System Protection Schemes in Eastern Denmark

Rasmussen, Joana

Publication date:
2006

Document Version
Publisher's PDF, also known as Version of record

System Protection Schemes in Eastern Denmark

Joana Rasmussen

System Protection Schemes Eastern Denmark

The author of the Ph.D. thesis is:
Joana Rasmussen

Supervisors:
Main supervisors from DTU:
Jan Rønne-Hansen (from 01/01/2002 to 16/06/2002)
Arne Hejde Nielsen (from 16/02/2002 to 21/12/2006)

Main supervisors from the industry:
Preben Jørgensen (from 01/01/2002 to 10/08/2005)
Jan Havsager (from 10/08/2005 to 21/12/2005)

Ørsted•DTU
Center for Power Electric Technology (CET)
Technical University of Denmark
Elektrovej, building 325
DK-2800 Kgs. Lyngby
Denmark

www.oersted.dtu.dk/cet
Tel: (+45) 45 25 35 00
Fax: (+45) 45 88 61 11
E-mail: cet@oersted.dtu.dk

ISBN: 87-91184-58-4

Publishing date:	21. December 2005
Class:	1 (public)
Version:	2.
Comments:	This Ph.D. thesis is enclosed as a part of the requirements to accomplish Industrial Ph.D. degree at The Technical University of Denmark.

Table of Contents

Table of Appendices

Summary (in English)

The Ph.D. project investigates different aspects of voltage stability in the power system of Eastern Denmark taking into account the large amount of wind power. In the project, a simple System Protection Scheme (SPS) against voltage instability in Eastern Denmark is developed. The SPS design is based on static and dynamic simulation analyses using a large-scale model[1] that considers a number of realistic power system conditions. The southern part of the 132-kV system is prone to voltage stability problems due to reactive power deficit in the area and the long distance to the large generating units. It was observed that the addition of large amounts of wind power to a relatively weak power system without reinforcements may cause voltage instability in the power system. The maximum power transfer in the heavily loaded system with two large off-shore wind farms is approached at about 70% of the wind generation capacity in Eastern Denmark. The restricted reactive power transfer from the 132-kV main system is the key indicator of voltage instability. The high load situation with high wind generation is considered a worst-case scenario in relation to serious problems with reactive power. Line outages in the southern part of the 132-kV system introduce further stress in the power system, eventually leading to a voltage collapse.

The local System Protection Scheme against voltage collapse is designed as a response-based scheme, which is dependent on local indication of reactive and active power flow in relevant 132 kV lines, violation of SVC rating and low voltages at selected 132-kV buses. As supplementary input, the SPS includes phase angle measurements from two separated locations in the 132-kV system. The phase angle recordings between the remote points can be used instead of measurement of active power in the tie-lines.

The power transfer in the 132-kV system is improved by additional reactive power support in the system using voltage control devices and/or SPS control actions: adjustment of adequate SVC setpoint, switching of additional capacitive shunts, start-up of Masnedø gas turbine etc. Stigsnæs power plant could possibly improve the reactive power support in emergency situations, as it is the closest power plant in the southern part of the system. In general, rescheduling power plants and voltage regulation at remote generators (MVAr adjustment) are not considered the most effective measures, because they are associated with large reactive power losses in the transmission system. Ordered reduction of wind generation is considered an effective measure to maintain voltage stability in the system. Reactive power in the system is released due to tripping of a significant amount of wind turbines based on induction generators. On the other hand, the wind turbine rejection is associated with loss of active power that has to be compensated using immediate reserves. To avoid unnecessary disconnection of wind turbines, fast fault clearance time is the main factor.

Phasor Measurement Units placed at strategic points are evaluated as an efficient tool for power system monitoring of important 400 kV and 132 kV transmission corridors in Eastern Denmark. The first PMU is connected to a 400 kV bus near Asnæs power plant, the largest generating unit in Eastern Denmark. The PMU in Radsted (RAD) is connected to a central bus in the southern part of the 132-kV system, which is close to a large concentration of wind turbines. The third PMU at Hovegård (HVE) is selected, because the bus terminates the interconnection to Sweden. Hovegård is geographically located near a number of power plants and the load centre in the Copenhagen area. The PMU at HVE is considered as a reference for the recorded phase angles at Asnæs and Radsted.

[1] Power system with 700 buses

Real-time phasor measurements are utilized for tracking power system dynamics during a number of severe power system disturbances that are characteristic for the Eastern Danish power system, such as wind farm rejection, cascading line outages and power oscillations. E.g. Nordic inter-area oscillation modes and damping were easily detected from phasor data during the outage of the 400 kV tie-line between Eastern Denmark and Sweden. It is concluded that recording of power oscillation frequencies is more convenient than computation of eigenvalues using a detailed dynamic model for the Nordic power system. One case study demonstrates that the recorded power system response is consistent with the simulation results. The application of synchronized phasor measurements for, e.g., validation of power system models used in stability studies, is seen as having a great potential in the future.

It was evaluated that PMU applications are mostly suitable in large interconnected networks, where abnormal dynamic changes in phase angles, power flows, frequency etc. can be easily observed. Great potential in the future is seen in advanced System Protection Schemes (SPS), where PMUs give precise input about the actual system state. In the future, the PMU units could enable the system operator to detect catastrophic events in due time and issue remedial orders in the power system. In that way, the power system capability could be extended beyond normal limits.

Resumé (in Danish)

Dette Ph.d. projekt undersøger forskellige aspekter af spændingsstabilitet i det østdanske elsystem med særlig fokus på vindkraftens påvirkning heraf. I projektet er der udviklet et koncept for systembeskyttelse (den såkaldte System Protection Scheme) mod truende spændingskollaps i det østdanske elsystem. Design af systembeskyttelsen er baseret på statiske og dynamiske analyser af elsystemet[2] under realistiske forhold. Den sydlige del af 132 kV systemet er specielt udsat for problemer med spændingsstabilitet pga. mangel af reaktiv effekt og den store afstand til de store kraftværker. Det fremgår af simuleringen, at store mængder vindkraft medfører spændingsustabilitet i elsystemet uden forstærkninger. Den maksimale effekt overført i systemet med højlast og to offshore vindparker svarer til ca. 70 % af den installerede vindproduktion i Østdanmark. Begrænsninger i 132 kV reaktiv effektoverførsel giver den bedste indikation for spændingskollaps. Den værste situation i relation til største problemer med reaktiv effekt forekommer ved højlast og højvind. Linieudfald i den sydlige del af 132-kV nettet svækker elsystemet yderligere med henblik på spændingsstabilitet.

Den foreslåede beskyttelse er et respons-baseret koncept, der er afhængig af lokale målinger af reaktiv/aktiv effekt i 132 kV linier, SVC kapacitet og lave 132 kV spændinger i udvalgte buser. Fasor målinger kan indgå som supplerende input i beskyttelsen, da fasen mellem to PMU (Phasor Measurement Unit) målepunkter giver indirekte information om aktivt effektflow i 132 kV linjerne mellem Radsted og Sjælland.

Effektoverførsel i systemet bliver forbedret ved brug af kontrol som nedregulering af vindproduktion, ændringer i SVC kapacitet, opstart af gasturbinen i Masnedø osv. Som følge af store reaktive tab ved reaktiv effektoverførsel er spændingsstyring på kraftværker ikke den bedste løsning for reaktiv effektstøtte i den sydlige del af 132 kV systemet. Stigsnæsværket kan muligvis bidrage gunstigt med reaktiv effekt i nødsituationer pga. den korteste elektriske afstand til Radsted. På den anden side er nedregulering af vindparker et godt alternativ for forbedring af spændingsforholdene i nettet. Dette skyldes, at en stor mængde reaktiv effekt bliver frigivet, efter at mange vindmøller kobler ud. Udfald af vindmøller medfører tab af aktiv effekt i nettet, som skal dækkes af reserver for aktiv effekt. Hurtig bortkobling af fejl i nettet spiller den største rolle, hvis større udfald af vindmøller skal undgås.

Tre PMU enheder placeret i strategiske punkter i nettet er udnyttet til overvågning af 400 kV og 132 kV transmissionskorridorer i Østdanmark. Den ene PMU er tilsluttet på 400 kV siden af Asnæsværket (ASV), det største kraftværk i Østdanmark. Den anden PMU i Radsted (RAD) ligger centralt i forhold til vindmølleproduktion i 132 kV nettet. Den tredje PMU sidder både på 400 kV og 132 kV skinnen i Hovegård (HVE), som er endepunkt på 400 kV forbindelsen til Sverige. PMUen i Hovegård betragtes som reference for vinkelmålinger fra de øvrige PMUer i nettet.

Realtids fasormålinger bruges til at analysere karakteristiske hændelser såsom udfald af vindmøller, kaskadeudkobling af linier og pendlinger i det østdanske system. F.eks. giver fasor datainformation om egenfrekvenser og dæmpning i forbindelse med karakteristiske effektpendlinger fremkaldt af udfald af 400 kV forbindelsen mellem Sverige og Østdanmark. Simuleringsresultater fra dette scenario er i overensstemmelse med de gennemførte PMU målinger. Der konkluderes, at måling af pendlingsfrekvenser ved hjælp af PMUer er mere praktisk end at beregne disse vha. detaljerede dynamiske modeller for det Nordiske elsystem.

[2] Realistisk model af elsystemet med 700 buser

Et stort fremtidigt potentiale ses i anvendelse af synkroniserede fasormålinger for verificering af stabilitetsmodeller for elsystemer. Det er vurderet, at PMU applikationer er mest egnede til brug i store elsystemer, hvor relevante dynamiske ændringer i fasevinkel, flow, frekvens etc. kan observeres. Fremtiden bringer nye muligheder for avancerede beskyttelseskoncepter, hvor PMUer giver nøjagtige input vedr. systemets tilstand. PMU enheder kan i fremtiden hjælpe netoperatører med i god tid at detektere kritiske hændelser for at beordre kontrol i elsystemet og udvide systemets muligheder ud over de normale stabilitets grænser.

Acknowledgments

First of all, I wish to express a gratitude to my family, my dear husband Kim Emil and our lovely daughters Andrea Emilie and Annika Helena Rasmussen for their understanding, support and help through the Ph.D. project as well as in the period of maternity leave with Annika. Sincere thanks are devoted to my caring mother Zagorka Bosbokilas, who came all the way from Macedonia to encourage me and relieve my work load at home at the end of my project.

This Ph.D. thesis is a result of an industrial research project carried out in close cooperation between the Technical University of Denmark and Elkraft System, the former Transmission System Operator in Eastern Denmark (now a part of the Danish TSO[3], Energinet.dk). The initial idea for the research project originates from my first university supervisor, Professor Jan Rønne-Hansen (in memoriam). In the past 4 years he was always in my mind as a motive power for my research. He was supervisor for my B.Sc. and M.Sc. projects at the Technical University of Denmark as well as my very first friend in Denmark since the autumn of 1995. I wish to honour his devotion and contribution to the field of power engineering at DTU and dedicate this thesis to him.

I acknowledge the enormous effort from my Elkraft System supervisors, Preben Jørgensen and Jan Havsager, who made the Ph.D. project succeed in spite of all the organizational changes and hectic activities in the company. I appreciate them as excellent, encouraging and incentive coaches as well as appreciated colleagues throughout my time at Elkraft System. They motivated me to understand and deal with the complex technical challenges in my research project. I wish to express my honest gratitude to Carsten Rasmussen, who was always willing to discuss PSS/E simulation related problems and long-term planning of the Eastern Danish power system. I am also thankful to my colleagues at Elkraft System, Søren Krüger Olsen (Transmission Department) and Lars Lind (System Operation Department), who were all the time inspiring and helpful.

I am thankful to associate professor Arne Hejde Nielsen for his support and involvement in my Ph.D. project. Together with Knud Ole H. Pedersen (Ørsted•DTU) he was fully engaged in the Phasor Measurements project at DTU. The hardware and software for PMU prototypes was developed at DTU and successfully implemented in the Eastern Danish transmission system. I am grateful to them having supplied real-time phasor data for my Ph.D. project. Without their hard work with the PMUs, I would not have been able to access the advanced measurements of the power system response to a number of severe disturbances.

I gratefully acknowledge the cooperation with associate professor Olof Samuelsson and Morten Hemmingsson (Lund Institute of Technology) within the PMU project at the Technical University of Denmark. I especially thank Olof Samuelsson for his excellent advices in relation to my Ph.D. project as well as his ability to simplify the most complicated technical and professional problems.

I highly acknowledge the contributions of Sture Lindahl and Daniel Karlsson (Gothia Power) for the valuable field experience with the ABBs PMU prototypes installed in Eastern Denmark and Southern Sweden. This PMU implementation prepared the way for further utilization of phasor measurements in Eastern Denmark and was used as case study in two scientific publications.

[3] Transmission System Operator

I wish to express my great gratitude to Dr. Arun Phadke, the father of synchronized phasor measurements, who enabled my study visit to Virginia Tech, Blacksburg, USA, in the period May-June 2002. He introduced me to different applications of phasor measurements and inspired me to be a dedicated PMU fan. I have always appreciated his lectures and discussions that made me learn more about his pioneering work in the field of phasor measurements.

I gratefully acknowledge the contributions of Kjetil Uhlen and Magni T. Palsson (Sintef Energy Research, Norway) in the development of a dynamic wind turbine model for the PSS/E simulation program. I thank them both for successful cooperation within the Nordic project "Utilization of the Nordic power system" as well as for the fruitful discussions on implementation of the wind turbine model that resulted in publication of a conference paper.

I wish to express great thanks to Professor Jacob Østergaard for his successful collaboration in the last phase of my project at DTU. I highly respect his intentions and enormous engagement to establish and lead DTUs Center for Electrical Technology.

At last and not least, I would like to thank all my colleagues from the former Transmission Department at Elkraft System for companionship and interesting discussions about power system related problems in Eastern Denmark. Besides, I thank Ms. Lisa Piil Pedersen (Energinet.dk) and Dorete Bendixen (Center for Electric Technology, DTU) for being kind and always helpful with the practical arrangements for my project. I would emphasize my appreciation of Ms. Anett Zemlov, COWI Consult A/S, who did a thorough and professional work in the final proofread of the Ph.D. thesis.

1 Introduction

1.1 Background for the project

The secure and reliable transmission of energy demands accurate and up-to date knowledge of the operational status of the transmission network. In many utilities, the operative safety margins are reduced due to restrained opportunities for network expansion caused by environmental, economic or political reasons. Such economic and regulatory changes may lead to less robust transmission system. Electric power utilities are forced to utilize more optimally the existing transmission capacity as well as to restrain their investments in network development. In relation to this trend in the electricity industry system protection schemes are seen as means for operating power systems closer to limits of safe operation. If the power system is to be operated close to the conventional stability limits, additional equipment and control measures and/or especially dedicated system protection schemes become necessary. System protection schemes can be related to manual operator instructions in the control centre or on-line automatic applications.

Automatic system protection schemes (SPS) are on-line applications that protect the power system against severe disturbances and preserve the capability and integrity of the entire system. Until now, system protection schemes have been implemented in many utilities, e.g. automatic load shedding schemes and generator tripping schemes. The SPS concept using classical relay technique may not be sufficient in the future, where the operational conditions in the network will come closer to the limits of safe operation. E.g. the classical relays used in well-known System Protection Schemes for under voltage and under frequency load shedding are dependent on local measurements. Local measurements may not be sufficient input in some of the advanced SPS applications. Remote measurements from widely separated points in the power system become often necessary as SPS input. The recent advances in synchronized phasor measurements open new opportunities in relation to system-wide System Protection Schemes.

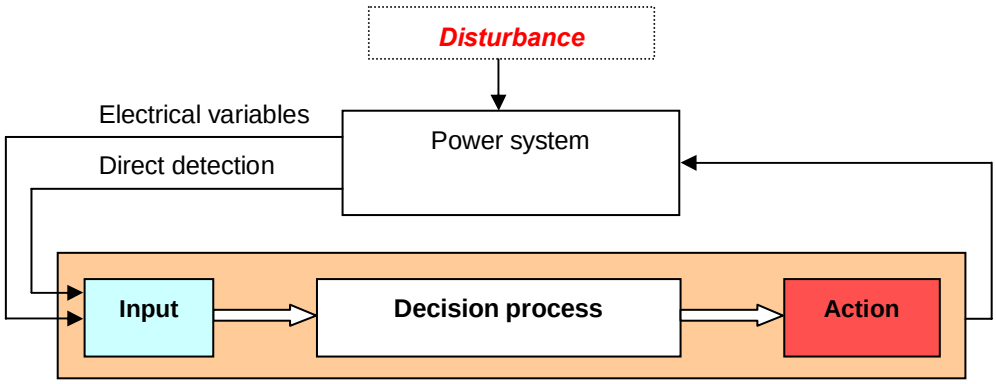

Fig. 1 Concept of System Protection Scheme, adapted from [1]

Fig. 1 illustrates a System Protection Scheme that relies on input from selected electric variables or direct detection of predefined events in the power system. The decision process is an automatic process that issues remedial control actions to counteract instability or insecure operation of the power system.

Increased security and wind power perspective:

The key issue in SPS applications for improved power system security is to counteract power system instability. SPS are typically applied to avoid wide-area disturbances and prevent (partial or total) blackouts in the power system. The large number of power system blackouts experienced world-wide puts an emphasis on system protection solutions as means to prevent future blackouts and to increase the level of security in the power system. This can be done by integrating power system monitoring, analysis and control in an automatic SPS platform for system-wide protection. System protection schemes can be designed to counteract a number of different power system instability phenomena (e.g. transient instability, frequency instability, voltage instability and cascading outages).

The Transmission System Operator of Eastern Denmark is concerned in investigation and application of System Protection Schemes as a means to increase the security in the Eastern Danish system. The main motivation for the Ph.D. project is to mitigate a number of problems related to large-scale integration of wind power. The increasing amount of wind power is a topic of immediate interest in many countries, where the wind turbines displace production from conventional power plants. Consequently, the TSOs have to handle a changing pattern of electric energy production. Furthermore, the deregulation of the electric energy market makes the power flow less predictable. The introduction of independent /dispersed generation in power systems contributes to continuously changing operating conditions.

The problem is currently highly relevant both in the eastern and the western parts of Denmark. During the last 15 years, the amount of wind production in Denmark has increased rapidly. The amount of wind power in Eastern Denmark took a further step upwards when a 150 MW offshore wind farm near Nysted south of Sealand was commissioned in 2003. This wind farm together with the majority of the existing wind turbines is placed in the sparsely populated areas, where the transmission system is significantly weak. System protection in Eastern Denmark becomes more complicated as a result of the following challenges in relation to the large share of installed wind power:

- Limited thermal capacity in parts of the system (weak transmission network);
- Significant amount of dispersed units are not dispatched in the Control Operational Centre;
- Difficulties in adequate voltage control (due to uncertain and unpredictable pattern of wind production);
- Difficulties in active power control (determine and control the power flow direction).

The issues of voltage stability, reactive power compensation and transient stability of wind turbines are extremely important for large-scale integration of wind power in areas distant from the main transmission system in Eastern Denmark. From an analysis point of view, the study of wind turbine generator performance during grid faults can be characterised as a transient stability problem. In case of induction generators, this problem is also related to the degree of reactive power support in order to magnetize and stabilize the generators after fault clearing. Detailed simulations using the PSS/E program are supposed to determine potential problems with voltage stability as well as transient stability of wind turbines considering a time scale up to ten seconds.

Nordic perspective: The power system security in Eastern Denmark is to a great extent dependent on the overall security of power supply in the interconnected Nordic system that encompasses transmission system of Denmark, Sweden, Norway and Finland. In the Nordic countries, there is an increased interest in utilizing the transfer capacity of the transmission network in the most efficient and economical manner. This was the main topic of a joint R&D project "Increased utilization of the Nordic power system" that was initiated by the Transmission System Operators in the Nordic countries. One of the benefits in this project is strategic coordination and utilization of phasor measurements in the Nordic countries.

1.2 Objective of the Ph.D. project

Objective 1: Design of system protection scheme against voltage instability

The main focus in the Ph.D. project is to develop a concept for system protection schemes (SPS) against voltage instability in the power system of Eastern Denmark taking into account the large amount of wind power. The project aims at evaluating general voltage stability criteria for the power system under normal operation and subjected to relevant contingencies. Static and transient voltage stability analyses are used to access the power system behaviour as well as the impact of wind generation.

The main task of the Ph.D. project is to design a system protection scheme against voltage instability of the large-scale power system in Eastern Denmark. The SPS design is especially dedicated to detect abnormal system conditions in due time and, if necessary, to give warning and/or launch corrective actions to counteract voltage instability. The system protection scheme is supposed to detect voltage instability and preserve the power system capability with respect to wind generation. Hereby, the project aims to illustrate the main principles for voltage stability, derive indicators and criteria (based on simulations and phasor measurements), to determine the voltage stability limits and constraints as well as to evaluate the feasibility of different indicators and different remedial control actions in the SPS system. The investigations in the project deal in particular with the following challenges:

A) Detect voltage instability

Large-scale wind power is integrated in a weak part of the Eastern Danish 132 kV network with a long distance to the main 400 kV transmission system, where the majority of central power plants (spinning generation) are located. Voltage stability and reactive power compensation are important issues for large-scale integration of wind power in areas distant from the main transmission system in Eastern Denmark. When adding large amounts of wind power, the system may become voltage unstable if it is operated too close to its stability limit. Furthermore, this may turn into a voltage collapse problem if after contingencies the network becomes too weak to maintain stable operation of a large share of wind farms without active voltage control. Thus it is necessary to know how closely the network can be operated to its voltage stability limits with respect to wind power constraints.

As shown in Fig.1, the detection of voltage instability is closely associated to identification of relevant indicators in the System Protection Scheme input and derivation of relevant criteria and setting values for the SPS decision process. In fact, the project searches the solution of the following problems:

SPS input:

- What are the best indicators for a System Protection Scheme against voltage collapse (where and what to measure?)

- What are the advantages of using phase angle monitors in system protection schemes against voltage stability? This subject is closely related to the general utilization of phasor measurements in Eastern Denmark.

SPS decision process:

- What maximum wind power can be transferred in a weak 132 kV intact network and in a network with transmission line outage(s)?

- How is the reactive power demand influenced by a variable degree of wind power in the system?

- What is the most significant impact of wind turbines with respect to voltage stability in the system?

- What is the dynamic impact of wind turbines on the power system transient stability?

- What are the main factors in ride-through capability of wind turbines?

- What is the impact of wind turbine rejection for preserving the voltage stability (tripping of on-land wind turbines in the power system)?

In order to design the SPS decision process, both static and short-term voltage stability is studied with special focus on wind generation. The impact of large generating units is not approached in detail. Long-term voltage stability (effects on tap-changers, field current limiters etc.) was not in the scope of studies.

B) Evaluate remedial controls for voltage stability

The **SPS output** acts when voltage instability is detected by the System Protection Scheme shown in Fig.1. In this context, the project evaluates general applicability of different control actions that are able to counteract voltage instability in Eastern Denmark. Time-domain simulations are performed in the Ph.D. project in order to illustrate the effect of different remedial control actions such as wind turbine rejection, application of reactive power support from additional generation units and a Static Var Compensator. The investigations here focus on central aspects for ride-through capability of wind turbines in Eastern Denmark. Some time-domain simulations are used to analyse possible feedback actions in the power system, but not all relevant remedial control actions are analysed in detail. For the system studies, the following limitations are valid: Determination of setting values and time delays for different controls was out of the scope of the analysis. Coordination of different control actions in the SPS scheme was not taken into account. Related problems with voltage collapse in Sweden are not considered.

The main challenge in unit protection of wind turbines today is the conflicting requirements for on-land and off-shore wind turbines. On one hand it is desired to keep large wind farms in operation under faults in the transmission system and thus benefit from the active power balance in the power system. The consequence of wind turbine rejection is loss of active power that has to be compensated by immediate reserve in the system. On the other hand tripping of wind turbines on-land is beneficial in case of problems with power system voltage stability, because significant reactive power is released in the system. The challenge of avoiding unnecessary disconnection of wind turbines can be solved using dedicated System Protection Schemes.

Objective 2: Utilize phasor measurements

The focus on increased power system security is closely related to improved methods for monitoring the system, where utilization of synchronized phasor measurements plays an important role. For this purpose the Ph.D. project aims to:

C) Investigate the potential of phasor measurements for detection and analysis of power system events in Eastern Denmark. The investigations are based on off-line analysis of phasor measurements in case of known severe disturbances or planned revisions;

D) Evaluate the potential for application of phase angles[4] in the suggested SPS against voltage instability due to large wind power penetration in Eastern Denmark;

E) Evaluate the future perspectives for system protection schemes using PMU input.

1.3 Project organization

The Industrial Ph.D. project is carried out at the Technical University of Denmark (Ørsted•DTU, power engineering section) in close cooperation with the Danish transmission system operator Energinet.dk (previously Elkraft System which is now merged with Eltra and Gastra). The research activities in Joana Rasmussen's Ph.D. project are primarily related to investigation of System Protection Scheme design against voltage instability in the power system of Eastern Denmark. The project has a special focus on the impact of wind power impact on the power system of interest. Fig. 2 shows the organisational diagram for the Ph.D. project and its interface to other related projects.

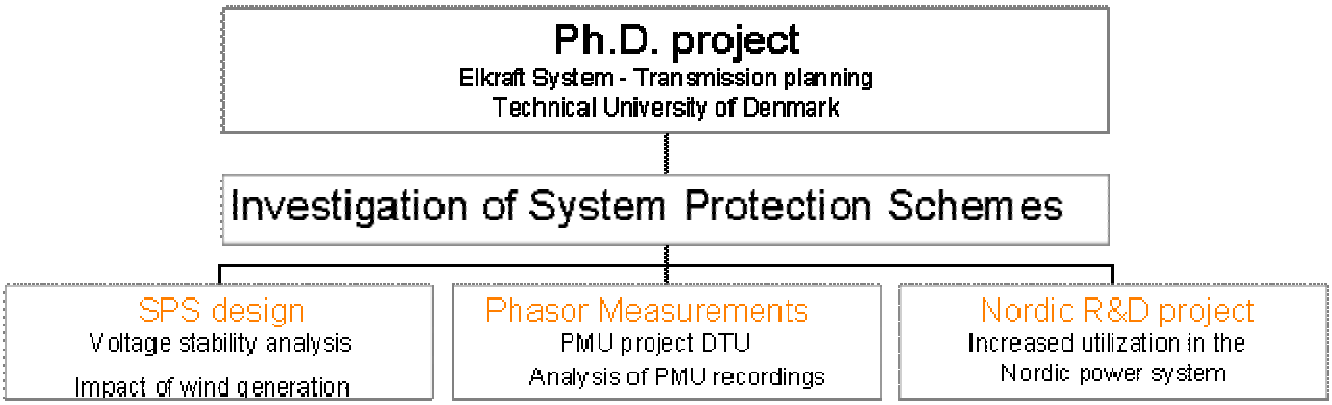

Fig. 2 Organisational diagram of the Ph.D. project

In parallel with the Ph.D. project, the research project "Complex voltage & current measurements in the transmission system" is initiated as a joint project among Energinet.dk, DTU and Lund University (LtH). The PMU project activities were related to practical problems concerning:

- Development of hardware for synchronized phasor measurements;
- Establishment of three PMUs with communication to a central location;

[4] Measured by Phasor Measurement Units (PMUs)

- Installation of the PMUs at widely separated points in the transmission system;

- Data acquisition and methods for advanced data analysis.

In the frame of the Ph.D. project, Joana Rasmussen was engaged in a number of activities in relation to phasor measurements. She focused on planning of the PMU network in Eastern Denmark, identification and analysis of relevant power system events using PMU recordings. Joana Rasmussen was also involved in planning and coordination of PMU activities in Eastern Denmark and Sweden. In relation to the PMU project at DTU, Joana Rasmussen prepared a number of scientific publications in the field of phasor measurements.

The Ph.D. project "System protection schemes in Eastern Denmark" is a part of the joint Nordic R&D project "Increased utilization of the Nordic transmission system". The Nordic project was carried out by the Transmission System Operators (TSOs) in cooperation with Nordic universities and research institutions i.e. SINTEF Energy Research. In the frame of the Nordic cooperation, a dynamic wind turbine model was developed at Sintef, Energy Research with the affiliation of Joana Rasmussen from Energinet.dk. Sintef Energy Research was involved in development and verification of the wind turbine model. In the Ph.D. project, Joana Rasmussen implemented this model for investigation of the dynamic impact of wind turbines in the Eastern Danish system.

Results from the Ph.D. project should enable system planners and operators at Energinet.dk to evaluate recent possibilities of using system protection schemes in the Eastern Danish power system. The SPS schemes are expected to enable better utilization of the existing transmission network as well as to contribute to increased power transfer in the Nordic region. The economic benefits related to practical implementation of SPS are referred to savings due to extended operational security and reduced risk for system instability. Detailed description of the commercial benefits for the Ph.D. project is enclosed in a separate business report [82]. The contents in the business report are based on a business-targeted course in technology management organized by The Danish Academy for Technical Sciences (ATV).

1.4 List of publications

1. Rasmussen J., Jørgensen P., "Synchronized Phasor Measurements of a Power System Event in Eastern Denmark", IEEE Transactions on Power Systems, Vol.21, No.1, pg. 278-284, February 2006.

2. Rasmussen J., Jørgensen P., "Synchronized Phasor Measurements of a Power System Event in Eastern Denmark", Conference proceedings for IEEE Bologna Power Tech 2003, 23-26. June 2003, Bologna, Italy.

3. Rasmussen J., Jørgensen P., Palsson M.T., Uhlen K., "Wind Power Impact to Transient and Voltage Stability of the Power System in Eastern Denmark", published in IASTED PES 2005 Conference proceedings, 8th IASTED International Conference on Power and Energy Systems , October 23-26, 2005

4. Samuelsson O., Hemmingsson M., Nielsen A.H., Pedersen K.O.H., Rasmussen J., "Monitoring of power system events at transmission and distribution level", accepted for publication in IEEE Transaction on Power Systems.

5. Nielsen A.H., Pedersen K.O.H., Jørgensen P., Havsager, J., Olsen S.K., Rasmussen J., "Phasor measurement units in the Eastern Danish power system", expected for publication at CIGRE general conference 2006.

Re. 1 and 2. The first and the second papers present synchronized phasor measurements of a power system event in April 2002. Joana Rasmussen initiated the overall planning of a temporary installation of ABB's Phasor Measurement Unit prototypes in Denmark and Sweden. In the paper, she emphasizes the advantages of using phasor measurements in monitoring of power oscillations between Eastern Denmark and Sweden. Besides phasor data analyses, she carried out a simulation analysis of the power system event using a large-scale power system model of Eastern Denmark. Joana Rasmussen stands for the complete preparation of the paper for the IEEE Trans. on Power Systems, which in fact is an upgrade of the conference paper with the same title previously presented at the Bologna Power Tech conference 2003.

Re. 3. In this paper, Joana Rasmussen demonstrates the dynamic impact of wind power integration in Eastern Denmark using an advanced wind turbine model in the large-scale power system model of Eastern Denmark. The dynamic wind turbine model was developed at Sintef, Energy Research in close cooperation with Elkraft System (the former Transmission System Operator in Eastern Denmark). The paper was presented at IASTED International Conference on Power and Energy Systems, 2005.

Re. 4. The publication is closely related to the joint PMU project between Ørsted•DTU, The Technical University of Denmark and Institute for Industrial Automation, Lund University on phasor measurements and development of a prototype for phasor measurement unit (PMU). One PMU prototype is connected to the 400 V mains in a laboratory at the Danish Technical University (DTU), and few PMU monitors are implemented at 400 and 132 kV busbars in the transmission system in Eastern Denmark. The paper deals with advanced monitoring of real-time power system disturbances using phasor measurements. The concept developed in the paper supports the advantages of using PMUs at low voltage level (400 V) for events that take place in the transmission system (400 kV). Ph.D. student Joana Rasmussen was involved in data acquisition and analysis of the PMU recordings at 400 kV level, interpretation of results and comments on the final manuscript.

Re. 5 The final manuscript of this paper is accepted for the upcoming CIGRE 2006 general conference in Paris.

1.5 Outline of the thesis

The Ph.D. thesis is divided in the following main chapters:

- Introduction
- Theory
  - Conventional unit protection
  - Fundamentals of power system stability
  - Fundamentals of System Protection Schemes (SPS)
  - Voltage stability analysis

- Models
- Simulations studies
    - Static voltage stability analysis
    - Design of SPS against voltage instability
    - Transient stability analysis
- Phasor measurements
- Conclusion
- Future work.

The theoretical part introduces concepts for conventional unit protection and system protection, including general principles and methods for power system stability. The next chapter deals with modelling issues for the Eastern Danish power system, where special attention is given to models of devices that have impact on voltage stability limits in the system of interest. Simulation models of power plants, loads, wind turbines and reactive power compensation devices are presented.

The simulation chapter describes extensive simulation studies performed in the PSS/E program. Steady-state and to some extent dynamic analyses are used to investigate voltage and transient stability limits in the Eastern Danish system. Special attention is paid to design of voltage stability criteria and requirements for a System Protection Scheme against voltage instability. The response of wind turbines systems to selected critical contingencies is analyzed with respect to transient and voltage stability of the power system.

The Phasor Measurements chapter involves fundamentals of synchronized phasor measurement and a number of case studies concerning different applications of synchronized phasor measurements for enhanced power system monitoring in Eastern Denmark.

2 Theory

The conventional relay methods may not be a sufficient practice, when the operational conditions in the power system come closer to the overall limits of safe operation. The aim of conventional unit protection is namely to detect faults and abnormal states in power system components and initiate trip of associated circuit breakers in order to prevent damage of the units. In contrary to unit protection system protection schemes are system-wide applications involving different units.

2.1 Conventional unit protection

Unit protection detects faults and abnormal states in power system components and prevents hazardous currents and/or over- or undervoltage from damaging equipment such as MV and LV distribution feeders, distribution and network transformers, busbars, circuit breakers, generators, HV transmission lines etc. Protective relays are designed to detect abnormal conditions in the network and, if necessary, activate disconnection of a particular circuit giving commands to circuit breakers/disconnectors. Unit protection is supposed to be stable, fast and sensitive enough in order to isolate efficiently faults in the network. Possible failure in the main protection is covered by means of back-up protection. Some relaying principles for protection of lines and transformers in transmission networks are previewed without going into details about functions of different relays [57].

2.1.1 Line protection

Combination of different relaying principles can be used for protection of lines and busbars in power systems. In the following section, special attention is paid to main principles for distance relays and the selectivity of distance protection.

Distance relays are commonly used for protection of 132 and 400 kV transmission lines in Eastern Denmark. The operating principle is based on detection of distance to the fault, which is proportional to the measured impedance[5] to the fault location. The majority of system faults occur as single-phase-to-ground faults, where the clearance time is highly dependent upon the neutral grounding and the required sensitivity of the zero-sequence detection used. As a matter of fact, the same fault type occurring in different sections of a network would result in different fault currents, and thus different impedance magnitudes would be measured between the power source and the fault. Selectivity in distance protection means that only circuit breakers nearest to the fault are supposed to trip, leaving the other circuit breakers to supply the healthy sections of the network. Fig. 3 illustrates a simple stepped characteristic, where A, B, and C represent the location of substations linked by feeders AB and BC. A fault occurring on the BC feeder introduces a fault current that activates the distance protection at substation C on the right side and substations A and B on the left side of the circuit.

In the last case zone-2 and zone-3 are activated. If the fault is correctly cleared by the nearest relay (e.g. B) then the faulted current through relay A and C is stopped. Relay A and C reset, as they are not needed as back-up protection. Crucial element for relay selectivity is the composition of different protection zones and the operating time of the corresponding relays. A fault in the first zone-1 extends for 80 % of the feeder AB in order to avoid possible discrimination with relay B. The second zone-2 covers about 120 % of AB feeder.

[5] Using voltage and current measurement circuits

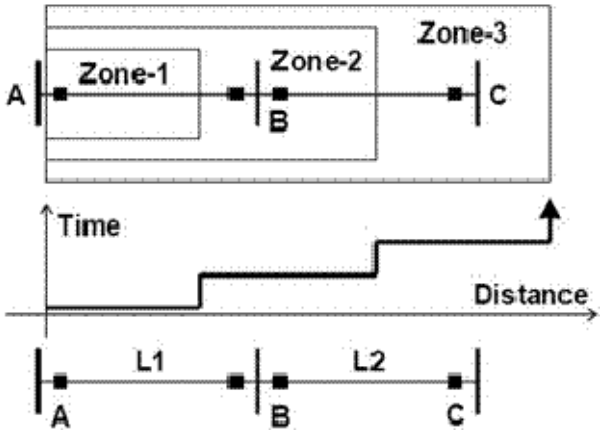

Fig. 3 Principle for distance relay operation [6]

2.1.2 Transformer protection

Protection of high-voltage transformers is commonly done using overcurrent and differential relays, detectors for severe internal faults etc.

Overcurrent relays operate when the feed current exceeds a preset value at a time determined by the relay characteristic. Hence, the relay initiates tripping of the associate circuit breaker after a time delay, which in many cases is inversely dependent on the value of overcurrent. The relay reacts at two levels: rapid operation in case of short circuit and delayed activation time in case of smaller currents.

Differential relays cover a single unit (a transformer or line) in the power system if a fault occurs within the protected zone. The protection scheme is based on the equality between the entering and the leaving currents in the circuit under normal conditions. The protection is activated when induced voltages on the primary and secondary side of the transformer attain different values as a result of different current values at each unit terminal.

2.1.3 Generator protection

The unit protection of large power plants in Eastern Denmark is designed according to the Nordic recommendations for operational performance of the generation units [15]. The recommendations specify operational and power control equipment characteristics, as well as the power unit's response capability to normal and contingency situations. The reference provides details about e.g. undervoltage, overcurrent, and frequency limitations for the power units in the Nordic system.

2.1.4 Wind turbine protection

The protection of wind turbines in Denmark is divided into two categories. The wind turbines on-land have relay protection that detects abnormal voltage, current and frequency variations and trips the wind turbine unit in case of violated thresholds in case of disturbances. From the other side, the requirements for ride-through capability of large off-shore wind farms are sharpened, because they have to withstand the majority of faults in the transmission system. The off-shore wind farms are considered to be wind power plants, as they are expected to some extent to take part in the voltage and frequency control in the power system. The Danish Transmission System Operator has well-defined technical regulations for the properties and

the control of wind turbines. The first set of recommendations is related to wind turbines connected to grids below 100 kV [36], while the second set is related to large wind farms connected to grids above 100 kV [37]. The regulations describe the active and reactive power control features and dynamic properties of wind turbines needed for operation of the power system with respect to short- and long-term stability and power quality.

The main challenge in the unit protection of wind turbines in Eastern Denmark is seen in the conflicting requirements for on-land and off-shore wind turbines. The benefit of using the present protection principle for wind turbines on-land is that they help to maintain voltage stability in the system. After a fault in the transmission system, a significant amount of on-land wind turbines would trip, and the released reactive power contributes to voltage recovery at system buses. The drawback of wind turbine protection on-land is the loss of active power, as a large number of wind turbines trip after a fault in the transmission system. The situation is opposite for off-shore wind turbines, as they are designed to remain in operation in spite of faults that occur in the transmission system. The drawback here is that the large off-shore wind farms are associated with increasing reactive power demand in case of faults in the transmission system. The need for additional reactive power support is thus more pronounced when off-shore wind farms are present in the system.

2.2 Fundamentals of power system stability

According to [41], power system stability is defined as "the ability of an electric power system, for a given initial operating condition, to regain a state of operating equilibrium after being subjected to a physical disturbance, with most system variables bounded so that practically the entire power system remains intact". Different types of SPS can be used to minimize or reduce the severity of power system phenomena such as angle instability (transient and small signal), frequency instability and voltage instability (Fig. 4).

The first two phenomena are mainly related to active power control, while voltage stability is influenced by reactive power control in the power system. Angle stability can be understood as generator stability, and it deals with aspects such as small signal stability and transient stability. The phenomenon of transient stability is closely connected to the ability of synchronous machines to withstand large disturbances and remain in synchronism. From the other side, small-signal stability is related to the power system oscillatory or non-oscillatory response to small disturbances, such as change in scheduled generation or small increase in system load. Reactive and active power balance as well as constant frequency and acceptable voltage levels are crucial for secure and stable power system operation. Voltage stability is related to the power system ability to maintain reactive power balance and acceptable voltages in all system buses. In general, voltage stability can be viewed as load stability that covers stationary and transient stability phenomena. Voltage stability and reactive power control are important issues in power systems with significant wind generation. From an analysis point of view, the wind turbine injections are considered as negative loads in the system. The ride-through capability of wind turbines based on induction generators is here considered as a special kind of transient voltage stability phenomena, as it is closely related to voltage recovery and wind turbines response after disturbances in the system.

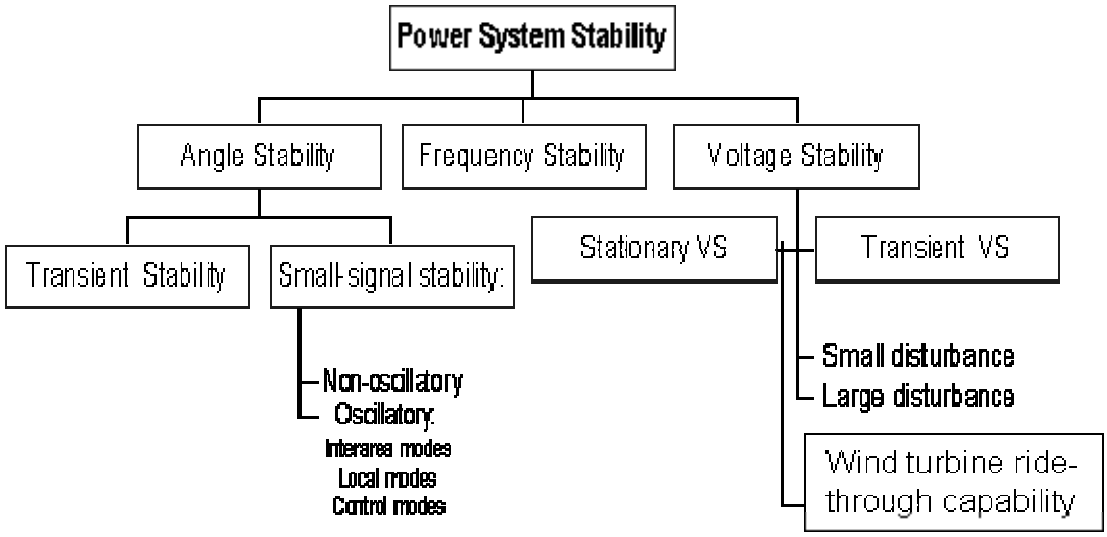

Fig. 4 Classification of power system stability phenomena, adapted from [41]

In the following section, some fundamentals of power system stability are approached using the simple transmission system shown in Fig. 5.

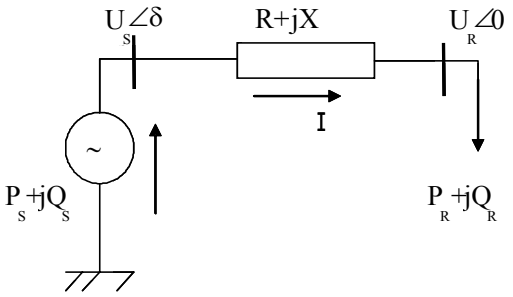

$$S_R = P_R + jQ_R = \left(U_R \cdot e^{j0}\right) I^* =$$

$$S_R = \underbrace{\frac{U_R\left(U_S R\cos(\delta) + U_S X\sin(\delta) - U_R R\right)}{R^2 + X^2}}_{P_R} + j\underbrace{\frac{U_R\left(U_S X\cos(\delta) - U_S R\sin(\delta) - U_R X\right)}{R^2 + X^2}}_{Q_R} \quad (1)$$

Fig. 5 Simple radial network

The radial network in Fig. 5 transfers power from a generator to a constant load via a transmission line with impedance Z=R+jX, where the assumption X>>R is valid. The sending node has complex voltage (magnitude U_S and phase angle δ), while the receiving bus has real voltage magnitude U_R. The transmitted active and reactive power from the sending to the receiving node is calculated in (1) taking into account a number of approximations.

$$P_R \propto \frac{U_R U_S X \sin(\delta)}{X^2} \propto \frac{U_R U_S \sin(\delta)}{X} \propto \sin(\delta) \propto \delta \quad (2)$$

The relation (2) describes the proportionality between active power and angle difference in steady-state operation, which is associated with constant frequency and small angle changes. During major disturbances, the steady-state description (1) of power transmission is no more valid, since the power system frequency can deviate significantly. Large frequency deviations and severe upsets in power systems have to be sustained in order to maintain stable frequency. In general, frequency stability is determined by active power balance and control in the system. Large frequency deviations are controlled by adjusting active power generation. Equation (3) reveals the close relation between reactive power and voltage control.

$$Q_R \propto \frac{U_R X (U_S \cos(\delta) - U_R)}{X^2} \propto \frac{U_R (U_S \cos(\delta) - U_R)}{X}$$
$$Q_R \propto U_S \cos(\delta) - U_R \propto U_S - U_R \qquad (3)$$

The physically weak coupling between active power P_R and voltage difference (U_S-U_R), and between the reactive power Q_R and δ is valid only in case of normal power system operation. E.g. the fast decoupled load flow method [44] takes advantage of this weak coupling and solves the load flow algorithm using a decoupled set of P-δ / Q-U equations. In case of imminent voltage instability, the coupling between P_R and (U_S-U_R) as well as between Q_R and δ can not be neglected.

2.3 Fundamentals of System Protection Schemes

According to [1], "System Protection Schemes[6] are designed to detect abnormal system conditions and take predetermined corrective action to preserve system integrity and provide acceptable system performance". System protection schemes are related to the capability of the entire power system to remain in stable operation and do not coincide with unit protection of power system equipment illustrated previously. A typical structure of an on-line system protection scheme is shown on Fig. 6. The central part of a system protection scheme is the decision process, which is based on input criteria and indicators for power system stability. The remedial control actions are issued as output, which in most cases is predetermined using the decision process logic. The time range of SPS actions associated with different power system phenomena is related to the time needed to mitigate the system-wide consequences.

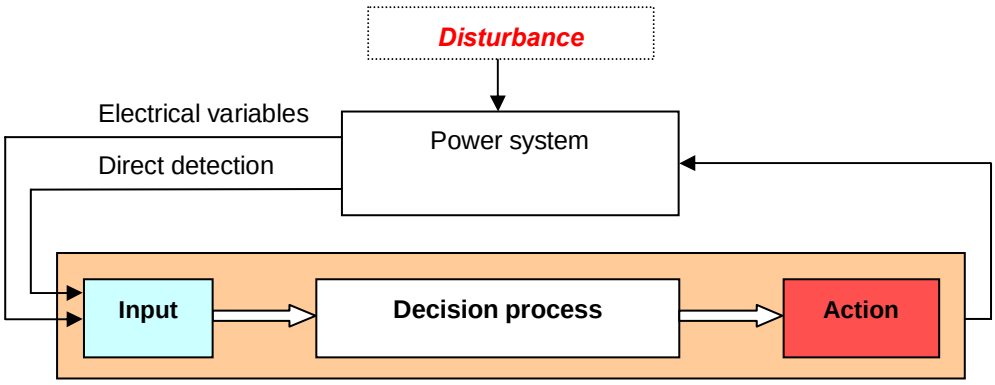

Fig. 6 Concept for automatic System Protection Schemes, adapted from [1]

As illustrated in Fig. 6, a System Protection Scheme is a complex application capable to receive a great amount of measurements, process them in order to select the correct solution (action) from variety of possible solutions of an impeding system-oriented problem and if necessary send appropriate orders to the proper power system equipment.

System Protection Schemes refer typically to various schemes for load shedding, generator tripping and network separation based on local or/and system remote signals or through fast continuous control of OLTC[7], HVDC[8] or FACT[9]s devices [2]. The purpose of these system

[6] Known also as Remedial Action Scheme (earlier acronym Special Protection Scheme)
[7] On-Load Tap Changers
[8] High Voltage Direct Circuit
[9] Flexible AC transmission

protection functions is to avoid or reduce adverse consequences of contingencies (such as severe line or generator outages) that would lead to overload or voltage/frequency excursions beyond acceptable limits. The control actions can be initiated by a local detection system in a region of the network, where all measurements are available at the same location where the control action is performed.

On the other hand, the protection scheme can rely on a wide area detection system, where complex and large disturbances can be detected by means of SCADA[10] or/and WAMS[11] data from Phasor Measurement Units (PMU) and Voltage Instability Predictors (VIP), which are connected at widely separated points via telecommunication channels, see Fig. 7. System protection schemes are expected to become more important in future transmission systems as means to operate the systems closer to their physical limits [7]. Wide area control and monitoring facilities would enable enhanced and more flexible use of system protection [9], [10].

According to input variables, the System Protection Schemes are classified in event –based SPS and response-based SPS.

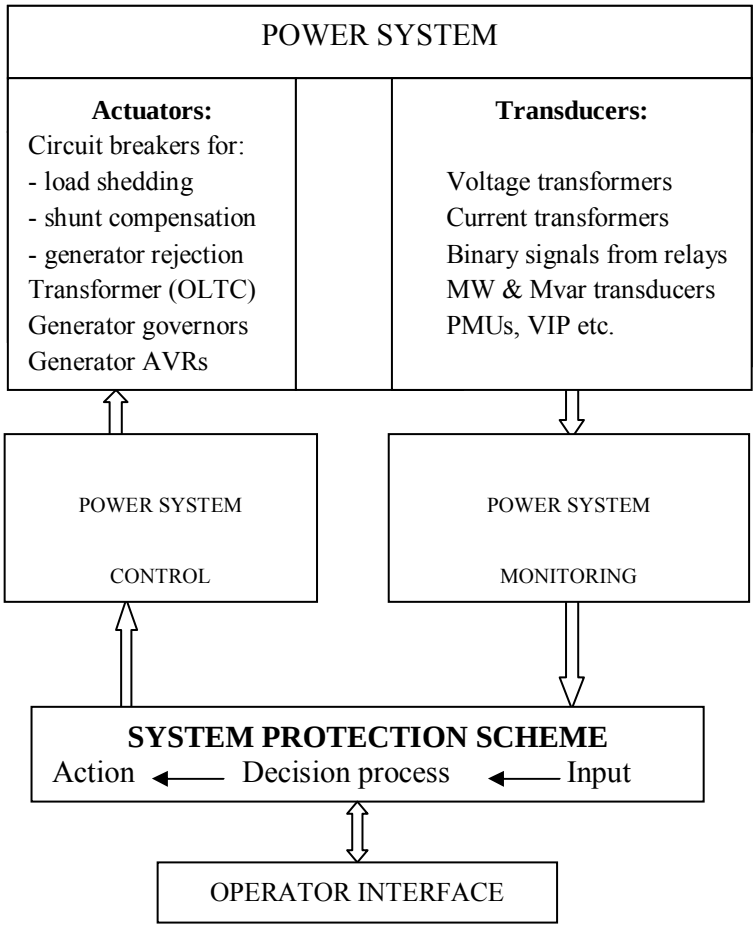

Fig. 7 *On-line concept for system protection scheme*

[10] Supervisory Control And Data Acquisition System (SCADA)
[11] Wide Area Measurement System (WAMS)

Event-based SPS (feed-forward schemes) react fast upon recognised limited number of critical events or a particular combination of events in the power system, which are easy to identify and detect. Event-based protection is required as mandatory in applications where:

- The severity of the event exceeds the system robustness;
- The speed of the control action is crucial;
- The monitored system parameters evolve slower than the desired time delay of action.

E.g. this type of protection is efficient in case of transient angle instability, which requires emergency control within a second. This SPS type is rule-based, with rules derived from off-line simulation and analytical studies of relevant phenomena. The predetermined control actions can be local or remote. A drawback of this approach is that it is difficult to predict all multiple contingency events that cause major incidents. For events omitted from the contingency list, the corresponding SPS would disoperate. The event-based SPS are characterised as open-loop type (a predefined event is followed by a predefined control action taken). The remedial actions are designed and evaluated using off-line simulation studies of the power system performance and system response to events and contingencies. Depending on the system response, the power system attains an acceptable state or successive SPS action(s) have to be executed as a new "remedial event" in the contingency list.

Response-based SPS (feed-back schemes) are based on a power system response to a specific contingency, where measured electrical values (power, voltage, frequency etc.) are used as input to the SPS. Specific input variables are selected according to the type and severity of the system-wide disturbances. The SPS triggers proper protection action(s) after the disturbance has caused the measured variables to significantly deviate from "normal" values. This SPS type can be applied even for events that are not explicitly identified in the power system. The operation of this SPS type is considered as the most dependable (upon local measurements) and in the same time most secure, since the effect of unintended SPS operation is minimal due to restricted and localised actions. The reaction time of the system protection can be rather slow, because they have to wait for the system response e.g. frequency or voltage drop under a certain setting. As examples of response-based SPS undervoltage or underfrequency load shedding can be mentioned.

There are two potential problems with dedicated system protection schemes that should be addressed in the future. One is that system protection can trip when it is not supposed to, resulting in unnecessary tripping of generators or unwanted interruptions of power supply.

Secondly, unexpected conditions and system changes can lead to critical operating situations, where the system protection does not trip when it ideally should, and thus contributes to a more serious system collapse. Thus the ultimate system protection should be a scheme which adapts to the changing conditions and provides a balance between the following contradictory requirements on reliability:

- **Dependability –**certainty that SPS will operate when required
  A protection scheme should always act when it is supposed to;
- **Security -** certainty that SPS will not operate when not required
  A protection scheme should never act when it is not supposed to;

- **Selectivity** - ability to activate minimum amount of control action
  A SPS should not act excessively, i.e. it should be able to shed the appropriate amount of load or generation in order to keep the system as much as possible intact;

- **Robustness** - ability to operate properly over the entire range of steady-state and dynamic system conditions.

The following table summarizes the general requirements for a System Protection Scheme against power system voltage instability in Eastern Denmark.

Response –based SPS		
SPS PERFORMANCE	Input signals	- Local voltage level - Generator output (reactive power, excitation current) - Power flow data (pre- & post disturbance)
	Output signals	- Trip signal to shunt devices: capacitors & reactors - Trip signal to wind turbine circuit-breaker - Change of voltage setpoint (for power plants,SVC)
	Control action speed & type	- Short term voltage stability - Fixed pre-determined control - Control sensitive to system conditions - Control optimised for minimum switching action
SPS DESIGN CRITERIA	Dependability	- Critical, complete design redundancy required - Prohibited coincided failure of more than 2 SPS components
	Security	- Very high security
	Robustness	- Proper function under all system conditions
	Selectivity	- SPS should operate only for design conditions - SPS should be disarmed if operation is not needed - Minimize inappropriate operation and human error
	Coordination with other control actions	- Capacitor & shunt reactor switching - Overfrequency generator tripping - Transmission overload protection

Table 1 Requirements for SPS against voltage instability, adapted from [1]

2.3.1 Examples of System Protection Schemes

The state-of-art for existing System Protection Schemes is summarized in a comprehensive technical report [1]. The report approaches general considerations about SPS implementation and includes a number of examples of different existing System Protection Schemes world-wide. At the end, the report views future needs for new System Protection Schemes, including application of phasor measurements for system protection.

The Ph.D. thesis is especially treating investigation of conventional and advanced concepts for system protection that are applied in the Nordic countries. In the Nordic power system consisting of Eastern Denmark, Sweden, Finland and Norway, a number of System Protection Schemes are used in case of extreme contingencies causing generation loss greater than the largest unit in operation. These SP Schemes consists of active power control by HVDC links, automatic start of gas turbines, load shedding etc.

The transmission system in **Sweden** has a generator disconnection SPS in operation that acts in case of outage of an important 400 kV transmission corridor. The total generation is reduced by automatic disconnection of generators in order to avoid a major system-wide disturbance. The loss of generation is compensated by the spinning reserve. Another protection scheme was introduced against voltage collapse in South Sweden. This SPS intends to increase the power transfer limits from the north to south in Sweden and/or to increase the system security in case of a severe system fault [3].

The Transmission System Operator in **Norway** has implemented across the country a large number of different system protection schemes, which demand a significant effort for coordination and supervision in the Operational Control Centre. Reference [5] deals with experiences related to System Protection Schemes in Norway as well as PSS/E user models for SPS design and test. It describes many Norwegian protection schemes in operation, e.g. SPS for generation tripping or regulation downwards (in relation to angle stability, overload, and voltage collapse), load shedding (in relation to line overload and voltage collapse) and SPS for automatic grid separation in relation to power oscillations.

Voltage Instability Predictor (VIP)

A Voltage Instability Predictor is installed at the Hasle transmission corridor between Norway and Sweden. It is a special monitoring system or an adaptive relay for tracking the distance to voltage instability, which is closely related to the notion of maximum loadability limit of a transmission network. As seen in Fig. 8, the VIP measures the apparent impedance of the load $Z_L=U/I$, as the ratio between the local voltage U and current I phasors at a particular bus and simultaneously estimates the network (Thevenin) equivalent impedance (Z_{th}). When the system loading is normal, the load impedance exceeds significantly the net impedance, i.e. $|Z_L| >> |Z_{th}|$. When maximum power transfer occurs at the inception of voltage stability, the difference between the two impedances approaches zero. The main idea in the VIP is to track the distance between $|Z_L|$ and $|Z_{th}|$ and by comparing the time varying impedances to track the proximity to voltage instability. The main problem with the device is that Z_{th} is not a fixed quantity, because it is being continuously updated. It represents a lumped equivalent of the total network consisting of many components that can change operating status at a given time. More likely during typical voltage instability problems, the network impedance Z_{th} increases (as the network gets weakened) and $|Z_L|$ decreases (loads become heavier). In real environment, the measurements are not precise, and the Thevenin parameters drift due to the changing conditions in the network. Thus, it is more appropriate to achieve a more accurate representation of $|Z_{th}|$ e.g. using input from PMUs. Further description, simulation studies and field test of the VIP unit are available in references [48] and [49].

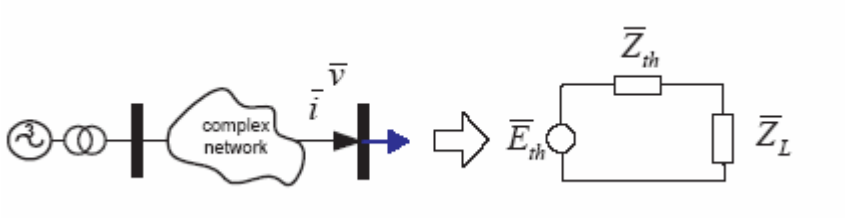

Fig. 8 *Thevenin equivalent representation for VIP approach*

In principle, the VIP application can be used as an input to a System Protection Scheme to issue proper preventive or corrective control actions to avoid the danger of voltage collapse. Generally, the VIP unit(s) can be integrated together with PMUs in a more powerful system-wide voltage stability monitoring scheme. Unfortunately, the potential for VIP application at e.g. the tie-line between Eastern Denmark and Sweden is limited, because of the changing direction of power flow (import/export) between the interconnected power systems.

2.3.1.1 System Protection Schemes in Eastern Denmark

The motivation for use of system protection in Eastern Denmark is to improve the transfer capacity in the transmission grid without jeopardising the security of supply. The present system protection schemes in Eastern Denmark are based on automatic process of remote signal monitoring from one spot in the electricity system to another. When a contingency occurs in the electricity system, system protection can be activated by intervening somewhere else in the system [16]. Different system protection schemes can be applied according to the operating situation. The following section illustrates major features and field experiences of installed SPS in the transmission network of Eastern Denmark.

Scheme 1: **HVDC emergency control**

The trading capacity between Eastern Denmark and Sweden is strongly dependent on the transfer capacity in the Swedish transmission grid. The transmission capacity in the Swedish transmission system can be increased by using a System Protection Scheme that will benefit the trading capacity between Eastern Denmark and Sweden. The activation of emergency control of the HVDC interconnection to Germany (Kontek) is highly dependent on the operating situation and the configuration of the interconnected system. In case of **large imports** from Sweden to Eastern Denmark, the trading capacity is often determined by the transfer capacity in the southbound direction via the transmission grid in Southern Sweden. When the voltage level in Southern Sweden is too low, the system protection will be activated to reduce the power flow on the Kontek HVDC link[12]. The lowered southward flow from Sweden to Eastern Denmark will lead to an almost instantaneous increase in voltage (due to the reduced voltage drop). The system protection scheme makes it possible to utilize better the capacity in the South Swedish system by exporting 500 MW[13], of which some 170 MW benefit the trading capacity from Sweden to Eastern Denmark. A precondition is that a number of operating conditions have been met, i.e. most importantly: Barsebäck unit 2 is in operation, consumption in Southern Sweden is less than 4500 MW, and the bottleneck is in the South Swedish transmission grid and not in the northern part of the Swedish transmission system.

In case of **large exports** from Eastern Denmark to Sweden, the trading capacity is often determined by the transmission capacity in the northbound direction via the transmission grid

[12] In the same time the generation from local power plants in Eastern Denmark is increased.

[13] This was otherwise reserved for contingencies.

along the Swedish west coast, "West Coast Corridor". System protection will be activated at two generating facilities in Eastern Denmark if one of the connections in the Swedish transmission grid near Gothenburg trips. The capacity at the generating facilities will then be reduced almost instantaneously by full or partial disconnection of the facilities. Alternatively, the signal from Sweden can be used for almost instantaneous reduction to zero import from Germany to Eastern Denmark via the Kontek HVDC Link. However, this latter function requires manual switching activation at a substation in Sweden. A similar system protection scheme has been established on the Kontiscan 2 interconnection between Sweden and Western Denmark. These system protection schemes contribute to increased trading capacity in the West Swedish system. This normally means that Eastern Denmark gets 1700 MW for export to Sweden (full trading capacity) provided that a number of operating conditions are fulfilled.

Scheme 2: **Generation control**

The System Protection Scheme for the power plants of Asnæs and Avedøre in Eastern Denmark will be activated, if one of the 400 kV interconnections across Øresund trips in case of an extremely stressed power system. The generation control is designed as ordered reduction of active power (fast valving) at the affected generation unit. I.e. at Avedøre power plant the active power reduction is either done by tripping of a gas turbine or by decreasing the output from the steam turbine.

Scheme 3: **Underfrequency load shedding**

The underfrequency load shedding scheme in the Eastern Danish power system consists of the following elements: load shedding (at 10 kV substations), tripping of 50 kV capacitor banks and automatic power system separation (at 132 kV and 400 kV level). The underfrequency load shedding is performed in accordance to the Nordic regulations for acceptable frequency deviations.

2.4 Voltage stability analysis in power systems

2.4.1 Introduction to voltage stability in power systems

"*Voltage stability* is defined as the ability of a power system to maintain acceptable voltages at all system buses under normal operation and after being subjected to a severe disturbance" [41].

Voltage instability is manifested in progressive and uncontrollable drops in voltage after a power system disturbance, e.g. increase in load demand, outage of equipment (generation unit, transmission line, transformer etc.) and/or weakening of voltage control. The main cause for voltage instability is the inability of a power system to meet the reactive power demand in a heavily stressed system. Problems with voltage stability occur typically in power systems with large electrical distance between generation and load centres. As a matter of fact, voltage instability is a local phenomenon, but its consequences can have a wide-spread impact on the entire power system. Voltage collapse is the catastrophic result of a sequence of events suddenly leading to an unacceptable low voltage profile in a significant part of the system.

In general, voltage stability is related to the ability of the power system to maintain steady acceptable voltage and reactive power balance. In reference [42], voltage stability is referred to as "load stability". Voltage instability problems are typically related to "ordinary" loads in power systems that are not able to meet the reactive power demand in case of heavy system loading and system faults. The essence of the voltage stability problem is the voltage drop

across inductive reactance(s) associated with active and reactive flow in transmission network. The reactive characteristics of AC transmission lines, transformers and loads restrict the maximum power transfers in the system. Generation plants are often placed far away from load centres, and increasing an amount of electricity is being imported (exported) in the power system. The central issue is power system impact on large disturbances such as loss of main transmission lines (mainly between load and generation centres), loss of crucial generation (mainly generator units supporting the voltage in the vicinity of loads).

The power system lacks the capability of transferring reactive power over long distances or through high reactances due to the requirement of a large amount of reactive power when a critical value of distance/power is exceeded. Transfer of reactive power over long distances is connected to extremely high reactive losses (due to high voltage gradients). The intention is, thus, to provide and consume reactive power for voltage control in a local area.

In the present work, the voltage stability problems seem mainly to be connected to the characteristics of the wind turbine (induction) generators rather than the ordinary loads in the system. On the other hand, generation can be viewed as a complex load with a negative sign contrary to "ordinary" loads representing power consumption. Using this assumption, the voltage stability definition can be extended to encounter both induction motors and generators. The main principles for voltage stability are theoretically illustrated using a simple network with wind power injection [34].

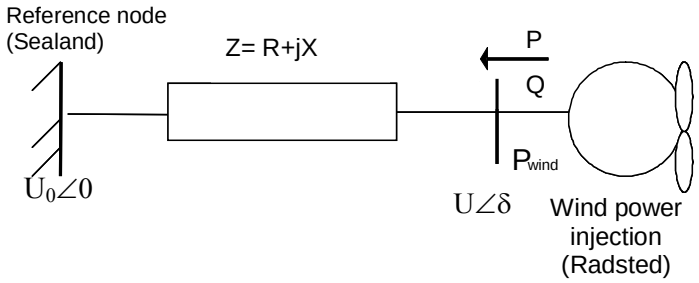

Fig. 9 Simple equivalent network with wind generation

The network equivalent shown at Fig. 9 shows a wind turbine (without any load or shunt elements installed) against a reference bus (stiff network with constant voltage). The complex voltage at the sending $\overline{U}$ end is dependent on the wind power injected in the bus ($S=P+jQ$) and the network short circuit impedance Z. The difference in voltage between the reference node (U_0) and the wind turbine terminal (U) in the simple network can be calculated as:

$$\Delta U = U - U_0 = Z \cdot I = (R + jX) \cdot \left(\frac{P + jQ}{U} \right)^* \tag{4}$$

$$\Delta U = \frac{P \cdot R + Q \cdot X}{U} + j \frac{(P \cdot X - Q \cdot R)}{U} \tag{5}$$

It is assumed that U_0 is real and U is a complex quantity:

$$\overline{U_0} = U_0 = const.$$
$$\overline{U} = U \cos\delta + jU \sin\delta = U_R + jU_I$$

The complex expression for the voltage at the sending end is:

$$U = U_0 + Z \cdot I = U_0 + Z \cdot \left(\frac{S}{U}\right)^* \tag{6}$$

The relation for the sending voltage is further derived as:

$$\begin{aligned} U \cdot U^* &= U_0 \cdot U^* + Z \cdot S^* \\ (U_R + jU_I)(U_R - jU_I) &= U_0(U_R + jU_I) + (H_R + jH_I) \\ U_R^2 + U_I^2 &= U_0 U_R + H_R + j(H_I + U_0 U_I) \end{aligned} \tag{7}$$

The imaginary part of the above equation is isolated yielding to:

$$0 = H_I + U_0 \cdot U_I \quad \rightarrow U_I = -\frac{H_I}{U_0} \tag{8}$$

The achieved value for U_I is inserted in the last expression:

$$\begin{aligned} U_R^2 + \left(\frac{H_I}{U_0}\right)^2 &= U_0 U_R + H_R \\ U_R^2 - U_0 U_R + \left(\frac{H_I}{U_0}\right)^2 - H_R &= 0 \end{aligned} \tag{9}$$

The real part of the sending end voltage is calculated assuming U_0=1.p.u.

$$\begin{aligned} U_R &= \frac{1}{2}\left[U_0 \pm \sqrt{U_0^2 - 4\left(\frac{H_I^2}{U_0^2} - H_R\right)}\right] \\ U_R &= \frac{1}{2} \pm \sqrt{\frac{1}{4} - (H_I^2 - H_R)} \quad for\ U_0 = 1 p.u. \end{aligned} \tag{10}$$

The complex value of the sending end voltage becomes:

$$U = U_R + jU_I = \frac{1}{2} \pm \sqrt{\frac{1}{4} - \left(H_I^2 - H_R\right)} + jH_I \tag{11}$$

The possible mathematical solution of U is given by:

$(H_R - H_I^2) > -1/4$ No physical solution

$\left(H_R - H_I^2\right) = -1/4$ The collapse point is reached

$\left(H_R - H_I^2\right) < -1/4$ Double solution (stable and unstable)

The solutions of the equation (11) can be presented as a characteristic P-U curve that illustrates the relation between the voltage (U) at sending bus and the wind power transferred in the simple system. The set of stable solutions are placed at the upper part of the P-U curve and the unstable solutions are at the lower part of the curve. The tip of the P-U curve determines the maximum power transfer to the receiving bus. This is very interesting as a critical point, where the stationary voltage stability limit is achieved [33].

$$U = \frac{1}{2} \pm \sqrt{\frac{1}{4} - (PX - QR)^2} + j(PX - QR) \tag{12}$$

The following factors influence the voltage stability in the power system of Eastern Denmark:

1) Transmission system
    a) System short circuit capacity
    b) Special concern for long distance between generation and wind power penetration
2) Lack of reactive power support[14]
3) High power transfers
4) Wind turbines based on induction machine
5) Load characteristics
6) Voltage control devices
7) Underload tap-changers (OLTC)
8) Generator reactive power capability

The system characteristics voltage vs. wind power generation is plotted in Fig. 10 for a realistic case in Eastern Denmark [23]. The wind generation is increased linearly (from nominal production) until the voltage collapse occurs at the tip of the curve. The upper part of the P-U curve is related to stable power system operation.

[14] Insufficient reactive power from generators (fast reserve) and capacitors (slower reserve)

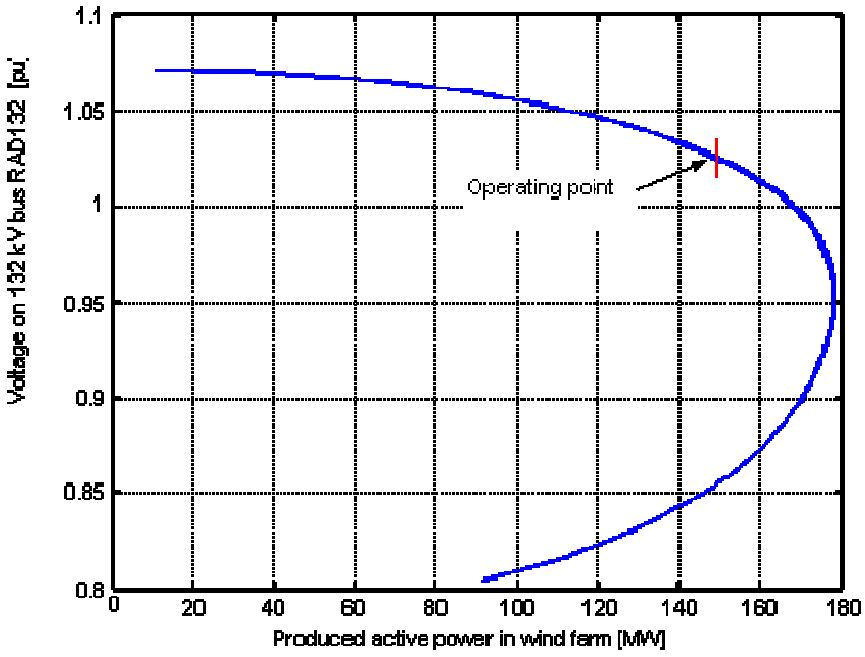

Fig. 10 *Voltage vs. wind power characteristics [23]*

According to the time frame of load restoration, voltage stability can be classified in short-term and long-term stability. Fig. 11 considers a number of factors that have impact on short- and long-term voltage stability with different duration time on the time scale.

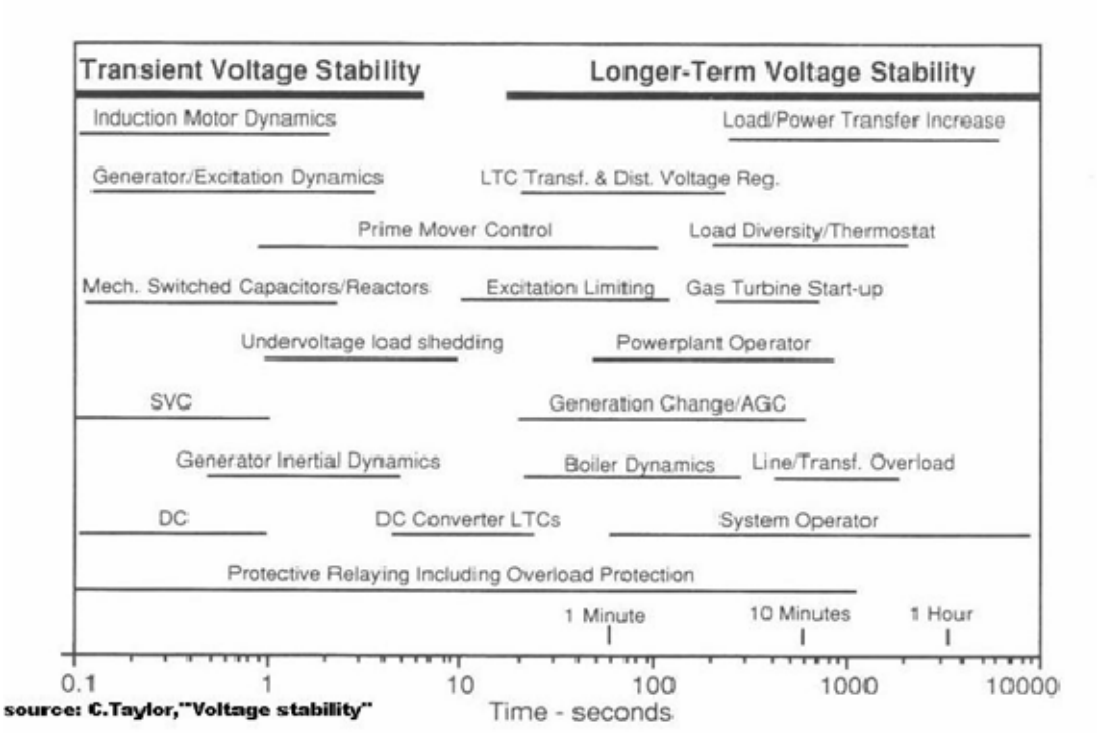

Fig. 11 *Classification of voltage stability phenomena in time-domain [42]*

I.e. induction machines restore their load within a second (short-term), while thermostatically controlled loads and loads fed via OLTC (on-load tap changers) restore over the time of one

to several minutes (long-term). The long-term scale is also characteristic for field current limiters, which protect generators from thermal stress by removing the voltage support.

The short-term voltage stability is particularly important in power systems with large-scale wind power integration, since the majority of wind turbines in Eastern Denmark are based on induction generators. The power output of such wind turbine generators varies significantly within a timeframe of tens of seconds reflecting the incoming speed variations at the wind turbine or the wind turbine response to severe faults in the transmission network.

The following section approaches methods and tools for voltage stability analysis and evaluates their applicability for the investigations in the Eastern Danish power system.

2.4.2 Stationary voltage stability analysis

2.4.2.1 Theory about Q-U stability curves

Since voltage stability is closely related to reactive (rather than active) power it would be appropriate to depict Q-U curves (together with P-U curves) for the power system of interest.

In a simple radial system (Fig. 5) with a single load, Q-U curves can be generated as voltage at a critical bus vs. reactive power in the same bus, where a fictitious synchronous condenser injects reactive power to maintain a certain voltage [42]. Series of power flow computer simulations can be used to obtain the Q-U curves at the critical bus, represented as a generation (PV) bus without reactive power limits. The steeper the Q-U curve is, the more reactive power is required to raise the voltage at the busbar.

In addition to the Q-U curve for the system, a Q-U curve for a capacitor (with reactive power rating corresponding to the system consumption at 1 p.u. voltage) can be generated. If the steepness (dQ/dU) for the system is higher than for the capacitor, the system will consume less reactive power than the capacitor delivers for voltages below 1 p.u. and vice versa.

Another method is considered more suitable for the large-scale simulations. The Q-U curves can namely be mapped from the corresponding P -U curves as follows: for each value of P the values of U and Q (two pairs) are replotted. A power system at a given operating condition is voltage stable if every system bus experiences increase in voltage magnitude as the reactive power injection at the same bus is increased. On the other hand, a system is voltage unstable if at least one bus in the system is associated with voltage magnitude decrease, while the reactive power injection in the same bus is increased.

- Stable situation: positive U-Q sensitivity $(\Delta U/\Delta Q)>0$ for every system bus;
- Unstable situation: negative U-Q sensitivity $(\Delta U/\Delta Q)<0$ is valid for at least one bus;
- Voltage stability limit reached: zero sensitivity $(\Delta U/\Delta Q) =0$, bottom of the U- Q curve.

This method is applied in the project investigations rather than conventional Q-U curves, because the transfer of active power changes direction (e.g. between the main 132 kV system and the southern part of the system) and can not be isolated from the injection of Q from/ to the southern part of the 132 kV system.

2.4.2.2 Q-U sensitivity analysis

In this section, the basic equations of sensitivity analysis for voltage stability evaluation [41] are derived and explained. Because the branch impedances in high-voltage systems are predominantly reactive, voltage magnitudes depend primarily on reactive power injections in the system and the voltage angles on active power injections. For analysing the voltage controllability of a power system, voltage variations (∂U) due to small variations in reactive power injections (∂Q) are examined.

Linearizing the load flow equations around the actual operating point leads to the following set of equations:

$$\begin{bmatrix} J_{P\theta} & J_{PU} \\ J_{Q\theta} & J_{QU} \end{bmatrix} \begin{bmatrix} \partial\theta \\ \partial U \end{bmatrix} = \begin{bmatrix} \partial P \\ \partial Q \end{bmatrix} \tag{13}$$

The matrix equation (13) shows that sensitivities of the type $\partial U/\partial Q$ can directly be calculated from the load flow Jacobian matrix $\begin{bmatrix} J_{P\theta} & J_{PU} \\ J_{Q\theta} & J_{QU} \end{bmatrix}$. By setting dP=0 in the previous equation the vector of voltage angles can be eliminated.

$$\partial\theta = -\left(J_{P\theta}\right)^{-1} J_{PU}\,\partial U \tag{14}$$

$$\underbrace{\left(-J_{Q\theta}J_{P\theta}^{-1}J_{PU}+J_{Qv}\right)}_{\tilde{J}_{QU}}\partial U = \partial Q \tag{15}$$

The inverse of the matrix $\tilde{J}_{Qv}$ is equivalent to the matrix of sensitivities $\partial U/\partial Q$.

$$\partial U = \tilde{J}_{QU}^{-1} \cdot \partial Q = S_{UQ}\partial Q \tag{16}$$

The variation of the voltage magnitude at each bus can hence be described as a linear combination of reactive power variations:

$$\partial U_i = S_{i1}\partial Q_1 + ... + S_{ii}\partial Q_i + ... + S_{in}\partial Q_n \tag{17}$$

where the diagonal elements S_{ii} from the S matrix describe the voltage variation at bus *i* due to variation of reactive power in the same bus and the diagonal element S_{ij} describes the voltage variation at bus *i* due to reactive power variation at another bus in the system. Hence, a high sensitivity $\partial U/\partial Q$ at a load bus explains that even a small increase of reactive power leads to high-voltage gradients, which cause significant decrease in the bus voltage. When the limit of voltage stability is approached, the sensitivity $\partial U/\partial Q$ increases drastically. High-voltage sensitivities indicate therefore weak areas in the network. This main idea behind the method is applied to interpret simulation results based on voltage vs. reactive power curves for the large-scale model of Eastern Denmark.

2.4.2.3 Simulation tool

The PTI Power System Simulator© (PSS/E) is a commercial program applied for computer analysis of the large-scale power system of Eastern Denmark. The program is utilized at many Transmission System Operators as well as other utilities world-wide. The PTI Power System Simulator (PSS/E) is a package of programs for studies of power system transmission network and generation performance in both steady-state and dynamic conditions. PSS/E handles load flow, fault analysis (balanced and unbalanced), network equivalent construction and dynamic simulation. The PSS/E load flow calculation is the common tool for simulation of balanced power systems. The objective of the load flow calculation is described in the following statement: "Given the load consumption at all buses of the power system and the generator power production at each power plant, find the power flow in each line and transformer in the network."

In steady-state operation, the power system must operate without overloading transmission lines or transformers, stay within acceptable voltage limits at all buses, and maintain generator reactive power outputs between acceptable limits. Dynamic simulation of the power system behaviour in case of contingencies is relevant for time-domain studies.

PSS/E is evaluated as a valuable tool for voltage stability analysis. Besides, the data for the Eastern Danish power system are easily accessed in PSS/E. The PSS/E program is used in load flow and dynamic simulation studies of a large-scale power system model of Eastern Denmark.

2.4.2.4 Continuation power-flow analysis

The advantage of the Continuation Power Flow method is that it can generate P-U and Q-U curves beyond the maximum loadability point without any divergence problems. The continuation Power Flow method and tools for voltage stability analysis are evaluated in reference [53]. The free-share research tool UWPflow[15] is a continuation power flow program tailored for IEEE or WSCE/BPA/EPRI input formats [54]. The program calculates local bifurcations related to system stability limits and non-singularities in the system Jacobian. This program can not be used for commercial applications, and it presupposes that it is possible to convert the PTI input data for the large-scale model used in the PSS/E simulation program.

[15] Developed by Canizarez C.A. (University of Waterloo, Ontario, Canada) and Alvarado F.A.(University of Wisconsin-Madison, USA)

3 Models

3.1 Power system model

The large-scale simulation model of the power system in Eastern Denmark comprises 700 buses at transmission and distribution level, from which 200 buses are associated with the 400 kV and 132 kV transmission system. The transmission system in Eastern Denmark encompasses overhead lines and cables at 132 kV and 400 kV level, as well as interconnections to Sweden and Germany. The tie-line to Sweden consists of two 400 kV cables and two 132 kV cables, which serve as AC interconnection to the Nordic system. Fig. 12 shows the 400 kV[16] and 132 kV[17] transmission system together with the interconnection to Sweden and the southern 400 kV DC link to Germany[18]. The maximum load in Eastern Denmark is about 2870 MW, and the total installed capacity is 4360 MW. The power system incorporates wind power capacity of approx. 600 MW, which is connected on-land to local distribution networks, either as single installations or as few wind turbines in clusters. Additionally, the off-shore wind farm Nysted in southern Lolland is AC-connected to the southern part of the 132 kV transmission system. The Nysted offshore wind farm has 72 active stall wind turbines with maximum installed power of 2.3 MW each.

Installed capacity	Generation units in total (central plants)	4360 MW
Embedded generation	Wind power units	700 MW
	(incl. Nysted Wind Farm 1)	
	Cogeneration units	500 MW
Transmission capacity of interconnections	Sweden (400 & 132 kV lines)	1900 MW
	Germany (HVDC link Kontek)	600 MW
Load	Maximum system load	2870 MW
Reserve	Slow reserve units:	300 MW
	Operational reserve:	625 MW
	Frequency regulating reserve:	65 MW
	Spinning disturbance reserve	60 MW
	Fast reserve units	300 MW

Table 2 Key numbers for the power system of Eastern Denmark [17]

During the last fifteen years, the amount of wind production has increased rapidly. The amount of wind power took a further step upwards when a 150 MW offshore wind farm at Nysted was commissioned in the autumn 2003. This wind farm together with majority of the existing wind turbines is placed in the sparsely populated areas, where the transmission system is significantly weak. The wind generation is intended to displace some production from conventional power plants in the power system. The wind turbines on-land are connected to

[16] Red lines
[17] Black lines
[18] Blue line

the distribution system either to supply the consumption in the local area (positive direction of power flowing from wind turbines to loads) or to inject power in the main transmission system (negative direction of power flowing from wind turbines upwards in the main system). Thus the power flow can vary between positive and negative values, all dependent upon the size of the wind turbine units, their location in the system and the seasonal load demand in the same area.

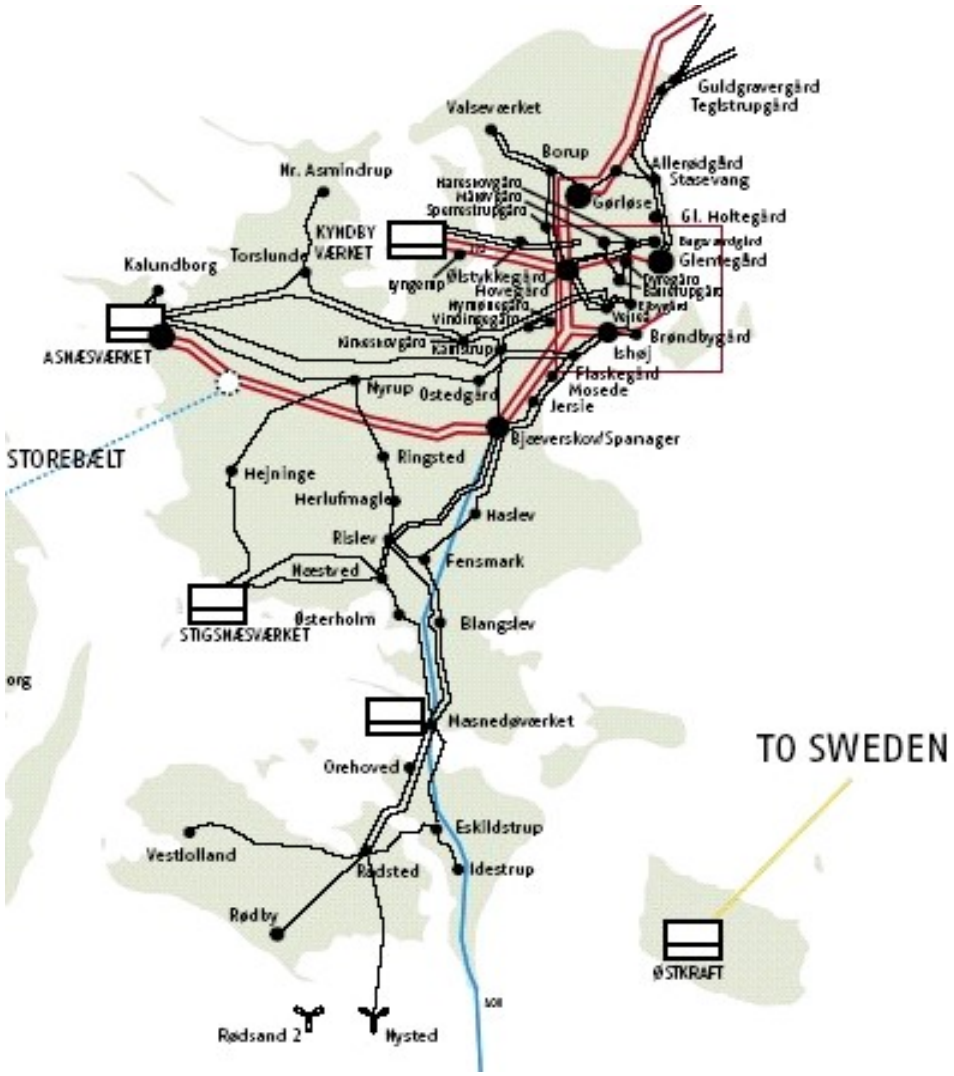

Fig. 12 The 400-kV and 132-kV transmission system in Eastern Denmark

For voltage stability studies, it is crucial to establish an appropriate system model and component models for wind turbines, load models, voltage control devices etc.

3.2 Load model

For simplicity, the constant power load model is used in all simulation studies in the Ph.D. project. In case of constant load, the maximum loadability limit and the voltage collapse point coincide with the tip of the Power-Voltage stability curve used as system characteristic. This is not the case if the load characteristic is modelled in the stability studies. The accurate modelling of loads is essential in voltage stability analysis. For future static analysis of voltage stability, it is important especially to account for the voltage dependence of loads. The voltage dependence is usually modelled using an exponential or a polynominal model. The impact of

load models to the power system voltage stability is documented in a large number of references [41], [42], [47], [51] and [52].

The dynamic behaviour of loads in long-term voltage stability studies includes the operation of on-load tap changers (OLTC), thermostatic loads, operation of compensation devices in the distribution network etc. Dynamic load models can be based on field measurements [51]. This approach requires time-consuming measurements of load and voltage at different substations during different seasons, weather conditions, days of the week, time of the day etc. In practice, the voltage dependence of loads can be estimated using component-based approach [47], which represents different combinations of load classes (industrial, residential, commercial, agricultural etc.).

3.3 Generation models

Synchronous generators are the primary source for voltage and reactive power control in power systems. In general for voltage stability studies, active (P) and reactive power (Q) generator capability need to be considered in order to achieve accurate results [43]. The limiting P and Q of generator power capability are commonly depicted in P-Q diagrams. In the simulation studies the generator P-Q diagrams were not included in the analysis due to lack of accurate generator data.

The active power limit of a generating unit is constant, because it is determined by the design of the turbine and the boiler. The reactive power limit of a generator has circular form. Representation of the voltage dependence of generator reactive power limit is important in analysis of the generator impact to voltage stability. The reactive power limitation is caused by the generator stator currents as well as its field current (over-excitation and under-excitation limits). Here it is relevant to mention that fast increase in generator voltages can be used as remedial action in System Protection Schemes. This control action uses set point change in the Automatic Voltage Regulators (AVR), which are able to increase their reactive power output until they reach their heating limit. Automatic Voltage Regulators are independent of the system voltage and can efficiently raise the low voltage the system buses.

The reactive power support from the large generators does not have a high priority in the present project, because the area of reactive power deficit (southern part of the 132 kV systems) is not located near significant generation units.

3.4 Dynamic wind turbine model

3.4.1 Introduction on wind turbine technology

The wind system model shown in Fig. 13 consists of a wind characteristic describing the variation in the incoming wind speed, and a wind turbine model which consists of a mechanical and an electrical part. The mechanical part includes an aerodynamic rotor and a mechanical transmission system. A typical electrical system consists of a generator, which is connected to a power grid via a step-up transformer. The generator is normally equipped with a reactive power compensation unit.

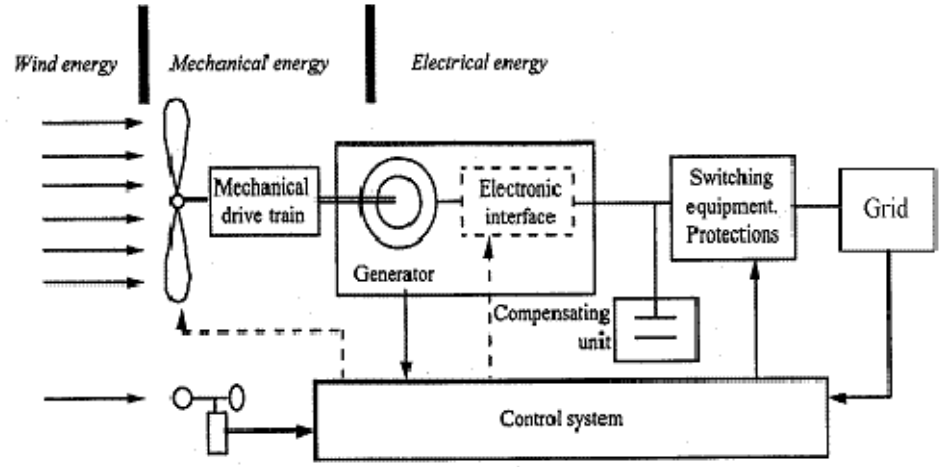

CIGRE TF38.01.10 "Modeling New Forms of Generation and Storage, fifth draft, June 2000

Fig. 13 Concept for wind generation in wind turbines based on induction generator

The wind energy arriving at the rotor blades of the wind turbine is transformed to a rotational torque T_m at the mechanical drive train. The mechanical power P_m arising at the wind turbine shaft is determined by the following expression [40]:

$$P_m = \omega_r T_m = \frac{1}{2} C_p(\lambda) A \rho v^3 = \frac{1}{2} C_p(\lambda) \cdot \left(r^2 \pi\right) \rho \left(\frac{\omega_r r}{\lambda}\right)^3$$

$$P_m = \frac{1}{2} \frac{C_p(\lambda) \cdot \pi \rho r^5 \omega_r^3}{\lambda^3} \tag{18}$$

where $\boldsymbol{\rho}$ is the air density (kg/m^3), $\boldsymbol{r}$ is the rotor radius (m), $A=r^2\pi$ is the affected rotational area (m^2), $\boldsymbol{\omega_r}$ is the rotational speed (rad/s) of the rotor and $\boldsymbol{C_p}$ is aerodynamic power coefficient.

In general, the power coefficient $C_p(\lambda)$ is a function of the tip speed ratio $\boldsymbol{\lambda}$, which is defined as a function between blade tip speed and the wind speed as follows:

$$\lambda = \frac{\omega_r \cdot r}{v} \tag{19}$$

The mechanical torque at the generator shaft is thus:

$$T_m = \frac{P_m}{\omega_r} = \frac{1}{2} \frac{C_p(\lambda) \cdot \pi \rho r^5 \omega_r^2}{\lambda^3} \tag{20}$$

Different wind turbine concepts

Each wind turbine is capable to control the mechanical power either by stall control (fixed blade position, where stall of the wind appears along the blade at higher wind speed), active stall (the blade angle is adjusted to create stall along the blades) or pitch control (the blades are turned out of the wind at higher wind speed) [39]. The fixed speed wind turbine is typi-

cally associated with stall control. The wind turbine stalls when it loses the possibility to obtain energy from the wind due to increasing wind speed.

The variable speed wind turbine is usually equipped with pitch control, where the blades can be turned to increase or decrease lift forces on the blade profile and thereby continuously control energy absorption from the wind. The active pitch control is designed to optimize the power obtained from the wind by changing the rotational speed of the rotor and the pitch angle and thus gain an optimum current flow around the blades.

In variable speed machines, the generator is connected to the grid via a power converter, or a generator field is fed by a power converter. Then the rotational speed of the generator rotor is decoupled from the frequency of the grid, and the rotor speed can be adjusted to the wind speed by an appropriate control.

The wind turbines are commonly classified in two major categories of "fixed speed turbines" and "variable speed turbines". A thorough discussion of a these concepts can be found in references [20], [38]. In fixed-speed machines, the generator is directly connected to the AC grid whose frequency, along with the number of the machine's poles, determines the rotational speed of the generator rotor. The wind turbine voltage and reactive power consumption vary as the generated real power output varies. Thus power factor capacitors or other reactive compensation is employed in the wind system. The different wind turbine concepts are summarized in Fig 14.

Concept 1 a) Fixed-speed wind turbines equipped with induction generators directly connected to the grid is one of the oldest and simplest concepts which was first used in Denmark, and therefore known as the "Danish concept". The turbine is connected to an induction generator through a gearbox. The speed of the generator may differ from the power system frequency due to the slip variation of the generator, which typically is up to 1%.

Variable speed turbines with induction or synchronous generator, directly or indirectly connected to the power system (concepts b) – f)) have become more important in recent years. The more efficient energy production, due to intelligent control strategies, and the possibility to independently control the speed decoupled from the grid, make these concepts a beneficial economic solution. Furthermore, these types are better grid compliant compared to the fixed speed turbines. The converter integrated in variable-speed wind turbines gives the possibility to actively control the power output of the wind turbine, which is increasingly important for the integration of wind turbines into the network.

Concept b) Induction generator connected to grid network through a step-up transformer and power converter. In this kind of wind turbines, the terminal voltage and/or power factor can be controlled. Reactive power consumption depends on the applied control method.

Concept c) In this concept, the induction generator is equipped with dynamic slip control using slip rings, which actually is a variant between the fixed-speed turbine and a variable-speed turbine. The so-called OptiSlip© wind turbine is based on the concept of speed or torque control while using variable impedance at the rotor of the induction machine. The advantage of the slip control is the possibility to achieve a speed variation of 10%.

Concept d) and e) The synchronous machine can not be directly coupled to the power system. To enable an efficient power production at a huge range of different wind speeds, it is neces-

sary to decouple the mechanical speed from the power system frequencies. This is done by using a full-scale power converter between the generator and the power system.

Concept f) The doubly fed induction generator (DFIG) is a variable-speed wind turbine using a back-to-back voltage source converter. The wind turbine is able to perform speed and pitch angle control as well as full real and reactive power control. The terminal voltage and generator power factor can be regulated using reactive power variation. Wind turbines equipped with DFIG have become more and more common during the last years, because they combine the advantages of pitch control with an efficient transmission of the power to the grid and the possibility of dynamic control of active and reactive power.

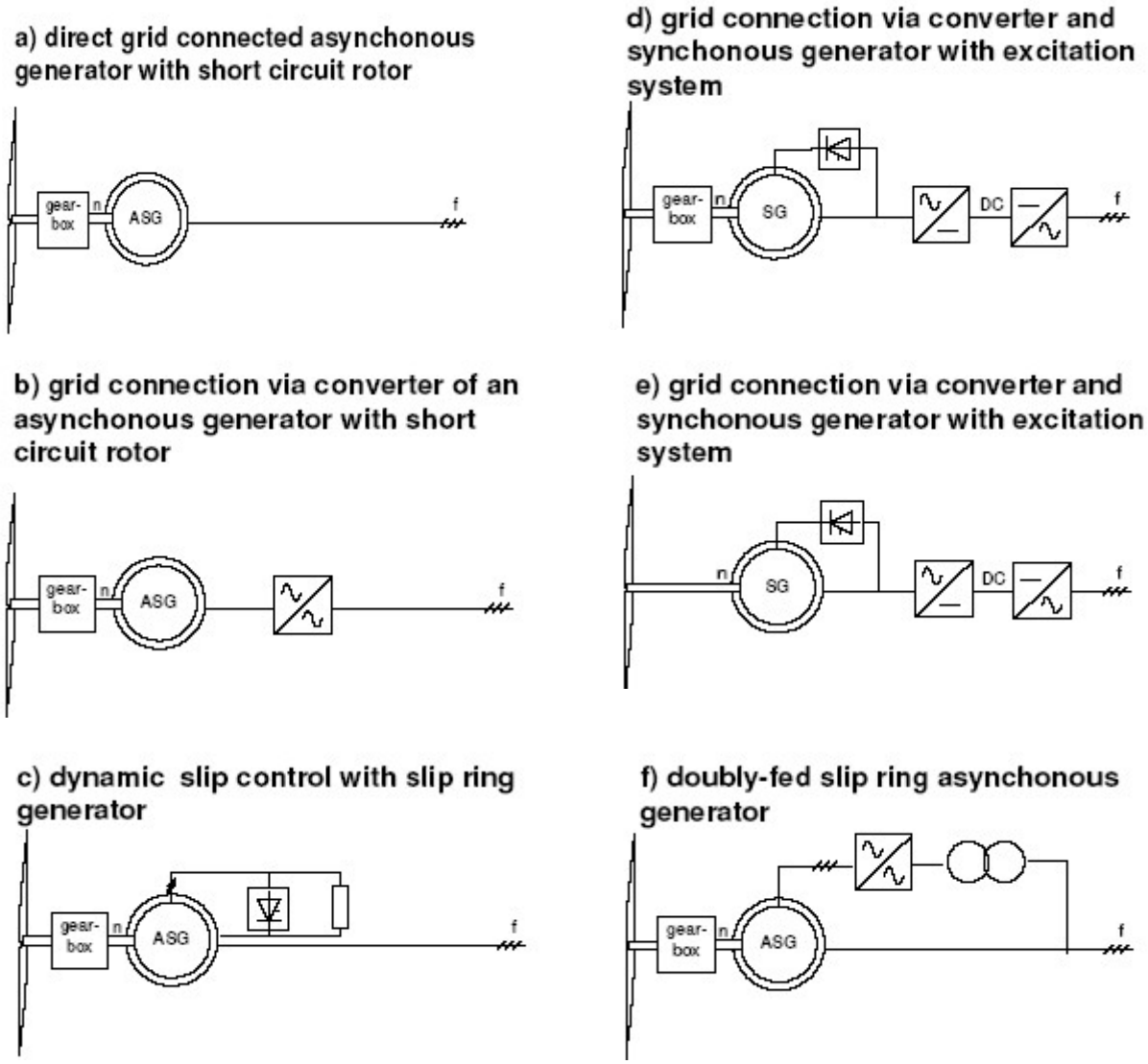

Fig. 14 Overview of wind turbine concepts

3.4.2 Dynamic wind turbine model in PSS/E

A dynamic model for passive stall wind turbines was developed in the PSS/E program[19]. It consists of a mechanical module [21] that incorporates the incoming wind speed characteristics with the mechanical representation of the wind turbine, and a standard induction generator model in PSS/E. The dynamic wind turbine model in PSS/E can be applied to investigate performance of single wind turbines as well as equivalent wind farms (aggregated model) in a power system. Wind farms are modelled as a large, single wind turbine equivalent that clusters a number of individual turbines. The wind farm representation assumes that the power fluctuations from all wind turbines coincide. The dynamical model of a single wind turbine describes the main features of the mechanical and the electrical part of the wind turbine system. A detailed model of a mechanical drive train takes into account the turbine shaft and gearbox. Fig. 15 shows a schematic diagram of the mechanical part of the model. The mechanical output P_{MECH} is introduced at the generator shaft as an active power interface to the existing induction generator model (CIMTR3) in PSS/E.

3.4.3 Mechanical system modelling

The mechanical part of the two-mass model describes the aerodynamic rotor of the wind turbine and a mechanical drive train represented by a shaft system with a low-speed and high-speed shafts coupled by a gearbox. The wind energy arriving at the rotor blades of a single fixed-speed passive stall wind turbine is transformed to a rotational torque T_{TURB} at the mechanical drive train. The mechanical output P_{MECH} from the wind turbine is introduced as input to the 3rd order induction generator model (CIMTR3) in the PSS/E program.

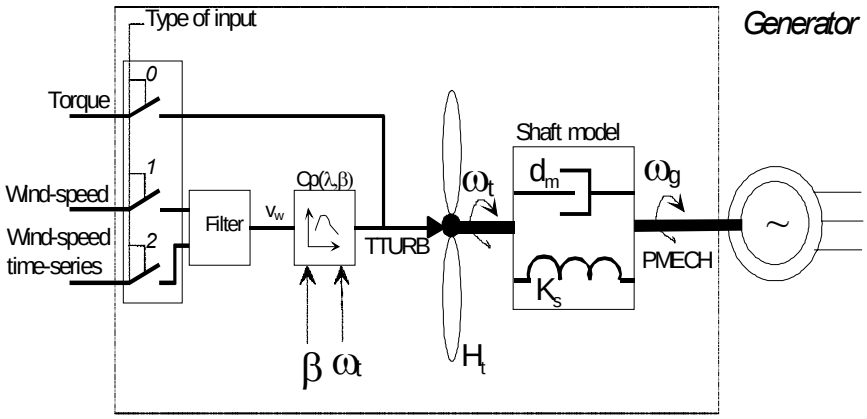

Fig. 15 Dynamic wind turbine model in PSS/E©

As illustrated in Fig. 15, the model may be initiated either by using fixed-torque input or variable wind speed / wind speed time series that introduce fluctuations in the wind power output. The following input options are available in the model initiation:

0) constant wind speed i.e. constant turbine torque (TTURB) as direct input
1) wind speed with variance
2) wind speed series (from actual recordings)

[19] Power System Simulator for Engineering® from Power Technologies, Inc. (PTI).

The fixed-torque mode is a suitable input for short-term transient analysis as well as for voltage stability analysis [22]. In this mode, the constant turbine torque T_{TURB} corresponds to the mechanical power needed to produce electrical power specified from the load flow calculation. The wind turbine model enables representation of wind farms as a single large aggregated wind turbine, assuming that the wind speed fluctuations in each turbine are uncorrelated [25]. The model represents the mechanical system of wind turbine(s) with sufficient degree of detail and has a direct interface to a 3.order induction generator model[20] (CIMTR3) in PSS/E. The wind turbine model was verified using three input options: constant mechanical torque, constant wind speed and measured wind speed series.

3.4.4 Induction generator modelling

The PSS/E model of a squirrel cage induction generator (CIMTR3) represents the generator internal voltage E´ behind a transient reactance X´$_s$. The induction machine equivalent [41] is determined as follows:

$$\frac{dE'}{dt} = -\frac{1}{T'} \cdot \left[E' + j\left(X_s - X'_s\right)I\right] + j \cdot s\omega_0 E' \qquad (21)$$

In equation (21) X_s is stator reactance, X'_s is transient stator reactance, I is stator current and the slip s is denoted from the generator speed ω_G (rad/s) and synchronous speed ω_0 (rad/s) as $s=(\omega_G - \omega_0)/\omega_0$. The rotor transient time constant T'(s) characterizes the decay of the rotor transients when the stator is open-circuited. The terminal voltage at the wind turbine generator E´ is determined by the load flow initial conditions of the grid. Besides the network impedances, the generator terminal voltage is strongly dependent on induction machine parameters such as slip s as well as active power production and reactive power consumption [30]. An iterative calculation of initial conditions for the dynamic wind turbine model was performed in PSS/E in order to initialize correctly the reactive power consumption at wind turbines. In PSS/E small and medium wind turbines (P<0.66 MW) are modelled with no-load compensation, while large wind turbines (P>0.66 MW) are simulated with full-load reactive power compensation.

3.4.5 Wind turbine protection model

The on-land wind turbines are protected by relays, whose settings are determined to match the actual network configuration and the wind turbine model used. The relay protection model in PSS/E detected abnormal voltage and frequency and trips the wind turbine unit in case of violated thresholds [35]. Wind turbine relays are included in the simulations (see Appendix data) in order to trip wind turbines affected by a severe fault in the power system. They are designed on one hand to protect the power system against internal faults in the wind turbine and on the other hand to protect the wind turbine against power system disturbances. The last task is fulfilled by disconnecting the wind turbine in case of exceeding a speed threshold and/or overcurrent (typically twice the rated current) and/or frequency and voltage at the wind turbine terminals are outside of the permitted interval. If the relay settings (Fig. 16) are violated after corresponding predefined time delays, a circuit breaker is activated to disconnect the wind turbine and its reactive compensation unit from the system. The capacitor shunts for reactive power compensation of the wind turbine are supposed to trip shortly after the wind turbine to avoid resonance and overvoltage problems.

[20] Stator transients are not taken in account

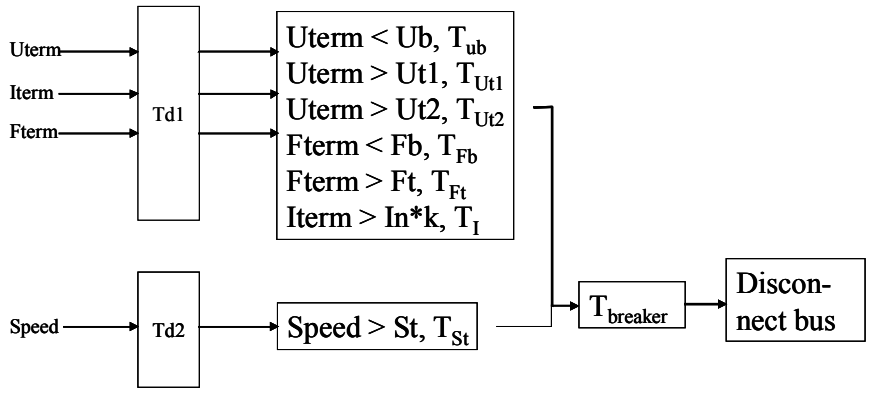

Fig. 16 Relay model for wind turbines

Large off-shore wind farms like Nysted (150 MW capacity) are supposed to withstand the majority of faults and remain in operation [36].

3.5 Dynamic sources for reactive power

A Static VAr Compensator (SVC) is a combination of shunt capacitor and reactor, which is able to control the voltage at a bus. The effect of controlled firing of the SVC thyristors is to control the effective fundamental frequency admittance of the thyristor-reactor unit as seen from its high-voltage terminals.

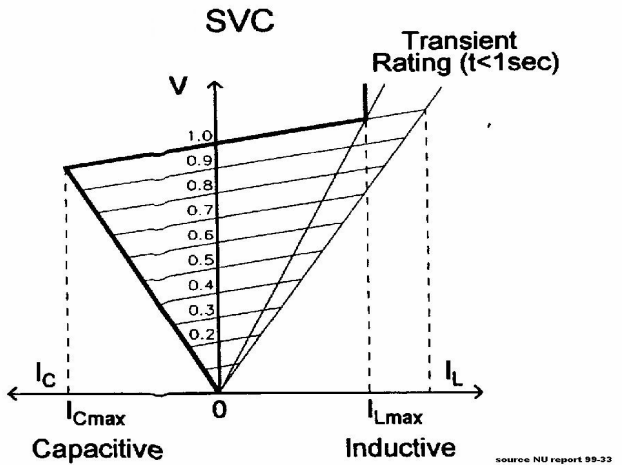

Fig. 17 SVC characteristics

With the reactor is turned off, the SVC installation is a shunt capacitor that will supply reactive power to the system. The reactor may be turned on to absorb reactive power, giving the flat section of the characteristic until it is fully on. Once the reactor is fully on, the characteristic is that of the reactor, which may saturate extensively at high voltages, in parallel with the capacitor. The characteristic shown in Fig. 17 is achieved by turning the reactor on in proportion to bus voltage. Virtually, any static and dynamic characteristic can be obtained within the range offered by the rating of the reactor and capacitor [55].

4 Simulations

The simulations use a large-scale power system model of Eastern Denmark. The 700-bus model includes a number of wind turbines on-land and two off-shore wind farms, i.e. the existing wind farm Nysted 1 and Nysted 2, which is planned in the near future. The main idea of the static analysis in the project is to detect imminent voltage instability in the system and to illustrate the main mechanisms that lead to voltage collapse in Eastern Denmark. The load flow module in the PSS/E program[21] is used to determine reactive power support requirements and transfer capability of wind generation in the power system of interest. The simulated voltage stability limits are used as setting values for design of a System Protection Schemes against voltage collapse.

The static analysis of voltage stability is not sufficient when the dynamic behaviour of wind turbines based on induction generators is to be accounted. The problems with short-term voltage stability of wind turbines require time-domain simulations in PSS/E in order to investigate aspects of wind generation and possible solutions in terms of additional voltage and reactive power support.

4.1 Static simulation analysis

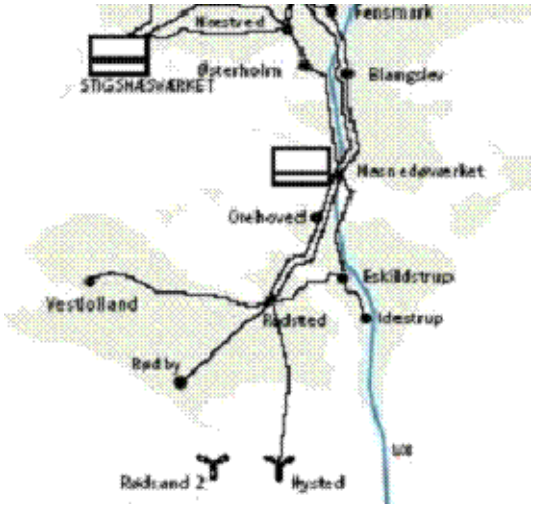

Fig. 18 *The southern part of the132 kV system*

In the project, the voltage stability limits are defined using static stability curves. The total wind power in the system is gradually increased until the maximum transfer is reached near the point of voltage collapse. At this point, there is no real steady-state solution to the load flow problem, and the system Jacobian becomes singular.

This approach is analogous to the method illustrated in Fig. 9, where wind power is injected in a simple radial network with one wind turbine connected to a reference bus. In this case, the set of convergent load flow solutions illustrate the relation between voltage (U) at the sending bus and the power flow (P, Q) transferred in the simple system. The last point plotted at the respective simulation curves is associated with the last convergent load flow solution.

Both (Q-U) and (P-U) stability curves are used to determine the maximum wind power transfer to the receiving bus. In the large-scale power system model, Radsted substation corresponds to the sending bus with wind power injection, while Hovegård substation in Sealand is

[21] Power System Simulator for Electrical Engineering

assumed as a reference bus in the main 132-kV system. Fig. 18 shows the 132 kV tie-line from Radsted to Sealand, which consists of three north-going lines Radsted-Orehoved (RAD-ORH), Radsted-Blangslev (RAD-BLA) and Radsted- Eskildstrup (RAD-ESK). The objective of the stability analysis is to determine the maximum power transfer in the tie-lines connecting Radsted to the main transmission system. The limiting factor here is the active and reactive power flow due to large wind generation in the region around Radsted. The challenge in the power system simulation is that a large number of parameter variations have to be considered in the load flow[22]calculations. The procedure for static simulations shown in Fig. 19 is summarized as follows:

1. Four initial cases are analysed for intact network with particular system loading (100%, 75%, 50% and 35% of total system load) and generation scheduling from power plants[23]. Initially, zero wind generation is assumed. For each particular initial case, the total wind generation is increased in steps. A large number of load flow simulations are run for different operating conditions, where the wind power is increased in steps 0%, 20%, 70% and 100% of total installed wind capacity. The generation at all wind turbines in the system is increased simultaneously.

2. For each operating condition[24], the reactive power balance is tuned in the network adjusting i.e. switched shunts, generator reactive power output and wind turbine reactive compensation. The objective is to obtain acceptable voltages at 132 kV buses within the range $0.95<U<1,05$ p.u.

3. For each system loading, a large number of load flow simulations are performed increasing the wind generation in the system. For each convergent load flow solution (% of wind power and load), the voltage magnitude at 132 kV buses and phase angle difference (between Radsted and Hovegård) as well as active and reactive power flow in relevant 132 kV lines are registered. The relevant pairs of convergent solutions for voltage magnitude U, relative phase angles as well as active and reactive power in the tie-lines ($P_{tie\text{-}line}$, $Q_{tie\text{-}line}$) are plotted until a non-convergent solution is reached. The characteristic stability curves are thus generated for relevant buses in the transmission corridor connecting Radsted to the main 132 kV system.

4. A global picture of the system and its limits with regard to voltage stability is gained. Critical reactive power flows and buses with greatest gradients in voltage are pointed out. The limits for maximum active and reactive power flow in the tie-lines and maximum wind power transfer in the system are determined.

5. One of the 132 kV tie-lines from Radsted to Sealand is disconnected, and the procedure for plotting stability curves and determination of limits is repeated in case of the contingency (e.g. single outage RAD-ORH).

[22] Based on the Newton-Raphson algorithm

[23] In all cases Stigsnæs power plant is not initially operated.

[24] Total load and generation (incl. wind power)

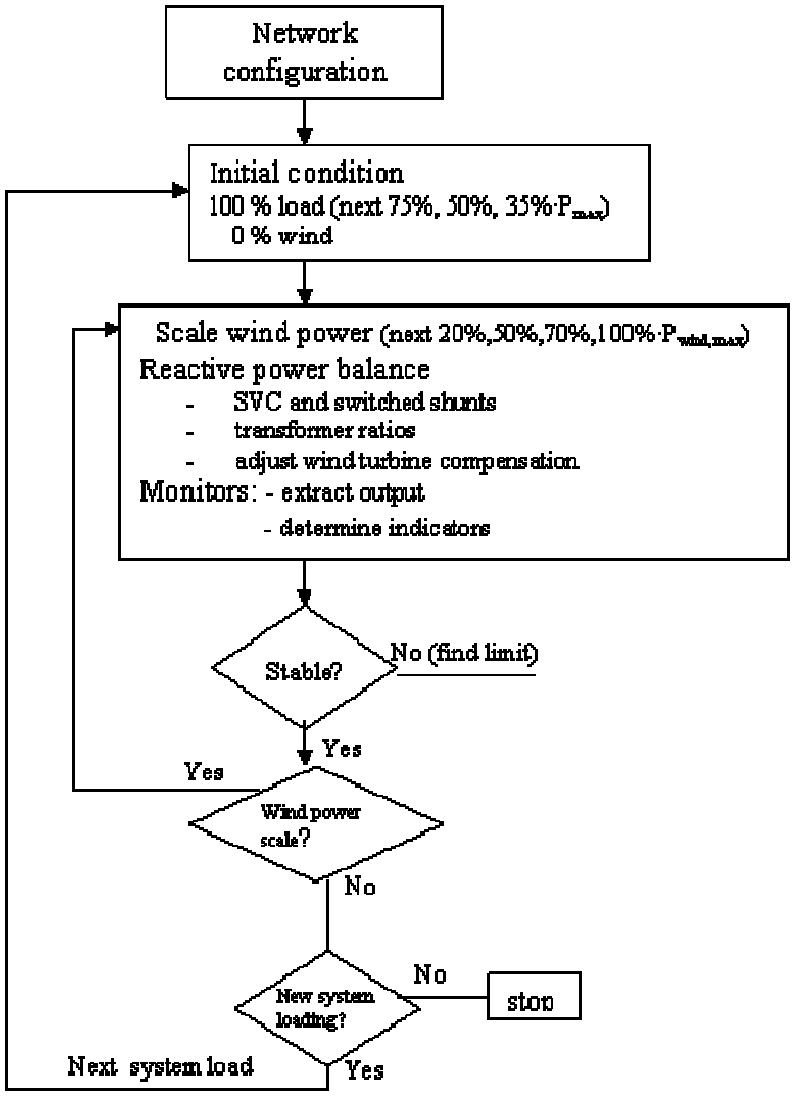

Fig. 19 *Flow-chart for static simulations*

4.1.1 Intact network with SVC

The direction of the power flow in the 132-kV system as well as the amount of injected power from wind turbines depend on the operational condition (total load vs. total generation) in the local area. The studied network is characterized with inadequate reactive power support and particular generator scheduling, see Table 2A in Appendix 2. The special interest is to find out the worst-case operating conditions with respect to voltage collapse in the system. For stationary simulations, a Static VAr Compensator (SVC) with 65 MVAr rating is introduced at 132 kV bus Radsted. The winter peak load in the southern part of the 132-kV system is 159 MW. Besides the maximum 350 MW wind production at Nysted 1 and Nysted 2 wind farms, wind power is produced on-land across the area adjacent to Radsted. E.g. wind turbines installed in the distribution network under the 132/50 kV substations of Vestlolland, Rødby and Eskildstrup can feed wind power in the transmission system. The load flow simulations in PSS/E use a detailed model of the power system in Eastern Denmark connected to a simple Swedish equivalent.

Fig. 20 shows the southern part of the 132 kV system, where the maximum wind power from on-land wind turbines is 470 MW and off-shore 406 MW arise from wind farm Nysted 1 (150 MW in operation), Nysted 2 (200 MW planned in the future) and Middelgrund (40 MW). All wind farms are modelled as a large, single wind turbine equivalent in PSS/E. The wind turbines on-land are connected to the grid via 10/0.69 kV step-up transformers, which have direct connection to 50/10 kV substations. The "local load" at Radsted 132/50 kV substation represents the flow in the 132/50 kV transformer, and the power flow size and direction depend upon the total system loading as well as the amount of local wind power generation[25]. E.g. the "local load" in case of high load (100% system loading) and no wind generation (0% wind) means that 32 MW are supplied from the 132 kV to the 50 kV grid via the 132/50 kV Radsted transformer. A typical condition of low system load and high wind at Radsted is characterized by backwards injection of wind power from the 50 kV to the 132 kV system.

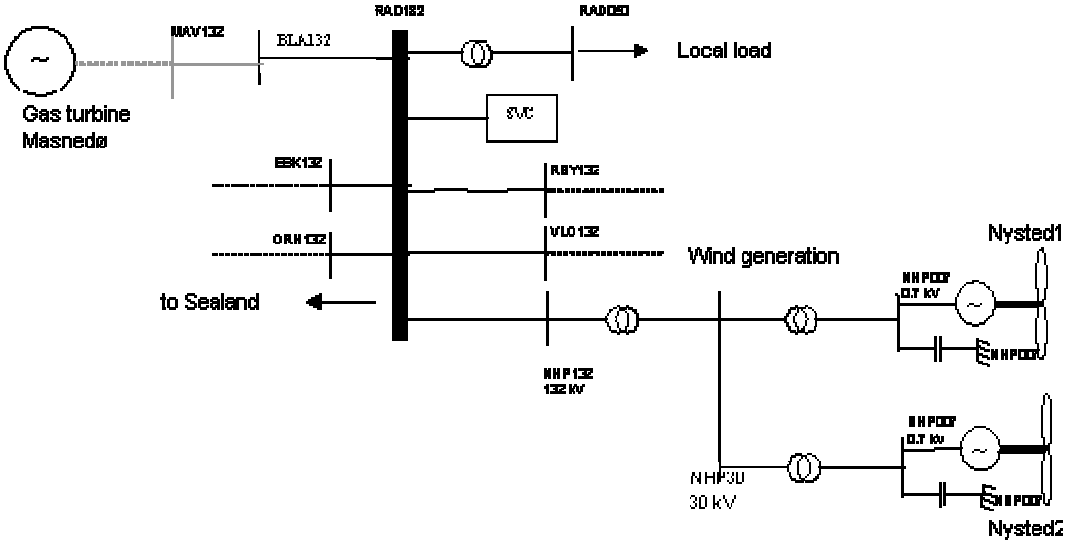

Fig. 20 Network with two off-shore wind farms Nysted 1 and Nysted 2

As shown in Fig. 20, the equivalent off-shore wind turbines at Nysted are connected via 30/0.69 kV and 132/30 kV transformers and a 132 kV line connecting the main 132 kV system to Radsted substation (RAD). This substation is the point of common connection, i.e. the first point in the system the wind farm shares with other customers. The wind turbine generators at Nysted 1 and Nysted 2 wind farm are modelled with full reactive compensation from capacitors shunts, and both wind farms are designed to be MVAr neutral at the 30 kV point at the 132/30 kV transformer connection. The key numbers for load and generation in the power system are submitted in Appendix 2. The accounted wind power on-land is actually 90% from the maximum installed capacity on-land, because it is most likely that the geographically spread wind turbines do not produce at the same time. Fig. 21 and Fig. 22 illustrate the flow of active and reactive power from/to Radsted substation. The black lines represent active and reactive power flow in the respective lines, while the red lines stand for total active and reactive power transfer from / to Sealand as well as the wind generation from the two Nysted wind farms (NHP1 and NHP2). The positive values denote power flow away from the bus bar (RAD) and negative values denote flows towards the bus.

[25] From on-land wind turbines connected to the 10 kV network under the Radsted 50/10 kV substation

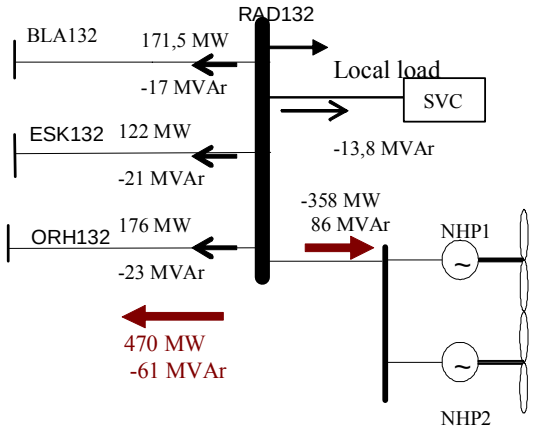

Fig. 21 *Power flows in intact network (35% total system load / 100% wind)*

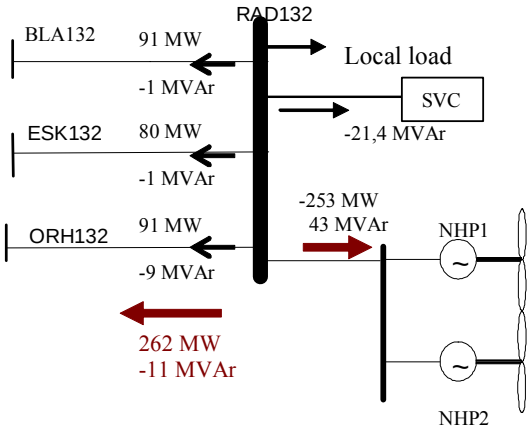

Fig. 22 *Power flows in intact network (100% total system load / 70% wind)*

Power flows from Radsted to the adjacent buses have positive sign. Here, the positive power flows are from Radsted in the northern direction to ESK132, BLA132 and ORH132. On the other hand the power flows from the adjacent buses to Radsted have negative sign. Here the negative power flows to Radsted from the large-scale wind farms e.g. off-shore: Nysted 1 and Nysted 2, on-land: VLO132 (Vestlolland), RBY132 (Rødby).

Fig. 21 and Fig. 22 show that in case of high wind, the active power transfer is from Radsted to Sealand, while a significant MVAr amount flows in the opposite direction (from Sealand to Radsted.). This situation occurs, because the SVC voltage set point at Radsted is set at a constant value of Vrad=1,01 p.u. (133,32 kV), regardless of low/high system loading. This is deliberately adjusted lower than the voltage at Sealand (e.g. V_{HVE} is adjusted in the interval 134 kV-136kV) in order to allow MVAr flow in the southern direction. The significant MVAr flow to Radsted is needed to supply local loads as well as to compensate for the reactive power losses in the 132 kV system e.g. 132 kV lines and 132/30 kV transformers near the wind farms. The negative power flow (-13,8 MVAr) is defined with regards to the reference direction from RAD132 to the SVC, which here means that the SVC delivers MVAr to the grid. The power flows in Fig. 21 and Fig. 22 can not be compared directly, because the two cases are related to different voltage profiles in the network. This is caused by the different reactive power balance conditions in the network due to a number of parameter variations as to changing settings for 50 kV capacitor shunts and reactive power output for central power plants and wind turbine compensation.

In low-load situation, the voltage magnitudes in Sealand are generally higher than in the southern system and MVAr flow from Sealand to Radsted. The difference in magnitudes between the southern part and the main 132 kV system at Sealand is flattened due to generally lower voltages in case of high load situation. Thus the reactive power flow from Sealand to Radsted is significantly reduced and local reactive power support is especially needed in the southern part of the heavily loaded system. The change of direction for the MVAr flow to/from Sealand is visualized for different loading conditions in Fig. 23. Here the x-axis presents the sum of active power flows in the three 132 kV tie-lines (RAD-ORH, RAD-BLA, RAD-ESK) that connect Radsted with Sealand. The positive values on the x-axis mean that the active power from Radsted is directed up north to the main system (typically when the wind power exceeds 20 % of the maximum capacity). The negative values are associated with active power flow from Sealand to Radsted, where the transferred wind power is rather small.

Fig. 23 illustrates clearly that the reactive power flow from Sealand to Radsted[26] is increased as the system loading decreases. E.g. the maximum reactive power flow from Sealand to Radsted is limited to approx. 60 MVAr in case of low load (35% of peak load), while the respective flow reaches approx. 40 MVAr in case of 75 % of peak load. In case of 100% winter peak load the 10 MVAr supplied from the main system to Radsted are not sufficient to maintain reactive power balance, which introduces voltage stability problems in the power system.

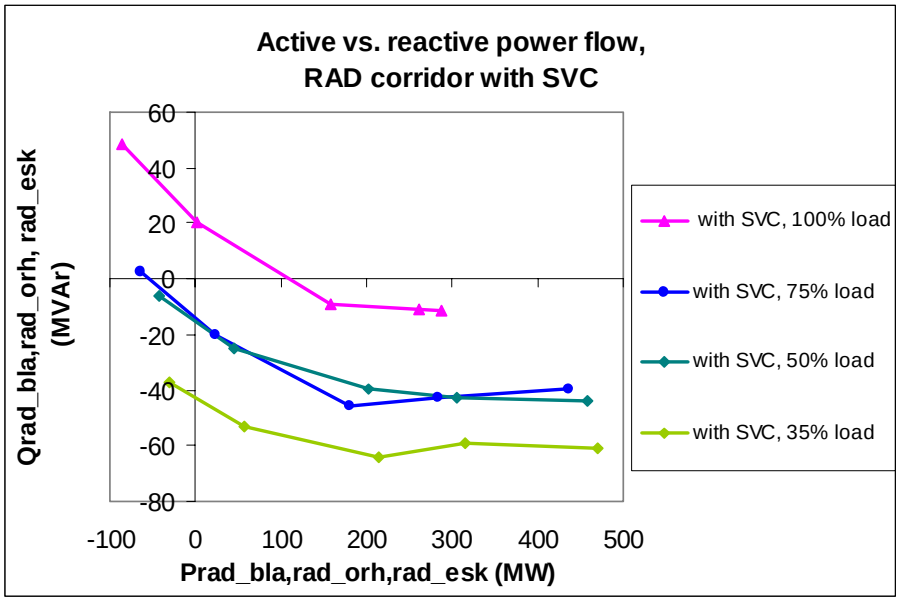

Fig. 23 Active vs. reactive power flow in the 132 kV tie-lines

The load flow calculation becomes non-convergent in case of heavily loaded system (100% load) with high wind penetration, which corresponds to total wind generation above 660 MW and 300 MW active power flow in the tie-lines. Here the 132-kV system is not able to transfer the increasing amount of wind power and the system becomes voltage unstable. Besides the high load/ high wind condition, convergent load flow solutions (stable system operation) are found for all other loading conditions.

The next figure depicts the flow from Radsted to the SVC ($Q_{RAD\text{-}SVC}$) as a function of the total tie-line flow. The x-axis in Fig. 24 represents the sum of line flows in the 132 kV tie-lines RAD-ORH, RAD-ESK and RAD-BLA. The y-axis in Fig. 24 represents the MVAr flow from Radsted to the SVC according to:

$Q_{RAD\text{-}SVC} > 0$ MVAr flow from Radsted to the SVC
$Q_{RAD\text{-}SVC} < 0$ MVAr flow from the SVC to Radsted

In fact, the positive values at the y-axis ($Q_{RAD\text{-}SVC}>0$) in Fig. 24 reveal that the SVC absorbs reactive power from RAD (coming from the main 132 kV grid). E.g. in case of 75% total load (pink curve), the increase of wind from 0% to approx. 50% of total wind generation in the system introduces greater reactive power flow from the main 132 kV system and thus greater MVAr flow from RAD to the SVC. For wind generation exceeding approx. 50% of the total wind power, the reactive power flow from RAD to the SVC decreases due to limited reactive

[26] Negative values on the y-axis

power transfer from the main 132 kV grid (shown in Fig. 23). The sign of $Q_{RAD\text{-}SVC}$ in Fig. 24 changes as the reactive power is supplied locally from the SVC to RAD. Problems with insufficient reactive power support especially in the heavily loaded system with high wind generation are caused by the limitation of the SVC rating. The above formulation should be adapted to the convention for reactive power flow to/from the SVC device. The negative part of the y-axis $Q_{RAD\text{-}SVC}$ in Fig. 24 is associated with reactive power flow from the SVC to RAD substation (SVC pumps MVAr in the 132 kV system). In case of 100% total load, the flow $Q_{RAD\text{-}SVC}$ flow becomes negative when the tie-line flow from Radsted to Sealand exceeds 200 MW.

The power flow directions for $Q_{RAD\text{-}SVC}$ in case of high wind/low load and high wind /high load are given in Fig. 22. The output in Fig. 24 reveals that in case of no wind, the 132 kV tie-line transfers active power from Sealand to Radsted (negative values on the x-axis). E.g. in case of 75% and 35% of the total system load the SVC absorbs the excessive reactive power from the main 132 kV system as the wind power increases from 0% to 50% of the total wind generation in the system.

The reactive power flow $Q_{RAD\text{-}SVC}$ begins to decrease after the total wind power generation exceeds approx. 440 MW (50% of the maximum wind power). This situation is seen in Fig. 24 for different system loading, where the total tie-line flow exceeds 150-200 MW. In case of high wind penetration, the sign of $Q_{RAD\text{-}SVC}$ changes, so that reactive power flows from the SVC to Radsted. For 100% load and wind generation higher than 70% of the maximum, it is not possible to obtain a convergent load flow solution. In this case, the SVC is not able to meet the high reactive power demand for the local load in the southern part of the 132 kV system. The simulation analysis confirms that adequate design of reactive power rating for the SVC is the crucial factor for maintaining reactive power balance when the wind generation is significantly increased in the system.

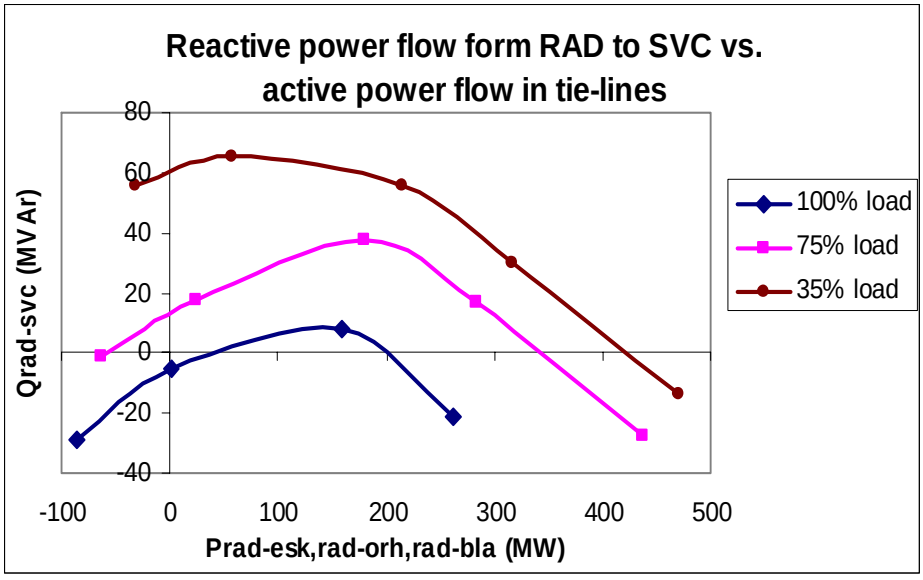

Fig. 24 *Reactive power flow $Q_{RAD\text{-}SVC}$ vs. active power flow in tie-lines*

Series of conventional load flow simulations are used to plot P-U, Q-U and P-Angle system characteristics for the intact network. The static system characteristics are calculated for increasing active power transfer in the tie-lines, which correspond to uniform increasing in wind generation at all wind turbines. The amount of wind power in the system is scaled up until a non-convergent load flow solution is reached, where problems with voltage stability become

obvious. The point of voltage instability for the case 100% load and high wind generation is not determined precisely, because the wind generation is varied in too large steps. The different stability curves are plotted for few 132 kV system buses in case of an intact network with SVC and the network subjected to a single line contingency. Different system loading is used as parameter variation.

In the simulation study, Orehoved (ORH) is identified as a weak 132 kV bus without voltage control, where the voltage variations are mostly pronounced. The low-load situation is related to the largest voltage decrease at Orehoved due to high wind penetration.

Fig. 25 presents the voltage magnitude at Orehoved as a function of total active power flow in the three tie-lines RAD-ESK, RAD-BLA and RAD-ORH. The curve is plotted for different loading scenarios. The dotted curve in Fig. 25 connects approximately the locus of respective points related to about 50% of maximum wind power in the system.

The same figure shows that higher level of voltage magnitude at Orehoved is associated with decreasing system loading. For all load levels it is observed that the voltage decreases significantly, when the total wind generation in the system exceeds the limiting 50% of the maximum wind power capability. This is though considered critical only for the case of high load/ high wind. The other loading conditions appear to be stable.

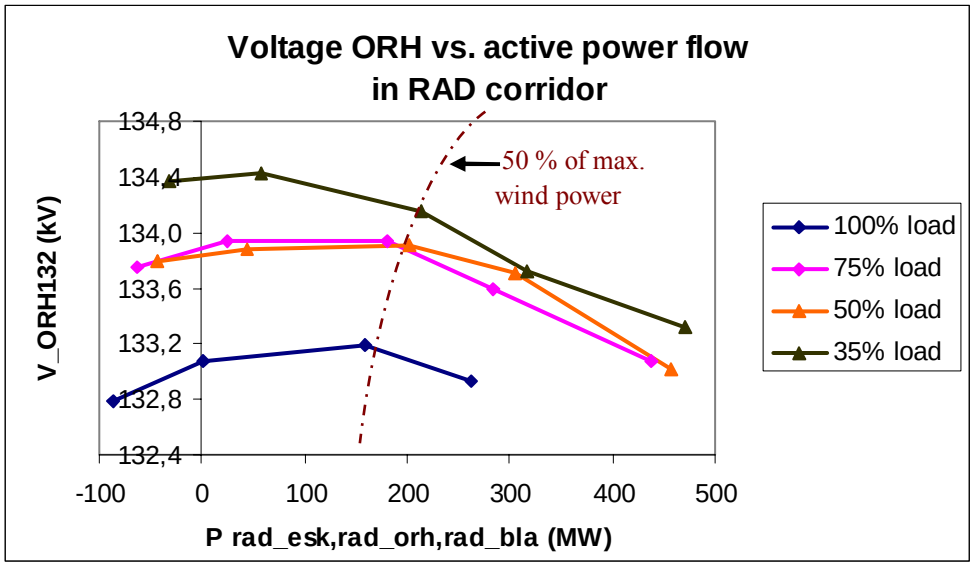

Fig. 25 *Voltage at Orehoved vs. active power flow in 132 kV tie-lines*

Since voltage stability is closely related to reactive (rather than active) power, it is most appropriate to depict voltage vs. reactive power (Q-U) curves for the system. The Q-U curves for the Eastern Danish system are generated by monitoring voltages at bus Orehoved (Fig. 26) as a function of the total reactive power flow in the 132 kV tie-lines. Under normal operation, the reactive power flow from Sealand to Radsted tends to support the voltage at ORH inside a predefined voltage range of (0.95-1.05) p.u. The voltage begins to decrease significantly when the wind generation exceeds 50% of the total wind capacity. This is a result the decreasing reactive power flow from Sealand to Radsted.

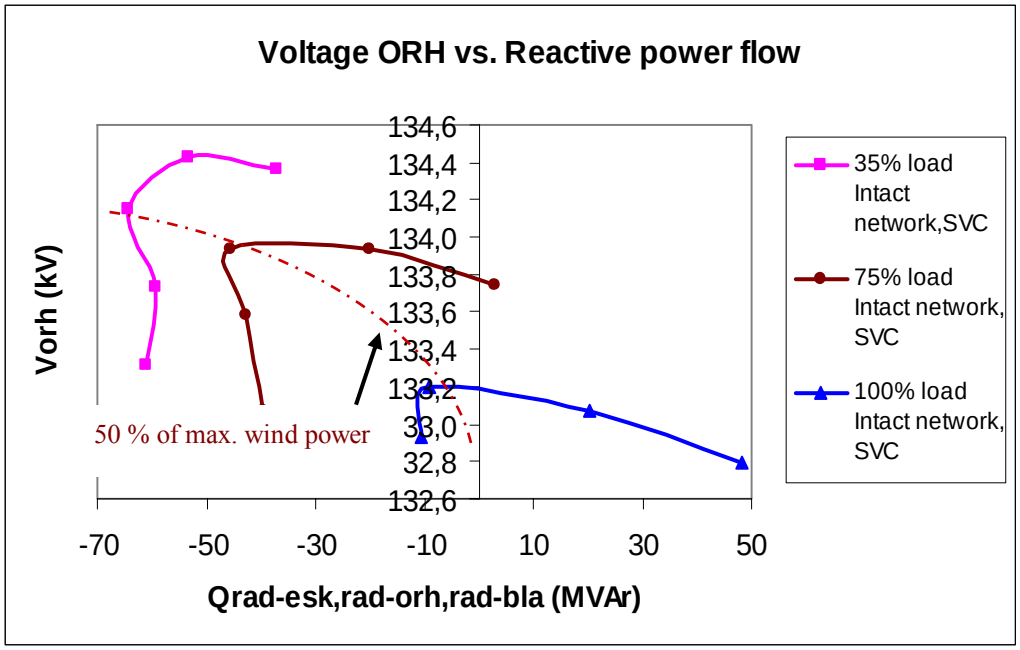

Fig. 26 Voltage at Orehoved vs. reactive power flow in tie-lines

Beyond the tip of the Q-U curve, the reactive power flow from Sealand to Radsted is reduced in the same time as ORH bus voltage decreases. The locus for points related to 50% of wind generation connects the tip of the curves for different system loading in Fig. 26.

This situation emphasizes once again the need for appropriate design of reactive power support in the area with two off-shore wind farms. Fig. 26 shows that the heavily loaded system with a large amount of wind power is pushed beyond its static voltage stability limit due to inappropriate reactive power support in the area [41], which arises from the insufficient reactive power flow from the main 132 kV system as well as the insufficient rating of the existing SVC device. It is suggested to apply an upgraded SVC rating (minimum 110 MVAr) or to use the existing SVC (65MVAr) and add capacitors banks of at least 45 MVAr at e.g. Radsted substation. E.g. the intact network using a 110 MVAr SVC has improved its reactive power balance, and the wind power transfer in the area is increased. Besides the upgraded SVC at Radsted, different remedial control actions in a dedicated System Protection Scheme open up for the possibility to be utilized in emergency situations in case of stressed or weakened network due to contingencies.

4.1.2 Single line outage

The outage of the 132 kV line Radsted-Orehoved introduces significant changes in the reactive power flow in the 132 kV tie-lines from Sealand to Radsted. As expected, the total active power flow in the northern direction is only slightly affected by the line outage. Relevant line flows for the contingency network in case of low load/ high wind are given in Fig. 27, while Fig. 28 illustrates the high load/ high wind situation in the network with a single 132 kV line outage.

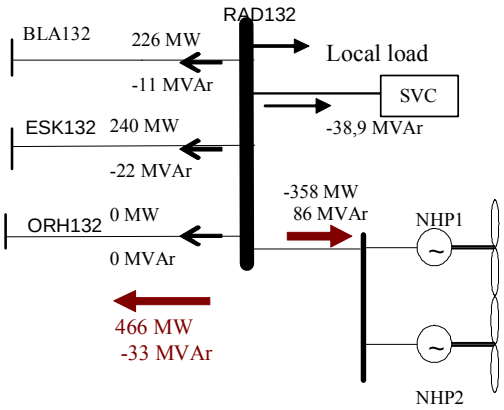

Fig. 27 *Power flows in contingency network (35% total system load / 100% wind)*

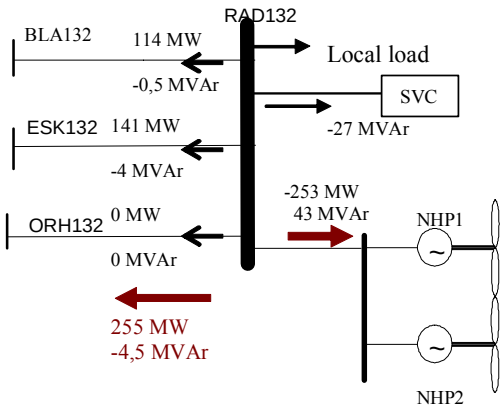

Fig. 28 *Power flows in contingency network (100% total system load / 70% wind)*

A number of characteristics, e.g. P-U, Angle-P and Q-U curves, are plotted in order to illustrate relevant changes in voltages, phase angles and reactive power flows due to the line outage. The bus voltage at Hovegård is depicted as a function of reactive power in the remaining tie-lines from Radsted to Sealand (RAD-ESK, RAD-BLA). The voltage profile at HVE (Fig. 29) is almost unaffected as far as the reactive power flow from Sealand to Radsted is increased until the limit of maximum transfer of reactive power. The bus voltage at Hovegård is less sensitive to reactive power changes in the tie-lines, because it is located in a stronger part of the 132-kV system close to large generating units.

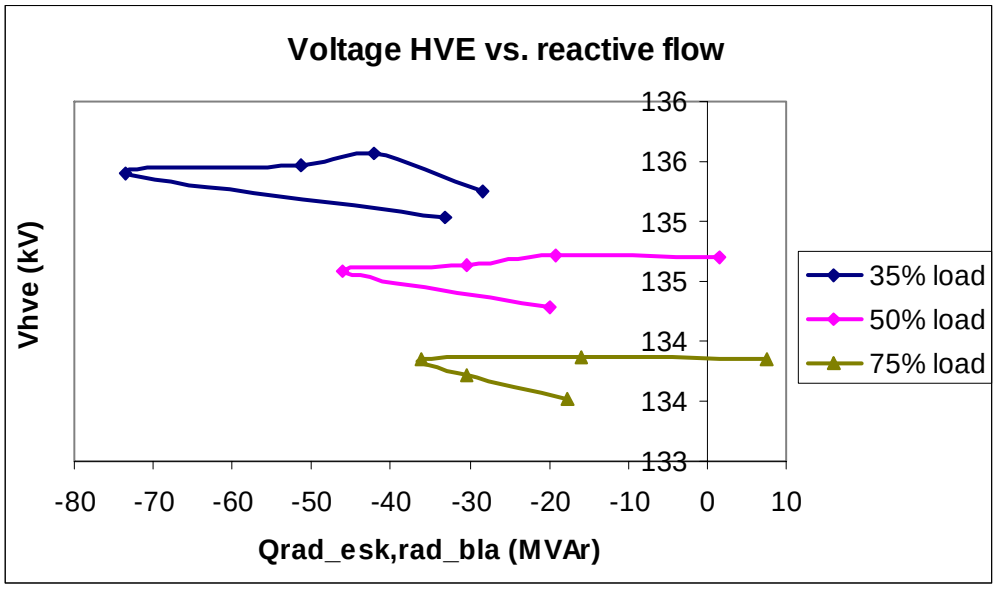

Fig. 29 *Voltage at Hovegård vs. reactive power flow in tie-lines*

The lower part of the Q-U curves at Orehoved is seen beyond the point of maximum reactive power transfer from the main 132 kV system. It is associated with a sudden decrease in both bus voltage and reactive power flow from the main system, because the flow $Q_{RAD\text{-}SVC}$ is reduced and becomes negative. It means that the reactive power flowing from the SVC towards Radsted is not sufficient to avoid decrease in the respective bus voltages. Fig. 30 illustrates that in case of contingency network, the voltage at bus Orehoved is much more sensitive to reactive power changes than Hovegård.

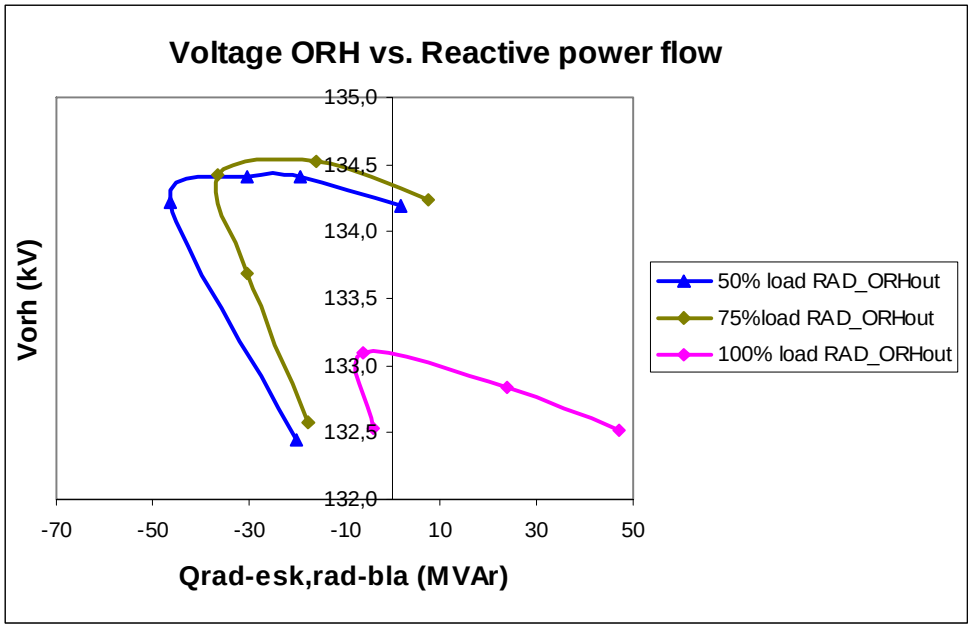

Fig. 30 *Voltage at Orehoved vs. reactive power flow in tie-lines*

The critical active power transfer from Radsted to Sealand[27] is significantly decreased as the system loading increases from low to high system loading. The main reason for this is the decreasing reactive power flow from Sealand to Radsted, which in turn constrains the tie-line active power.

The voltage profiles for bus Orehoved are enclosed in Fig. 31 in case of 100% load in intact network and 100% load in the network with a single line outage (Radsted-Orehoved). The figure illustrates that the voltage shifts down to lower values due to the tripping of a tie-line between Radsted and Sealand. This is explained by the increased equivalent impedance in the transmission corridor between Radsted and Sealand after the line outage. As expected, the contingency curve for wind generation above 50% of the maximum wind power capacity is associated with greater voltage decrease than the base case.

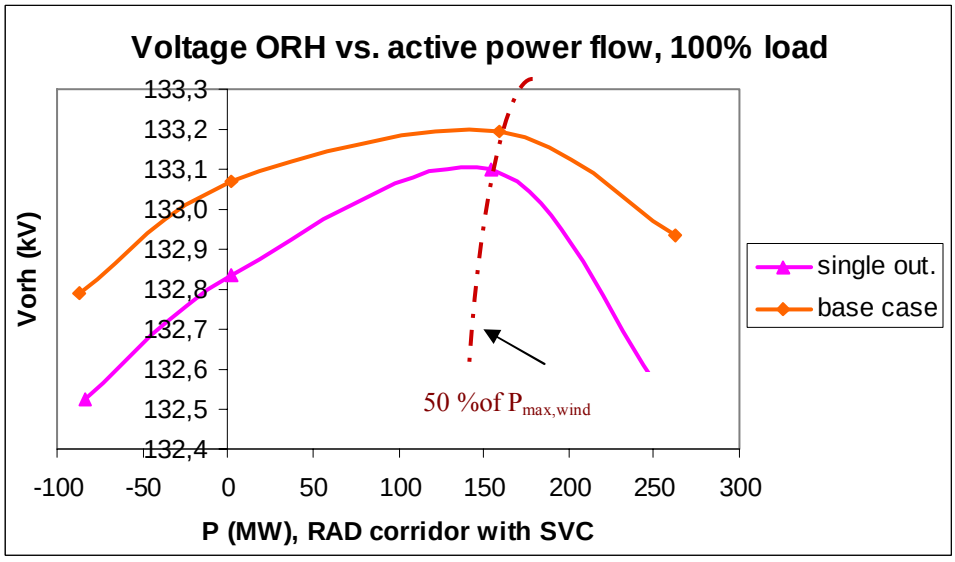

Fig. 31 *Voltage at Orehoved vs. active power flow in 132 kV tie-lines*

[27] In case of high wind power transfer in the northern direction

The uncontrolled voltage decrease can be avoided if remedial control actions e.g. using a System Protection Scheme are performed. E.g. wind generation shedding can be used to reduce the active and the reactive power transfer in the 132 kV tie-lines as a remedial control action to prevent voltage instability. The shedding of wind generation can be done either by downwards regulation of the power output from off-shore wind farm(s) or by tripping of a significant amount of wind turbines on-land.

Fig. 32 illustrates a non-linear shape of the phase angle difference between the 132 kV busbars Radsted and Hovegård as a function of the reactive power flow in the tie-lines connecting Radsted to Sealand in case of intact and contingency network. The angle RAD-HVE increases almost linearly as the reactive power flow from Sealand to Radsted increases concurrently with the increase of wind penetration up to 50% of maximum wind capacity. For wind penetrations of 70% and 100% of the maximum wind capacity, the relative voltage angle RAD-HVE is still increasing, but the reactive power flows from the main 132 kV system are reduced. This is explained by the fact that in case of high wind penetration, the reactive power in the southern part of the system is mainly supplied from the SVC to Radsted. The reactive power transfer in the tie-lines is mainly governed by the reactive power demand from wind turbine generators in the area and the reactive power flow between Radsted and the SVC at the same bus. The active power flow in the 132 kV tie-lines and the difference in voltage angle between Radsted and Hovegård are seen as secondary factors that influence the reactive power flow in the tie-lines that connect Radsted with the main 132 kV transmission system.

The outage of the 132 kV line RAD-ORH weakens the system, because the reactive power transfer in the network is significantly reduced in comparison to the intact network. As expected, the relative phase angle $\delta_{\text{RAD-HVEpostfault}}$ in case of a line outage is increased in comparison to the corresponding prefault value $\delta_{\text{RAD-HVEprefault}}$. Hence, the tip of the angle–reactive power curve is shifted as a result of the line outage. The increase in critical voltage angle $\delta_{\text{RAD-HVE}}$ after the line outage is explained by the increase in equivalent reactance between busbar Radsted and Hovegård, see equations (22), (23).

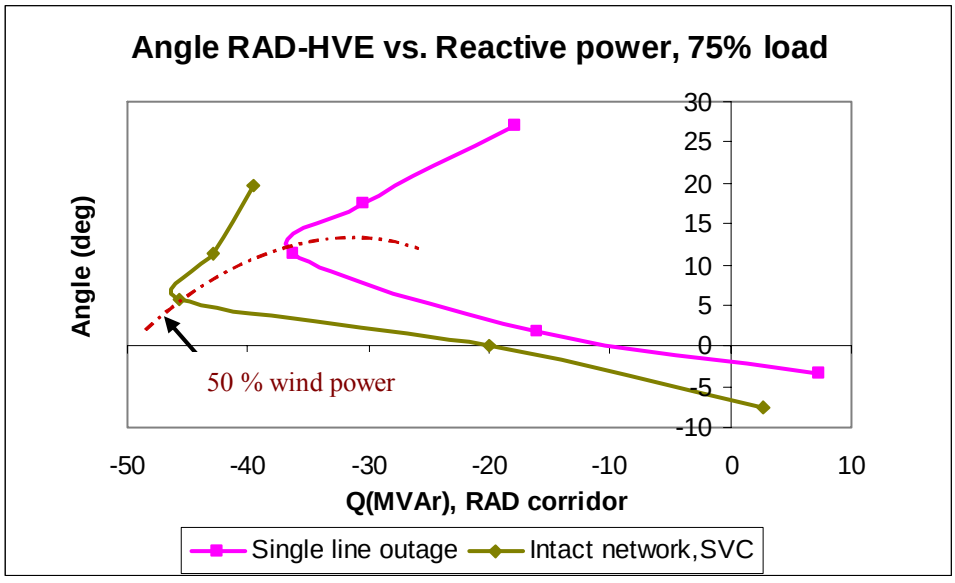

Fig. 32 Angle difference vs. tie-line reactive power flow for intact and contingency network

The relation between the angle difference ($\delta_{\text{RAD-HVE}}$) and active power flow between Radsted and Sealand is shown in Fig. 33. The simulated angle difference vs. active power flow characteristics can be approximated with a linear function.

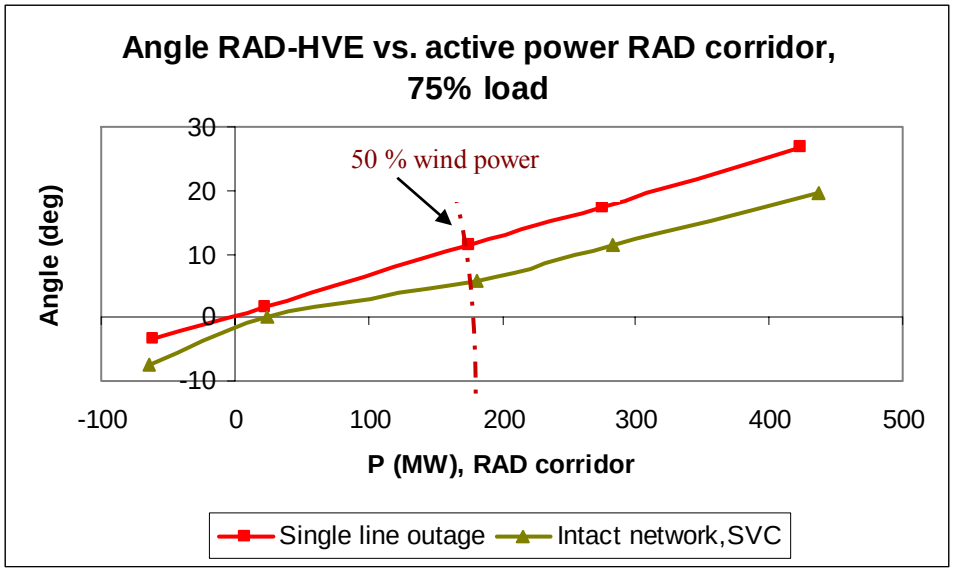

Fig. 33 *Angle difference vs. active power flow in 132 kV tie-lines*

The angle difference between RAD and HVE in case of intact network (prefault) and line outage (postfault) are theoretically described by the following relation:

$$\sin \delta_{RAD-HVEprefault} = \frac{P_{prefault} \cdot X_{eq,pre}}{U_{RAD} \cdot U_{HVE}} \tag{22}$$

$$\sin \delta_{RAD-HVEpostfault} = \frac{P_{postfault} \cdot X_{eq,post}}{U_{RAD} \cdot U_{HVE}} \tag{23}$$

$\boldsymbol{P}_{prefault}$ and $\boldsymbol{P}_{postfault}$ in equations (22) and (23) denote the power flow in the tie-lines from Radsted to Sealand before and after a transmission line outage. U_{RAD}, U_{HVE}, δ_{RAD} and δ_{HVE} are the voltage magnitudes and phase angles at the 132 kV buses Radsted and Hovegård, while $X_{eq,pre}$ and $X_{eq,post}$ are the respective equivalent reactances between RAD and HVE before and after the line outage. The relations for the prefault and postfault phase angle difference are derived from equations (24) and (25) respectively.

$$P_{prefault} = \frac{U_1 \cdot U_2}{X_{eq,pre}} \sin(\delta_1 - \delta_2)_{prefault} = \frac{U_1 \cdot U_2}{X_{eq,pre}} \sin \delta_{12\_prefault} \tag{24}$$

$$P_{postfault} = \frac{U_1 \cdot U_2}{X_{eq,post}} \sin(\delta_1 - \delta_2)_{postfault} = \frac{U_1 \cdot U_2}{X_{eq,post}} \sin \delta_{12\_postfault} \tag{25}$$

Phase angle information could possibly be applied to improve the performance of system protection scheme in case of impeding voltage instability. The most important benefit of using PMUs in the suggested SPS against voltage instability is to detect severe disturbances (line outages, wind turbine rejections) in terms of severe phase shifts.

4.1.3 Conclusion on static simulations

The static simulations show that voltage instability occurs in Eastern Denmark, if two large off-shore wind farms near Nysted are to be integrated in the existing transmission system with high loading and high wind power generation without any reinforcements. The studied 132-kV transmission system is rather weak and prone to voltage stability problems because of its limited reactive power control capability and the long distance to the large generating units. The voltage stability limit in the heavily loaded system (100% load) is approached when the total wind generation in the system is increased above 70% of the maximum capacity. The problems with voltage stability appear due to the characteristic of wind turbine generation as well as the inability of the power system to meet the reactive power demand in the southern 132 kV system.

The permissible active power transfer from Radsted to the main 132 kV system is mainly constrained by the degree of wind generation and the system loading conditions (high load). In the proximity of voltage collapse, the system is associated with high reactive power losses in the affected area eventually followed by low voltage at critical buses. In case of a 132 kV tie-line outage, the limiting transfer of reactive power between Radsted and Sealand is significantly reduced, which indicates problems with voltage stability in the heavily loaded power system.

The calculated reactive power losses for intact $\Delta Q_{prefault}$ and contingency network $\Delta Q_{postfault}$ are compared in Table 3A in Appendix 2. It is illustrated that the largest voltage gradients and the largest reactive power losses are associated with largest power flows in relevant 132 kV lines that typically occur in case of low load and high wind. The losses are further increased if a tie-line outage occurs in the network. On the other hand, the increase in the total system loading (100% load) in case of relatively small wind power generation[28] also raises the total system losses.

The outage of a single 132 kV tie-line leads to a greater voltage angle difference between Radsted and Hovegård and lower limit of wind power transfer in comparison to the base case (intact network). After contingencies, the heavily loaded network becomes even weaker, because the stress is associated with decreasing margins to voltage instability. The wind power transfer in the 132 kV network is improved by application of additional voltage control devices (e.g. dynamic reactive power compensation from SVC and Masnedø gas turbine) or SPS remedial control measures (e.g. change of SVC set-point etc.).

In practice, phase angle differences can be easily monitored using Phasor Measurement Units (PMUs) at a number of system buses. In general, PMUs can be applied for disturbance detection and warning about severe phase shifts that are identified in case of outage of lines, generating units or significant load rejection. The static analysis clarifies the following points:

- The worst-case scenario with respect to reactive power deficit in the southern part of the 132 kV system is the situation with high system loading and high wind generation. It was not possible to achieve a convergent load flow solution for the situation 100% load and 100% wind generation due to the insufficient SVC rating as well as the limited flow of reactive power from the main system. The operating scenario related to high load (100% load) and wind generation above 70% threatens the system voltage stability. The critical situation can be avoided by using a more powerful SVC e.g. with rating of minimum 110 MVAr and/or activation of System Protection Scheme control actions.

[28] Up to 20% of Pmax,wind

- The largest voltage and reactive power gradients are seen in case of 35% load and 100% wind generation. This situation is caused by the large 132 kV line flows in the intact and in the contingency network.

- In general, it is difficult to derive simple voltage stability limits that are valid for a large range of operating conditions, where many parameter variations are present. Good knowledge of the network behaviour is crucial.

- It is difficult to determine precisely the voltage stability limits for the heavily loaded system using Q-U (and P-U) curves with a limited number of points. The simulated wind power is scaled in relatively large steps of 0%, 20%, 50%, 70% and 100% of the total wind generation in the system. For more accurate determination of the voltage stability constraints and generation of smoother stability curves, it is recommended to use a more appropriate wind power scaling (e.g. with increments smaller than 5%). This is especially important for correct identification of voltage stability sensitivities related to proximity to voltage collapse. On the other hand, the increased amount of data will require an improved procedure for data management and better tools for data mining.

- The used method for voltage stability analysis illustrates a typical mechanism of voltage instability in systems with significant wind generation. Advanced studies using voltage stability indices [53] can be used in future off-line or on-line applications to help the power system operator determine how close the system is to voltage collapse. Different performance indices to predict the proximity to voltage collapse can be defined as scalar magnitudes, which are easy to monitor as critical parameters that change in the power system (such as total wind power generation, reactive power flows etc.).

- The conventional load flow methods (Newton-Raphson or Fast Decoupled) provide solutions up to the critical point [46]. The continuation power flow method becomes necessary only if solutions exactly at and past the critical point are required. For this purpose, reference [54] suggests application of a continuation power flow tool.

- The approach using static P-U and Q-U curves is not persistent when a large number of wind turbines are introduced in the power system. The wind turbine performance is strongly dependent on the wind speed and voltage variations in the power system. Thus dynamic P-U and Q-U characteristics (rather than the respective steady-state curves) are acquired for more adequate representation of the wind generation impact [23].

4.2 System Protection Scheme design

In practice, SPS is designed as a system-wide solution that incorporates monitoring, analysis and control on an automatic platform. SPS relies on monitoring input from the power system, which initiates an on-line decision-making process about the security status of the power system. The characteristics incorporated in the suggested SPS decision process are unique and dependent upon the specific power system and its operational practices. SPS can be armed or disarmed depending upon the network operating conditions. If necessary, the SPS output issues remedial control action(s) to improve the security of the power system.

Both event- and/or response-based SPS can be used as concept for a protection scheme against voltage instability. E.g. reference [1] proposes implementation of event-based SPS as a primary control with response-based SPS acting as a backup in case of failure of the event-based SPS. In the particular case, the SPS against voltage stability is designed as an open-loop

response-based scheme that enables the power system to preserve its capability with respect to wind generation. The simplified concept for SPS design illustrated in Fig. 34 does not take into account the impact of feedback control(s). The SPS is designed as a simple response-based scheme that is able to react with respect to critical system contingencies whatever the cause of the disturbance.

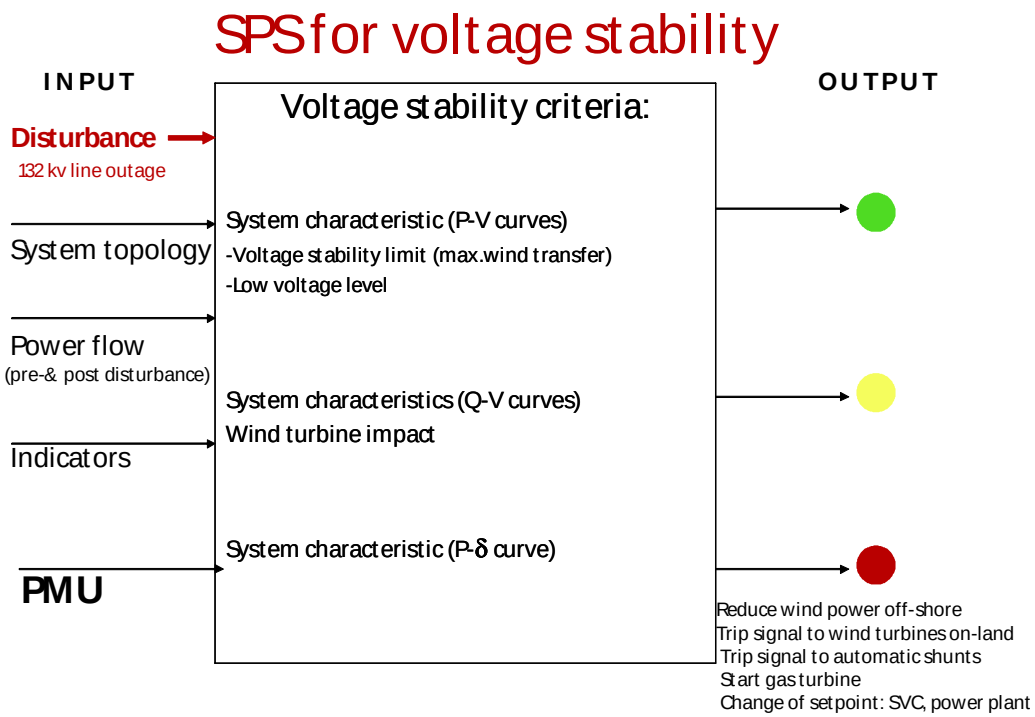

Fig. 34 Concept for System Protection Scheme design

Accordingly, the response-based system protection scheme is considered efficient for disturbances that are not explicitly identified or foreseen, because its reliability depends mainly on the selection of variables and their behaviour. The main challenge in the particular SPS design is associated with the input considerations (detect abnormal system conditions) and output considerations (give warning in case of imminent voltage instability).

Input considerations: For design purposes, it is necessary to access information about the system configuration and **power flow** (input parameters from the off-line simulation analysis). Each load flow case study is related to a single operating point characterized by a particular system configuration, total generation and total load and load flow solution in terms of power flows, bus voltages (magnitude U and phase angle δ), reactive power generation etc. For operational purposes, the key input to the SPS is based on **indicators** of voltage instability in relation to conventional input (from the SCADA system) and to supplementary input from Phasor Measurement Units (PMUs). Besides, it is crucial to know the **system topology** (circuit breaker status from the SCADA system) that is especially used for identification of disturbances.

The decision process is based on off-line simulation analyses in PSS/E of a wide range of predetermined system conditions and contingencies for the large-scale power system model.

A considerable number of case studies are analyzed in order to determine SPS settings for relevant operating conditions.

Output considerations: As illustrated in Fig. 34, the output of the scheme can give the control centre information about the security status of the network. The *green* lamp is given in case of normal operation. The *yellow* lamp issues warning if the power system is approaching a security margin for safe operation; while the *red* lamp gives an alarm that the system is close to voltage instability. A control action can be executed after the yellow or the red lamp gives warning. The alarms for critical conditions can automatically activate remedial control(s) in the system, such as reduction of wind power, additional reactive power support in the system or emergency start of a gas turbine.

Additional investigations are not performed to determine more precisely security margins and control action(s) that are most appropriate for particular operating conditions. In the future, a separate protection scheme should be designed for each control action, and the different schemes have to be coordinated.

The design objective for the system protection is to avoid a voltage collapse after a very severe disturbance in the power system of Eastern Denmark. The following requirements are relevant:

- Maintain balance of reactive power generation and demand;
- Avoid uncontrollable voltage decrease at any part of the power system;
- Avoid uncontrollable voltage increase (reactive power overshoot from switched capacitors and SVC);
- Attain acceptable voltage recovery at load centres and at wind turbine terminals in post-disturbance state;
- Avoid load shedding requirements.

4.2.1 Identification of indicators for voltage stability

Reactive power flow

Reactive power imbalance is the most important indicator of potential voltage stability problems. It is primarily relevant to monitor the reactive power demand Q (MVAr) in the southern part of the 132 kV system. Secondly it is relevant to monitor the reactive power compensation of wind turbines and the reactive output of generating units electrically close to the southern 132 kV system. The reactive power demand is divided in the local reactive power consumption and reactive power losses in transmission lines and transformers. The reactive power loss ΔQ_i arises from voltage drop ΔU_i across a transmission line i. In transmission grids, the line reactance exceeds the line resistance ($X_i >> R_i$), and thus reactive losses due to R_i are neglected in equation (26). The losses in the transmission system ΔQ_{system} can be calculated as a sum of ΔQ_i for each line, where P_i and Q_i denote the active and reactive power line flow.

$$\Delta U = \frac{R \cdot P_i + X \cdot Q_i}{U_n} \approx \frac{X \cdot Q_i}{U_n}, \quad for \quad X_i >> R_i \tag{26}$$

The reactive power losses are used to classify scenarios with regard to largest reactive power losses, due to largest voltage gradients in transmission lines. For each particular case of interest, a load flow calculation is performed for the initial operating situation and following a

contingency. Severe voltage depressions during a contingency are often associated with deficient reactive power Q in the system. The reactive power deficiency can be attributed to increase in reactive power losses in transmission circuits due to increased line loading. E.g. maximum power flows from Lolland-Falster to Sealand and maximum power losses are experienced in case of low system loading and high wind generation. Table 3A (Appendix 2) summarizes reactive power losses in the southern region for different operating conditions in the respective cases of intact network with SVC (with 65 MVAr rating) as well as for the network with outage of a single 132 kV line (RAD-ORH) and double outage of 132 kV lines (RAD-ESK, RAD-BLA).

Voltage magnitude is not the best indicator of voltage stability due to:

- Stiff voltage regulation in transmission systems and voltage control at power plants, where generator units attempt to keep constant voltage at their terminals;
- Large voltage variations are not necessarily related to voltage stability problems. Besides, sudden voltage changes are experienced due to shunt capacitors and reactors switching;
- Inherent bias error on voltage transformers (measuring voltage transformers are inaccurate due to aging and faults in capacitors);
- Under normal operation, the voltage at Radsted is insensitive to system loading conditions, because it is held constant using SVC.

Phase angle

Phase angle difference between buses in distant areas of the power system can vary significantly according to the network loading and generation conditions. Shift in phase angles can be caused by line outage, generator (power plants, wind turbines) tripping or load rejection, system stress or a combination of these. The SPS phase angle monitors focus on angle deviations due to significant change in power flows P that can cause voltage stability problems. E.g. a simple radial system corresponding to the one in Fig.9 is associated with sending and receiving node parameters U_1, δ_1, U_2, δ_2 and active power flow P in the equivalent line impedance X. As described in equation (27) the system operation is considered stable, if the phase angle difference between the sending and receiving node (δ_{12}) does not exceed a critical value (δ_{max}).

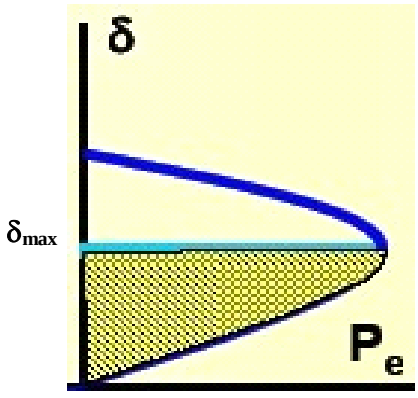

$$P = \frac{U_1 \cdot U_2}{X} \sin\left(\delta_1 - \delta_2\right)$$

$$P = \frac{U_1 \cdot U_2}{X} \sin\ \delta_{12}$$

$$\delta_{12} < \delta\text{max} \qquad (27)$$

Fig. 35 Ideal power-angle characteristics of a generator

4.2.2 Criteria for voltage stability

The system protection scheme suggested in Fig. 36 detects voltage instability as violation of relevant criteria from the SPS decision-making process. The scheme is designed to give an alarm for unstable operation if all three of the following criteria are fulfilled:

- $Q > Q_{max}$ reactive power flow
- $U < U_{low}$ low local voltage **(** associated with a voltage gradient ΔU)
- $P > P_{max}$ active power flow in tie-lines
  $(\delta > \delta_{max}$ supplementary indicator instead of active power flow in tie-lines).

The suggested SPS settings such as active and reactive power flows and voltage gradients are enclosed in Table 3 in case of intact network and network with outage of a 132 kV tie-line for the critical case 100% load and 70% wind generation.

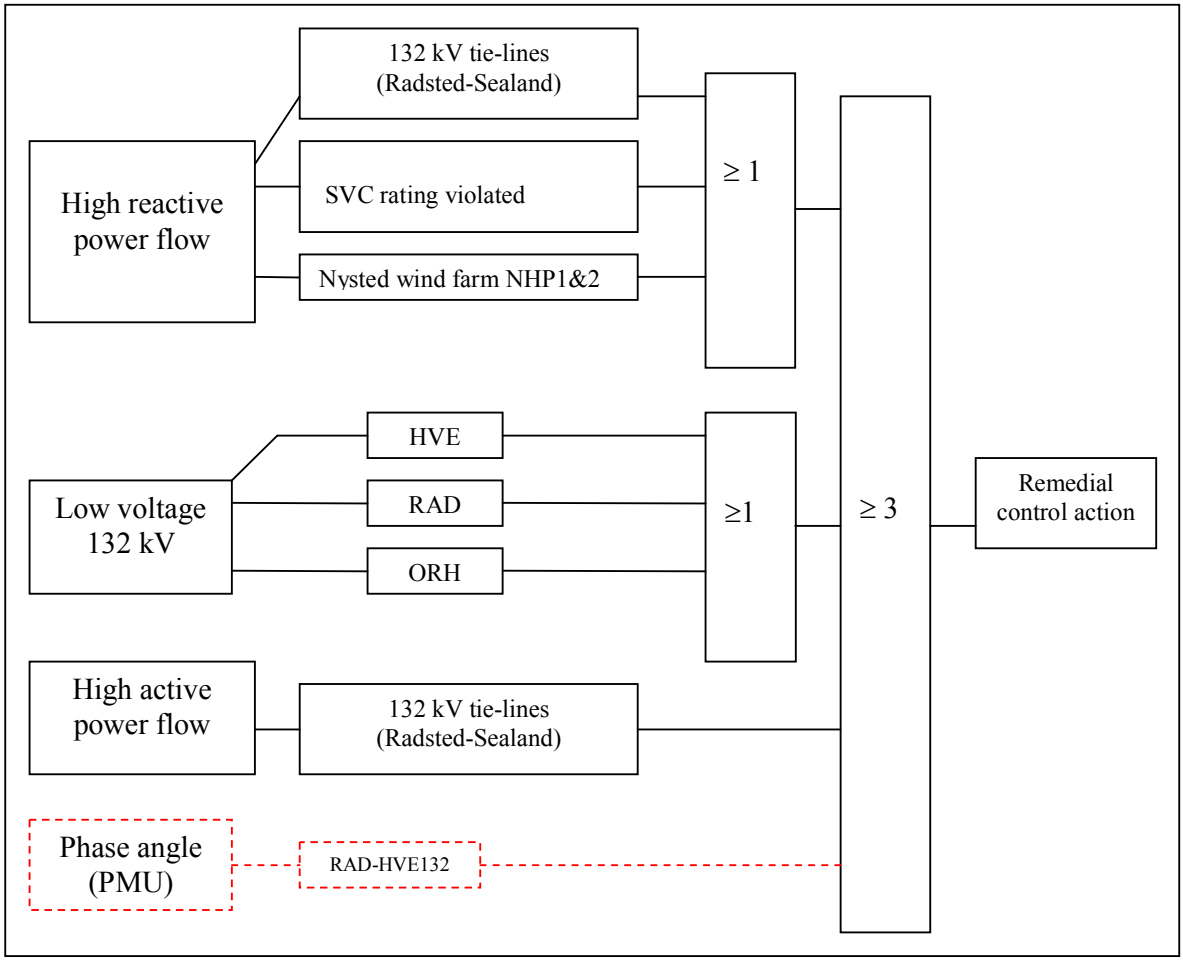

Fig. 36 Design of SPS against voltage instability in Eastern Denmark

The SPS settings are determined from simulated static stability curves for the high load/ high wind operating scenario.

	Base case with SVC			Contingency case with SVC		
Total load (MW) (% of peak load)	Critical active power transfer		Critical reactive power transfer	Critical active power transfer		Critical reactive power transfer
2800 MW (100%)	Ptie-line (MW) 280 MW	Wind power (% of total) 70%	Qtie-line (MVAr) -10.0 MVAr	Ptie-line (MW) 155 MW	Wind power (% of total) 70%	Qtie-line (MVAr) -5.94 MVar

Table 3 *Simulation results for SPS settings in intact vs. contingency network with high system loading and high wind generation*

The stationary voltage stability limit is reached when the wind power exceeds 70% of the total wind capacity in Eastern Denmark. This voltage stability limit is closely related to the maximum active P_{max} and reactive power Q_{max} transfers from Radsted to the main 132 kV system and is strongly dependent on the system loading condition (high load).

One of the SPS criteria is that the reactive power transfer in the 132 kV tie-lines exceeds a critical value $Q_{tie\text{-}line}$. As to Fig.23 the critical threshold means that 10 MVAr flow from Sealand to Radsted. The reactive power flow from the main 132 kV system to Radsted is significantly reduced in case of contingency network.

The conventional SPS relies on measurement of active flow in the 132 kV tie-lines from Radsted to Sealand, as it gives a very good indication of the system loading (e.g. high active power flow to Sealand is representative for low load and high wind generation, while active power flow from Sealand to Radsted is typical for no wind and high load situation). The system protection scheme detects critical active power transfer when the 132 kV tie-lines exceed a critical value $P_{tie\text{-}line}$.

It was considered crucial to focus on identification of simple criteria for the SPS decision process that are easy to implement in a TSO control centre. A large number of advanced rules will increase the level of complexity and requirements of the SPS. A remedial control action can be issued in the SPS, if the three criteria related to reactive and active power flows as well as low voltage are fulfilled at the same time. The SPS decision process is based on the following logic:

If active power flow $P_{tie\text{-}line}$ is critical[29] *and*
monitored reactive power flow is critical
($Q_{tie\text{-}line}$ or $Q_{RAD\text{-}SVC}$ or $Q_{RAD\text{-}Nysted}$)[30] *and*
monitored voltage is low (U_{RAD} or U_{ORH} or U_{HVE})[31]

then execute a remedial control action.

Simple decision laws can be expressed for a network with high system loading and maximum wind generation in case of a single contingency (trip of the 132 kV tie-line Radsted-Orehoved) and inadequate reactive power support:

[29] 1 out of 1
[30] 1 out of 3
[31] 1 out of 3

If ($P_{tie\text{-}line}$>280 MW) and ($Q_{tie\text{-}line}$≈ -5 MVAr) and (V_{ORH} < 132.5 kV) and (V_{RAD}<133.32 kV) and (Stigsnæs is out of operation) and (violated SVC rating) **then** activate control (e.g. provide additional reactive power support).

These criteria are only representative for the studied data set for the Eastern Danish power system model. They are associated with a number of modelling assumptions and constraints for the particular network configuration. Thus the criteria can not be generalized to operational rules that are valid for arbitrary power system conditions related to different total system loading and generation. Sophisticated methods of data mining and automatic learning techniques [14] can be used to advance the decision rules.

If this investigation is to be extended to a real-time application, the design has to be refined taking into account a comprehensive set of simulation data that covers more systematically operating scenarios, contingencies and other system constraints [45]. If event-based SPS is chosen, it is rather time-consuming to identify credible contingencies and to prioritize relative impacts of all contingencies in a contingency list. As many as possible operating scenarios have to be covered systematically as events. For this purpose, a large number of time consuming calculations for single and double contingencies are required.

Alternatively, Phasor Measurement Units can be utilized in a wide-area system protection scheme. The voltage angle difference between Radsted (RAD) and Hovegård[32] (HVE) can be used as one of the inputs in the SPS. This phase angle difference gives valuable indication of active power flow in the 132 kV tie-line Radsted to Sealand.

With the two PMUs implemented in the 132 system, it is possible to gain significant input for the system protection scheme of interest (see Fig. 49). The PMUs at Radsted and Hovegård incorporate measurements of phase angle between Radsted and Hovegård, voltage magnitude at Radsted and Hovegård, active and reactive flow in outgoing lines from Radsted. Presently, the PMUs in Eastern Denmark do not record voltage at Orehoved and MVAr output from the SVC at Radsted. Besides the mentioned indicators in the SPS, it is necessary to have information about the network topology (circuit breaker status for detection of tripped equipment). The additional information can be supplied either by PMUs or by the SCADA system.

4.3 Transient analysis of power systems with wind turbines

Transmission system operators (TSOs) are defining specific requirements for grid connection of wind farms in terms of performance and control e.g. during fault situations [26]. To fulfil these requirements, careful planning and design of control and system protection are needed. One of the objectives is to maintain transient stability of the power system, which is related to the ability of each machine in the system to sustain a severe disturbance.

In this context, investigation of the “ride-through” capabilities of different wind turbine types (passive vs. active stall models, fixed speed vs. variable speed machines, etc.) plays an important role in transient stability analysis in the Eastern Danish system [27], [28]. Thus, transient stability studies are carried out in PSS/E to investigate the impact of the wind turbines to the system and vice versa. The case studies demonstrate the close relation between the ride-through capability of wind turbines and the power system impact to loss of wind generation or to reactive power imbalance under fault.

[32] HVE is used as a reference point

In principle, the transient stability phenomenon of a two-mass wind turbine model is described [31], [32] by a set of time-domain equations for motion of the wind turbine and the induction generator:

$$
\begin{aligned}
2H_G \frac{d\omega_G}{dt} &= K_S\theta_S - D_G\omega_G - T_E \\
2H_T \frac{d\omega_T}{dt} &= T_{TURB} - K_S\theta_S - D_m\omega_T \\
\frac{d\theta_S}{dt} &= \omega_0(\omega_T - \omega_G)
\end{aligned}
\tag{28}
$$

The set of equations (28) uses quantities such as turbine torque (T_{TURB}), generator torque (T_G), turbine rotor speed (ω_T) and generator rotor speed (ω_G), inertia constant for wind turbine (H_T) and generator (H_G), damping coefficient for wind turbine (D_m) and generator (D_G), shaft stiffness (K_S) and torsional twist (θ_S). Two-mass wind turbine models are appropriate for transient stability studies, since they take into account the interaction between the wind turbine mechanical and electrical system [29].

Among crucial parameters for the dynamic response of the model are the different sizes of inertia for the wind turbine and the generator as well as the degree of soft or stiff coupling between turbine and generator (shaft stiffness K_S). For appropriate integration of the wind turbine models in the dynamic simulation, correct initialization of the initial conditions is important [24]. Thus, an iterative method was used for appropriate initialising of the induction generator model CIMTR3 with respect to reactive power compensation of wind turbines.

The PSS/E simulation program uses a large-scale model of the 400 kV and 132 kV transmission systems in Eastern Denmark. The power plants are modelled with excitation and governor control, as they contribute to primary voltage and frequency control in the transmission system. Besides, the reactive power output from shunt capacitors and reactors was adjusted to the actual operating condition. Simple constant load is included in the model. The following limitations concern for the wind turbine model in the short-term transient stability study (up to 10 seconds):

- The dynamic wind turbine model uses fixed wind speed as input. Wind speed variations and power fluctuations using measured wind series are not considered to be relevant input to the wind turbine model in case of voltage stability analysis;

- The wind farms are modelled by an aggregated model, which represents each farm as a large, single wind turbine equivalent in PSS/E;

- In normal operating conditions, all wind turbines are assumed to be connected to the grid. Besides, it is assumed that all on-land and off-shore wind turbines trip in case of a fault in the transmission system. In the real operation, the off-shore wind farm Nysted 1 is designed to withstand severe faults in the system.

- Active stall control and emergency power reduction at Nysted 1 wind farm is not implemented in the model, due to lack of data.

4.3.1 Case study with Nysted 1 off-shore wind farm

In the case study, the large-scale power system model includes on-land wind turbines in the underlying distribution networks as well as the 150 MW large off-shore wind farm (Nysted 1) connected to the 132-kV system in Eastern Denmark. All wind turbines are represented by the fixed-speed passive stall wind turbine model. Steady-state and dynamic simulations are performed for the power system operated in low load (1000 MW) and high wind power (490 MW) generation on-land. The generated wind power covers about 50% of the total generation, and the rest is supplied by three central power plants (580 MW) in the main 400 kV system. No production from local combined heat and power units is taken into account. As shown in Fig. 37, the equivalent wind turbine at Nysted is connected via 30/0.69 kV and 132/30 kV transformers and a 132 kV line to the main 132 kV grid at Radsted substation (RAD). This substation is the point of common connection (PCC), i.e. the first point in the system that the wind farm shares with other customers.

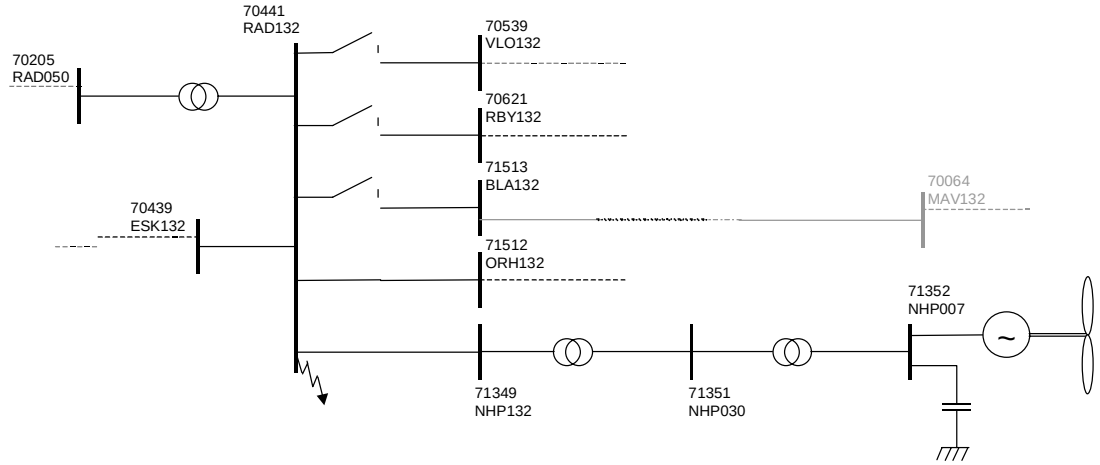

Fig. 37 Equivalent for the southern part of the 132 kV system

The power system was subjected to a three-phase short-circuit at the 132 kV busbar at Radsted substation located in the southern part of Eastern Denmark, where the transmission system is relatively weak in terms of short-circuit capacity. The impact of wind turbines on voltage stability of the Eastern Danish power system is analyzed for a base case (without stabilising control) as well as for cases with stabilising controls such as: wind turbine rejection and dynamic compensation of reactive power (application of **S**tatic **V**Ar **C**ompensators).

The base case investigates transient stability in the power system, without any stabilizing measures applied in a time frame up to 10 seconds. The wind turbine response to the 132 kV fault is monitored for a single 0.3 MW turbine near the fault location (RAD) as well as for the equivalent wind turbine representing Nysted wind farm. The voltage stability of the power system is observed at the 132 kV busbar at Radsted substation and at the wind turbine terminal at Nysted wind farm. The transient behaviour of the particular wind turbines is accessed with respect to relative speed deviation and active power output using variable fault clearance time.

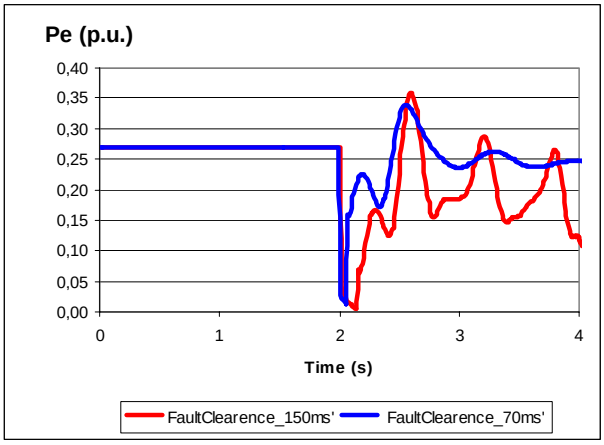

Fig. 38 Electrical power at wind turbine near Radsted, variable fault clearance time

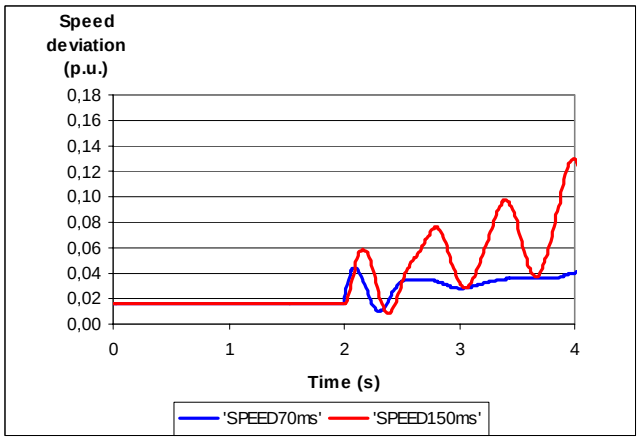

Fig. 39 Speed deviation at wind turbine near Radsted variable fault clearance time

During the 132 kV busbar fault at Radsted, the active power reduces to zero immediately followed by a large voltage decrease. If on-land wind turbines continue uninterrupted operation during and after a short-circuit fault, their induction generators will absorb reactive power from the electric system in attempt to re-establish the magnetic field between rotor and stator winding. The increase in reactive power consumption at wind turbines causes the postfault voltage at Radsted to depress further (see V_RAD curve in Fig. 42).

The electrical output for a single wind turbine near Radsted is shown in Fig. 38 for fault clearance time 70 ms and 150 ms. As expected the fast fault clearance enables active power recovery at the wind turbine. When the induction generator is subjected to e.g. a fault with 150 ms duration[33], the rotor accelerates rapidly (Fig. 39), unless precautions are taken to trip the generator from the network. The short circuit initiates torsional oscillations between the turbine and the generator, because the turbine inertia H_T is significantly larger than the generator inertia constant H_G, see equation (28).

The impact of these oscillations is observed in the postfault variation of generator speed (Fig. 39) and electrical power for fault clearance time 150 ms (Fig. 38). In case of rapid[34] fault clearance (70 ms), the speed deviation shown in Fig. 39 is limited to a postfault value that is slightly higher than the prefault value. The postfault value is caused by the weak 132 kV network and the voltage dependence of the generator torque-slip characteristic.

The simulations shown in Fig. 40 and Fig. 41 are performed in case of network without SVC and network with SVC (100 MVAr) installed at Radsted. In all cases Nysted wind farm is modelled as an equivalent passive stall wind turbine. Fig. 40 reveals the active power output from the 132 kV bus near Nysted prior and after a 100 ms fault at Radsted. In case of network without SVC, the active power at Nysted decreases to zero due to unsatisfactory voltage recovery after the fault. If no voltage control is applied immediately after the disturbance, the equivalent wind turbine generator will trip. The simulations show that the modelled Nysted wind farm is unable to withstand a temporary short-circuit due to insufficient amount of dynamic reactive power compensation in the area with large wind power penetration. This is because the power system lacks the capability to transfer reactive power from the main 132 kV system [19]. These simulations reveal that integrating 150 MW from the Nysted off-shore

[33] Typical clearance time for old relays

[34] Typical clearance time for modern relays

wind farm, and using passive stall controlled wind turbines equipped with conventional induction generators without any extra reactive power compensation (apart from the no-load consumption), are not viable due to voltage stability problems.

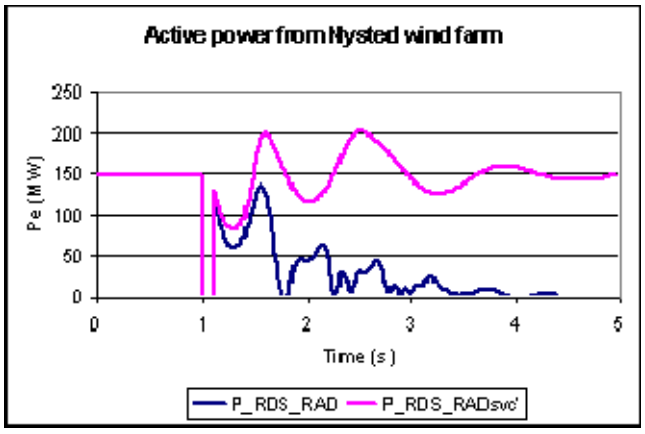

Fig. 40 Active power output at Nysted with/without SVC

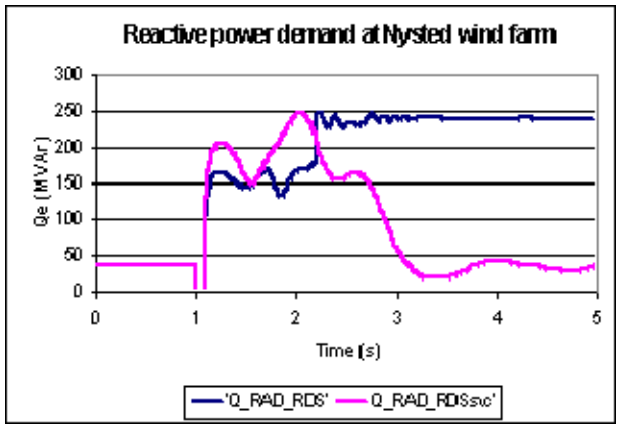

Fig. 41 Reactive power flow to Nysted with/without SVC

Fig. 41 shows that the reactive power demand to Nysted is extremely increased from 40 MVAr in normal operation to 250 MVAr after the fault clearance. This may result in voltage collapse of the power system, unless the relay protection at Nysted orders disconnection of the farm shortly after the fault occurrence. The voltage collapse at Nysted leads also to problems with voltage recovery at Radsted substation (unless appropriate voltage control is activated). Tripping of Nysted does not comply with the TSO specifications [36] that recommend uninterrupted operation of large wind farms at grid faults. The subsequent loss of about 150 MW wind power requires activation of immediate power reserves in the power system. The situation is significantly improved when dynamic compensation of reactive power is supplied by the SVC together with disconnection of a large amount of wind turbines on-land. The rejection of on-land wind turbines protects the power system from increase in reactive power demand. Fig. 41 illustrates that the additional reactive power released by the wind turbines as well as the MVAr contribution from the SVC device contributes to successful voltage and active power recovery. The postfault active power output achieves the prefault level 2 seconds after the fault is cleared.

The real off-shore farm is based on active stall wind turbines that can be ordered to reduce the active power supply to less than 20% of the rated power within 2 seconds. The accurate simulation of the active-stall wind model at Nysted is out of the scope of the present study due to lack of modelling data. The extended control features for adjustment of active and reactive power at Nysted enable the farm to withstand transmission system faults and stabilise the terminal voltage at the farm after a severe fault efficiently. Application of advanced model of Nysted wind farm is considered to be a subject of future investigations.

Fig. 42 shows the voltage magnitude at Radsted prior to and after a 100ms fault at RAD in case of no wind turbine rejection (V_RAD) and in the case where wind turbine rejection is activated alone (V_RADgenrel) or together with the SVC (V_RAD_SVCmax). Wind turbine rejection is activated in the dynamic simulation, if any of the relay settings at the wind turbine terminal is violated. The wind turbine reactive compensation units are also automatically disconnected from the network after predefined time. Relay settings for the wind turbines are enclosed in Table 5A and Table 6A, Appendix 2.

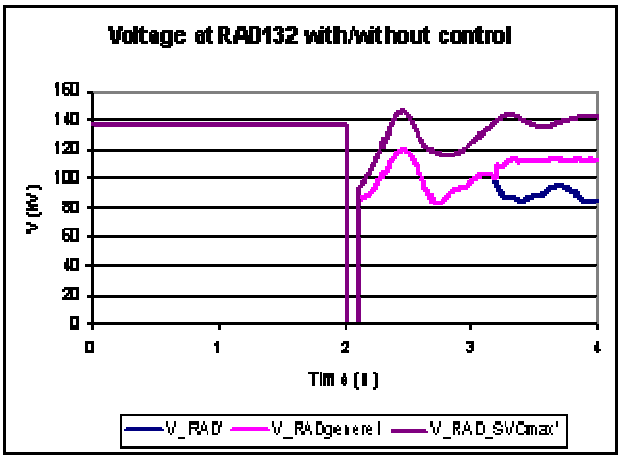

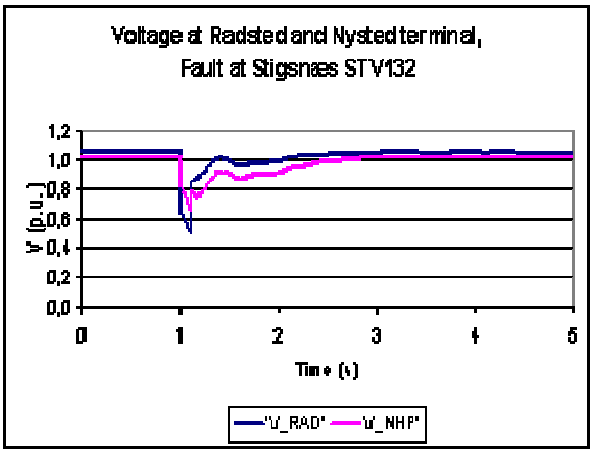

Fig. 42 Voltage at Radsted 132 kV busbar after fault at Radsted near Stigsnæs

Fig. 43 Voltage at Radsted and Nysted after 132 faul near Stigsnæs

The majority of on-land wind turbines in the southern part of the 132 kV system trip when their undervoltage threshold is reached about 1.1*s* after the system fault is cleared (see Fig. 42). The best voltage recovery is achieved using a SVC (with 100 MVAr rating), as the post-fault voltage reaches the prefault level 1 second after fault clearance. The simulated voltage curves at Radsted for the different cases (Fig.42) are compared to the voltage profile given in Fig. 44 [37]. The wind turbine rejection improves significantly the voltage recovery as the postfault voltage exceeds the acceptable level of 0.7 p.u. Besides the obvious advantage for dynamic reactive power compensation, the SVC increases the transfer capability of the 132-kV system and improves significantly the static voltage stability limit [19].

The impact of tripping of Stigsnæs power plant in the 132-kV system is shown in Fig. 43. The fault at Stigsnæs has only a moderate effect on the selected wind turbines, since the voltage at Radsted achieves an acceptable value 0.5 seconds after the fault clearance.

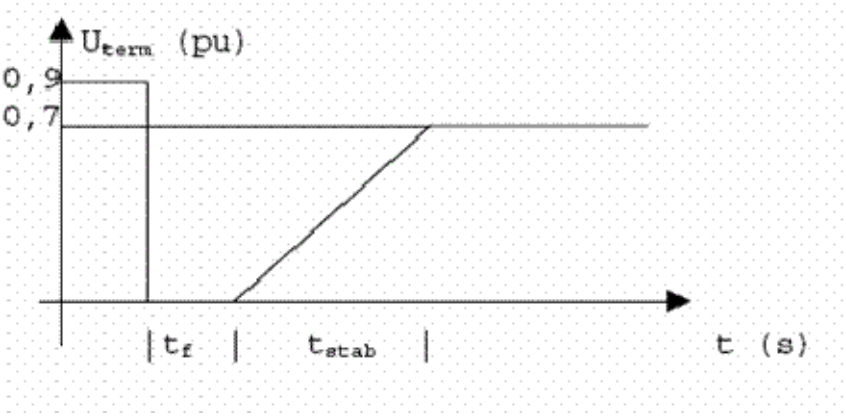

Fig. 44 Acceptable voltage profile after a three-phase short circuit [37]

The degree of rejection of on-land wind turbines for different fault durations and different reactive capability in the power system is illustrated in Table 4. The successful voltage recovery in Radsted in case of 70 ms fault clearance justifies no need for wind turbine rejection The transmission system fault cleared at 100 ms induces tripping of twice as much wind power as in the base case with insufficient reactive power capability in the power system.

CASE:	Base case		Base case with additional power plants	
Fault clearance $t_{f.c}$(ms)	t=70	t=100	t=70	t=100
Loss of wind power (MW)	0	198	0	98

Table 4 Rejection of on-land wind turbines for different cases studied

The loss of wind generation depends mainly on the fault location, wind turbine unit protection settings and the supplementary active control measures near the wind turbines. Besides the loss of power from on-land wind turbines, the simulated collapse of Nysted wind farm leads to further loss of 150 MW. The loss of maximum 348 MW (198+150) MW is not critical for active power control in the Eastern Danish power system, because it is designed to withstand a loss of 500 MW (corresponding to the largest generating unit) in the system. The disconnected wind power can be compensated with available immediate reserve in the system. Presently, it is not a serious problem to supply 348 MW in the power system in Eastern Denmark, because the Nordic system is designed to supply up to approx. 2500 MW emergency power reserve between the interconnected systems. Problems with frequency and angle stability in the overall system could appear, if the amount of rejected wind power is significantly above 348 MW.

4.3.2 Conclusion on time-domain simulations

The simulation studies describe real problems after severe disturbances in the Eastern Danish 132 kV system encountered when integrating large amounts of wind energy into a relatively weak system. To reveal these problems, a dynamic simulation model of a generic fixed-speed passive stall controlled wind turbine has been developed, verified and implemented in a complete model of the transmission system in Eastern Denmark. The case study demonstrates that the main reason for the particular problems with transient and voltage stability is seen in the characteristics of wind turbine generation. The passive stall fixed-speed wind turbines experience excessive rotor acceleration after a short circuit in the 132 kV system that may initiate uncontrollable voltage decrease and cascading outages in the transmission system. Fast fault clearance time is crucial in order to prevent fatal overspeeding and maintain wind turbine response within acceptable limits. Additional reactive power support from SVC and power plants Stigsnæs and Masnedø contributes to satisfactory voltage recovery. The remaining central power plants are not capable of maintaining the necessary voltage regulation in relation to wind power, because they are electrically distant from Radsted, and the MVAr transfer to the southern part of the 132 kV system is associated with large transmission losses. Both wind turbine rejection on-land and application of a Static VAr Compensator are effective solutions to improve reactive power capability of the system and to recover the transmission system voltage after faults.

The time-domain simulations confirm that integrating 150 MW from the Nysted off-shore wind farm, and using passive stall controlled wind turbines equipped with conventional induction generators without any extra reactive power compensation (apart from the no-load consumption) may jeopardise the power system transient and voltage stability. The results justify the need for an accurate model of the active voltage control at Nysted 1 wind farm. Additional emergency control at off-shore wind farms is considered an issue of further investigations.

4.4 Evaluation of remedial control actions

Coordination of different local reactive power controls (change of SVC set-point, automatic switching of reactors/ capacitors banks in the power system and appropriate reactive power control of wind turbines) is necessary when a large amount of wind power is introduced in the power system. This section gives a general evaluation of different remedial control actions for voltage stability. It summarizes how relevant and realistic the applicability of remedial control actions in the suggested System Protection Scheme in Eastern Denmark is. The following actions are initially considered:

4.4.1 Change of SVC set point

The case studies with SVC in the network illustrate that the power system transfer is increased for higher rating of reactive power compensation from the SVC at Radsted.

4.4.2 Wind power shedding

This remedial control is relevant in case of a limited transfer capability that constrains the wind power penetration in the system. E.g. the voltage collapse simulated in case of high system loading and maximum wind power can be avoided by ordered active power reduction at Nysted 1 and/or Nysted2 wind farms. This alternative becomes even more attractive in case of weakened network due to outage of important lines and/or generators. A severe fault (e.g. short circuit at a substation busbar or at a transmission line) can cause disconnection of a great amount of wind generation in the system, if the relay protection of the affected wind turbines is activated. The automatic disconnection of on-land wind turbines is primarily activated to protect the wind turbines from hazardous overspeeding and secondarily to avoid system-wide voltage instability. The outage of wind turbine units can be interpreted as a new contingency that introduces imbalance in active power in the system. The loss of wind generation is not critical for the Eastern Danish power system, since it can be compensated by the spinning reserve in the system. The impact of wind turbine rejection used as remedial control action to counteract voltage stability problems is illustrated in the previous section using time-domain analysis of the large-scale power system of Eastern Denmark.

4.4.3 Fast unit start-up

Activation of fast units (such as gas turbines) takes up to tens of minutes. The extra power supply is rather slow and can be used in case of risk of voltage collapse due to inappropriate generation scheduling. E.g. Masnedø gas turbine can be applied as additional short-term capacity in the system. Normally, the application of SVC is preferred for activation of the gas turbine, because the SVC at Radsted is closer to the area of local consumption. The gas turbine is more likely being used for emergency active power. The gas turbine can be a helpful remedial control action for reactive power support in a stressed or weakened network. In practise, this unit has limited application as a voltage control device due to design constraints.

4.4.4 Automatic reactive shunt compensation

Undervoltage control can be achieved by automatic disconnection of shunt reactors and connection of capacitor banks in selected substations. In practice, this is considered to be a cheap solution with a great availability, but the speed of response of the stepwise implementation of capacitors is rather slow [43]. The frequent connections and disconnections of the shunts lead to aging of the circuit breakers and the shunts. The ability to support voltage by capacitor

banks is poor in case of decreasing voltage magnitude, since the reactive power output of the units is dependent on the square of the applied voltage.

4.4.5 Emergency control of OLTC

Blocking of OLTC is used in many utilities to reduce the severity of voltage decrease and to preserve long-term voltage stability in stressed situations. This control action is not a common practise in Eastern Denmark. In general, tap changers are used to supply the voltage on the LV side of distribution transformers within a certain range. As load increases and the LV side voltage tends to decrease, the OLTC will raise the tap position in order to restore the load voltage to an acceptable value. When the system is close to voltage collapse, the current flow in the system is increased to maintain the load demand, which leads to further reduction of system voltage. The general effect depends on the type of load characteristics and degree of shunt compensation in the system. In an alert state, it is necessary to adjust the voltage set-point of OLTC, typically by returning to pre-defined settings. Normally, the OLTC transformers operate on local criteria and independent of each other. Besides local OLTC blocking, coordinated or centralised schemes can be performed:

- Local blocking schemes apply voltage relays with appropriate time delays to detect low voltage level at a substation;

- Coordinated blocking schemes use a number of independent undervoltage schemes in different substations; or

- Centralised schemes consist of interconnected undervoltage relays implemented in various substations within a region. The scheme detects low voltage pattern at key substations and is highly dependent upon the communication system from the substations to a central location, where the collected data are analysed, and based upon the central decision making-process, OLTC at affected substations in the region blocking is activated.

4.4.6 Undervoltage load shedding

Undervoltage load shedding is used to reduce load in the area with uncontrolled low-voltage levels as the last alternative to preserve the system voltage stability in extreme situations. Shedding of proper amount of load on certain locations (drop in predefined load areas) is recommended as the last option to restore acceptable voltage profile, if all other control solutions have failed. The scheme of undervoltage relays recognises impeding voltage decrease, which is below a pre-set threshold value during the time of few seconds and orders trip of a (circuit breaker to a) feeder. After the electricity supply to a certain amount of load is interrupted, the voltage is expected to recover to an acceptable value. The effect of undervoltage load shedding is extremely dependent upon the choice of load location and type of load to be shed [50].

4.4.7 Automatic Generation Control (AGC) actions

The objective of AGC is to ensure generation interchange between power areas according to the scheduled values. This task is performed by control of a reference set point of a selected group of generators in the power system. The action of AGC under normal conditions is limited in the individual area of generation. During abnormal operation, the area affected by mismatch between generation and load can be relieved using changes in AGC set points from other generation areas. This feature is presently not available in Eastern Denmark, because it

is rather slow in comparison with the primary frequency control, which also overrides this system.

4.4.8 HVDC emergency control

In general, the application of HVDC links is used for active power emergency control in the Nordic power system. The HVDC link between Eastern Denmark and Germany (Kontek) is based on conventional HVDC transmission using thyristor technology. In exceptional situations, the conventional HVDC link can deliver reactive power support by adjusting the setup point of the capacitive filters at the end stations. The capability of Kontek as voltage control device is though limited due to power quality problems (i.e. signal distortion due to significant harmonics content). The possibilities of reactive power control in normal and emergency situations are improved if HVDC transmission links based on voltage source converters technology[35] are available. This kind of HVDC links is not implemented in Eastern Denmark. Reference [35] discusses the advantages and drawbacks of this concept as especially attractive in case of integration of large wind farms in a weak transmission system.

4.5 Conclusion on SPS against voltage instability

The simulation studies reveal that the existing 132-kV transmission system in Eastern Denmark is rather weak and prone to voltage stability problems because of its limited reactive power control capability and the large distance to the large generating units. The problems with voltage stability are caused by the characteristic of wind turbine generation as well as the inability of the power system to meet the reactive power demand in case of high system loading. The stationary simulations show that voltage collapse occurs in Eastern Denmark, if two large off-shore wind farms near Nysted are to be integrated in the existing heavily loaded system without any reinforcements or improvements in the SVC rating.

The long-term solution is to invest in radical reinforcements of the existing 400 kV and 132-kV system, if Nysted 2 (200 MW) is to be integrated in the future system. E.g. the transfer capacity of the system can be significantly extended by introduction of a new 132 kV line from Vestlolland to Stigsnæs power plant and/or by upgrades of a number of existing 132 kV cable sections [17]. The reinforcements are considered to be the most expensive alternative, so if the power system is to be operated close to its voltage stability limit, additional equipment and control measures and/or especially dedicated system protection schemes become necessary.

The Ph.D. project suggests a simple System Protection Scheme as means to mitigate the voltage instability problems associated with large-scale wind generation in the heavily loaded system. The SPS design is especially dedicated to detect abnormal system conditions in due time and, if necessary, to give warning in case of voltage instability. The achieved SPS criteria are valid only for the limited simulation data set related to an intact network and network with a single line outage.

The SPS criteria detect violation of voltage stability limits. The SPS reveals the critical impact of wind power in the Radsted corridor using critical active power flow in the tie-lines (alternatively phase angle Radsted-Hovegård), critical reactive power flow in tie-lines, violation of SVC output and low local voltages. The simulation analysis reveals that reactive power flows are the best indicators for voltage instability. The voltage deviation is not a sufficient criterion

[35] Known as HVDC light concept

for impeding voltage collapse problems, because local deficit of reactive power is not necessarily associated with large voltage decrease. This is especially evident in the simulation of high load and high wind generation in the system.

The dynamic impact of wind turbines in the power system is approached using time-domain simulations. The studies show that it is a difficult task to achieve a compromise between the conflicting requirements between ride-through capability of wind turbines and wind turbine rejections, which counteract voltage instability in the power system. Fast fault clearance time is crucial for preserving the ride-through capability of fixed speed passive stall wind turbines. Possible voltage quality problems in wind farms may be overcome by selecting an appropriate wind turbine type, and/or adjusting wind turbine control parameters. Accurate representation of active control at Nysted off-shore wind farm is an important issue of future investigations.

Usually, it is preferred to keep as many wind turbines as possible in normal operation, but on the other hand wind turbine rejection helps to preserve voltage stability in contingency situations. The compromise between wind turbine rejection (rapid tripping of on-land wind turbines) and the lack of tripping facility for off-shore wind generation is a serious challenge in power system operation. In case of emergency, wind power shedding can be used as SPS control action in relation to reduction of the total wind generation. Both ordered rejection of on-land wind turbine and regulation of off-shore wind farms are possible solutions to avoid voltage collapse. The precise amount of wind generation to be shed is a subject of future investigations.

The reactive power support from the SVC at Radsted is evaluated as valuable measure for local reactive power balance in steady-state operation. The SVC serves also as an effective dynamic compensation device in case of power system disturbances. Change in SVC set point can be used as SPS remedial control action. Hence, the crucial issue in the SPS design is to apply appropriate settings for reactive power rating of the SVC device.

Gas turbine start-up at Masnedø is an attractive solution for reactive power support during contingencies. The gas turbine is normally used for emergency active power, but its performance is not fast enough. Rescheduling power plants and voltage regulation at remote generators (reactive power adjustment) are not considered the most effective measures, because they are associated with large reactive power losses in the transmission system. Stigsnæs power plant could possibly improve the reactive power support in emergency situations, as it is the closest power plant in the southern part of the system.

5 Phasor measurements

Traditionally, phase angles could not be measured due to difficulties with time synchronisation of measurement devices. Phasor Measurement Units (PMUs) introduce a unique opportunity to utilize synchronised phasors (magnitudes and phase angles) at different substations. This chapter describes the technology of synchronized phasor measurements and its potential uses in power system monitoring, protection and control. The principles of synchronized phasor measurements are reviewed, followed by a description of PMUs. The PMU data analyses illustrate the benefits of applying phasor measurements in disturbance monitoring.

5.1 Theory of synchronized phasor measurements

Phasors are useful in analysing the power system performance when the operating conditions are in steady state (pure sinusoidal signal) or the waveforms change rapidly. In general, phasors are specified either as a complex value (consisting of a real and an imaginary part) or an RMS value and a phase angle of a sinusoidal signal.

The waveform related to a phasor is sampled by the measurement system continuously, and each time a new sample is acquired, new phasor data are obtained with a data window including the latest sample [59]. In a digital measuring system, samples of the waveform for a nominal period are collected starting at time t=0. Then the fundamental frequency component of the Discrete Fourier Transform (DFT) is calculated according to the relation:

$$X = \frac{\sqrt{2}}{N} \sum_{k=1}^{N} x_k \cdot e^{-j2k\pi / N} \tag{29}$$

where N is the number of samples in one period
X is the phasor
x_k are the samples of the waveform.

When applying the DFT calculation, aliasing errors in the input waveform have to be eliminated using anti-aliasing filters. That means that the signal must not contain frequency above the Nyquist rate $N \cdot f_0$. Harmonics in the input signal that are not multiples of fundamental frequency f_0 are treated as noise. In this case, the influence of the harmonics has to be eliminated in order to calculate correctly the 50 Hz component of the signal.

The positive sequence phasor X_1 is computed from the measured phase values X_a, X_b and X_c according to its definition:

$$X_1 = \frac{1}{3}\left(X_a + a X_b + a^2 X_c\right) \tag{30}$$

where $a = e^{j\,2\pi/3}$

For the majority of applications, the positive sequence representation of phasors is sufficient to describe the behaviour of the power system. The negative and zero sequence can be calculated if needed to analyse asymmetries in three phase measurements. The positive sequence voltage and current phasors are used to calculate complex quantities of active and reactive power as follows:

$$\overline{S} = \sqrt{3} \cdot (\mathrm{Re}\{U\} + j\,\mathrm{Im}\{U\}) \cdot (\mathrm{Re}\{I\} + j\,\mathrm{Im}\{I\})^* \tag{31}$$

$$\begin{aligned} \overline{S} &= \sqrt{3} \cdot \overline{U} \cdot \overline{I}^* = \sqrt{3} \cdot U \cdot e^{j\theta} \cdot I \cdot e^{j(-\psi)} = \sqrt{3} \cdot UI \cdot e^{j(\theta-\psi)} \\ \overline{S} &= \sqrt{3} \cdot (U \cdot \cos\theta + jU \cdot \sin\theta)(I \cdot \cos\psi - jI \cdot \sin\psi) \end{aligned} \tag{32}$$

$$\begin{aligned} \overline{S} = P + jQ = \sqrt{3} \cdot (&U\cos\theta \cdot I\cos\psi + U\sin\theta \cdot I\sin\psi) + \\ &j\sqrt{3} \cdot (U\sin\theta \cdot I\cos\psi - U\cos\theta \cdot I\sin\psi) \end{aligned} \tag{33}$$

$$\begin{aligned} P &= \sqrt{3} \cdot (U\cos\theta \cdot I\cos\psi + U\sin\theta \cdot I\sin\psi) \\ Q &= \sqrt{3} \cdot (U\sin\theta \cdot I\cos\psi - U\cos\theta \cdot I\sin\psi) \end{aligned} \tag{34}$$

The PMU illustrated in Fig. 45 utilizes the Global Positioning System (GPS) to provide timing signals to synchronize sampling of all input signals. Phasor values can be computed related to a global reference with a precision of less than one microsecond [58]. PMUs that rely on satellite-based GPS clocks, give the opportunity of real-time monitoring of phasor measurements

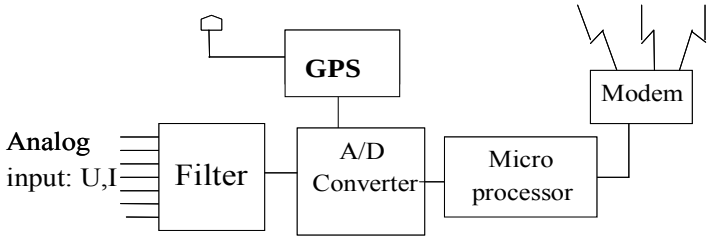

Fig. 45 Phasor Measurement Unit diagram

Measurements from widely separated locations in the power system can be synchronized at a common time reference and collected at a central location, see Fig. 46. PMUs placed on strategic buses in the network and communicating with a control centre form a Wide Area Measurement system (WAMS) [70]. Using PMUs, detailed information about the actual operational status of the power system can be preserved in a precise way. The most promising feature here is utilization of PMUs as angle comparator devices. Synchronized phasor measurements can be used as an efficient tool both in warning of abnormal system conditions in due time and in analysis of critical events after severe disturbances in the power system. By synchronizing the sampling processes for different signals - which may be hundreds of km away - it is possible to put their phasors in the same diagram.

The first category of PMU applications is related to the advanced power system monitoring. The basic motivation is to gain faster and more reliable on-line knowledge about the power system state that would reduce uncertainties with regard to determination of operating limits and congestion management. The second category of PMU applications focuses on system protection and control.

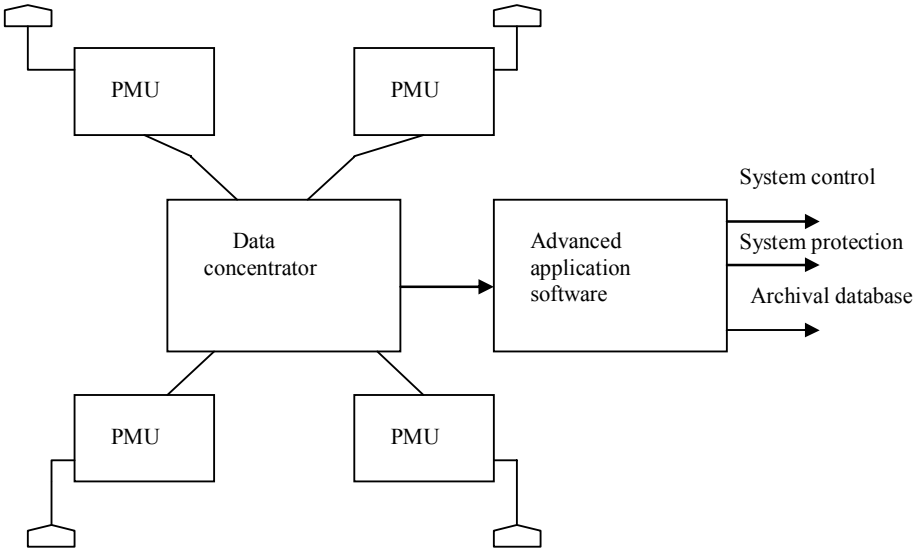

Fig. 46 Wide Area Measurement System

The pioneering work on synchronized phasor measurements was documented in a large number of publications [60], [74] and [84]. The early experiences on the first PMU prototypes are summarized in a number of reports from the North American Wide Area Measurements (WAMS) project [75]. State-of-the-art projects and recent advances of WAMS and PMU applications in system protection such as Wide Area Control Systems (WACS) can be found in reference [4]. Presently, a number of commercial PMU devices are available at the market either in form of a stand-alone unit [67] or as relays, where the PMU function is integrated in e.g. advanced distance relays. The recent trend is to manufacture intelligent devices that incorporate both monitoring and control. Besides, some digital fault recorders have a supplementary PMU module to the conventional power swings detection. The early experiences with phasor measurements world-wide and the future potential for wide-area measurement systems in the Nordic countries are elaborated in reference [65]. The recent developments in PMUs and PMU based applications world-wide are reviewed in reference [66]. PMU prototypes are used for research and development activities at a number of universities [64].

5.1.1 Phasor measurements applications

The traditional estimation of system states (voltage magnitudes and angles) employs a State Estimation (SE) procedure that extracts the system states from a measurement set such as voltage magnitudes, line active and reactive power flows. As a pre-requisite of the state estimation, the power system topology and its admittance matrix have to be known. However, the measurement set is biased by various types of measurement errors that have additive nature. The conventional state estimators are associated with a number of difficulties such as change of network parameters over time, aging of devices etc. In order to reveal the actual operating conditions, the network topology needs to be updated automatically or manually dependent on the switching status of the device (e.g. line outage due to service or contingency). Also new components installed in the network have to be entered into the SE system. Typical disadvantages of remote telemetric units used for state estimation in transmission networks are different origins (vendors, age etc.) as well as different accuracies and, most importantly, sampling frequencies. The key issue is the fact that traditional state estimators “align” measurements that have been taken in different time instants and the calculated snapshot of the system state is based on this incoherent data set.

PMU-based state estimators are time stamped, since they represent a snapshot of the system operation. They can be implemented locally and on a wide area system level. On-line measuring of the state of the power system with synchronised phasor measurements collected at a central location provides effective and accurate monitoring of the actual operating state of the power system.

Two approaches for state estimation tools with PMUs are distinguished. The first approach suggests complete observability of the power system state independently from the SCADA/EMS system. Experiences from system studies [71] show that at least one fourth of the system buses have to be provided by PMUs in order to obtain complete observability needed for correct PMU-based state estimation of power systems. A number of methods for PMU placement for complete and incomplete observability using graph theoretic approach are available in literature [72].

The required number of PMUs can be reduced by intentionally creating unobservable regions in the power system. The most probable approach is to start with a few PMU units and then increase the number of PMUs in stages until satisfactory observability is reached. The number of PMUs depends on the predefined depth of unobservability related to the buses, where phasor quantities are not directly measured nor derived indirectly.

The principle for "depth of unobservability" is illustrated in Fig. 47, which shows an arbitrary 7-bus network with generator buses (B and G) and load buses (A, C, X, E and F). Buses B and F are equipped with PMU units (directly observable buses), indirectly observable buses are A, C, E and G. At each of the four buses, the attached bus voltages and current injections for these buses are known. The unknown currents can be calculated using Kirchhoff's law for sum of currents at a bus. The unknown voltage can be calculated as voltage drop across a line using the information at the neighbouring buses. Bus X is unobservable, as its parameters can not be determined from the known parameters for the neighbouring buses. Optimum positioning strategies for PMUs are based on a prioritised list of location sites so that the area of observability and controllability will expand uniformly as more sites are included. Redundant measurements are required in order to represent more correctly critical dynamics of the investigated power system as well as to improve the measuring accuracy. In general, the planning of minimum number of PMUs is dependent upon the investigated dynamic phenomena and the choice of representative locations for the PMUs depends on the application objective, network size and characteristics, as well as communication and data transfer constraints.

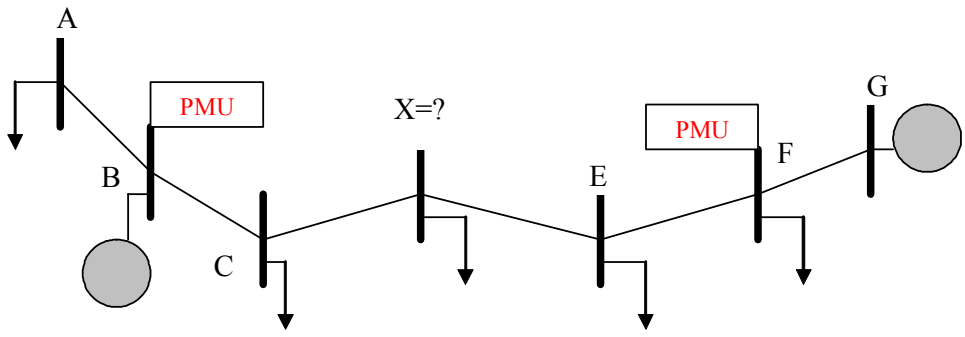

Fig. 47 Depth-one observability

The second approach for state estimation is to combine synchronized phasor measurements with SCADA[36] measurements in a hybrid state estimator with few PMUs. PMU measurements from a limited number of widely dispersed locations in the power system can be used to improve the conventional state estimator based on SCADA system.

The mixture of PMU and SCADA measurements can be used for simpler, more robust and more accurate state estimation than the present SE implementations. The practical application is associated with lower costs of installation, operation and maintenance, but it requires hardware and software changes in the existing monitoring system.

On the hardware side, PMUs can easily be integrated within the conventional SCADA system as any other measurement device i.e. RTU (Remote Telemetry Unit). The biggest challenge is on the software side, as PMUs imply modification of the state estimation algorithm and its implementation. It is believed that in near future PMUs can provide data to commercial state estimators [11].

Another category of PMU applications enables more accurate design for monitoring and control system tools. It includes improved design of automatic controllers e.g. Power System Stabilizers (PSS) and other generator controllers, Static VAr Compensators (SVC), High Voltage Direct Current (HVDC) and Flexible AC Transmission (FACT)s devices as well as system protection schemes and emergency control.

Phasor measurements, either directly or through state estimators, can provide the necessary input to develop and implement system protection schemes. In both cases, the objective is to improve the power system performance and to increase the transfer capacity. Future perspectives for application of phasor measurements in system protection are documented in references [8], [12] and [13].

5.2 Phasor measurements in Eastern Denmark

5.2.1 Experimental PMU prototype

The PMUs are low-cost units built at The Technical University of Denmark, and are based on an industrial PC design with analogue and digital I/O card and a GPS clock especially designed for timing purposes rather than positioning [68]. The UTC time has global simultaneity, and phases measured with this reference are comparable even if they are measured hundreds or thousands of kilometres apart. The uncertainty in phasor measurements is due to measurement errors in magnitude and phase shift of the conventional voltage and current transformers used in the transmission system.

The experimental PMU prototype shown in Fig. 48 is used for real-time phasor measurements in Eastern Denmark. The following section describes some overall considerations about planning of PMU placement and utilization of phasor measurements in the transmission network of Eastern Denmark. The focus is placed on application of phasor measurements in disturbance monitoring.

[36] Supervisory Control And Data Acquisition

Fig. 48 PMU installation at substation Asnæs

5.2.2 Planning of the measurement system

The PMU locations in Eastern Denmark are planned at widely separated strategic points in the transmission system in order to observe significant 400 kV and 132 kV transmission corridors under different operational condition (outage of lines, generators, network islanding etc.). PMUs are placed on system buses with available communication facilities. Thus, the PMU prototypes are placed in three strategic buses, i.e. Asnæs (400/132 kV), Hovegård (400/132 kV) and Radsted (132/50 kV) substations.

Asnæs (ASV) substation has a key power generating unit, Radsted (RAD) is the central point with regard to concentration of wind turbines, and Hovegård (HVE) is chosen as a strong point that terminates the interconnection to Sweden. The geographical location of Hovegård is near Copenhagen (the load centre), where a number of central power plants are also placed. HVE is considered a reference PMU for the relative voltage phase angles in ASV and RAD.

The geographical location of the PMUs in the Eastern Danish transmission system is presented in Fig. 49. Each PMU unit measures frequency, positive sequence voltage and a number of positive sequence currents from outgoing lines in the substation of interest. The positive sequence values are calculated from the respective three phase quantities. Fig. 50 illustrates schematically the PMU network, while the overview with PMU measured quantities is enclosed in Table 5. Appendix 3 contains further details about PMU input signals.

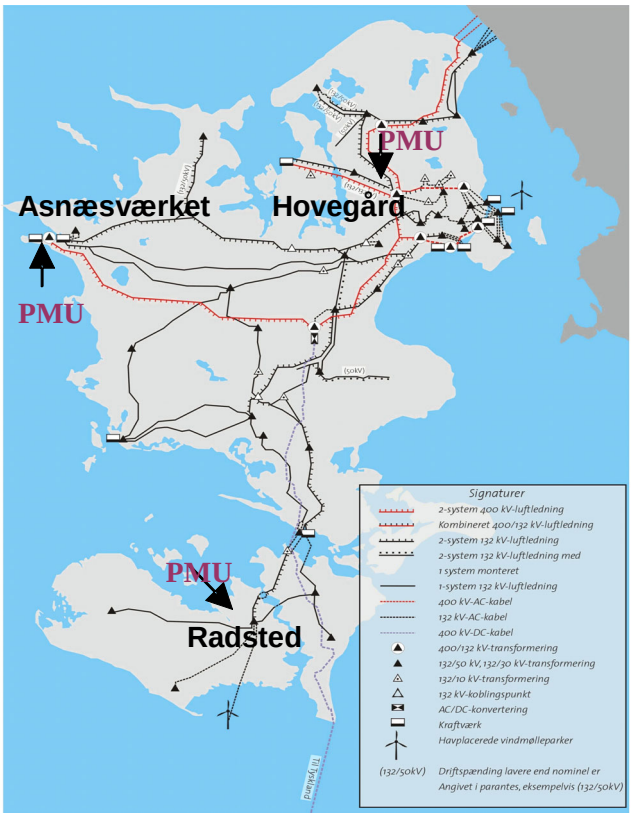

Fig. 49 *The 400 kV and 132 kV system with PMUs in Eastern Denmark*

The three PMU units collect data continuously and store them in a circular buffer. This means that irrelevant data will eventually be overwritten unless they are selected for more permanent storage. Measurements from the three locations in Eastern Denmark are synchronized at a common time reference and collected at a central location at DTU.

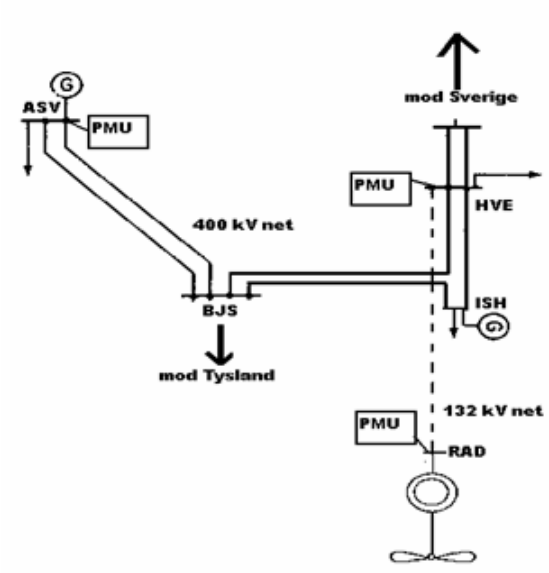

Fig. 50 *Schematic diagram of the PMU network in Eastern Denmark*

	PMU anal	ASV400	HVE400	HVE132	RAD132
1	V (kV)	UASV	UHVE400	UHVE132	URAD
2	Θ (deg)	ΘASV	ΘHVE400	ΘHVE13	ΘRAD
3	I1 (kA)	IASV-BJS1	IHVE-SAN		IRAD-RDS
4	ψ1 (deg)	ψASV-BJS1	ψHVE-SAN		ψRAD-RDS
5	I2 (kA)	IASV-BJS2	IHVE-GØR		IRAD-VLO
6	ψ2 (deg)	ψASV-BJS2	ψHVE-GØR		ψRAD-VLO
7	I3 (kA)	IASV400/132			IRAD-BLA
8	ψ3 (deg)	ψASV400/132			ψRAD-BLA
9	I4 (kA)				IRAD-ORH
10	ψ4 (deg)				ψRAD-ORH
11	Δ f (Hz)	fASV	fHVE400	fHVE132	fRAD
12	df/dt	fASV/dt	fHVE/dt	fHVE/dt	fRAD/dt

Table 5 Overview of PMU measurements in Eastern Denmark

In the future, the process of data selection should be controlled automatically by means of triggering logic in each PMU unit and at the phasor data concentrator. PMUs are expected to preserve detailed information about the actual operational status and to record severe disturbances in the power system of interest. The PMUs could reveal power system dynamics related to different system stability problems. The suggested PMU at Radsted captures phasor data for analysis of potential voltage stability problems in the southern part of the Eastern Danish power system.

5.3 PMU data analysis

The section starts with a general introduction to the power oscillation phenomena in power systems, since the central case study is related to power oscillations monitoring using a commercial PMU prototype from ABB [67]. The case presents comparisons between real-time PMU recordings and results from dynamic PSS/E simulations that reproduce the power system event. The other case studies are based on phasor data from the PMU prototypes developed at the Technical University of Denmark. The PMU data are used for off-line analysis of a number of severe disturbances in the Eastern Danish power system.

5.3.1 Power oscillations analysis in interconnected systems

Inter-area power oscillations are dependent on the power system response to small disturbances, such as change in scheduled generation or small increase in system load. These electro-mechanical oscillations in interconnected power systems are manifested by an exchange in mechanical kinetic energy between groups of generators as electric power flows through the transmission system. Using the analogy between electrical and mechanical systems, the number of generator masses in each power system can be represented by the inertia of the generators, while the electric transmission lines constitute the network of elastic springs connecting the generator masses.

The power system in Fig. 51 illustrates a two-area model of major generation/load areas connected by a tie-line [77]. In large systems, the power flow P in tie-lines is described by equation (35), where the line reactance is denoted by X, while U_1, U_2, δ_1 and δ_2 are the magnitudes and angles of the voltages at the line terminals.

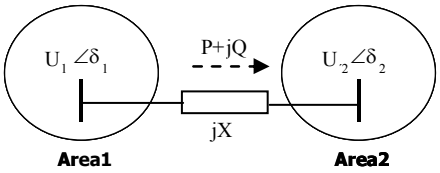

$$P = \frac{U_1 \cdot U_2}{X} \sin\left(\delta_1 - \delta_2\right) \tag{35}$$

Fig. 51 Power oscillations involving two areas.

In the following section, the theoretical background for tie-line oscillations is approached using the concept for small signal stability [76], [78]. In general, the dynamics of power oscillations can be analysed using the small-signal stability method. The theoretical study is conducted for an ideal unregulated multi-machine power system. The power system has been perturbed from a steady-state condition introducing small changes of system quantities such as power and machine angle ($\Delta\delta$).

The equation of motion for an ideal single synchronous machine in a multi-machine system is given by the well-known swing equation:

$$\frac{2H_i}{\omega_R} \cdot \frac{d^2\delta_i}{dt^2} = P_{m,i} - P_{e,i} \tag{36}$$

$P_{m,i}$ and $P_{e,i}$ in (36) denote the mechanical and electrical power output of machine *i,* with electrical angle δ_i and inertia constant H_i, *while* ω_R (rad) is rated system frequency.

The electrical power $P_{e,i}$ into node *i* for an n-machine system is given by the following expression:

$$P_{ei} = E_i^2 G_{ii} + \sum_{\substack{j=1 \\ j \neq i}}^{n} E_i E_j (B_{ij} \sin \delta_{ij} + G_{ij} \cos \delta_{ij}) \tag{37}$$

where

$$\delta_{ij} = \delta_i - \delta_j$$
$$\overline{Y}_{ii} = G_{ii} + jB_{ii}$$
$$\overline{Y}_{ij} = G_{ij} + jB_{ij}$$

$\overline{Y}_{ii}$ and $\overline{Y}_{ij}$ are a diagonal and an off-diagonal element of the respective network short-circuit admittance matrix Y.

Ei is constant voltage behind transient reactance for machine i
Ej is constant voltage behind transient reactance for machine j.

It is assumed that the power system has been perturbed from a steady-state condition introducing small changes of system quantities such as machine angle and power.

$$\delta_i = \delta_{0j} + \Delta\delta_i$$
$$P_{ej} = P_{oj} + \Delta P_{ej}$$
$$P_{mj} = P_{moj} \tag{38}$$

The increment $\Delta P_{e,i}$ of electric output of machine *i* is obtained as a derivative of eq. (38) with respect to δ_{ij}.

$$\Delta P_{ei} = \sum_{j=1}^{n} E_i E_j \left(B_{ij} \cos \delta_{ij0} - G_{ij} \sin \delta_{ij0} \right) \cdot \Delta \delta_{ij}$$
$$\Delta P_{ei} = \sum_{j=1}^{n} P_{sij} \Delta \delta_{ij} \tag{39}$$

$$P_{sij} = \left. \frac{\partial P_{ei}}{\partial \delta_{ij}} \right]_{\delta_{ij0}} = E_i E_j \left(B_{ij} \cos \delta_{ij0} - G_{ij} \sin \delta_{ij0} \right)$$

for (40)

P_{sij} is a synchronizing power coefficient. It stands for the change in electrical power in machine *i* due to angle change between machines i and j, with all other machine angles held constant.

$$\frac{2H_i}{\omega_R}\cdot\frac{d^2(\Delta\delta_i)}{dt^2}+\Delta P_{e,i}=0 \tag{41}$$

The linearized version of the swing equation is divided by the factor $2H_i/\omega_R$, and the expression for $\Delta P_{e,i}$ is inserted. The differential is then solved with respect to $\Delta\delta_i$ using Taylor series expansion about the initial point ($\delta_{o,i}$).

$$\frac{d^2(\Delta\delta_i)}{dt^2}+\frac{\omega_R}{2H_i}\cdot\sum_{\substack{j=1\\ j\neq i}}^{n}P_{sij}\Delta\delta_{ij}=0 \qquad \text{for } i=1,2,\ldots n \tag{42}$$

The set of (n-1) independent second-order differential equations (44) can be modified to a set of 2(n-1) first-order differential equations by subtracting the equations for n^{th} and i^{th} machine. For $\Delta\delta_{ij}=\Delta\delta_{in}-\Delta\delta_{jn}$ the linearized system equations attain the following form:

$$\frac{d^2(\Delta\delta_{in})}{dt^2}+\sum_{j=1}^{n-1}\alpha_{ij}\Delta\delta_{jn}=0 \qquad i=1,2\ldots n \tag{43}$$

The state-space representation of the power system from Fig. 51 is used to obtain the free response of the system.

$$\begin{bmatrix} \frac{d(\Delta\delta_{1n})}{dt} \\ \frac{d(\Delta\delta_{2n})}{dt} \\ \frac{d(\Delta\ddot{\delta}_{(n-1)n})}{dt} \\ \frac{d^2(\Delta\delta_{1n})}{dt^2} \\ \frac{d^2(\Delta\delta_{2n})}{dt^2} \\ \frac{d^2(\Delta\ddot{\delta}_{(n-1)n})}{dt^2} \end{bmatrix} = \begin{bmatrix} 0 & 0 & 0 & 0 & 1 & 0 & .. & 0 \\ 0 & 0 & 0 & 0 & 0 & 1 & .. & 0 \\ 0 & 0 & 0 & 0 & .. & .. & .. & .. \\ 0 & 0 & 0 & 0 & 0 & 0 & .. & 1 \\ A_{11} & A_{12} & .. & A_{1,n-1} & 0 & 0 & 0 & 0 \\ A_{21} & A_{22} & .. & A_{2,n-1} & 0 & 0 & 0 & 0 \\ .. & .. & .. & .. & 0 & 0 & 0 & 0 \\ A_{n-1,1} & A_{n-1,2} & .. & A_{n-1,n-1} & 0 & 0 & 0 & 0 \end{bmatrix} \cdot \begin{bmatrix} \Delta\delta_{1n} \\ \Delta\delta_{12} \\ .. \\ \Delta\delta_{(n-1)n} \\ \frac{d(\Delta\delta_{1n})}{dt} \\ \frac{d(\Delta\delta_{2n})}{dt} \\ \frac{d(\Delta\ddot{\delta}_{(n-1)n})}{dt} \end{bmatrix} \tag{44}$$

The A matrix coefficients are calculated as:

$$A_{ii}=-\sum_{\substack{j=1\\ j\neq i}}^{n}\frac{\omega_R}{2H_i}P_{sij}-\frac{\omega_R}{2H_n}P_{sni}$$

$$A_{ij}=\frac{\omega_R}{2H_i}P_{sij}-\frac{\omega_R}{2H_n}P_{snj} \tag{45}$$

In general, computation of eigenvalues in large power systems is a complex task, since it involves a systematic procedure for simultaneous solution of differential equations representing synchronous machines with associated prime movers, excitation systems and Power System Stabilizers (PSS), extensive transmission networks, load dynamics, power electronic devices

(such as HVDC links, SVC) etc. Analysis of inter-area oscillations in large interconnected power systems requires comprehensive off-line studies, such as eigenvalue analysis and dynamic simulations using a detailed model of the entire system including a wide range of non-linear devices [80]. E.g. the identification of Nordic system modes is to a great extent dependent upon the actual configuration of the interconnected power systems [81]. It means that detailed information about a number of machines in operation (system inertias), the impedance path of the tie-lines and the transmission corridors (transmission stiffness between the inertias) is the key issue for determination of oscillation modes associated with a particular eigen-frequency and damping. A more effective way to observe inter-area oscillation modes and system damping is using phasor measurements from PMUs [79]. Future perspective of real-time phasor data is seen in developing tools for detecting and preventing dynamic problems rather than simply analyzing critical power system events. The application of synchronized phasor measurements for, e.g., validation of power system models used in stability studies, is seen as having a great potential in the future.

5.3.1.1 Case 1: Power oscillations, April 2002

The advantage of phasor measurements for detection of power oscillations is discussed in the papers [62], [63]. The full version of the paper is enclosed in Appendix 1. The Nordic system shown in Fig. 52 consists of synchronized power systems in Norway, Finland, Eastern Denmark and Sweden. The installed capacity of the Nordic system is about 90 GW (including 4360 MW total installed capacity in Eastern Denmark), while the Nordic peak load is approx. 60 GW (2870 MW peak load in Eastern Denmark).

Fig. 52 The transmission system of the Nordic countries

The transmission system of Eastern Denmark (Fig. 54) consists of 132 kV and 400 kV lines as well as the interconnections with South Sweden and Germany. The link to Germany is a 400-kV DC interconnection with a transmission capacity of 600 MW. The link to Sweden also serves as an interconnection in the Nordic system. The interconnection to Sweden consists of four AC links terminated at Söderåsen - two 400-kV and two 132-kV cable systems with a total transfer capacity of some 1600 MW (before Gørløse). The 400-kV system includes a double 400-kV tie-line connection (red dotted lines in Fig. 53) between substation Hovegård (HVE) in Denmark and Söderåsen (SAN) in Sweden. The 132-kV tie-line (shown by black dotted lines in Fig. 53) is terminated at Mörarp (MRP) in Sweden and Teglstrupgård substation (TEG) in Denmark. MEQ represents a local load equivalent in Sweden.

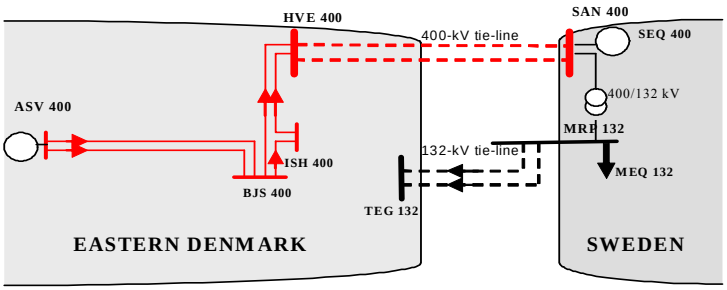

Fig. 53 *Two-area model of interconnected power systems*

The power system event studied is a planned outage of the 400-kV tie-lines between Söderåsen and Hovegård substations. The lines were deliberately disconnected during a 3-week period in April 2002 due to connection of a new substation in the 400-kV transmission system. Due to market and effect balance constrains during the outage period, the power transfer was deliberately limited to 100 MW (import or export to Sweden) compared to some 1600 MW at normal conditions.

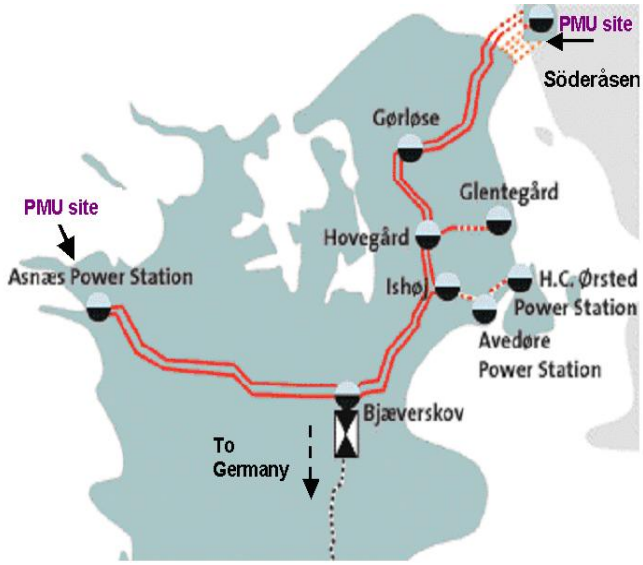

Fig. 54 *The 400-kV transmission system in Eastern Denmark.*

The outage of the 400-kV tie-line appeared as a small disturbance that weakened the Eastern Danish power system and excited power oscillations in the interconnected power systems.

The disconnection of the 400-kV tie-lines between Eastern Denmark and Sweden can be understood as decoupling of an important spring in the interconnected system followed by fluctuating forces in the other springs (transmission lines). Power oscillations occurred on the tie-lines connecting different groups of machines as a result of temporary unbalance between power input and output.

During this event, prototype PMUs gave the opportunity of real- time monitoring of positive sequence voltage and current phasors using satellite-based Global Positioning System (GPS). Two sets of synchronized phasor measurements have been performed during the planned outage of the double 400-kV tie-line between Eastern Denmark and Southern Sweden. One PMU was placed at Asnæs Power Station (ASV) and another PMU 200 km apart at Söderåsen substation (SAN), Sweden. The two PMU prototypes, ABB RES 521 PMU β version, were commissioned independently of each other at Asnæs Power Station (ASV) and Söderåsen substation (SAN) in Southern Sweden in order to record frequency and positive sequence phasor quantities such as 400-kV busbar voltages, currents in 400/132 kV transformers and currents in outgoing 132 kV lines at the respective locations, which are 200 km apart.

The voltage and current phasor values were sampled every 20 ms and synchronized using time transmissions from the GPS satellites. The recordings were stored on a PC near the PMUs during the 3-week period in April 2002. After normal operation was re-established, the data from the remote substations were aligned according to a common time reference. The synchronized recordings at ASV and SAN were compared directly due to the fact that the voltage and current measurements are assigned the same time stamp and phase reference supplied by GPS clock. The accuracy of phasor measurements [79] is quoted:

- Frequency accuracy ± 0.005 Hz
- Angle value accuracy ± 0.1 deg

The measurement accuracy of phasors is primarily caused by transducers at transmission level. In general, the precision of the synchronization is up to 1 µs, which introduces a negligible measurement error in phase angles. The measurement accuracy of phasors is primarily caused by transducers at transmission level. In general, the precision of the synchronization is up to 1 µs, which introduces a negligible measurement error in phase angles.

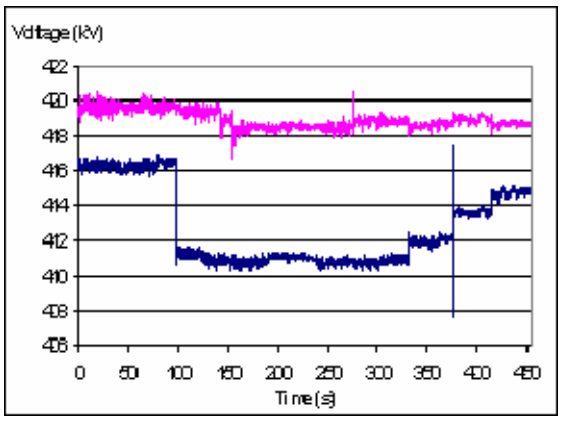

Fig. 55 Voltage measured at SAN and ASV

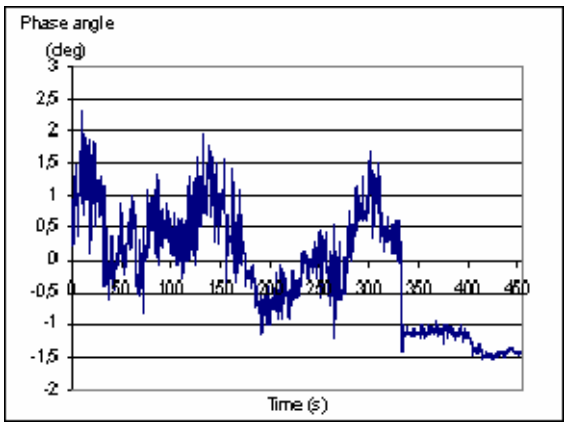

Fig. 56 Phase angle difference measured between SAN and ASV

The upper curve in Fig. 55 indicates the measured voltage at ASV, where the voltage variations are limited within 2 kV due to the voltage regulation at the power plant. The lower curve shows the voltage magnitude at SAN during the reconnection sequence, which is presented on Fig. 55 as the lower curve. The voltage decrease after 90 s was caused by the connection of a 150 MVAr reactor in SAN. The first 400-kV tie line was energized from the Danish side, and the line reconnection to Sweden was completed at 330 s. The second 400-kV line inserted at SAN gave rise to a transient peak at 370 s. Subsequently, the voltage builds up until the second line reconnection is completed at about 400 s.

The phase angle dynamics (Fig. 56) reproduce accurately the dynamic behaviour of the Eastern Danish power system with respect to the Swedish interconnection. A phase shift of about 1.3 deg. occurs after the first 400-kV connection is established at 330 s. Due to the reconnection of the second 400-kV tie-line, the voltage angle difference between ASV and SAN is further decreased, and the oscillation was stabilized to lower amplitude at about 400 s. The weakened system with a 400 kV outage shows evident oscillation in the relative phase angle between SAN and ASV busbars in comparison to the angle oscillation in intact network. The recorded disturbance had a small effect on the power system resulting in a moderate phase shift. The recorded phase shift of 1.3 deg. is within the phase angle accuracy, which according to the PMU manufacturer is quoted to be 0.1 degrees. Thus, the presented recordings can not be used as a benchmark case nor generalised for a number of sudden disturbances or outages.

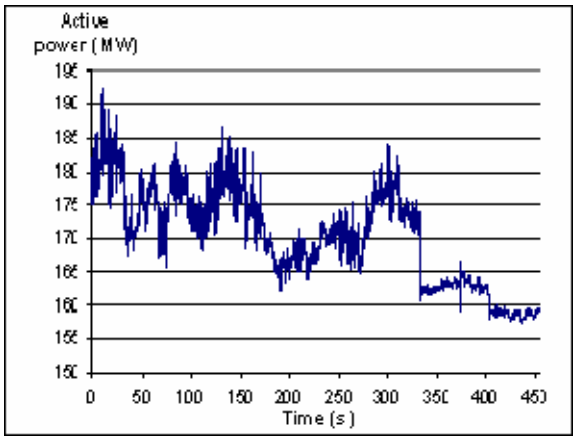

Fig. 57 *Active power flow in from MRP in the 132-kV tie-line*

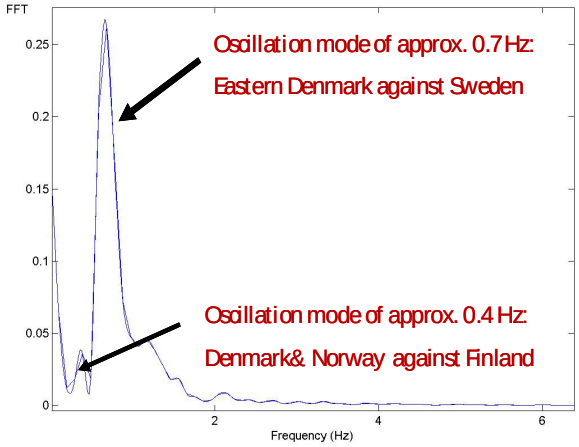

Fig. 58 *Spectral analysis of tie-line flow*

The relative change in phase angle between SAN and ASV during the tie-line outage affected power oscillations, which were superimposed on the stationary line flow in the power system [41]. The correlation between the change in tie-line power flow (Fig. 57) and difference in voltage phase angles (Fig. 56) is obvious, which is evidently described by equation (37). The power flow in the tie-line was computed using the 132 kV voltage and current phasor measurements at SAN. Fig. 57 shows that prior to the 400-kV tie-line connection, power swings were excited between the systems interconnected via a double 132-kV line only. The active power flow in the 132-kV interconnection was reduced by 10 MW immediately after the double 400-kV tie-line was taken into operation. Afterwards, it was observed that the power swings were damped sufficiently, and finally the system was settled down to equilibrium.

A harmonic analysis of the active power flow on the 132-kV tie-line was performed after the switching event (t >330 s) using the FFT function in Matlab® Signal Processing Toolbox. Inter-area oscillation modes of the Nordic system are identified in the low frequency range (0.1-1.0) Hz, see Fig. 58. The largest peak reveals a dominant eigenfrequency of about 0.7 Hz

corresponding to the oscillation mode between Sweden and Eastern Denmark [69]. A less distinct peak is evident at a frequency of about 0.4 Hz, which is related to an oscillation mode involving all the generators in the Nordic system, where Denmark and Norway swing against Finland.

The measured frequency variation at SAN substation is given in Fig. 59. The rapid frequency transients at 330 s and 370 s are caused by reconnection of the first and the second 400-kV line at SAN, where the frequency is also registered. The graph of the respective frequency at ASV is not depicted, as it follows the same trend as SAN due to the strong 400-kV connection between ASV and SAN measuring locations.

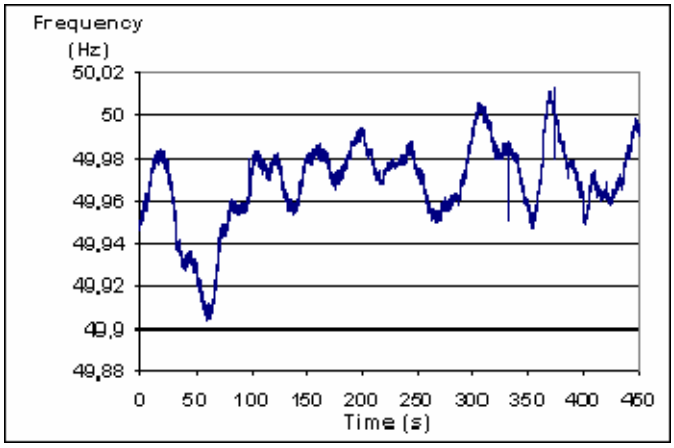

Fig. 59 *Frequency measured at SAN substation*

The main features from the simulation analysis are successfully verified by corresponding synchronized phasor measurements. The objective of the simulation analysis in the PSS/E[37] program was to reproduce the behaviour of the Eastern Danish transmission system during the reconnection of the double 400-kV tie-line. Static and dynamic simulation of the reconnection sequence was performed using a detailed power system model for Eastern Denmark with a simplified representation of the Swedish grid equivalent. To make the reference load flow case as exact as possible, the initial conditions for the 400 kV and 132 kV power system are based on actual data for generation dispatch and transfers to Sweden and zero transfer to Germany, which are captured by the control centre at the Transmission System Operator of Eastern Denmark.

Steady-state initial condition: During the actual situation in April 2002 the power system was not severely stressed as the tie-line transfer was low and the total system load was about 65% of the maximum winter load. For the load flow calculation, the Swedish generator equivalent is accounted as a slack node with a zero phase angle. The power transfer with Sweden is rather low compared to the transfer limit in normal operation, because it is set intentionally as a precaution measure against wide-spread disturbance. This initial condition is characterized by a small phase angle change (about 0.5 deg) between ASV and SAN substations. The small initial angles are indeed indicative for a strong and lightly loaded system.

The power plant at Asnæs (ASV) delivers about 244 MW via the 400 kV lines towards HVE station, which is electrically close to the load centre near Copenhagen. After the reconnection of the 400-kV tie-line, the steady-state phase angle difference between ASV and SAN is slightly changed to about 1,3 deg., and about 10 MW are transmitted via the 400- kV tie-line

[37] Power System Simulator for Engineering® from Power Technologies, Inc. (PTI).

HVE-SAN. The active power towards 132-kV busbar MRP was reduced by the same amount of power. In the intact network, the active power from MRP supplies mainly the local load at MEQ, and the remaining active power is directed to Denmark via the 132-kV tie-line MRP-TEG.

The dynamic simulation in PSS/E presumes steady-state initial condition prior to the reconnection of the 400-kV tie-lines. Each power plant generator was presented together with a power system stabilizer, a detailed governor model and excitation model. The line impedances and bus loads are represented using lumped constant parameters. Further, switching shunts and voltage control at specified points in the 400-kV and 132-kV transmission network were considered in the dynamic simulations.

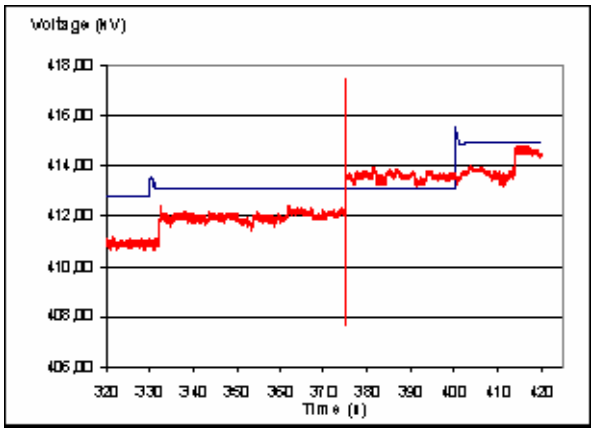

Fig. 60 *Simulated vs. measured voltage at SAN*

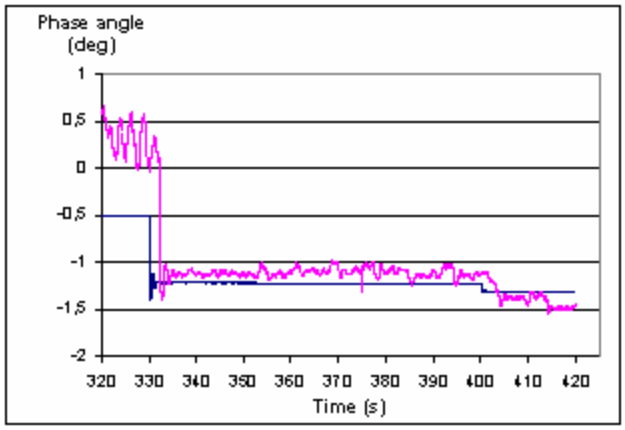

Fig. 61 *Simulated vs. measured angle difference between SAN and ASV*

The voltage magnitude at SAN was simulated during a 100-second period, under the assumption that each 400-kV tie-line is re-energized simultaneously at both ends. Starting from a 413 kV initial value, the voltage at SAN increases in steps after reconnecting the first line (330 s) and second 400-kV tie-line (400 s), see Fig. 60. When the SAN voltage is stabilized, it attains a final value of 415 kV, which corresponds exactly to the average measured value for the intact network in Fig. 55.

Analogous to the measured curve, the calculated difference in voltage angles between SAN and ASV is illustrated in Fig. 61. A characteristic shift of about - 0.9 deg. is registered immediately after the simulated reconnection of the first line (330 s), while the subsequent line connection (400 s) results in a minor shift in the relative phase angle. The simulated post-disturbance value of relative phase angle after 400 s is relatively close to the corresponding measured quantity. Fig. 61 reveals a discrepancy of some 0.75 deg. during the disturbance in the period 320-330 s. This initial difference is caused by inexact representation of the Swedish network equivalent and the uncertainty of the load situation in Sweden at the particular condition. The measured oscillatory behaviour in both phase angle and power flow prior to the switching event is most likely caused by internal impacts from Swedish generators.

A complete match between the simulated and the monitored system conditions is a difficult task due to some discrepancies between the pre-fault load flow in the simulation and the actual conditions prevailing in the power system. The main reason is the fact that the system loads are not exactly known at the time when the phasor measurements were realized. The simulated post-disturbance value of 162 MW is about 2 MW higher than the corresponding value measured as average in the intact network.

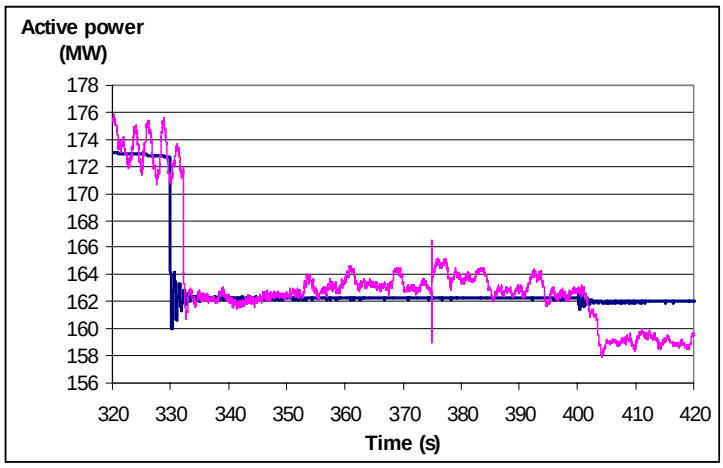

Fig. 62 Simulated (black) vs. active power flow (pink) measured from MRP

The simulated active flow at 330 s is about 13 MW less than the initial value of 173 MW, which is in good correspondence with the shift observed at the corresponding point in the measured curve. The simulated power flow in the 132-kV tie-line (Fig. 62) is in good agreement with the actual measured power flow during the reconnection sequence. The recorded active power oscillations prior to the switching event are not considered critical, since they are damped successfully in the intact network. This discrepancy results are caused by the fact that the exact operating situation in the entire power system is not precisely known.

The case study presents one of the first phasor measurements applications in the Nordic transmission system during a disturbance. Synchronized phasor measurements were used as a valuable tool in post-disturbance analysis during the switching of a 400-kV tie-line between Eastern Denmark and Sweden.

Two ABB RES 521 PMU β prototypes provided a simultaneous system-wide data set, e.g. tie-line power flow and dynamics in the voltage phase angles. The voltage and current phasors at the 400 and 132-kV buses reproduced the dynamic behaviour of the Eastern Danish power system with respect to the Swedish interconnection. Due to the high precision of synchronization using GPS with sampling accuracy up to 1 μs, the introduced error is considered negligible. Though the presented recordings can not be used as a benchmark case nor generalised for a number of sudden disturbances or outages.

Inter-area oscillation modes were easily detected from the positive sequence phasors. The PMU data revealed valuable information about low frequency oscillation of a group of machines within a large area (Sweden) against the neighbouring area (Eastern Denmark). This approach is more convenient than computation of eigenvalues using a detailed model of a specific network configuration.

The case study demonstrates that the recorded power system response is consistent with the simulation results. The simplified model of the Swedish power system was insufficient for detailed simulation of power swings. A more precise simulation of power oscillations was difficult due to the limited availability of a detailed small signal stability model for the Nordic system.

5.3.1.2 CASE 2: Power oscillations 11. March 2005

A reactor outage in the PMU monitored substation Hovegård (04:52 h) caused tripping of a number of outgoing lines including one of the 400 kV tie-lines between Eastern Denmark and Sweden (Hovegård-Söderåsen). The connection to Sweden was limited to the 400 kV tie-line Gørløse-Sweden and the double 132 kV tie-line Mörarp-Teglstrup. The event weakened the system, and at 06:15 h introduced power oscillations between Sweden and Denmark involving oscillations at several generating units near the fault location.

After the critical 400 kV line outages, the central power plants were rescheduled, and the generation capacity was limited to maximum 350 MW per production unit. The transfer to/from Sweden was constrained to 100 MW in both directions. Since the 400 kV busbar was de-energized, the PMU analysis uses available voltage recordings from the 132 kV busbar at Hovegård besides the recordings from Asnæs and Radsted substation. In addition, these phasor measurements are documented in a case study in reference [83].

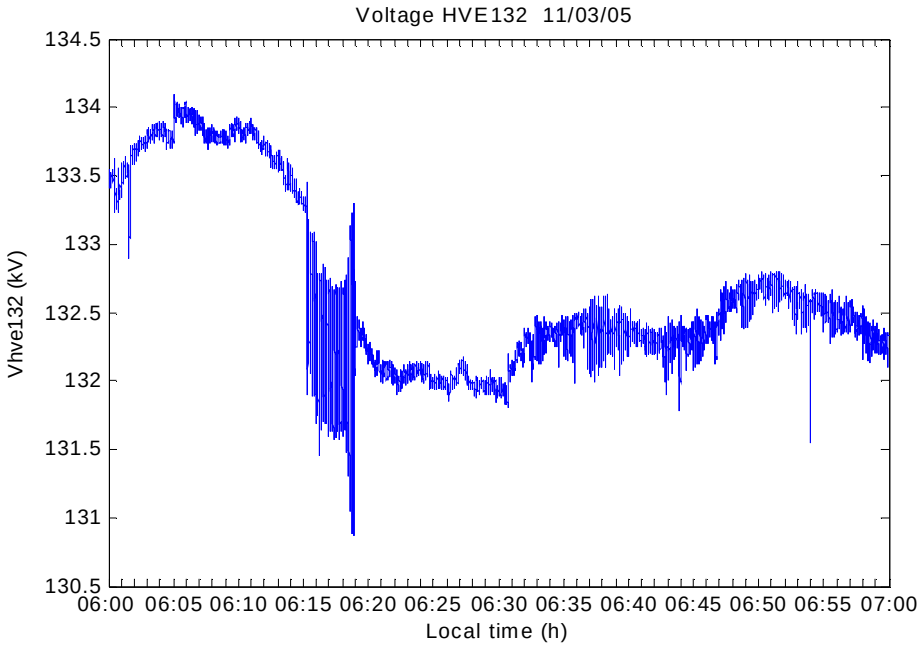

Fig. 63 PMU measurement of voltage at 132 kV busbar at Hovegård

The 132 kV voltage magnitude at HVE (Fig. 63) has decreasing trend in the interval 06:05-06:20h, but it smoothens after the system stabilizes. The power oscillations are clearly visible, when the voltage was zoomed in a 10-minute window (Fig. 64). Here it is seen that the oscillations are characterized by an almost constant magnitude in the first three minutes. The magnitude of oscillations increases as a result of reduced power system damping. The undamped oscillations are terminated at 06:19h after the affected generation unit(s) were disconnected from the system.

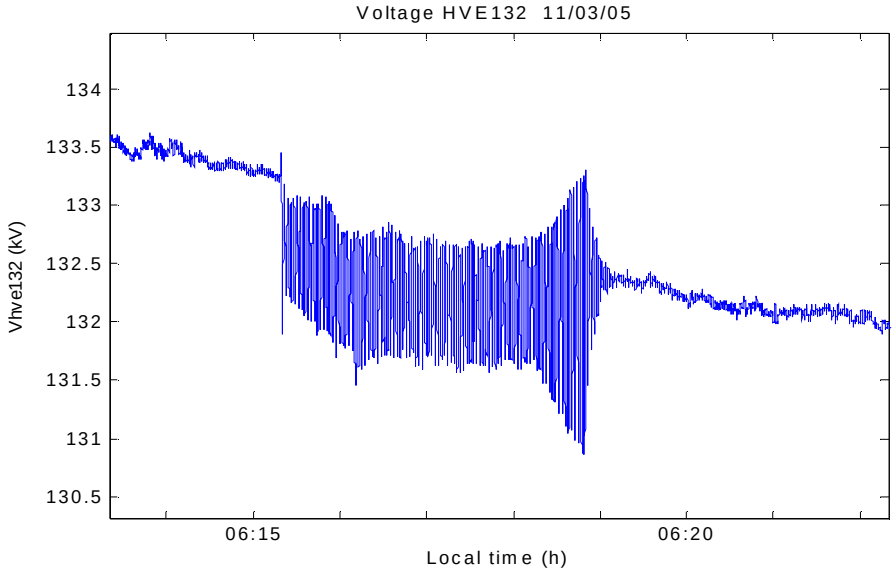

Fig. 64 Zoom of voltage recording in the interval 06:13-06:22h

As seen from the power spectrum plot in Fig. 65, the power oscillations were associated with a frequency mode of approx. 0.5 Hz. The undamped oscillations with frequency mode of 0.5 Hz are superimposed to the ordinary 50 Hz frequency variations shown in Fig. 66.

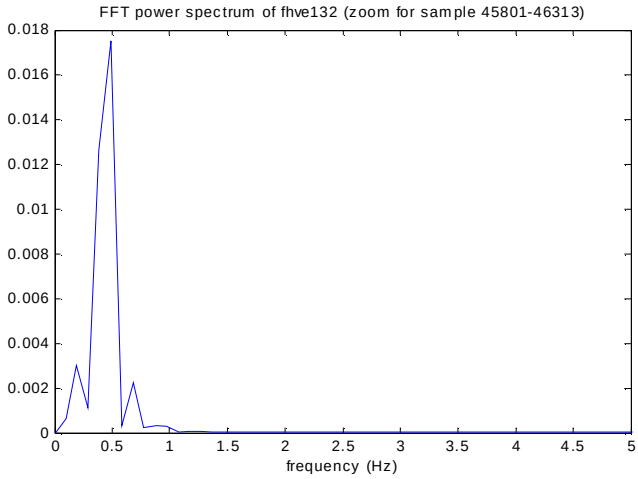

Fig. 65 FFT analysis of power oscillations

Until 06:30 h, the system frequency experiences a decreasing trend, but afterwards it changes to increasing frequency. The variation in the 50 Hz frequency signal is most likely caused by the temporary limitation in tie-line transfer from/to Sweden as well as the ordered regulation of some generation units in Eastern Denmark.

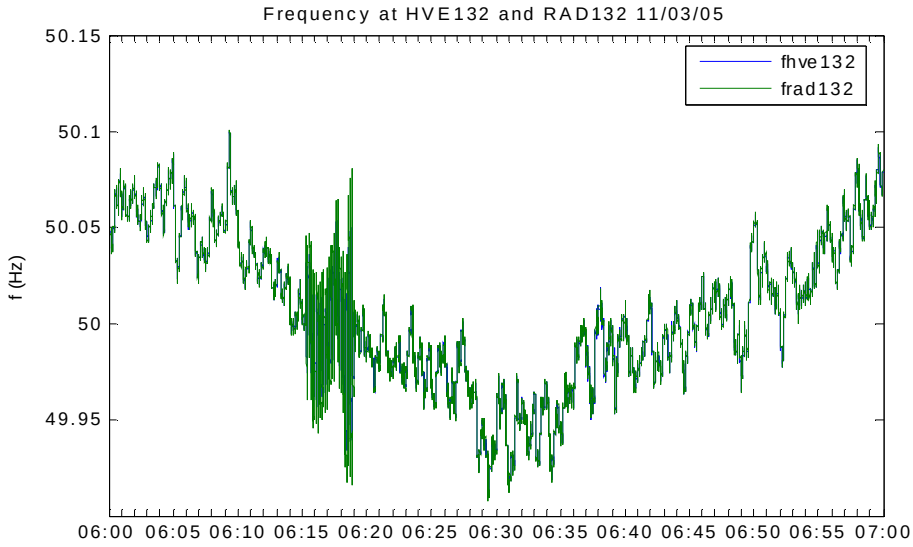

Fig. 66 Frequency measured at 132 kV buses Radsted and Hovegård

E.g. the production at Asnæs power plant is reduced from approx. 480 MW to 320 MW, which is obvious in the PMU recording of the active power flow at one of the outgoing 400 kV lines from Asnæs to Bjæverskov (Fig. 67). In the period (06:15-06:19 h), the monitored active power flow in the 400 kV line Asnæs- Bjæverskov and in the 132 kV line Radsted-Orehoved reveal undamped oscillations.

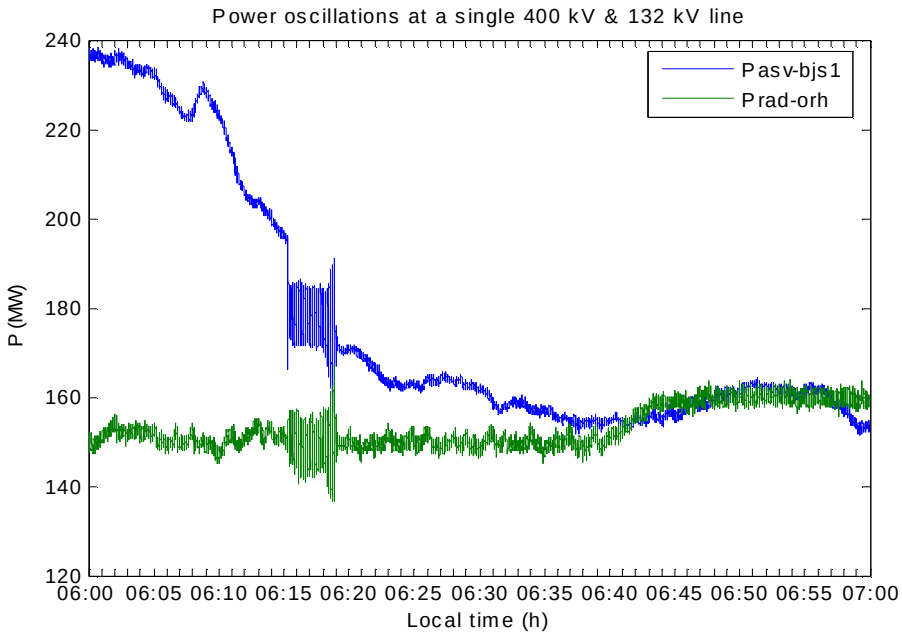

Fig. 67 Active power flow in 400 kV line ASV-BJS1 and 132 kV line RAD-ORH

The average magnitude of oscillation for both line flows is about 13 MW which is superimposed as variation in the active power. The plot for RAD-ORH shows that the wind power transfer from Radsted towards Sealand was not changed drastically as it remains about 150 MW until 06:40 h and up to 160 MW afterwards. This is due to the large electrical distance from Radsted and Nysted to Hovegård substation, where a number of adjacent 400 kV lines tripped.

Fig. 68 presents the respective recordings for the phase angle differences: Asnæs400-Hovegård132 (ASV400-HVE132) and Radsted132-Hovegård132 (RAD132-HVE132). In both phase angle recordings ASV400-HVE132 and RAD132-HVE132, a sudden increase of 4-5 degrees is evident at 06:15 h. In on-line PMU applications, the phase shift can be used to give warning about intensive power oscillations in the system.

The recent information provided by PMUs (such as phase angles, critical power flow in transmission lines, system frequency and power oscillation modes and damping) can be further utilized in systematic identification of power oscillations in Eastern Denmark. In the future, PMUs can provide a valuable input for a new System Protection Scheme that counteracts impeding problems with power oscillations in the Nordic power system.

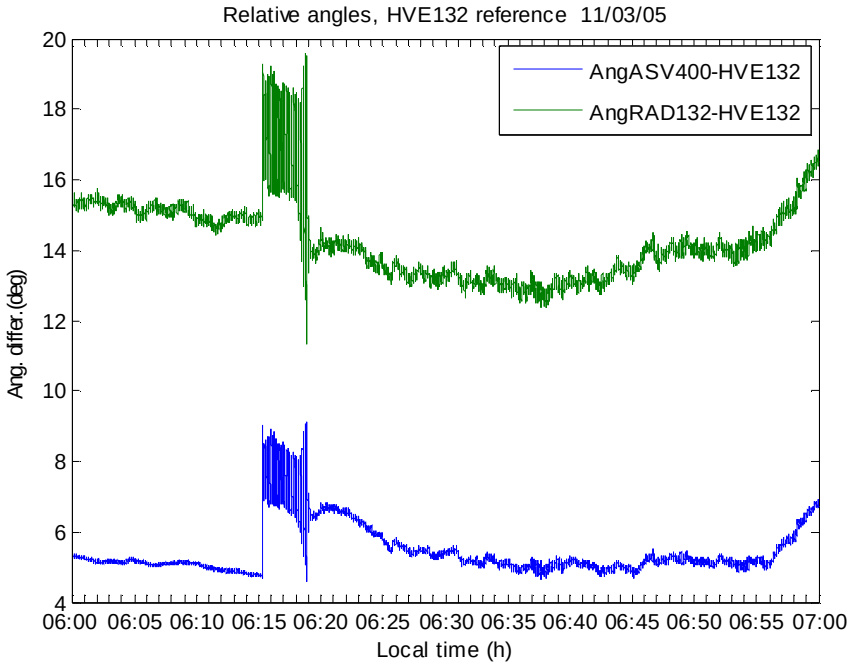

Fig. 68 Angle difference recordings ASV400-HVE132 and RAD132- HVE132

E.g. the scheme can be designed as an automatic solution able to detect an important tie-line outage that excites power oscillations in the Nordic system. If necessary, the SPS can issue remedial control actions such as HVDC modulation, set point change of Power System Stabilizers PSS, generation trip etc. The design of such system protection can be a subject of future work.

5.3.2 Case 3: Wind power impact, hurricane 08/01/2005

The hurricane on 8 January 2005 caused massive disconnection of wind turbines all around Eastern Denmark, because all wind turbines in the region are designed to trip from the network when the wind speed exceeds 25 m/s. The rejection of the Nysted wind turbines was captured using both SCADA and PMU recordings for the day. The PMU recordings of the rejection of Nysted wind farm are plotted for a one-hour period (13-14 h). The plot in Fig. 69 shows that around 13:30 h the generation at Nysted was reduced from 156 MW to 0 MW within 5 minutes. The respective wind turbines in the wind farm trip subsequently when the maximum wind speed limit is reached. After 10 minutes, the wind farm attempted to reconnect in the system, but without any success, and the wind farm is tripped again at about 14: 50h.

The PMU plots during this abnormal operating condition are compared to the corresponding data identified in the 24 h (1 minute sampling) SCADA measurements for 08/01/05. Both the PMU and the SCADA measurements show that Nysted wind farm was controlled to zero production due to extremely high wind.

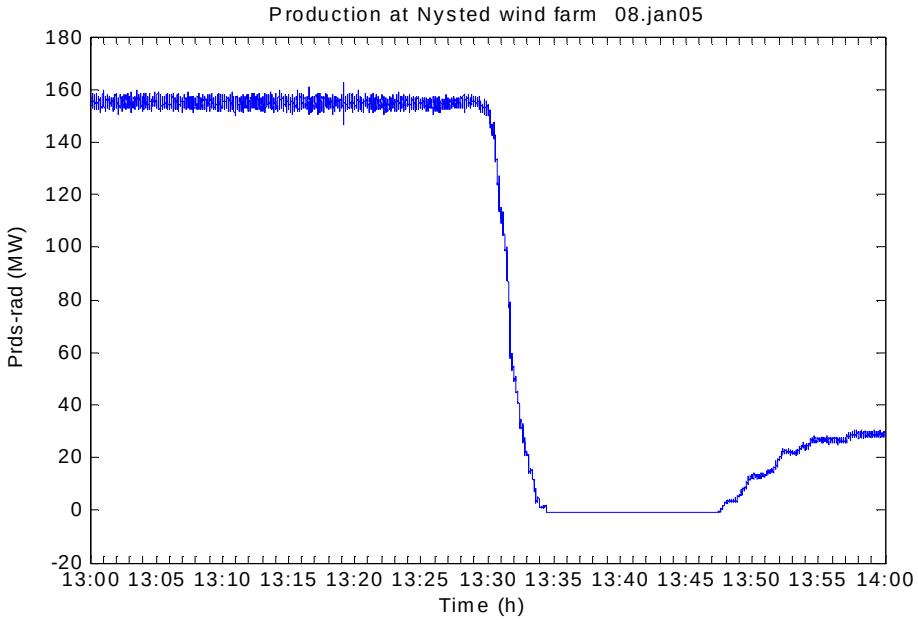

Fig. 69 Active power production at Nysted wind farm

The benefit of using phasor measurements instead of SCADA measurements is the better sampling and the time synchronization of different PMUs. The frequency and phase angle data give a more dynamic picture of the event. Fig. 70 shows that Nysted wind farm was disconnected from the network in 400 minutes (6,7 hours).

The unsuccessful re-connection sequence of up to 50 MW wind generation is also obvious at the SCADA plot. Due to extreme wind conditions, all affected wind turbines in Nysted tripped again after 80 minutes. The reactive power flow has opposite direction (from Radsted to Nysted) compared to the direction of active power flow (from Nysted wind farm to Radsted). The transfer of 40 MVAr is necessary to cover the reactive power losses in the 132/ 30 kV transformer and the 132 kV connection to Nysted.

At the particular day of interest, the total consumption was swinging between approx. 1400 MW (50% of the winter peak load) in the morning, until 2000 MW in the afternoon (70% of the winter peak). That day, about one third of the load consumption in Eastern Denmark was covered by approx. 620 MW wind power, as Stigsnæsværket and Masnedø were not in operation. The loss of significant wind generation introduced temporary imbalance in active power. The system maintained an acceptable frequency using emergency power control.

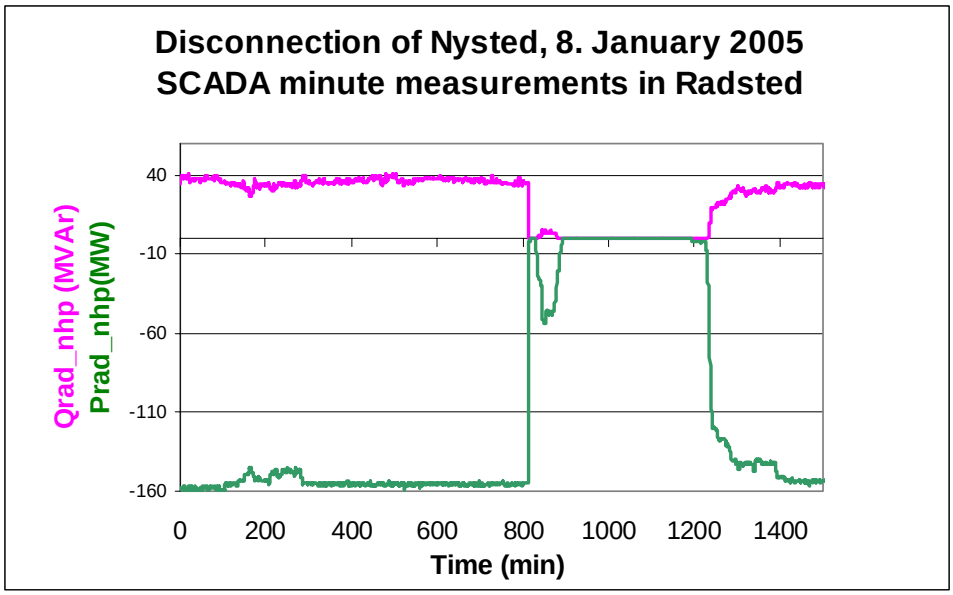

Fig. 70 *SCADA recording of active and reactive power flow from Radsted to Nysted*

The positive value of the recorded phase angle difference between Radsted and Hovegård indicates power transfers in the northern direction (from Radsted to the main 132 kV system), see Fig. 71. The phase angle curve corresponds to the respective active power flows at e.g. lines Radsted-Orehoved and Radsted-Blangslev. The consequence of sudden angle increase around 13:10 h is not evident in Fig. 69 as it is influenced by the increased reactive (and active) power demand from Sealand to Radsted (Fig. 73).

The phase angle difference was decreased gradually at 13:30h which is incidental with the downwards regulation of the wind generation. As 155 MW wind generation was removed, the angle difference was reduced from 11 to 4 degrees. The final phase angle reaches 5 deg. after the temporary reconnection of some Nysted wind turbines in the network.

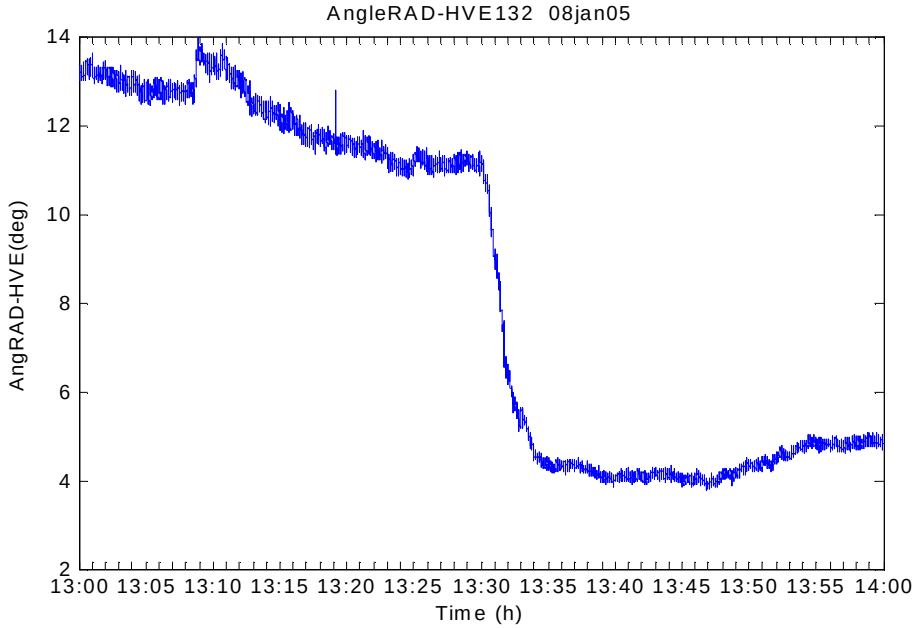

Fig. 71 *PMU recording of angle difference between Radsted and Hovegård*

The stepwise change in reactive power flows to Radsted (Fig. 73) is explained by a subsequent voltage control at Radsted substation. Switching off capacitor shunts was done intentionally at the regional control centre in order to avoid extreme voltage rise caused by disconnection of wind turbines. Fig. 72 shows that the first gradual increase in voltage around 13:05 h is most likely to be caused by tripping of on-land turbines in the region.

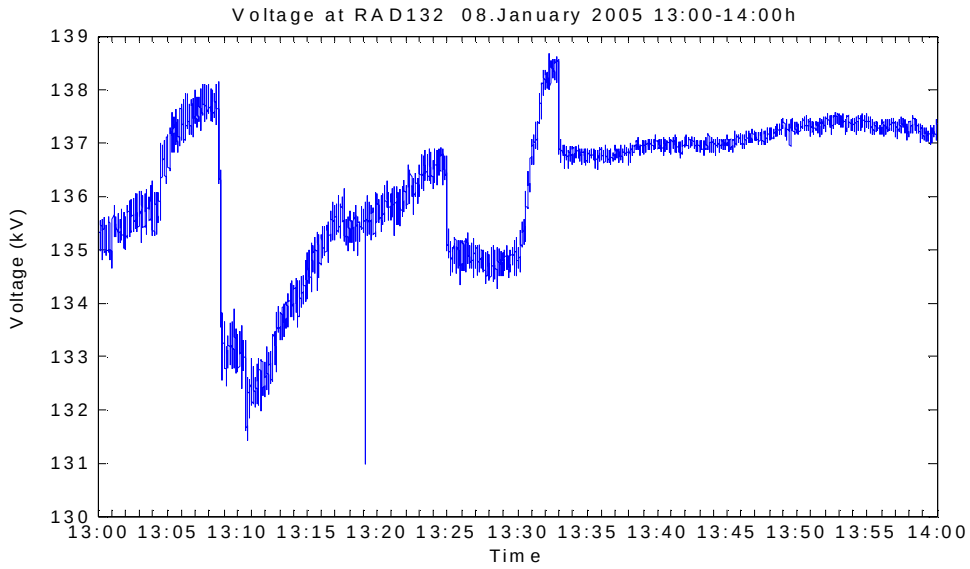

Fig. 72 PMU recording of voltage at Radsted

The most distinct voltage increase of 4 kV at 13:30 h is obviously due to tripping of 150 MW at Nysted. The switching of reactive shunt compensation capacitor shunts introduces respective voltage drops that are experienced as sudden shifts of 5 kV (at 13:10 h), 2 kV (at 13:25 h) and 1,7 kV (at 13:30 h). The postfault voltage stabilises at an acceptable value of 137 kV, which is 3,8% higher than the rated voltage.

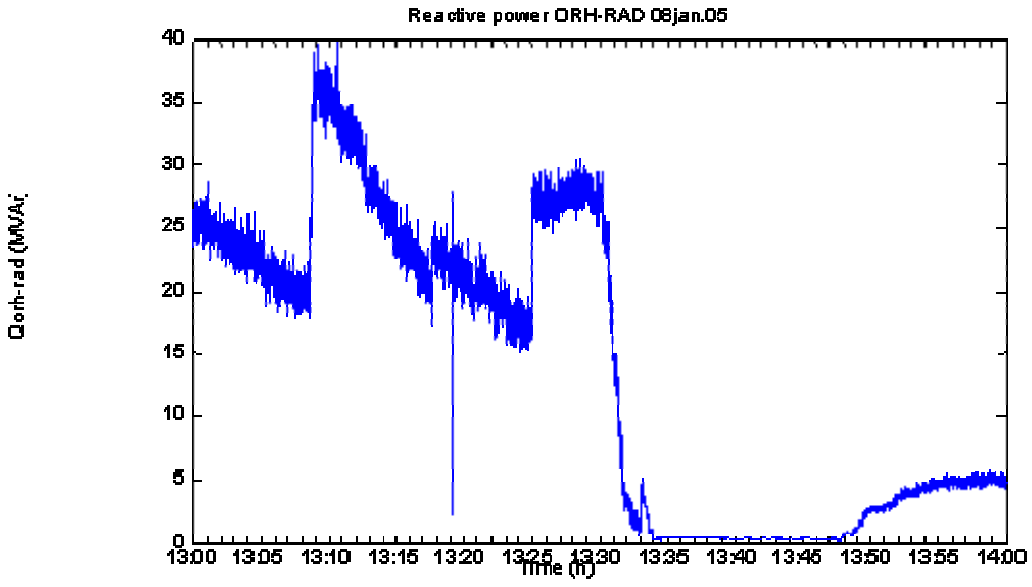

Fig. 73 Reactive power flow in the 132 kV tie-line Radsted-Orehoved

The reactive power flow on the line RAD-ORH from Orehoved to Radsted (Fig. 73) is a mirrored version of Fig. 72. E.g. the decreasing reactive power flow from Sealand is related to the increased voltage level at Radsted that arises from the wind turbine rejection. The tripping of capacitor shunts near Radsted is immediately manifested in 20 MVAr increased reactive power flow from Sealand to Radsted.

The subsequent voltage shift at 13:25 h introduces some 10 MVAr extra reactive power flow from Sealand, while the last shift at 13:35 h is seen as a small shift in flow from 0 to 5 MVAr. This reactive power adjustment from 30 to 0 MVAr corresponds to the downward regulation of the generated power from Nysted.

The trial for reconnection of Nysted is also recognized (at 13:50 h) in the gradual increase of reactive power flow from 0 to 5 MVAr. The recorded voltage profile at Radsted and the capability to supply reactive power from Sealand to Radsted illustrate that the voltage variations are obviously a local phenomenon which is not related to voltage variations in a large area of the main 132 kV system.

5.3.3 Case 4: Outage of 132 kV lines

An extraordinary outage of two 132 kV tie-lines from Radsted to Sealand (Radsted-Blangslev, Radsted-Eskildstrup) took place on 13 February 2005, because of heavy snow storm conditions. The lines RAD-BLA and RAD-ESK tripped at time 02:20 h (Fig. 75). The double line outage constrained the further transfer of wind power from Radsted in the northern direction. However, the situation was not critical because the wind generation from Nysted wind farm was only about 10 MW (Fig. 74).

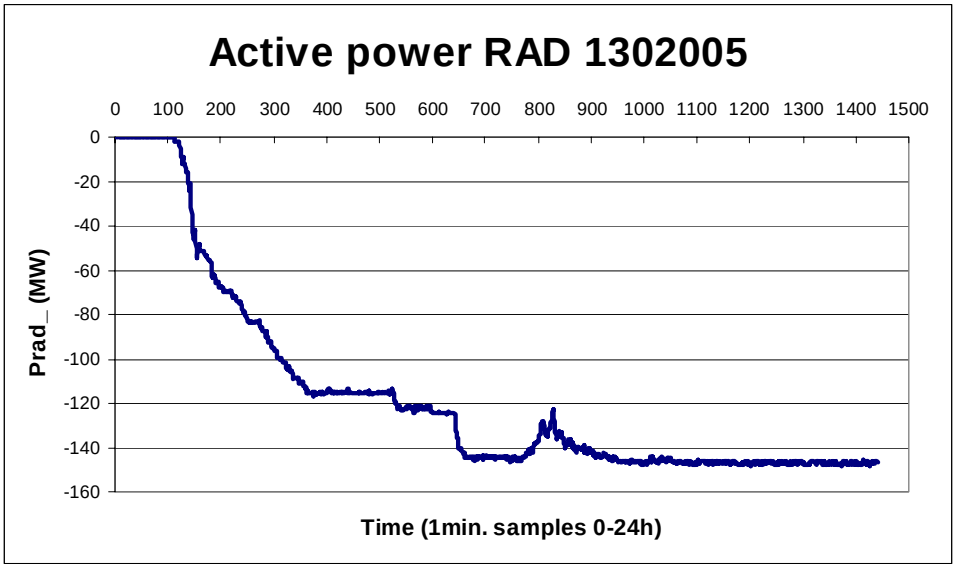

Fig. 74 SCADA data of active power flow from Nysted to Radsted for 24 hours

During the event, the PMUs at RAD132 and HVE132 were unfortunately out of service, but the double line outage was detected by the PMUs in the 400-kV system (ASV400 and HVE400).

In order to obtain a physical meaning, the angle measurement at ASV was referred to the 400 kV reference measurement point at HVE. The phase angle difference recorded between the PMUs at 400 kV level (Fig. 75) shows a 0.3 deg phase shift precisely at the time of the line outages. The small phase shift leads to 10 MW reduction in the 400 kV line flow from one of the 400 kV lines from Asnæs to Bjæverskov (ASV-BJS) seen in Fig. 76.

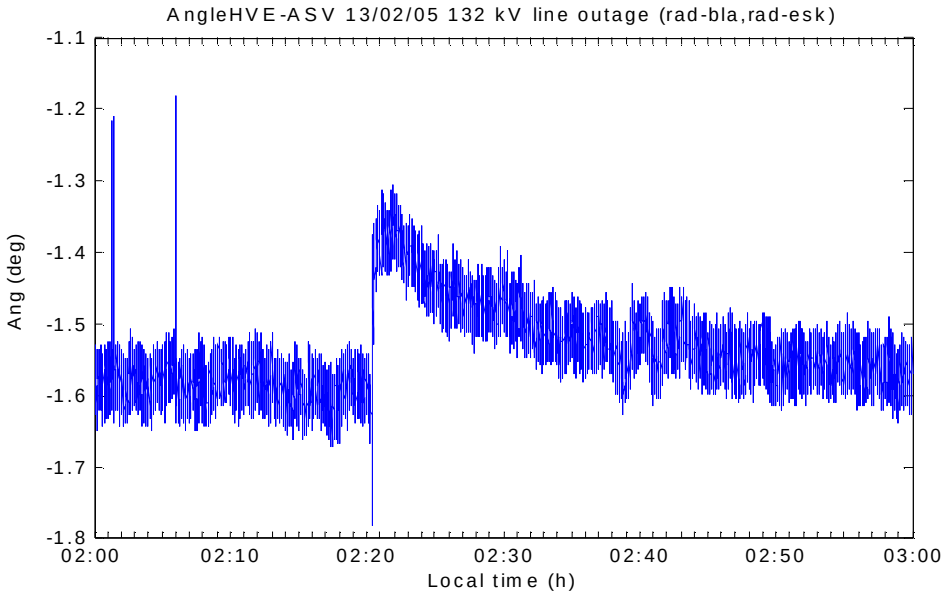

Fig. 75 *PMU recorded angle difference between Hovegård and Asnæs*

After 02:20, both the phase angle difference ASV-BJS and the active power flow in the line were increased to postfault values that are slightly lower than the respective prefault values.

The gradual upgrade of the active power is most likely caused by regulation in the nearby power plant Asnæs. It can be concluded that the 400 kV system is rather robust to small changes in tie-line flows from Radsted to Sealand.

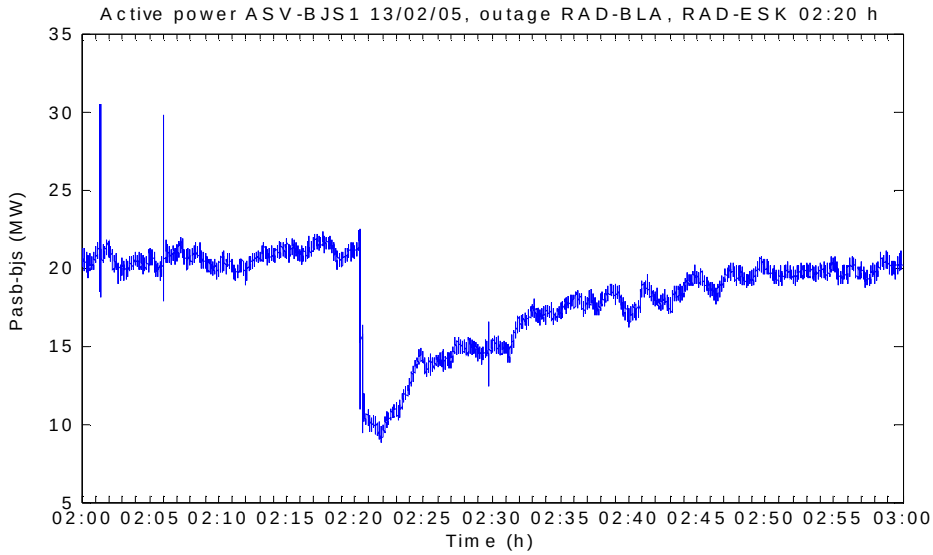

Fig. 76 *Active power in the 400 kV line Asnæs-Bjæverskov*

5.3.4 Case 5: Cascaded outage of 400 kV lines

The PMU recordings from 12 February 2005 show that the 400 kV transmission lines Bjæverskov-Ishøj and Bjæverskov-Hovegård were tripped at 14: 30 and 14:33 h, respectively. The line outages were influenced by the galloping lines effect that also caused disconnection of the submarine cable connection to Sweden, Söderåsen-Hovegård (SAN-HVE) at 14:52 h.

The monitored power flow (Fig. 77) in tie-line shows power import to Denmark that was gradually decreased from 200 MW to 100 MW and then immediately reduced to zero, as the 400 kV tie-line from Sweden was tripped.

The cascaded line tripping is manifested as three severe transient peaks in the 400 kV power flow from Sweden. The synchronized recordings of the 400-kV voltage at Asnæs and Hovegård substations (Fig. 78) were compared directly due to the fact that the voltage and current measurements are assigned the same time stamp and phase reference supplied by GPS clock. About 15 kV (3,7 %) voltage rise at ASV at time 14: 33h is a result of the reduced reactive power consumption in the transmission system due to the tripped 400 kV lines Bjæverskov-Ishøj and Bjæverskov-Hovegård.

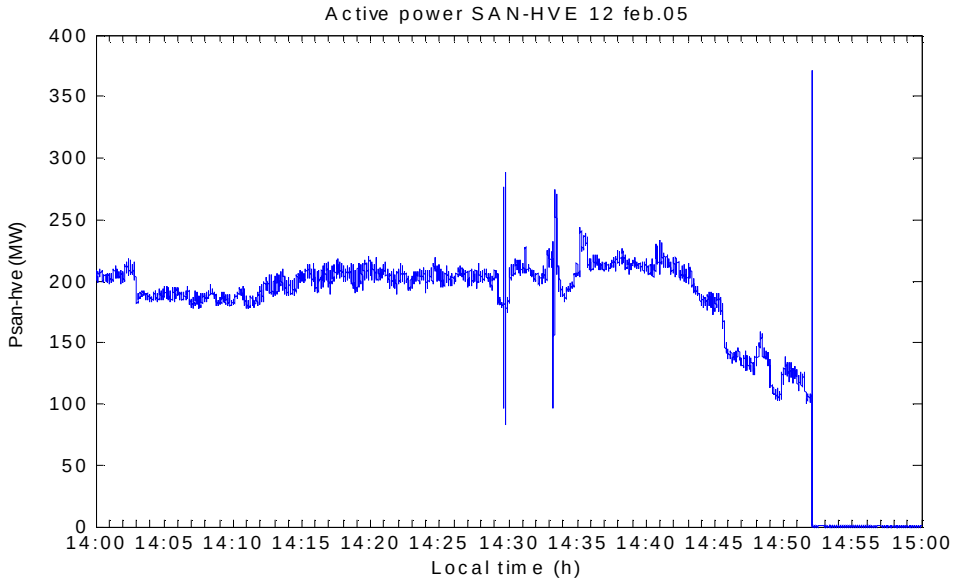

Fig. 77 Tie-line active power flow from Sweden

The cascaded line outage caused splitting of the 400 kV system into two separate parts, and the power transfer was redirected via the 132 kV system. This introduced a larger impedance of the new transmission path and consequently a significant change in phase angles at the 400 kV buses.

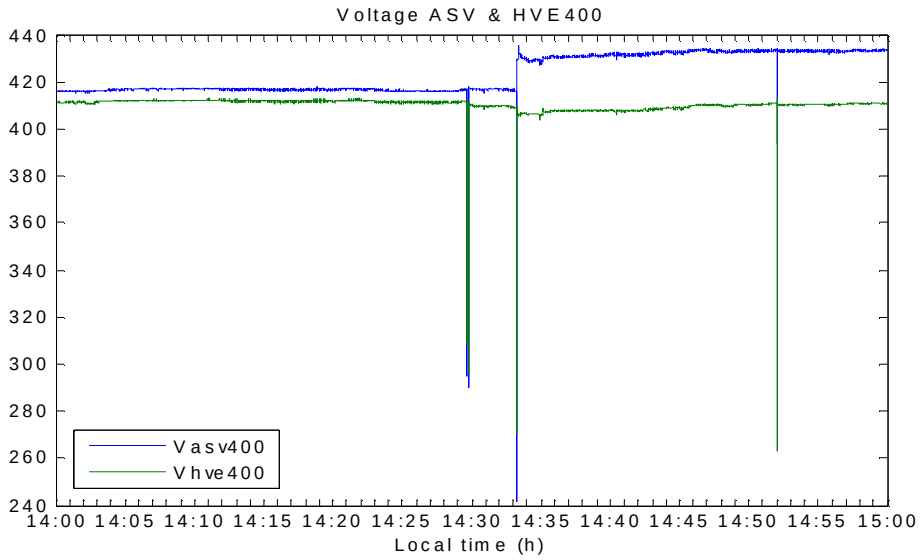

Fig. 78 *Voltage measured at ASV and HVE*

The tripping of the first 400-kV line (BJS-ISH) introduces a phase shift of 1 deg., while the second 400-kV line tripping leads to a further change to approx. 12 deg. phase angle difference between ASV400 and HVE400. The event of line tripping is identified in Fig. 79 as subsequent transients at time 14:30h and 14:33h. The phase angle plot between ASV and HVE supports the fact that the power system was severely stressed during the recorded disturbance.

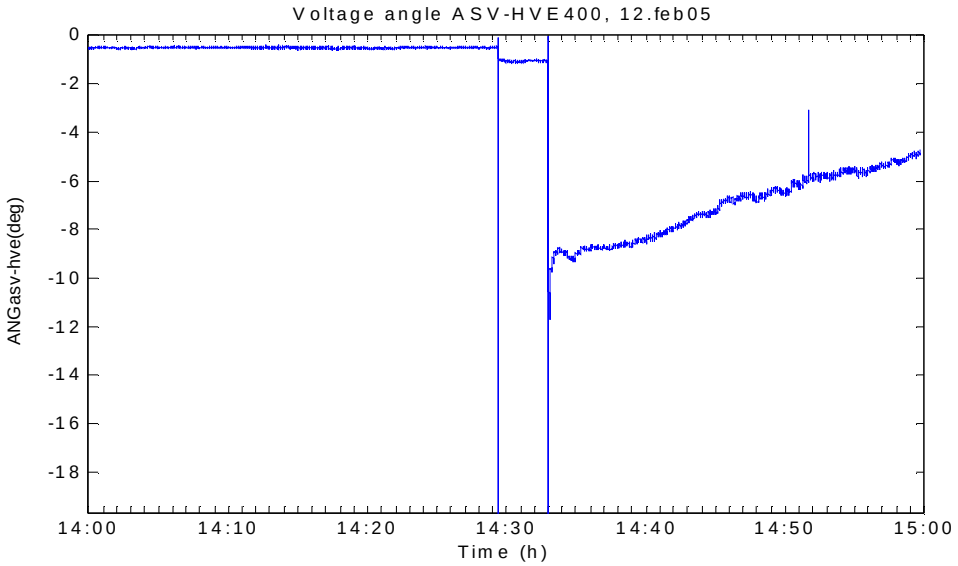

Fig. 79 *Voltage phase angle difference between ASV and HVE*

The event analysis presented in this section illustrates clearly the benefit of using PMUs in disturbance monitoring and tracking system dynamic phenomena that are characteristic for the Eastern Danish power system i.e. wind farm rejection, cascaded line outages and power oscillations between Denmark and Sweden. It is believed that the PMU application in Eastern Denmark can become a significant segment in a Nordic wide-area PMU network.

5.4 Conclusion on phasor measurements

Three PMUs are placed at strategic points in important 400 kV and 132 kV transmission corridors in Eastern Denmark. In general, the choice of representative location for PMU units is dependent upon the investigated stability phenomena, network characteristics and communication constraints.

Real-time phasor measurements are utilized for tracking power system dynamics during a number of severe power system disturbances that are characteristic for the Eastern Danish power system, such as wind farm rejection, cascading line outages and power oscillations. E.g. Nordic inter-area oscillation modes were easily detected from phasor data during the outage of the 400 kV tie-line between Eastern Denmark and Sweden. The recording of power oscillation frequencies is more convenient than computation of eigenvalues using a detailed dynamic model for the Nordic power system. The application of synchronized phasor measurements for, e.g., validation of power system models used in stability studies, is seen as having a great potential in the future.

PMUs are evaluated as an efficient tool to enhance power system monitoring using the existing SCADA/EMS system. Further on, it is believed that phasor data can be utilized as additional information in monitoring of system security. In future applications, PMUs can be used as a supplementary input in future System Protection Schemes that give warning in case of an emergency situation.

5.4.1 Nordic perspective of phasor measurements

It is believed that the synchronized phasor measurements technology is mature and capable of utilization in large-scale applications in the Nordic transmission system. The future perspective of phasor measurements in the Nordic power system is to extend a system-wide PMU network in the Nordic countries. Norway and Denmark have already installed PMU prototypes in the respective transmission networks. It could be highly relevant to place a limited number of PMUs at important transmission corridors in Sweden and Finland as well as to harmonize the PMU utilization in the eastern and the western part of Denmark with the general objective of enhancing the monitoring of the Nordic power system.

An obvious application could be PMU monitoring of sustained frequency and phase angle changes in relation to angle and frequency stability as well as power system oscillations in the interconnected systems in the Nordic countries. E.g. power oscillation modes and potential angle stability problems can be deducted from synchronized phase angle recordings at selected buses in the Nordic system. PMU can also be integrated in sophisticated applications for voltage security etc. In general, the future benefits are seen in enhancement of transmission system capability and reliability of the entire Nordic system. Special efforts have to be made to coordinate and harmonize different wide-area measurement projects in the Nordic countries.

In general, the following points are relevant to be considered for a future Nordic PMU network:

1) **Level of investment**: The measured information can be considered as insurance against operational uncertainty. How much insurance is enough? How much information is too much?

2) **Monitor applications** are necessary in addition to event recording.

a) Direct tests and analysis of the power system;

b) Real-time system operations (operator alerts, cross triggers, etc.)

3) **Monitor recording options**:

a) Evaluate data in real time, using event identification logic to trigger "snapshot" recordings of special activity or conditions;

b) Record all data continuously, and then apply event identification logic to archived records.

4) **Considerations on event identification**:

a) Event identification is an ongoing process. The automatic detection of significant abnormal system behaviour requires comprehensive examination and knowledge of normal behaviour;

b) Real-time event identification rarely detects the onset of distant events;

c) Event identification for scanning continuously recorded archives can be simplified for use in real time, as a refinement to the "triggers" now in use. Besides, it can be used for scanning and characterization of snapshot archives.

5) **Value engineering**:

a) Functionality is the key issue: Who needs to see what, where, when, in what form? Why – what decisions hinge upon the information?

b) Staff costs (engineering, operations, and maintenance) are dominant in power system monitoring;

c) Continuous recording, in combination with a competent archive scanner, provides value engineering for wide area measurements of power system dynamics;

d) User participation is essential to development and operation of high performance monitor facilities.

6 Conclusion

The Ph.D. project suggests a simple System Protection Scheme (SPS) for the power system of Eastern Denmark. The SPS is an automatic solution to mitigate the voltage instability problems related to a heavily loaded power system with high wind generation. The suggested SPS against voltage instability should only be activated when the voltage stability limits can not be maintained with any other conventional measure. The benefits from the introduced System Protection Scheme concept are seen in increased power system security (especially for extreme contingencies) as well as in the possibility of operating the power system closer to its limits.

The SPS design is based on analysis of a large-scale power system model[38] with two off-shore wind farms. For design purposes, a number of realistic system conditions are considered. The System Protection Scheme against voltage collapse is designed as a response-based scheme, which is dependent on local indication of reactive and active flow in relevant 132 kV lines, violation of SVC rating and low voltage at Radsted substation. Besides the local measurements, voltage magnitudes at two other 132 kV buses are used for the SPS input. The introduced SPS concept is rather simple and efficient, but it does not include redundant measurements and is associated with great uncertainties in the SPS settings. The drawback of the System Protection Scheme is its robustness, i.e. the SPS ability to operate properly in a wide range of operating conditions and disturbances. The SPS limits and criteria can not be generalized for an arbitrary data set for the system of interest. The uncertainties are affected by the selected voltage stability method and tool as well as the limitations in the modelling data and simple models used for loads and generator capabilities.

PMUs can be utilized in the system protection scheme leading to a system-wide SPS solution. As supplementary input, the SPS includes phase angle measurements from two separated locations in the 132-kV system, besides the conventional indicators of reactive power flows and low voltages. The phase angle difference between Radsted (RAD) and Hovegård (HVE) is used instead of active power measurements in the 132-kV lines connecting Radsted with the main 132 kV system. The PMUs are especially valuable in detection of disturbances in the system, because the respective phase angles change significantly in case of severe wind turbine rejections as well as generator or line outages. This benefit can possibly improve the performance of the system protection scheme.

The maximum power transfer in the heavily loaded system with two large off-shore wind farms is approached at about 70% of the total wind generation capacity. The low-load situation with high wind generation gives rise to largest voltage gradients and reactive power losses, because this situation is associated with the greatest line flows in the 132 kV system. Due to the high wind generation, the active power flows from Radsted to the main 132 kV system, while the direction of the reactive power is opposite. The key limitation used in the SPS design is seen in the restricted reactive power transfer from the main system as well as insufficient SVC rating. A single line outage weakens further the southern part of the 132-kV system due to reduced transfer of reactive power.

The reactive power can not be transmitted over long distances, therefore local reactive power support from the SVC at Radsted or start of Masnedø gas turbine are suggested as potential voltage controls in case of heavy system loading. In fact, the existing SVC has inadequate rating, because it is not designed to cope with two off-shore wind farms. For system protection

[38] Power system with 700 buses

purposes, it is important to upgrade the SVC output to minimum 110 MVAr or to install minimum 45 MVAr additional capacitor shunts near Radsted.

The main challenge in protection of wind turbines on-land in Eastern Denmark is seen in the conflicting requirements for on-land and off-shore wind turbines. After a fault in the transmission system, a significant amount of on-land wind turbines would trip, and the released reactive power contributes to voltage recovery at system buses. The benefit of using the present protection principle for wind turbines on-land is that they help maintain voltage stability in the system. The drawback of the protection principle for on-land wind turbines is the loss of active power, as a large number of wind turbines will trip after a fault occurs in the 132-kV system. The main factor to avoid unnecessary disconnection of wind turbines is the fast fault clearance time. Possible voltage quality problems in wind farms may be overcome by selecting an appropriate wind turbine type and/or adjusting wind turbine control parameters.

The System Protection Scheme uses the positive impact of wind turbine rejection with respect to voltage stability. Wind power shedding is suggested as an efficient remedial control in case of imminent voltage collapse. The automatic reduction of the total wind generation is done by the SPS either by issuing tripping signals to wind turbines on-land or by downwards regulation of active power at one of the Nysted wind farms.

Synchronized phasor measurements from three separated locations are successfully used for improving the power system monitoring in Eastern Denmark. PMUs revealed the power system response to different disturbances in Eastern Denmark, such as wind turbine rejection, cascading outages and power oscillations excited by tripping of the 400 kV tie-lines to Sweden. The greatest potential for PMU application is seen in detection of power oscillation modes and damping in the Nordic power system as well as verification of dynamic simulation models.

The PMUs could enable the system operator to achieve more precise information about the actual system state and detect catastrophic events in due time. PMUs applications are mostly suitable in large interconnected networks, where large abnormal dynamic changes in phase angles, power flows, frequency etc. can be easily observed. PMUs can be utilized to give early warning of e.g. severe power system stress (e.g. outage of important transmission corridors), so that an automatic System Protection Scheme or the system operator can react in a proper way. Hence, the power system capability could be extended beyond normal limits.

A common problem with system protection schemes in operation today is that they act on very precise pre-determined criteria. The SPS parameter values are adjusted only to major changes in the system configuration. Some SPS systems take into account the actual switching status and power flow of the network. In general, the SPS complexity is increased by introducing enormous amounts of data, where complicated SPS rules have to be processed. This can lead to reduced reliability of SPS operation.

7 Future work

For future practical application of the SPS scheme it is necessary to improve the detection of voltage instability and propose some more realistic SPS settings. The static simulations performed in the project are mainly concerned with identification of voltage instability (for limited number of contingencies and operating scenarios) in the Eastern Danish transmission system. Enhanced procedure for SPS design is important for future studies. In the future studies it is crucial to improve the identification of voltage stability limits and to access systematically the critical impact of large number of contingencies and operating scenarios with respect to voltage stability and wind power generation in the power system. The automatic procedure for scaling of wind power and total system loading has to be improved in order to facilitate better the parameter variations in case of different operating scenarios. The uncertainties in the simulation studies are possibly reduced if voltage dependence in load models is represented as well as generator capabilities[39] are encountered. For the dynamic simulations an accurate wind turbine model with active power control for Nysted wind farm is recommended.

In practice, the design of SPS against voltage instability in a large power system should be based on exhaustive set of coordinated defensive measures, whose design and implementation concern a high level of complexity. For practical implementation it becomes too complicated to meet a variety of advanced requirements in case of many protection schemes.

The detailed evaluation of feedback control in the suggested SPS design is a subject of future work. In real applications, the response-based SPS design should encompass the feedback control of relevant remedial actions. Thus, the next step is to perform further static and dynamic simulations for critical contingencies and corrective actions included. On the basis of these simulations, settings and time delays for corrective measures can be selected for the particular operating conditions. In the future investigations, it is relevant to generate a set of stability curves for each control action and compare the system characteristics for remedial control with the respective characteristics for intact and contingency network. Further on, it is recommended to coordinate different control actions in the specific SPS scheme(s) and, if necessary, coordinate the purposed SPS with other schemes in operation.

In the future, a specific cost-benefit analysis is necessary to point out advantages and drawbacks in relation to increased security and/or increased power system capability of the suggested System Protection Scheme against voltage instability. Increased security can be estimated as reduced costs for utility power interruptions and undelivered energy for the customers. The benefit of increased power transfer capability is reduced investments for network reinforcement. The calculated savings have to justify the investments for development and installation of the particular SPS. In general, the compromise between dependability and security of SPS remains a challenge for future investigations. Great potential is seen in adaptive System Protection Schemes (SPS) based on state estimators with PMUs. Such sophisticated solutions are able to track the dynamics of the power system state and adapt the SPS settings to the actual operating condition. The benefits and drawbacks of adaptive SPS based on state estimators is a subject of future work.

[39] For power plants electrically close to the southern part of the 132 kV system

8 References

System Protection

1. CIGRÉ SCTF 38.02.19: " System Protection Schemes in Power Networks ", June 2001

2. CIGRE WG 39.05, B. K. Lereverend, et al.: "Industry Experience with Special Protection Schemes", Electra, No. 155, August, 1994.

3. B. Ingelsson, P. O. Lindström, J. O. Sjödin, D. Karlsson, G. Runvik: "Special Protection Scheme against Voltage Collapse in the South Part of the Swedish Grid", CIGRE report 38-105, Paris, 1996

4. Taylor C., Erickson D., Martin K.E., Wilson R.E., Venkatasubramanian V.: "WACS – Wide-Area Stability and Voltage Control System: R&D and Online Demonstration", Proceedings of the IEEE, Vol. 93, No. 5, May 2005

5. Kirkeluten Ø.: "Systemvern i Norge og modeller i PSS/E", Statnett SF, presentation at Nordic PSS/E Users group meeting, 18-19. June 2003, Copenhagen, Denmark

6. Lindahl S.: "Principles of relaying", Seminar on Wide-Area Measurements in Power Systems, Lund University, Sweden, 06. September 2004.

7. Jonsson M.:"Protection Strategies to Mitigate Power System Blackouts", Ph.D. thesis Department of Electric Power Engineering, Chalmers University of Technology, Götteborg, Sweden, 2003, ISBN 91-7291-293-6

8. Rehtanz C., Bertsch J.: "A new wide are protection system", IEEE Porto Power Tech Conference, 10-13th September 2001, Porto, Portugal

9. Rehtanz C.: "Wide Area Protection and Online Stability Assessment based on Phasor Measurements", Bulk Power System Dynamics and Control V, August 26-31, 2001, Onomichi, Japan

10. Rehtanz C., Bertsch J.: "Wide Area Measurement and Protection System for Emergency Voltage Stability Control", IEEE Winter Meeting 2002

11. Larsson M., Rehtanz C., Bertsch J.: "Monitoring and Operation of Transmission Corridors", IEEE Bologna Power Tech Conference, June23-26th, 2003 - Bologna, Italy

12. Zima M., Andersson G.: "Stability Assesment and Emergency Control Method Using Trajectory Sensitivities", Bologna Power Tech Conference, June23-26th, 2003,Bologna, Italy

13. Rehtanz C., Larsson M., Zima M., Kaba M., Bertsch J.: "System for wide area protection, control and optimization based on phasor measurements", Power Systems and Communication Systems Infrastructures for the Future, Beijing, September 2002.

14. C. Olaru, P. Geurts, L. Wehenkel: ”Data mining tools and applications in power system engineering”, Proc. 13th Power Systems Computation Conference, pp. 324-330, Trondheim, Norway, 1999.

15. “Operational performance specifications for thermal power units larger than 100 MW”, NORDEL 1995

16. www.elkraft-system.dk, Note on agreements for system protection schemes 2003.

17. Transmission plan 2005, Elkraft System, Denmark

18. Grande O.S., Uhlen K., Bakken B.H., Hernes M., Foss O.B: ”Operational Security Assessment- Planning and Control”, SINTEF Energy Research, TR A5294, October 2000

Wind Power Generation

19. Rasmussen J., Jørgensen P., Palsson M.T., Uhlen K., “Wind Power Impact to Transient and Voltage Stability of the Power System in Eastern Denmark” (accepted for publication in IASTED PES 2005 Conference proceedings), 8th IASTED International Conference on Power and Energy Systems , October 23-26, 2005

20. Tande J.O.G., Uhlen K.: ”Assessment of electrical conversion systems for wind turbines”, GWEC’2002, Paris, France 2-5 April 2002.

21. Tande J.O.G.: “Wind Farm Models for Power System Studies”, IEEE Transactions on Energy Conversion”, October 2002.

22. Pálsson M.T., Toftevaag T., Uhlen K., Norheim I., Warland L., Tande J.O.G.: ”Wind farm modelling for network analysis – Simulation and validation”, Conference paper presented at EWEC 2004, London UK, 22-25 November 2004.

23. Palsson M.: ”System operation and control with increasing integration of wind power and distributed generation”, Technical report SINTEF Energy Research, Trondheim, Norway, December 2002.

24. Slootweg J.G., Polinder H., Kling W.L.: “Initialization of Wind Turbine Models in Power System Dynamics Simulations”, BPT 2001, IEEE Porto Power Tech Conference, 10-13th September; Porto, Portugal

25. Slootweg J.G., Kling W.L.: ”Aggregated Modeling of Wind Parks in Power System Dynamic Simulations”, IEEE Bologna Power Tech Conference, June23-26th, 2003 - Bologna, Italy

26. Bruntt M., Havsager J., Knudsen H.: “Incorporation of wind power in the East Danish power system”, IEEE Power Tech’99 Conference, Budapest – Hungary, August 29 – September 2, 1999, BPT99-202-5.

27. Akhmatov V., Knudsen H., and Nielsen A.H.: "Advanced simulation of windmills in the electric power supply", Electrical Power and Energy Systems 22 (2000) p.421-434, 2000 Elsevier Science Ltd.

28. Akhmatov V., Knudsen H, Nielsen A.H., Pedersen J.K., Poulsen N.K.: “Modeling and transient stability of large wind farms” Electrical Power and Energy Systems 25 (2003) p.123-144, Elsevier Science Ltd.

29. Akhmatov V., Knudsen H, Nielsen A.H.: ”Electromechanical interaction and stability of power grids with windmills”, Proceedings of the IASTED International Conference Power and Energy Systems”, September 19-22, 2000, Marabella, Spain, International Association of Science and Technology for Development – IASTED, ISBN 0-88986-300-8, ISSN 1482-7891

30. Akhmatov V., Knudsen H.: "Modeling of windmill induction generators in dynamic simulation programs", IEEE Power Tech'99, 29 August-2 September 1999, Budapest, Hungary, BPT99-243-12.

31. Akhmatov V., Knudsen H.: "Dynamic modeling of windmills", Proceedings of the International Conference on Power System Transients IPST'99, 20-24 June, Budapest, Hungary, 1999, p.289-295

32. Knudsen H, Akhmatov V.: "Induction generator models in dynamic simulation tools", Proceedings of the International Conference on Power System Transients IPST'99, 20-24 June, Budapest, Hungary, 1999, p.253-259

33. Rosas, P.A.C.; Rønne-Hansen, J.; Sørensen, P.; Bindner, H.; Feitosa, E.: “Wind energy influences on voltage stability”, (poster). In: Wind energy for the new millennium. Proceedings. 2001 European wind energy conference and exhibition (EWEC '01), Copenhagen (DK), 2-6 Jul 2001. Helm, P.; Zervos, A. (eds.), (WIP Renewable Energies, München, 2001) p. 1124-1127

34. Rosas P.: “Dynamic influences of wind power on the power system”, Ph.D. thesis, Ørsted • DTU, Section of Electric Power Engineering, Technical University of Denmark, ISBN: 87-91184-16-9, Technical Report RISØ R-1408, March 2003

35. ”Langsigtede analyser ved nettilslutning af havplacerede vindmøller, del 1”, Teknisk Rapport - NESA, TRAPLA - December 2002

36. “Wind turbines connected to grids with voltages above 100 kV”, Technical regulations for the properties and control of wind turbines, TF 3.2.5. Draft version, Elkraft System, ELTRA, September 2004

37. “Wind turbines connected to grids with voltages below 100 kV”, Technical regulation for the properties and control of wind turbines, TF 3.2.6., Elkraft System, ELTRA, May 2004

38. Bolik S.M., “Modelling and Analysis of Variable Speed Wind Turbines with Induction Generator during Grid Fault”, Ph.D. thesis, Institute of Energy Technology, Aalborg University, Denmark, October 2004, ISBN 87-89179-55-2.

39. Erich H.: “Wind-turbines – Fundamentals, Technologies, Application, and Economics”, Springer John Wiley & Son Ltd; ISBN: 3-540-57064-0, 2000.

40. Freris L.: “Wind Energy Conversion Systems”, Prentice Hall, ISBN: 0-13-960527-4, 1990

Voltage Stability Assessment

41. Prabha Kundur: “Power System Stability and Control”, EPRI Editors, Nea J. Balu and Mark G. Lauby. McGraw–Hill, 1993, ISBN: 0 – 07 – 035958 – X.

42. Carson W. Taylor: “Power System Voltage Stability”, McGraw Hill Text, 1994; ISBN: 0-07-063184-0, 1994

43. “Voltage Collapse Mitigation”, Report to IEEE Power System Relaying Committee, Substation Protection Subcommittee, Working Group K12, final version, December 1996.

44. Van Cutsem T., Vournas C.: ”Voltage stability of electric powers systems”, Kluwer academic publishers, Norwell, MA, 1998.

45. Nuqui R. F., Phadke A.G., Schulz R.P., Bhatt N.B.: “Fast On-Line Voltage Security Monitoring Using Synchronized Phasor Measurements and Decision Trees”, paper presented at the IEEE PES 2001 Winter Power Meeting, 01 WM 287-2-PWRS.

46. Begovic M. M: “Analysis, Monitoring and Control of Voltage Stability in Electric Power Systems” Ph.D. Thesis, Virginia Polytechnic Institute and State University, Blacksburg, Virginia.

47. Rapo S.: “On-line Voltage Stability Assessment of Power System- An Approach of Black-box Modeling”, Ph.D. thesis, Publications 344, Tampere University of Technology, October 2001

48. Warland L, Holen A.:” A Voltage Instability Predictor Using Local Area Measurements (VIP++)”, Conference Proceedings, IEEE Porto Power Tech Conference, 10-13. September 2001, Porto, Portugal

49. Vu K.T., Begovic M.M., Novosel D., Saha M.M.: ”Use of local measurements to estimate voltage stability margin”, IEEE Transactions on Power Systems, Vol. 14, No. 3, pp.1029-1034, August 1999.

50. Arnborg S.: “Emergency Control of Power Systems in Voltage Unstable Conditions”, March 1997, Ph.D. thesis, Electric Power Systems Department of Electric Power Engineering, Royal Institute of Technology, Stockholm, Sweden; TRITA-EES –9701, ISSN 1100 – 1607

51. Karlsson D.: “ Voltage stability simulations using detailed models based on field measurements”, Technical Report 230, Department of Electrical Power Systems, School of Electrical and Computer Engineering 1992

52. Price W.W., Wirgau K., Murdoch A., Mitsche J.V., Vaahedi E., El-Kady M.A.: “Load Modeling for Power Flow and Transient Stability Computer Studies”, IEEE Transactions on Power Systems, Vol.3, No.1, February 1988

53. Cañizares C.A.: “Voltage Stability Assessment: Concepts, Practices and Tools”, IEEE-PES Power Stability Subcommittee Special Publication SP101PSS, ISBN 0780378695

54. Cañizares C.A., Alvarado F.L.: “Continuation and Direct Methods to Locate Fold Bifurcations in AC/DC/FACTS power systems”, UWPflow free-software, available at www.power.uwaterloo.ca, Electrical and Computer Engineering, University of Waterloo.

55. Power Technologies, Inc.: PSS/E- version 29.5 Power System Simulator, Program Operational and Application Manual, Kostyniak T.E.

Wide-Area Measurements System

56. Phadke, A.G., "Synchronized phasor measurement in power systems", in IEEE Computer Applications in Power, vol. 6, no.2, pp. 10-15, April 1993.

57. Phadke Arun G., Thorp James S.: “Computer Relaying for Power Systems” John Wiley and Sons Inc., ISBN 0 471 92063 0 Research Studies Press Ltd. 1988, ISBN 0 86380 074 2

58. Martin K.E.: “Phasor Measurements at the Bonneville Power Administration”, Power Systems and Communication Systems Infrastructures for the Future, Beijing, September 2002.

59. IEEE Power System Relaying Committee of the Power Engineering Society, "IEEE Standard for Synchrophasors for Power Systems," The Institute of Electrical and Electronics Engineers, Inc., New York, September 1994.

60. Begovic M.M. and Phadke A.G.: “Voltage Stability Assessment Through Measurement of a Reduced State Vector,” IEEE Transactions on Power Systems, vol. 5, no. 1, February 1990, pp. 198-203.

61. Heydt G.T., Liu C.C., Phadke A.G., Vittal V.: “Solutions for the crisis in electric power supply”, IEEE Computer Applications in power, ISSN 0895-0156/01/2001 IEEE

62. Rasmussen J., Jørgensen P., “Synchronized Phasor Measurements of a Power System Event in Eastern Denmark”, IEEE Transactions on Power Systems, Vol.21, No.1, February 2006.

63. Rasmussen J., Jørgensen P., “Synchronized Phasor Measurements of a Power System Event in Eastern Denmark”, IEEE Bologna Power Tech 2003 Conference proceedings IEEE BPT June 23-26, 2003, Bologna, Italy

64. Samuelsson O., Hemmingsson M., Nielsen A.H., Pedersen K.O.H., Rasmussen J., “Monitoring of power system events at transmission and distribution level”, accepted for publication in IEEE Transaction on Power Systems.

65. ELFORSK report 99:50: “Wide Area Measurements of Power System Dynamics “

66. CIGRE report (draft): “Wide Area Monitoring and Control for Transmission Capability Enhancement”, TF in Power System Security Assessment WG C4.6.01, Christian Rehtanz

67. ABB Technical Overview Brochure, RES 521-PMU Beta 01, 2002

68. Nielsen A.H., Pedersen K.O.H., Samuelsson O.: ”An experimental GPS- based measurement unit”, Nordic and Baltic Workshop on Power Systems, Tampere 4-5 February 2002

69. Hemmingsson M., Samuelsson O., Nielsen A.H., Pedersen K.O.H.: “Estimation of Electro-Mechanical Mode Parameters using Frequency Measurements”, IEEE Winter Meeting 2001

70. Uhlen K.: ”Wide Area Control Concepts- A Pre-study”, SINTEF Energy Research, TR A5055, January 2000

71. Baldwin T.L., Mili L., Boisen M.B. and Adapa R. “Power System Observability With Minimal Phasor Measurement Placement,” IEEE Transactions on Power Systems, vol. 8, no. 2, May 1993, pp. 707-715.

72. Milosevic B, Begovic M.: “On Optimal Placement of Phasor Measurements in Power Systems”, Proceedings of North American Power System Conference (NAPS) 2001, Texas A&M University, College Station, USA – October 15- 16, 2001

73. Nuqui R.F. “State Estimation and Voltage Security Monitoring Using Synchronized Phasor Measurements” Ph.D. Thesis, Virginia Polytechnic Institute and State University, Blacksburg, Virginia, July 2001.

74. Burnett R.O., Butts M.M., Cease T.W., Centeno V., Michel G., Murphy R.J., Phadke, A.G., "Synchronized phasor measurements of a power system event", IEEE Transactions on Power Systems, Vol.9, No.3, pp.1643-1650, August 1994.

75. Hauer J. F., Donnelly M. K. , Mittelstadt W. A., Litzenberger W. H., Adapa R.: ”CRC Electric Power Engineering Handbook, chapter 11: Power System Dynamics and Stability, section 8: Direct Analysis of Wide Area Dynamics”.

Power Oscillations in Interconnected Systems

76. Anderson P.M., Fouad A.A., “Power System Control and Stability”, Volume I, The Iowa State University Press 1977.

77. Samuelsson O.: “Power System Damping- structural aspects of controlling active power”, Ph.D. thesis - Department of Industrial Electrical Engineering and Automation, Lund Institute of Technology, April 1997 ISBN 91-88934-05-5

78. Eliasson B. :“Damping of power oscillations in large power systems”, Ph.D. thesis 1990 - Department of Automatic control, Lund Institute for Technology

79. Hemmingson M., “Power System Oscillations, Detection Estimation and Control” , Ph.D. dissertation, Department of Industrial Electrical Engineering and Automation, Lund Institute of Technology, Lund University, ISBN 91-88934-27-6, March 2003

80. Lysfjord T., Messing L., Ingemars B., Keränen T., Østrup T., ”Improved damping of power oscillations in the Nordic grid using optimisation of adjustable control parameters for Power System Stabilisers”, (in Swedish) “Förbättrad dämpning av effektpend-

lingar i nordelnättet genom optimering av inställbara reglerparametrar för dämptillsatser", Nordel report 1982-06-15

81. Uhlen, Kjetil; Elenius, Stefan; Norheim, Ian; Jyrinsalo, Jussi; Elovaara, Jarmo; Lakervi, Erkki: " Application of Linear Analysis for Stability Improvements in the Nordic Power Transmission System", IEEE/PES General Meeting, Toronto, Canada, July 13–17, 2003

82. Rasmussen J.:"Research and development at Elkraft System", Business report, ATV business –targeted course "Technology management and technology emergence", June 2004

83. Samuelsson O., Hemmingsson M., Nielsen A.H., Pedersen K.O.H., Rasmussen J., "Monitoring of power system events at transmission and distribution level", accepted for publication in IEEE Transaction on Power Systems.

Appendix 1 - Selected publications

A. Rasmussen J., Jørgensen P., "Synchronized Phasor Measurements of a Power System Event in Eastern Denmark", IEEE Transactions on Power Systems, Vol.21, No.1, pg. 278-284, February 2006.

B. Rasmussen J., Jørgensen P., "Synchronized Phasor Measurements of a Power System Event in Eastern Denmark", Conference proceedings for IEEE Bologna Power Tech 2003, 23-26. June 2003, Bologna, Italy.

C. Rasmussen J., Jørgensen P., Palsson M.T., Uhlen K., "Wind Power Impact to Transient and Voltage Stability of the Power System in Eastern Denmark", published in IASTED PES 2005 Conference proceedings), 8th IASTED International Conference on Power and Energy Systems , October 23-26, 2005

D. Samuelsson O., Hemmingsson M., Nielsen A.H., Pedersen K.O.H., Rasmussen J., "Monitoring of power system events at transmission and distribution level", accepted for publication in IEEE Transaction on Power Systems.

E. Nielsen A.H., Pedersen K.O.H., Jørgensen P., Havsager, J., Olsen S.K., Rasmussen J., "Phasor measurement units in the Eastern Danish power system", expected for publication at CIGRE general conference 2006.

Publications A, C, D and E from the list are attached in Appendix 1

“Synchronized Phasor Measurements of a Power System Event in Eastern Denmark”,

Rasmussen J., Jørgensen P.

Published in IEEE Transactions on Power Systems, Vol.21, No.1, February 2006

Synchronized Phasor Measurements of a Power System Event in Eastern Denmark

J. Rasmussen and P. Jørgensen, *Senior Member, IEEE*

Abstract--**Two sets of synchronized phasor measurements 200 km apart have been performed during a planned outage of a double 400-kV tie-line between Eastern Denmark and Southern Sweden. The interconnection between Eastern Denmark and Southern Sweden comprises of a double 400-kV line and a double 132-kV line. The outage of the 400-kV tie-line weakened the Eastern Danish power system and excited power oscillations in the interconnected power systems. During this event prototype Phasor Measurements Units (PMU) gave the opportunity of real-time monitoring of positive sequence voltage and current phasors using satellite-based Global Positioning System (GPS). Comparisons between real-time recordings and results from dynamic simulations with PSS/E are presented. The main features from the simulation analysis are successfully verified by means of the corresponding synchronized phasor measurements.**

Index Terms—**Power system measurements, Power system monitoring, Power system stability.**

I. Introduction

PHASOR Measurement Units (PMUs) that rely on satellite-based GPS clocks, give the opportunity of real-time monitoring of phasor measurements. Measurements from widely separated locations in the power system can be synchronized at a common time reference and collected at a central location. In that way detailed information about the actual operational status of the power system can be preserved in a precise way. Synchronized phasor measurements can be used as an efficient tool both in warning of abnormal system conditions in due time and in analysis of critical events after severe disturbances in the power system.

Synchronized phasor measurements from a limited number of dispersed locations in the power grid can be used for enhanced monitoring of the power system, as well as for presentation of the critical dynamics in the power system [11]. The choice of representative locations for the PMU units is dependent upon the investigated dynamic phenomena, network size and characteristics, as well as communication and data transfer constraints [10].

Correct identification of oscillation modes using simulation of the Nordic power system requires exhaustive eigenvalue analysis. The authors of this paper were unfortunately not able to perform such simulation analysis, since the actual generation and load pattern in the Nordic power system was not sufficiently known. The exact computation of oscillation modes is dependent on extensive data on actual number of machines in operation as well as the impedance path of tie-lines and transmission corridors in the Nordic grid.

Instead Nordic inter-area oscillation modes are derived directly from phasor measurements captured during a tie-line switching between Eastern Denmark and Sweden. The recorded switching event excited well damped power oscillations that had a moderate impact effect on the power system. The case illustrated in this paper was among the first Nordic applications of synchronized phasor measurements for power oscillation monitoring. Important system-wide oscillation frequencies are easily detected using positive sequence phasors at respective buses in Sweden and Eastern Denmark. In fact this method is more convenient than modal analysis using a detailed model of a large interconnected system.

II. Power System Description

The Nordic system shown at Fig. 1 comprises of synchronized power systems in Norway, Finland, Eastern Denmark and Sweden. The installed capacity of the entire Nordic system is about 90 GW and the peak load is 60 GW. The total installed capacity in Eastern Denmark is 4360 MW and the maximum load is about 2870 MW. The transmission grid in Eastern Denmark encompasses overhead lines and cables at the two highest voltage levels, i.e. transmission at 132 kV and 400 kV, and the interconnections with South Sweden and Germany. The link between Eastern Denmark and Sweden has a total transfer capacity of some 1600 MW and it serves as an interconnection between two parts of the Nordic power system. Fig. 2 shows the Eastern Danish 400-kV grid together with the northeastern interconnection to Sweden and the southern interconnection to Germany. The link to Germany

Elkraft System Ltd and the Danish Academy of Technical Science supported this work.

J. Rasmussen is undertaking a Ph.D. study at the Technical University of Denmark in close cooperation with Elkraft System Ltd (e-mail: jor@oersted.dtu.dk).

P. Jørgensen is Director of the Transmission Department, Elkraft System Ltd, Lautruphøj 7, 2650 Ballerup, Denmark (e-mail: prj@elkraft.dk).

is a 400-kV DC interconnection with a transmission capacity of 600 MW. The interconnection between Eastern Denmark and Southern Sweden consist of two 400-kV circuits connected to the 400-kV busbar in Söderåsen and two 132-kV circuits connected to the 132-kV busbar in Mörarp (Fig.3). Each 400-kV circuit consists of overhead circuits in Denmark and Sweden and three 400-kV single-phase submarine cables and a seventh single-phase cable as spare.

Fig. 1. The transmission grid of the Nordic countries

Each 132-kV circuit consists of overhead circuits in Denmark and in Sweden and two three-phase submarine cables. There is a 400/132-kV transformer in Söderåsen and two 132-kV circuits between Söderåsen and Mörarp, each with a length of 8 kilometers.

A. Event Description

The 400 kV power system of Eastern Denmark with a simplified representation of the Swedish grid is represented at Fig. 3. The equivalent 400-kV backbone network includes the double 400-kV tie-line connection (shown in full lines) between substation Hovegård (HVE) in Denmark and Söderåsen (SAN) in Sweden. The 132-kV tie-line given by dotted lines in Fig.3. is terminated at Mörarp (MRP) in Sweden and Teglstrupgård substation (TEG) in Eastern Denmark.

Fig. 2. The 400-kV transmission grid in Eastern Denmark. One PMU was placed at Asnæs Power Station (ASV) and another PMU was placed 200 km away at Söderåsen substation (SAN), Southern Sweden.

The power system event studied is a planned switching of the 400-kV tie-lines between Söderåsen and Hovegård substations. The lines were deliberately disconnected due to connection of a new substation in the 400-kV transmission system. Due to technical constrains[1] during the outage period the power transfer was deliberately limited to 100 MW (import or export to Sweden) compared to some 1600 MW at normal conditions. Hence the line switching appeared as an event that weakened the Eastern Danish power system.

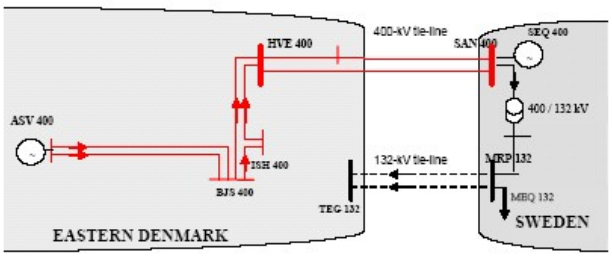

Fig. 3. Two-area model of interconnected power systems

The disconnection of the 400-kV tie-lines between Eastern Denmark and Sweden can be understood as interruption of an important corridor in the interconnected system followed by fluctuating forces in the other transmission lines. Power oscillations occurred on the tie-lines connecting different groups of machines as a result of temporary unbalance between power input and output.

[1] A previous disturbance in April 1985 demonstrated that there was a considerable risk for undamped power oscillations when the export from Denmark to Sweden increased to 300 MW.

III. POWER OSCILLATIONS IN INTERCONNECTED SYSTEMS

The power system at Fig. 4 shows a two-area model of major generation/load areas connected by a tie-line.

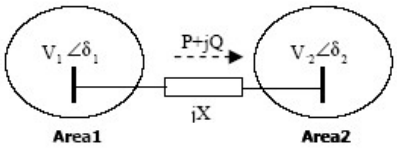

Fig. 4 . Inter-area power oscillations involving two areas.

In general, the dynamics of power oscillations in large systems [1] is related to the power flow P in a tie-line as follows:

$$P = \frac{V_1 \cdot V_2}{X} \sin(\delta_1 - \delta_2) \qquad (1)$$

where X is the line reactance and V_1, V_2, δ_1 and δ_2 are the magnitudes and angles of the voltages at the line terminals.

Inter-area power oscillations are dependent on the power system response to small disturbances such as change in scheduled generation or small increase in system load after the system has been perturbed from a steady-state condition [2]. The phenomenon of small signal stability is related to small changes of system quantities such as power and machine angles ($\Delta\delta$). The free response of n-machine power system is derived from the linearized version of the well-known swing equation of motion of an ideal unregulated machine i [16]:

$$\frac{d^2(\Delta\delta_{ij})}{dt^2} + \frac{\omega_R}{2H_i} \cdot \sum_{\substack{j=1 \\ j \neq i}}^{n} P_{sij} \Delta\delta_{ij} = 0 , \qquad (2)$$

According to (2) the power oscillations are dependent on the rated system frequency ω_R (rad), the inertia constant H_i for machine i and the synchronizing power coefficient P_{sij}, which is related to the change in electrical power in machine i due to angle change between machines i and j, with all other machine angles held constant. In general electro-mechanical oscillations in interconnected power systems are manifested by an exchange in mechanical kinetic energy between groups of generators as electric power flows through the transmission system. The small signal stability of large power systems is characterised by a number of complex eigenvalues for each oscillating mode. Each mode is associated with a single eigenfrequency and a damping factor. Successful damping of power oscillations indicate a stable system that is able to return to an acceptable steady state situation after being exposed to a disturbance. A damping factor of 3-5% is accepted as reasonable for damping of inter-area modes [8].

In general computation of eigenvalues in large power systems is a complex task, since it involves a systematic procedure for simultaneous solution of differential equations representing synchronous machines with associated prime movers, excitation systems and Power System Stabilizers (PSS), extensive transmission networks, load dynamics, power electronic devices (such as HVDC links, SVC) etc. Analysis of inter-area oscillations in large interconnected power systems requires comprehensive off-line studies, such as eigenvalue analysis and dynamic simulations using a detailed model of the entire system including a wide range of non-linear devices. E.g. the identification of Nordic system modes is to a great extent dependent upon the actual configuration of the interconnected power systems [14]. It means that detailed information about a number of machines in operation (system inertias), the impedance path of the tie-lines and the transmission corridors (transmission stiffness between the inertias) is the key issue for determination of oscillation modes associated with a particular eigenfrequency and damping.

A more effective way to observe inter-area oscillation modes and system damping is using phasor measurements from PMUs [7],[15]. The advantage of phasor measurements for tracking system dynamic phenomena is further discussed.

IV. MEASUREMENTS

Two PMU prototypes, ABB RES 521 PMU β version, were commissioned independently of each other at Asnæs Power Station (ASV) and Söderåsen substation (SAN) in Southern Sweden in order to record frequency and positive sequence phasor quantities such as 400-kV busbar voltages, currents in 400/132 kV transformers and currents in outgoing 132 kV lines at the respective locations, which are 200 km apart. The instantaneous values of the voltages and currents were sampled with a sampling rate of 36 kHz, aligned and downsampled in two steps to a sampling rate of 1 kHz. The synchronized phasors are calculated using these samples of the instantaneous values and reported every 20 milliseconds using time transmissions from the GPS satellites [4],[7]. The recordings were stored on a PC near the PMUs. After normal operation was re-established the data from the remote substations were aligned according to a common time reference [3].

The synchronized recordings at ASV and SAN were compared directly due to the fact that the voltage and current measurements are assigned the same time stamp and phase reference supplied by GPS clock. The accuracy of phasor measurements [12] is quoted to be ± 0.005 Hz for frequency accuracy and ± 0.1 deg for angle accuracy. The measurement accuracy of phase angles is primarily caused by transducers at transmission level. In general the precision of the

synchronization is up to 1 μs, which introduces a negligible measurement error [5].

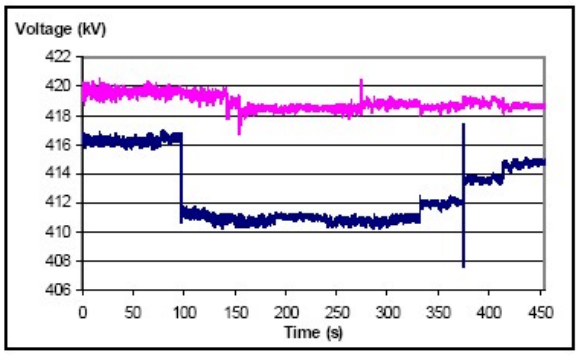

Fig. 5. The voltage magnitude measured as a function of time. The lower curve shows the voltage at SAN, while the upper curve shows the voltage at ASV.

The voltage magnitude at SAN during the reconnection sequence is presented on Fig. 5 as the lower curve. The voltage decrease after 90 s was caused by the connection of a 150 MVAr reactor in SAN. The first 400-kV tie line was energized from the Danish side and the line reconnection to Sweden was completed at 330 s. The second 400-kV line inserted at SAN gave rise to a transient peak at 370 s. Subsequently the voltage builds up until the second line reconnection is completed at about 400 s. Fig. 5 also indicates the measured voltage at ASV, where the voltage variations are limited within 2 kV due to the power plant voltage regulation.

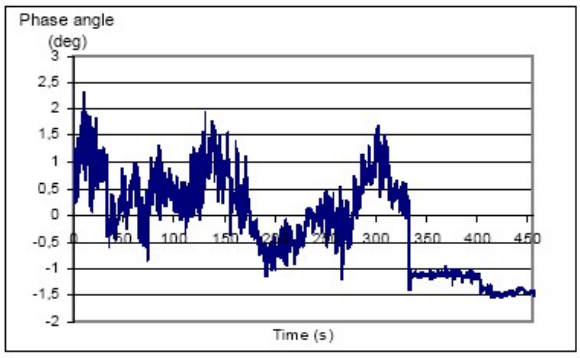

Fig. 6. Voltage phase angle difference between SAN and ASV busbars measured as a function of time.

The oscillations in relative phase angle (Fig. 6) between SAN and ASV are observed before the first 400-kV connection is established at 330 s. A phase shift of about 1.3 deg occurs after the reconnection of the first 400-kV tie-line. After the second 400 kV line is reconnected at about 400 s the voltage angle difference between SAN and ASV is further decreased to lower amplitude and the oscillation is successfully damped.

Fig. 6 shows that the power system was weakened (but not severely stressed) during the recorded switching event. The small effect on the power system (small initial angles and moderate phase shift) is influenced by low tie-line transfer[2] and total system load of about 65% of maximum load. The phase shift of 1.3 deg recorded is within the phase angle accuracy, which according to the PMU manufacturer is quoted to be 0.1 degrees. Thus the presented recordings can not be used as a benchmark case nor generalised for a number of sudden disturbances or outages.

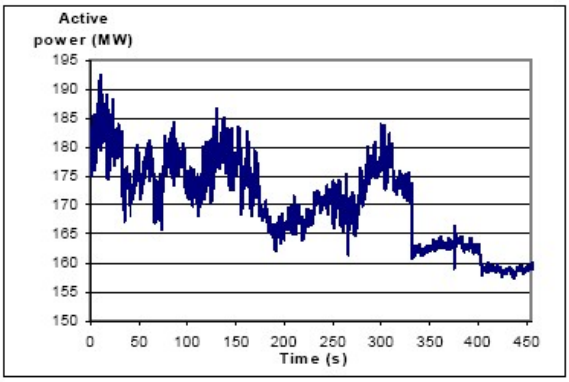

Fig. 7. Active power flow in the 132-kV interconnection measured at MRP as a function of time.

Fig. 7 shows that prior to the 400-kV tie-line connection power swings were excited between the systems interconnected via a double 132-kV line only. The relative change in phase angle between SAN and ASV during the tie-line outage affected power oscillations, which were superimposed on the steady-state line flow in the power system [1]. The correlation between the change in tie-line power flow (Fig. 7) and difference in voltage phase angles (Fig. 6) is obvious, which is evidently described by (1). The active power flow in the 132-kV interconnection was reduced by 10 MW immediately after the double 400-kV tie-line was taken into operation. It is observed that the power swings were damped sufficiently and finally the system was settled down to equilibrium.

A harmonic analysis of the active power flow on the 132-kV tie-line after the switching event (t >330 s) was performed using the DFT function[3] in Matlab® Signal Processing Toolbox. The horizontal axis shown in Fig. 8 is related to a frequency scale up to 6 Hz, while the vertical axis is related to the magnitude (complex modulus) of the DFT transformation

[2] was deliberately controlled to 100 MW in each direction
[3] Discrete Fourier Transform

of the power flow measurement. Inter-area oscillation modes of the Nordic system are identified in the low frequency range (0.1-1.0) Hz of Fig. 8. The largest peak reveals a dominant eigenfrequency of about 0.7 Hz, which corresponds to the oscillation mode between Sweden and Eastern Denmark [9].

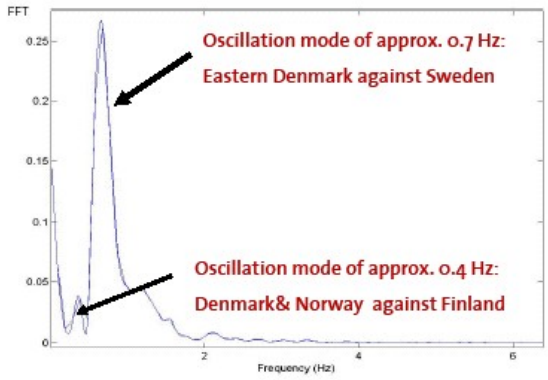

Fig. 8. Spectral analysis of 132 kV tie-line flow.

A less distinct peak is evident at frequency of about 0.4 Hz, which is related to an oscillation mode involving all the generators in the Nordic system. In this case the system inertias swing into two generators groups, where Denmark and Norway swing against Finland [14].

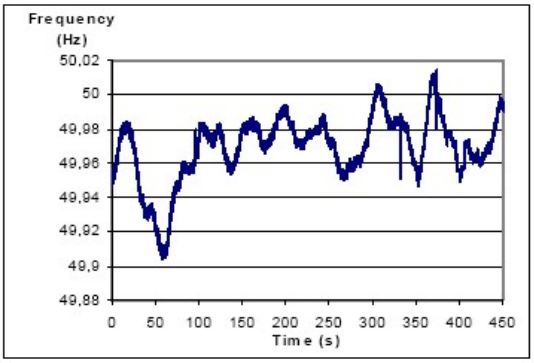

Fig. 9. Frequency measured at SAN substation

The measured frequency variation at SAN substation is given at Fig. 9. The rapid frequency transients at 330 s and 370 s are caused by reconnection of the first and the second 400-kV line at SAN, where the frequency is also recorded. The graph of the respective frequency at ASV is not depicted, as it follows the same trend as SAN due to the strong 400-kV connection between ASV and SAN measuring locations.

V. Simulations

The objective of the simulation analysis in the PSS/E[4] program was to reproduce the behavior of the Eastern Danish transmission system during the reconnection of the double 400-kV tie-line. Static and dynamic simulation of the reconnection sequence was performed using a detailed power system model for Eastern Denmark with a simplified representation of the Swedish grid equivalent (see Fig.3). To make the reference load flow case as exact as possible the initial conditions for the 400 kV and 132 kV power system are based on actual data for generation dispatch and transfers to Sweden and zero transfer to Germany, which are captured by a limited amount of SCADA[5] system data, which reveals the operating condition for the particular hour of the day in the control center at the Independent System Operator (ISO) of Eastern Denmark.

During the actual situation the power system was not severely stressed as the tie-line transfer was low and the total system load was about 65% of the maximum winter load. In the simulation model substation SAN is connected to a simple Swedish generation equivalent, which is accounted as a slack bus with zero phase angle. An estimate for the local load at the Swedish side (MEQ) is represented by load equivalent of 120 MW connected at MRP busbar. In the reference load flow case the line HVE-SAN is disconnected and about 52 MW are sent from Sweden to Eastern Denmark via the 132-kV tie-line MRP-TEG. The power transfer with Sweden is rather low compared to the transfer limit in normal operation, because it is set intentionally as a precaution measure against wide-spread disturbance.

This initial condition is characterized by small phase angle change (about 0.5 deg) between ASV and SAN substations. The small initial angles are indeed indicative for a strong and lightly loaded system. The power plant at Asnæs (ASV) delivers about 244 MW via the 400 kV lines. After the reconnection of the 400-kV tie-line the steady-state phase angle difference between ASV and SAN is slightly changed to about 1.3 deg. and about 10 MW are transmitted via the 400-kV tie-line HVE-SAN. The active power towards 132-kV busbar MRP (see Fig. 3) was reduced by the same amount power. In the intact network the active power from MRP provides the local load equivalent at MEQ and remaining 40 MW are directed to Denmark via the 132-kV tie-line MRP-TEG. The simulated power transfer from Sweden (SAN) to Denmark (HVE) complies with the calculated values from equation (1) for the tie-line flow taking in account the value for line impedance and the small increment in phase angles.

[4] Power System Simulator for Engineering® from Power Technologies, Inc. (PTI).

[5] The SCADA system at the Operational Control Center (ISO Elkraft System) collects data every 5-10 seconds. The data is typically averaged to values valid for the hour of question.

The dynamic simulation in PSS/E presumes steady state initial condition prior to the reconnection of the 400-kV tie-lines. Each power plant generator was presented together with a power system stabilizer, a detailed governor model and excitation model. Switching shunts and voltage control at specified points in the 400-kV and 132-kV transmission network were considered in the simulations.

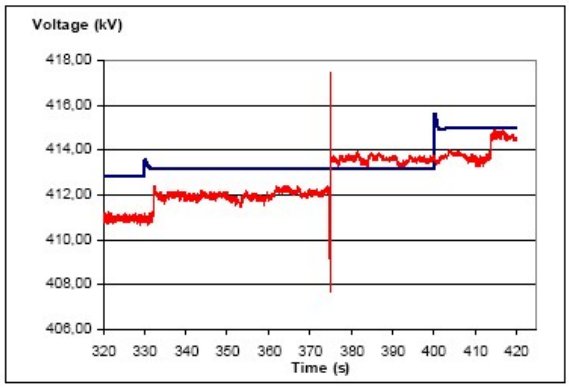

Fig. 10. Simulated vs. measured voltage magnitude at SAN as a function of time.

The voltage magnitude at SAN was simulated during a 100 s period, under the assumption that each 400-kV tie-line is re-energized simultaneously at both ends. Actually, the circuit-breakers were not closed simultaneously and four switching events can be spotted in the PMU recordings. Thus the previous assumption does not reveal to the exact power system operation. Starting from a 413 kV initial value the voltage at SAN increases in steps after reconnecting the first line (330 s) and the second 400-kV tie-line (400 s), see Fig. 10. When the SAN voltage is stabilized it attains a final value of 415 kV, which corresponds exactly to the average measured value for the intact network shown in Fig. 5. Analogous to the measured curve in Fig. 6, the calculated difference in voltage angles between SAN and ASV is illustrated in Fig. 11. A characteristic shift of about - 0.9 deg is recorded immediately after the simulated reconnection of the first line (330 s), while the subsequent line connection (400 s) results in a minor shift in the relative phase angle.

The simulated post-disturbance value of relative voltage phase angle after 400 s is relatively close to the corresponding measured quantity. Fig. 11 reveals a discrepancy of some 0.75 deg during the period 320 -330 s. This initial difference is caused by inexact representation of the 132 kV for the Swedish network equivalent and the uncertainty of the particular load condition. The measured oscillatory behavior in phase angle (Fig.11) and power flow (Fig.12) prior to the switching event arises from internal impacts from Swedish generators. A complete match between the simulated and the monitored system conditions is a difficult task due to discrepancies between the pre-fault load flow in the simulation and the actual conditions prevailing in the power system recorded by instantaneous phasor data from the PMU units.

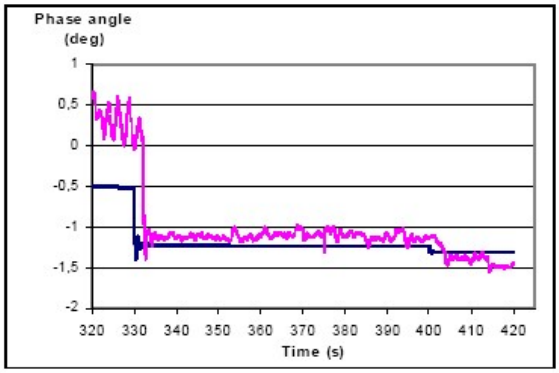

Fig. 11. Simulated vs. measured voltage phase angle difference between SAN and ASV bus bars as a function of the time.

The main reason is the fact that the initial load flow condition was based on SCADA[6] recordings reported as averaged values in the particular hour interest. Furthermore the system loads were not exactly known at the time the phasor measurements were realized.

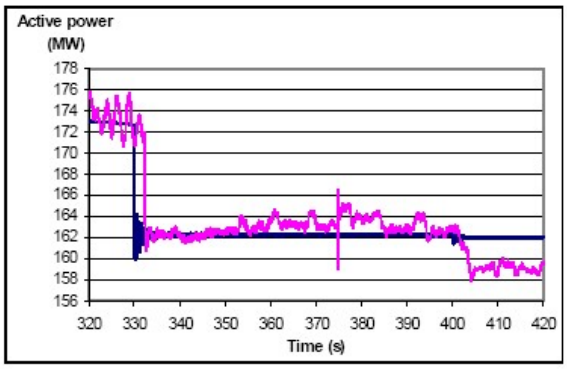

Fig. 12. Simulated vs. measured active power flow in 132 kV tie-lines to MRP transformer station.

The recorded active power oscillations prior to the switching event are not considered critical, since they are damped successfully in the intact network. This discrepancy results from the assumption that the dynamic simulation starts from a steady state initial conditions, which does not coincide with the real measurements [6]. This is due to the fact that the exact operating situation in the entire power system is not precisely known. From the other hand the simulated power flow in the 132-kV tie-line (Fig. 12) is in good agreement with the actual measured power flow during the reconnection sequence. The simulated post-disturbance value of 162 MW is

[6] Supervisory Control And Data Acquisition System

about 2 MW higher than the corresponding value measured as average in the intact network. The simulated active flow at 330 s is about 13 MW less than the initial value of 173 MW, which is in good correspondence with the shift observed at the corresponding point in the measured curve.

VI. CONCLUSION

The paper presents one of the first Nordic applications of synchronized phasor measurements in monitoring power system oscillations during a tie-line switching. Two ABB RES 521 PMU β prototypes provided simultaneous recordings of voltage and current phasors at key buses. The measured tie-line power flow and dynamics in the voltage phase angles revealed low frequency oscillations of a group of machines within a large area (Sweden) against the neighboring area (Eastern Denmark) in the Nordic system. The PMU data was a valuable tool in post-disturbance analysis of the dynamic behavior of the Eastern Danish power system with respect to the Swedish interconnection during the 400-kV tie-line switching. The presented recordings justify the high accuracy and feasibility associated with synchronized phasors. The phase angle accuracy is related to relatively small errors introduced by transducers. The synchronization using GPS has high precision, since the samples are time tagged with an accuracy of 1 microsecond.

The paper demonstrates that direct observation of inter-area oscillation modes using phasor measurements is more convenient than computation of eigenvalues using a detailed model of a specific system configuration. The recorded power system response is to some extent consistent with the dynamic simulation results. The initial condition assumptions as well as the imprecise model for the Swedish equivalent can explain the discrepancy between the simulated curves and the phasor recordings prior to the reconnection of the 400-kV tie-line.
The limited availability of detailed small signal stability models of the Nordic system demanded the simulation with a simplified Swedish power system model, which showed up to be insufficient for correct simulation of power oscillations and precise determination of eigenvalues. The application of synchronized phasor measurements for, e.g., validation of power system models used in stability studies, is seen as having a great potential in the future. Future perspective of real-time phasor data is seen in developing tools for detecting and preventing dynamic problems rather than simply analyzing critical power system events.

VII. ACKNOWLEDGEMENT

This paper is based on a contribution presented by the authors at the 2003 IEEE Bologna Power Tech, Bologna, Italy, June 23-26, 2003. The authors gratefully acknowledge the contributions of ABB, which made it possible to borrow prototypes of PMU.

VIII. REFERENCES

[1] Kundur P., "*Power System Stability and Control*", McGraw–Hill, 1993.

[2] Anderson P.M., Fouad A.A., "*Power System Control and Stability*", Volume I, The Iowa State University Press 1977.

[3] Heydt G.T., Liu C.C., Phadke A.G. and Vittal V., "Solutions for the crisis in electric power supply", *IEEE Computer Applications in Power*, vol. 14, no.3, pp. 22-30, July 2001.

[4] Phadke, A.G., "Synchronized phasor measurement in power systems", in *IEEE Computer Applications in Pow*er, vol. 6, no.2, pp. 10-15, April 1993.

[5] Martin K.E.: "Phasor Measurements at the Bonneville Power Administration", Power Systems and Communication Systems Infrastructures for the Future, Beijing, September 2002.

[6] Burnett R.O., Butts M.M., Cease T.W., Centeno V., Michel G., Murphy R.J., Phadke, A.G., "Synchronized phasor measurements of a power system event", *IEEE Transactions on Power Systems*, Vol.9, No.3, pp.1643-1650, August 1994.

[7] Phadke A.G., Thorp J.S.: "*Computer Relaying for Power Systems*" John Wiley and Sons Inc., ISBN 0 471 92063 0 Research Studies Press Ltd. 1988, ISBN 0 86380 074 2

[8] Hemmingsson M., Samuelsson O., Pedersen K.O.H. and Nielsen A.H.: "Estimation of Electro-Mechanical Mode Parameters using Frequency Measurements", in *Proc. 2001 IEEE Power Engineering Society Winter Meeting*, vol.3, pp. 1172-1177, 2001.

[9] Nielsen A.H., Pedersen K.O.H., Samuelsson O.: "An experimental GPS-based measurement unit", in *Proc. of Nordic and Baltic workshop on power systems*, February 4-5, 2002, Tampere University of Technology, Tampere, Finland.

[10] Samuelsson O.: "Wide area measurements of power system dynamics - the North American WAMS project and its applicability to the Nordic Countries", ELFORSK report 99:50, January 2000.

[11] Cigre TF 38.02.19 (Convenor: D. Karlsson): "System Protection Schemes in Power Networks", Electra, No. 196, pp. 50-61, June 2001.

[12] Hemmingson M., "Power System Oscillations, Detection Estimation and Control" , Ph.D. dissertation, Department of Industrial Electrical Engineering and Automation, Lund Institute of Technology, Lund University, ISBN 91-88934-27-6, March 2003

[13] Lysfjord T., Messing L., Ingemars B., Keränen T., Østrup T., "Improved damping of power oscillations in the Nordic grid using optimisation of adjustable control parameters for Power System Stabilisers", (in Swedish) "Förbättrad dämpning av effektpendlingar i nordelnättet genom optimering av inställbara reglerparametrar för dämptillsatser", Nordel report 1982-06-15

[14] Uhlen K., Elenius S., Norheim I., Jyrinsalo J., Elovaara J., Lakervi E., Application of Linear Analysis for Stability Improvements in the Nordic Power Transmission System, *IEEE/PES General Meeting,* Toronto, Canada, July 13–17, 2003, 7 p.

[15] Ballance J., Bhargava B., Rodriguez G.D.,Southern California Edison Co, USA, "Use of Synchronized Phasor Measurement System for Enhancing AC-DC Power System Transmission Reliability and Capability", C1-210, CIGRE Session 2004

[16] Eliasson B., "Damping of Power Oscillations in Large Power Systems", Ph.D. dissertation, Department of Automatic Control, Lund Institute of Technology, 1990

“Wind Power Impact to Transient and Voltage Stability of the Power System in Eastern Denmark”

Rasmussen J., Jørgensen P., Palsson M.T., Uhlen K.

Conference proceedings on 8th IASTED International Conference on Power and Energy Systems
International **A**ssociation of **S**cience and **T**echnology of **D**evelopment, 24-26.October 2005
Marina del Rey, California, USA

WIND POWER IMPACT TO TRANSIENT AND VOLTAGE STABILITY OF THE POWER SYSTEM IN EASTERN DENMARK

Joana Rasmussen,
Elkraft System, Ltd.,
Lautruphøj 7,
2750 Ballerup,
Denmark

Preben Jørgensen,
Elkraft System, Ltd.
Lautruphøj 7,
2750 Ballerup,
Denmark

Magni T. Palsson,
SINTEF Energy Research,
Sem Sælandsvej 11
7465 Trondheim
Norway

Kjetil Uhlen
SINTEF Energy Research
Sem Sælandsvej 11
7465 Trondheim
Norway

ABSTRACT

Voltage stability, transient stability and reactive power compensation are extremely important issues for large-scale integration of wind power in areas distant from the main transmission system in Eastern Denmark. This paper describes the application of a dynamic wind farm model in simulation studies for assessments of a large wind power penetration. The simulation results reveal problems with voltage stability due to the characteristic of wind turbine generation as well as the inability of the power system to meet the reactive power demand. Furthermore, the established model is applied to analyze challenges in system protection as means to reduce the risk of widespread blackouts.

KEY WORDS

Power system analysis, Transient stability, Voltage stability, Wind power modeling, Dynamic simulation, Ride-through capabilities.

1 Introduction

Transmission system operators (TSOs) are defining specific requirements for grid connection of wind farms in terms of performance and control e.g. during fault situations. To fulfil these requirements, careful planning and design of control and system protection are needed.

One of the objectives is to maintain transient stability of the power system, which is related to the ability of the synchronous machines in the system to sustain a severe disturbance and remain in synchronism. In this context investigation of the "ride-through" capabilities of different wind turbine types (passive vs. active stall models, fixed speed vs. variable speed machines, etc.) plays an important role in transient stability analysis in the Eastern Danish grid. Furthermore, voltage stability and reactive power compensation are important issues for large-scale integration of wind power in areas distant from the main transmission system in Eastern Denmark.

From an analysis point of view, the study of generator performance during grid faults can be characterized as a transient stability problem [1]. In case of induction generators this problem is also related to the degree of reactive power support in order to magnetize and stabilize the generators after fault clearing. Furthermore, this may turn into a voltage stability (or voltage collapse) problem if after fault clearing the network becomes too weak to maintain stable operation of a large share of wind farms without active voltage control.

The voltage instability phenomenon is manifested in progressive and uncontrollable drop in voltage after a power system disturbance e.g. outage of equipment (generation unit, transmission line, transformer etc.). The voltage stability is typically associated with increase in load demand and the power system response to large disturbances in the time range from few seconds to tens of minutes. Progressive drop in voltage at wind turbine terminals and power system substations can also be associated with rotor angle instability. The aim of this paper is to illustrate this problem through simulation studies, and to describe possible solutions in terms of dedicated protection schemes or additional voltage and reactive power support. In fact the case studies are not representative of the actual real-time behavior of the Eastern Danish system.

2 Power System Description

The transmission grid in Eastern Denmark encompasses overhead lines and cables at 132 kV and 400 kV level, as well as interconnections to Sweden and Germany. The tie-line to Sweden consists of two 400 kV cables and two 132 kV cables, that serve as AC interconnection to the Nordic grid. Figure 1 shows the 400 kV and 132 kV transmission grid together with the north-eastern interconnection to Sweden and the southern 400 kV DC link to Germany. The maximum load in Eastern Denmark is about 2870 MW and the total installed capacity is 4360 MW.

The power system incorporates wind power capacity of approx. 600 MW, which is connected on-land to local distribution networks, either as single installations or as few wind turbines in clusters. Additionally, the off-shore wind farm Nysted in southern Lolland is AC-connected to the southern part of the 132 kV transmission grid.

Figure 1: The 400-kV (red) and 132-kV (black) transmission grid in Eastern Denmark

3 Dynamic wind turbine model

The most common type of wind turbines installed in Denmark is the conventional passive stall fixed-speed wind turbines based on induction generators shown in Figure 2. The induction generator is equipped with a reactive power compensation unit[8] and connected to the power grid via a step up transformer.

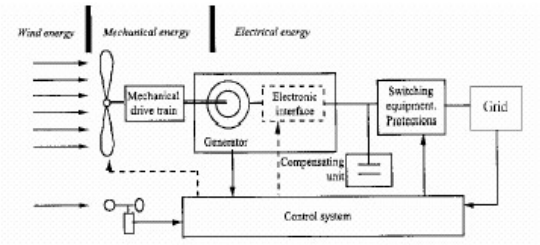

Figure 2: General concept of a passive stall wind turbine

[8] No-load or full-load compensation

A dynamic model for passive stall wind turbines [6] was developed in the PSS/E program[9]. It consists of a mechanical module [2] that incorporates the incoming wind speed characteristic with the mechanical representation of the wind turbine, and a standard induction generator model in PSS/E.

3.1 Mechanical wind turbine model

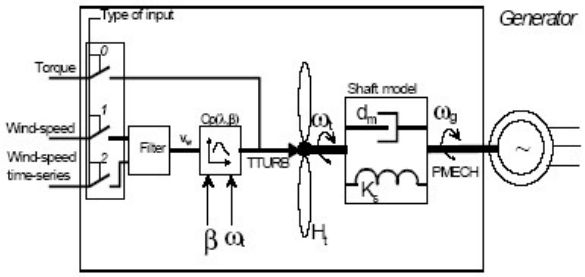

Figure 3: Two-mass model of a passive stall wind turbine

The mechanical part of the two-mass model describes the aerodynamic rotor of the wind turbine and a mechanical drive train represented by a shaft system with a low-speed and high-speed shafts coupled by a gearbox. The wind energy arriving at the rotor blades of a single fixed-speed passive stall wind turbine is transformed to a rotational torque TTURB at the mechanical drive train.

The mechanical output PMECH from the wind turbine is introduced as input to the 3rd order induction generator model (CIMTR3) in the PSS/E program.

The standard relationship between wind speed and mechanical power delivered to the shaft of the passive stall wind turbine is:

$$P_{MECH}=\frac{1}{2}C_p(\lambda)\cdot\rho\cdot\pi r^2 v^3 \qquad (1)$$

where ρ is the air density, $r^2\pi$ is the wind turbine rotor area, Cp (λ) is the power coefficient for a passive stall wind turbine and λ is the tip-speed ratio defined by the rotor rotational speed ω_r and the wind speed v.

$$\lambda=\frac{\omega_r\cdot r}{v}$$

The torque delivered to the shaft is derived as follows:

$$T_{MECH}= P_{MECH}/\omega_r \qquad (2)$$

[9] Power System Simulator for Engineering® from Power Technologies, Inc. (PTI).

As illustrated in Figure 3 the model may be initiated either by using fixed-torque input or variable wind speed / wind speed time series that introduce fluctuations in the wind power output. The fixed-torque mode is a suitable input for traditional stability analysis (e.g. short circuits, tripping of lines/generators etc). The fixed-torque input TMECH corresponds to the mechanical power needed to produce electrical power specified from the load flow calculation [7]. In the simulation studies (section 4) fixed-torque is applied as a convenient input for analysis of voltage stability and short-term transient stability.

Constant mean wind speed with variance is typically used input for studies of interaction resonance phenomena etc. The input with wind speed time series is considered in long term simulations of e.g. the impacts of wind speed trend variations. The last option is important for valuation of wind power fluctuations and model verification described in section 3.2.

In general the dynamic behaviour of turbine-drive train is represented by two-masses corresponding to the turbine inertia and the generator inertia coupled by a flexible shaft. The state equations for this model [4] are:

$$\begin{aligned} 2H_G \frac{d\omega_G}{dt} &= K_S\theta_S - D_G\omega_G - T_G \\ 2H_T \frac{d\omega_T}{dt} &= T_{TURB} - K_S\theta_S - D_m\omega_T \\ \frac{d\theta_S}{dt} &= \omega_0(\omega_T - \omega_G) \end{aligned} \qquad (3)$$

The set of equations (3) use quantities such as turbine torque (T_{TURB}), generator torque (T_G), turbine rotor speed (ω_T) and generator rotor speed (ω_G), inertia constant for wind turbine (H_T) and generator (H_G), damping coefficient for wind turbine (D_m) and generator (D_G), shaft stiffness (K_S) and torsional twist (θ_S). Two-mass wind turbine models are appropriate for transient stability studies, since they take into account the interaction between the wind turbine mechanical and electrical system. Among crucial parameters for the dynamic response of the model are the different size of inertia for the wind turbine and the generator as well as the degree of soft or stiff coupling between turbine and generator (shaft stiffness K_S).

3.2 Induction machine model

The PSS/E model of a squirrel cage induction generator (CIMTR3) represents the generator internal voltage E´ behind a transient reactance X´$_s$. The induction machine equivalent [3] is determined as follows:

$$\frac{dE'}{dt} = -\frac{1}{T'} \cdot \left[E' + j(X_s - X_s')I\right] + j \cdot s\omega_0 E' \qquad (4)$$

In equation (4) X_s is total stator reactance, I is stator current and the slip s is denoted from the generator speed ω_G (rad/s) and synchronous speed ω_0 (rad/s) as $s=(\omega_G - \omega_0)/\omega_0$. The rotor transient time constant T´(s) characterizes the decay of the rotor flux linkages when the stator is open-circuited. The terminal voltage at the wind turbine generator is determined by the load flow initial conditions of the grid. Besides the network impedances the generator terminal voltage is strongly dependent on induction machine parameters such as slip s as well as active power production and reactive power consumption. An iterative calculation of initial conditions for the dynamic wind turbine model was performed in PSS/E in order to integrate the wind turbine model in the dynamic simulation software and to initialize the dynamic simulation correctly.

The dynamical behaviour of a single induction machine is described by the rotor acceleration equation [1]:

$$\frac{d(\overline{\omega_r})}{dt} = \frac{1}{2H}(T_E - T_M) \qquad (5)$$

for (p.u.) - rotor rotational speed,
T_E (p.u.) – electromagnetic torque
T_M (p.u.) - mechanical torque
H(MW·s/MVA)- combined inertia constant of the generator and the mechanical load

In case of stable operation the rotor angle oscillates about an equilibrium position with moderate speed deviation. Severe power system disturbances may introduce uncontrollable increase in the generator rotor angle and speed.

3.3 Verification of the wind turbine model

The wind turbine model has been verified, as described in [7]. The verification is based on measurements of active power from a wind farm with twenty 2 MW fixed speed, active stall controlled wind turbines. The model verification is carried out by modeling the wind turbines and their connection to a detailed model of a large power grid. The simulations are performed with a single 2 MW wind turbine installed and 20x2 MW wind turbines, respectively. In both simulations, measured wind speed time-series are applied as input to the wind turbine model. In Figure 4a, the power spectral densities (PSD) of the simulated and measured active power for a single wind turbine are compared.
The tops of the graphs indicate enhanced power fluctuations. These appear at three times the turbine frequency, i.e. 3p = 0.8 Hz. and also at 6p, 9p and 12p since enhanced power

fluctuations from fixed speed three bladed wind turbines will appear at multiples of 3p due to the wind speed variations over the turbine blades. The relative magnitudes of these fluctuations are smaller for the wind farm than for the wind turbine, as shown in Figure 4b as power fluctuations from a number of wind turbines are unlikely to coincide.

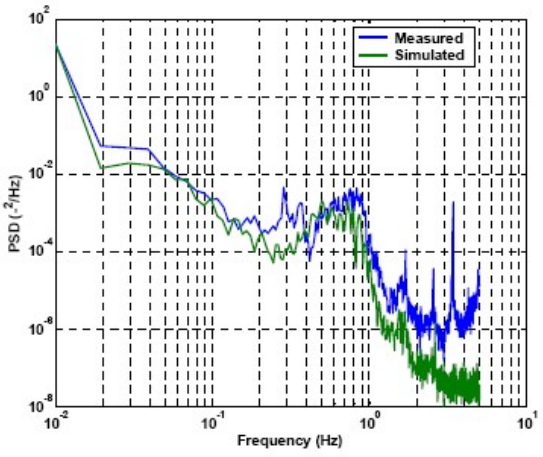

a) Wind turbine (2 MW)

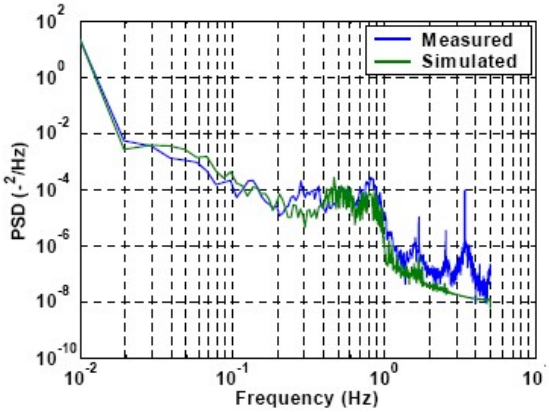

b) Wind farm (20x2 MW)

Figure 4: PSD of measured and simulated power from a 2 MW wind turbine (a) and 20x2 MW wind farm (b) [7].

The relative good match between the measurements and simulations verifies the dynamic wind turbine model. The power fluctuation around 0.3 Hz in the measured response is not reflected in the model. However this frequency component is likely to appear due to a power system oscillation not included in the grid model applied for the study. The representation of higher harmonic fluctuations (i.e. 6p, 9p and 12p) in the model is simplified, thus the measured and simulated responses deviate somewhat for frequencies above 2 Hz.

4 Simulation studies

4.1 General

A detailed model of the 400 kV and 132 kV transmission system in Eastern Denmark connected to a Nordic equivalent has been established in the PSS/E power system simulation program. Static and dynamic simulations in the PSS/E program are performed for the the main operational scenario i.e. low load (approx.1000 MW) and high wind power (in total 650 MW) situation. Three large thermal power plants produce 580 MW in total. In this case about 50% of the total generation is covered by wind production off-shore (150 MW) and on-land (500 MW). The fixed-speed passive stall model is applied for all wind turbines assuming fixed torque input. Nysted offshore wind farm has 72 active stall wind turbines with maximum installed power of 2.3 MW each, which are modeled as passive stall wind turbines in the simulation studies. Nysted wind farm is not represented accurately in any of the simulation results, in spite of the fact that it has significance on the transient and voltage stability of the system. Due to this assumption the simulation results are hypothetical and do not reflect the real-time behavior of Nysted wind farm.

The operating situation assumes zero exchange via the interconnections to Sweden and Germany as well as no production from local combined heat and power units. All power plants are modeled with excitation and governor control, as they contribute to primary voltage and frequency control in the transmission system. The reactive power output from shunt capacitors and reactors was adjusted to the actual operating condition. Another operating scenario considers change in generation dispatch, as Stigsnæs- and Masnedø power plant are used to supply additional reactive power reserve to the wind turbines in the southern part of the grid.

All wind turbines on-land are connected to the grid via 0.69 /10 kV step-up transformers, which have direct connection to 50/10 kV substations. Details about underlying distribution networks or dynamic load behavior were not included in the model. All wind farms are modeled by aggregated models that represent each wind farm as a large equivalent instead of a number of single wind turbine models in PSS/E. The equivalent wind turbine at Nysted is connected via 0.69/30 kV and 30/132 kV transformers and a 132 kV line to the main 132 kV grid at Radsted substation (RAD). This substation is the point of common connection (PCC), i.e. the first point in the system the wind farm shares with other customers. The power system was subjected to a three-phase short-circuit at the 132 kV busbar at Radsted substation located in the southern part of Eastern Denmark, where the transmission grid is relatively weak in terms of short circuit capacity. The simulation study did not include subsequent tripping of outgoing 132-kV lines from Radsted substation.

4.2 The base case – no stabilizing control

The base case investigates transient stability in the power system, without any stabilizing measures applied in a time frame of 4 seconds. The wind turbine response to the 132 kV fault is monitored for a single 0.3 MW turbine near the fault location (RAD) as well as for the equivalent wind turbine representing Nysted wind farm.

The power system behavior is observed at the 132 kV busbar at Radsted substation and at the wind turbine terminal at Nysted wind farm. The transient behavior of a single wind turbine on-land and the large wind farm at Nysted is accessed with respect to relative speed deviation, mechanical power as well as active power output using variable fault clearance time.

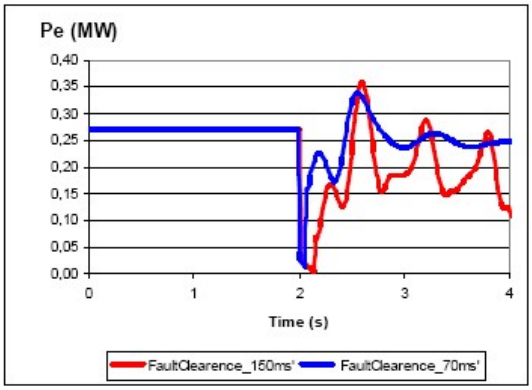

Figure 5: Electrical power at on-land wind turbine terminal near Radsted using fault clearance time of 70ms (upper curve) and 150 ms (lower curve).

When a 132 kV busbar fault occurs at Radsted substation the voltage decay propagates throughout the system and reaches the wind turbines in the Lolland region, where the largest concentration of wind turbine sites and no synchronous generation is present. As observed in Figure 5 especially large active power reduction during the fault is valid for a single wind turbine near Radsted.

The high current introduces increase in reactive power consumption at wind turbines and larger voltage drops in lines and transformers, which cause the post-fault voltage at the 132 kV busbar in Radsted to depress further (see base case curve in Figure 10). When the induction generator is subjected to e.g. a fault with 150 ms duration, the rotor accelerates rapidly (Figure 6) and ends in a run-away situation, unless precautions are taken in order to trip the generator from the grid. In case of rapid fault clearance (70 ms) the post-fault value of the speed deviation is established slightly higher than the pre-fault value, that is a result of a weak 132 kV network and the voltage dependence of the generator torque-slip characteristic.

The short circuit influences torsional oscillations between the turbine and the generator, because the turbine inertia HT is significantly larger than the generator inertia constant HG, see equation (1). The impact of these oscillations is also observed in the post-fault variation of generator speed (Figure 6) and electrical power (Figure 5).

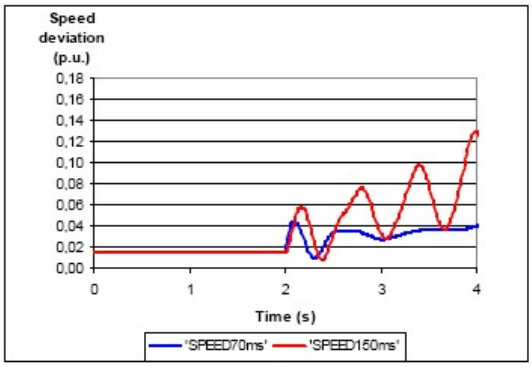

Figure 6: Relative speed deviation at a single on-land wind turbine near Radsted due to fault with 70 ms and 150 ms clearance time.

Figure 7 reveals unsatisfactory recovery of voltage and active power output from the off-shore wind farm. The simulation shows post-fault voltage at the wind farm terminal, which is less than 40% from the pre-fault value. Nysted wind farm is unable to withstand a temporary short-circuit due to insufficient amount of dynamic reactive power compensation in the area with large wind power penetration. The power system lacks the capability to transfer reactive power over large distances [1].

These simulations reveal that integrating 150 MW from the Nysted off-shore wind farm, and using passive stall controlled wind turbines equipped with conventional induction generators without any extra reactive power compensation (apart from the no-load consumption), is not viable due to voltage stability problems. Voltage instability at Nysted wind farm may result in voltage collapse of the power system, unless the relay protection at Nysted orders disconnection of the farm.

The assumption of passive stall control at the large off-shore wind farm results in unacceptable tripping of the wind farm and the subsequent loss of about 150 MW requires activation of immediate power reserves. This pessimistic solution does not comply with the TSO specifications [9], which ensure uninterrupted operation of large wind farms at grid faults. The real off-shore farm is based on active stall wind turbines that can be ordered to reduce the active power supply to less than 20% of the rated power within 2 seconds [5].

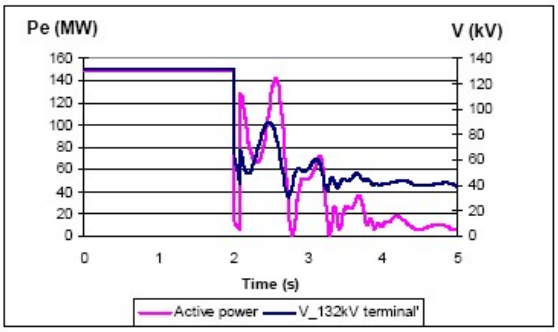

Figure 7: Active power output (pink curve) and voltage (blue curve) at 132 kV terminal for Nysted off-shore wind farm prior and after a 100 ms fault at Radsted.

The extended control features for adjustment of active and reactive power at Nysted enable the farm to withstand transmission system faults and stabilize the terminal voltage at the farm after a severe grid fault efficiently.

4.3 Cases with stabilizing control

The case studies investigate the impact of wind turbines to transient stability in the power system with a number of stabilizing measures applied. The simulations persist in passive stall representation of Nysted wind farm as a worst case scenario.

4.3.1 Base case with wind turbine rejection

The relay protection of wind turbines on-land is represented by a PSS/E user-developed model illustrated at Figure 8.

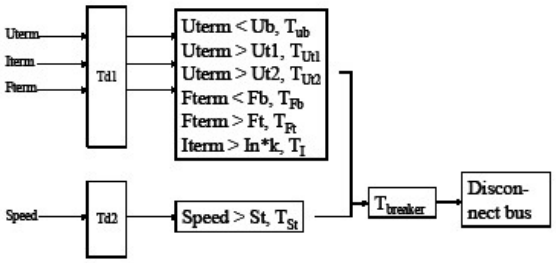

Figure 8: Relay model for wind turbines

The model includes a set of thresholds with appropriate activation time for e.g. underfrequency F_b (time T_{Fb}) and overfrequency F_t (time T_{Ft}), time T_I for an overcurrent limit, which is a multiple k of the generator rated curent I_n. The undervoltage relay has fast detection time T_{Ub} of voltages lower than Ub, while the overvoltage relay reacts in two steps i.e. fast activation (with time T_{UT1}) when the overvoltage limit Ut1 is exceeded and slow activation time T_{UT2} related to the next overvoltage step Ut2. The overspeeding logic is designed in separate relay that monitors the generator speed (St) using time setting T_{St}. Furthermore the relay incorporates a measuring delay T_{d1} for the advanced voltage/frequency relay and time delay T_{d2} for the overspeeding relay.

If any of the relay settings at the wind turbine terminal are violated during the dynamic simulation a tripping command is issued to a circuit breaker and the wind turbine and its reactive compensation unit are automatically disconnected from the grid after predefined time $T_{breaker}$. If on-land wind turbines continue uninterrupted operation during and after a short-circuit fault their induction generators will absorb reactive power from the electric grid in attempt to re-establish the voltage at the wind turbine terminals. The relay settings for on-land wind turbines [8] are applied to protect the power system from increase in reactive power demand that weakens the system further. In the base case the majority of wind turbines on-land in the Lolland region trip when their undervoltage threshold is reached about 1,1*s* after the system fault is cleared (see Figure 10). The protection of on-land wind turbines electrically close to the fault has to trip as fast as possible without tripping wind generation far away from the affected area. The compromise between rapid tripping of the affected wind turbines on-land and the lack of tripping facility for remote wind turbines is a difficult task in power system operation.

4.3.2 Case with wind turbine rejection and reactive power support from additional power plants

The power system becomes more robust to faults when Stigsnæs and Masnedø power plants (see Figure 1) with respective production of 50 MW and 30 MW are taken in operation. The synchronous generation of reactive power in the proximity of the fault leads to smaller voltage gradients and reduced over-speeding problems at wind turbines after the disturbance. As seen from Figure 9 the rejection of wind turbines at on-land sites improve significantly the voltage recovery at the 132 kV terminal at Radsted.

The fictitious SVC device[10] at the 132 kV terminal at Radsted contributes to satisfactory voltage recovery as well as to maintenance of the post-fault voltage within its acceptable operational limits. The benefit of using dynamic var devices (e.g. SVC) is discussed in the following subsection. The degree of wind turbine rejection (loss of wind power) for different fault durations and different reactive capability in the power system is illustrated in Table 1.

[10] with 90 MVAr rating

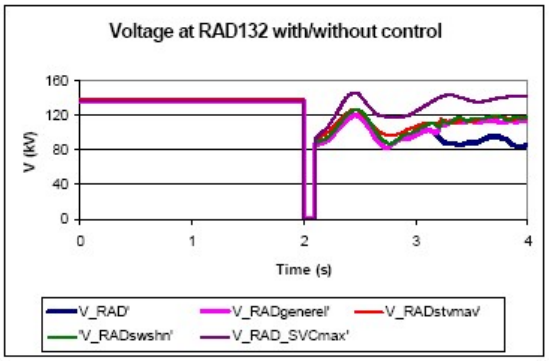

Figure 9: Voltage magnitude at 132 kV busbar in Radsted before and after a 100ms fault for: Base case without wind turbine rejection (lower curve V_RAD), Base case with wind turbine rejection (middle curveV_RADgenrel), Case with wind turbine rejection and reactive power support from STV and MAV power plants (upper curve V_RADstvmav)., Case with SVC voltage control (V_RAD_SVCmax).

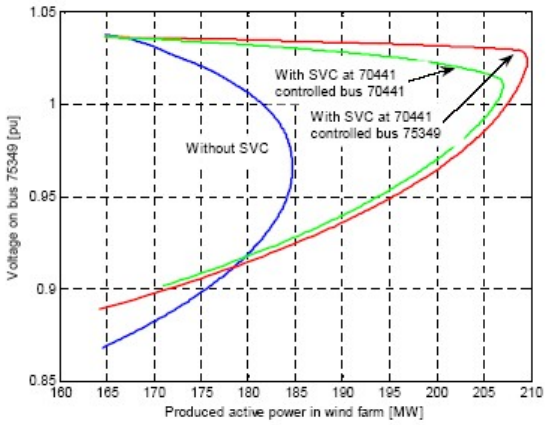

Figure 10: Voltage at Nysted terminal as a function of produced active power in wind farm. Comparison of case with no extra reactive power support and cases with a 90 Mvar Static Var Compensator (SVC)

The transmission system fault cleared at 100 ms induces tripping of twice as much wind power on-land in case of insufficient reactive power capability in the power system. The successful voltage recovery in Radsted substation justifies no need for wind turbine rejection in case of 70 ms fault duration. Although a large quantity of wind generation is tripped the power system remains stable in all analyzed cases.

CASE:	Base case		Base case with additional power plants	
Fault clearance $t_{f.c}$ (ms)	t=70	t=100	t=70	t=100
Wind power rejection (MW)	0	198	0	98

Table 1: Rejection of on-land wind turbines for different cases studied

4.3.3 Case with SVC device

The short-circuit capacity of the grid at the connection point RAD is rather low, and integrating a relatively large amount of power without active voltage control at this point is likely to increase the risk of voltage instability. Problems with voltage stability can turn into voltage collapse if after fault clearing the network with a large share of wind farms becomes too weak to maintain stable operation. Figure 10 shows a set of well-known static stability P-V curves without and with a SVC (rated at 90 Mvar) placed at Radsted substation and controlling the 132 kV voltage at Radsted (bus 70441) and at Nysted wind farm terminal (bus 75349), respectively.

The P-V stability curves are generated by simulating a linearly increasing wind production[11] and plotting the voltage on the 132 kV terminal at RAD as a function of the produced active power in the wind farm. The upper part of the P-V curves is related to stable operation, while operation beyond the tip of the curve refers to voltage instability.

For the case without SVC the operating point at full production (150 MW) is in the vicinity of the "nose-curve" tip, indicating that the system is operating close to the voltage stability limit. As indicated in Figure 10 the voltage stability limit is significantly increased by the use of a SVC device. The most effective way of controlling the voltage in the studied case is to keep a firm control of the voltage close to the wind farm.

5 Conclusion

The paper describes real problems after a disturbance in the Eastern Danish 132 kV grid encountered when integrating large amounts of wind energy into a relatively weak grid. To reveal these problems, a dynamic simulation model of a generic fixed-speed passive stall controlled wind turbine has been developed, verified and implemented in a complete model of the transmission system in Eastern Denmark. The paper demonstrates that the main reason for the particular problems with transient and voltage stability is seen in the characteristics of wind turbine generation. The passive stall fixed-speed wind turbines experience excessive rotor acceleration after a short circuit in the 132 kV grid that may initiate uncontrollable decay and cascading outages in the transmission grid.

[11] wind speed increased from 5 m/s to 25 m/s over a period of 30 s

Fast fault clearance time is crucial in order to prevent fatal overspeeding and maintain wind turbine response within acceptable limits. It has been shown that reactive power support from dynamic var devices (e.g. SVC) and two additional power plants[12] near the fault location contributes to satisfactory voltage recovery. The simulations illustrate that when wind power penetration increases, the Eastern Danish grid becomes weaker in respect to transient and voltage stability. In general, rejection of on-land wind turbines as well as improved reactive power capability of the system is necessary in order to stabilise the transmission system voltage efficiently.

The simulations confirms that integrating 150 MW from the Nysted off-shore wind farm, and using passive stall controlled wind turbines equipped with conventional induction generators without any extra reactive power compensation (apart from the no-load consumption), may jeopardize the power system transient and voltage stability. The study presented in this report shows that the presented production/load scenario is vulnerable with respect to faults in certain parts of the system (more precise; at the point where the offshore wind farm at Nysted is connected to the grid at Radsted substation).

Simulations on the base case (passive stall wind turbines, without extra stabilizing measures) show that Nysted wind farm is operated near the voltage stability limit. This means that relatively moderate disturbances may jeopardize the voltage stability unless measures for enhancing the voltage level (i.e. to produce the reactive power needed) are applied. The simulations indicate that the most effective way of increasing the voltage stability limit of the system is application of a fictive SVC device in the 132 kV grid close to Nysted wind farm.

In fact the simulation results are not representative of the actual behavior of the Eastern Danish system. The results justify the need for dynamic wind turbine model with active voltage control at Nysted wind farm. The accurate representation of the off-shore wind farm is highly important in order to investigate the wind turbine performance and its impact on security of power system operation. Additional control to counteract the inability of the weak grid to meet the reactive power demand due to large wind power penetration is an issue of further investigations.

6 Acknowledgements

The authors gratefully acknowledge the contributions of Jan Havsager and Carsten Rasmussen, Elkraft System Ltd., in the implementation of the wind turbine model.

[12] power plants used as spinning reserves

References:

[1] Kundur P., *Power System Stability and Control* McGraw–Hill, 1993.

[2] Tande J.O.G., Wind Farm Models for Power System Studies, *IEEE Transactions on Energy Conversion*, 2002

[3] Rodríguez J.M., Fernández J.L., Beato D., Iturbe R., Usaola J., Ledesma P., Wilhelmi J.R., "Incidence on Power System Dynamics of High Penetration of Fixed Speed and Doubly Fed Wind Energy Systems: Study of the Spanish Case", *IEEE Transactions on Power Systems, 17* (4) November 2002.

[4] Akhmatov V., *Analysis of Dynamic Behavior of Electric Power Systems with Large Amount of Wind Power*, Ph.D. thesis, Electric Power Engineering, Ørsted•DTU, Technical University of Denmark, April 2003, ISBN 87-91184-18-5.

[5] "Dynamic stability calculations for Nysted Off-shore Wind Farm", in Danish: "Nysted Havvinmøllepark-Beregninger af den Dynamiske stabilitet" Internal report NESA, Marts 2004 (Jørgen Nygård)

[6] Palsson M.T., "System operation and control with increasing integration of wind power and distributed generation", Internal technical report, SINTEF Energy Research, Trondheim, Norway, December 2002

[7] Palsson M.T., Toftevaag T., Uhlen K., Norheim I., Warland L., Tande J.O.G., "Wind farm modelling for network analysis – Simulation and validation", conference paper EWEC 2004, London UK, 22-25 November 2004.

[8] Wind turbines connected to grids to voltages below 100 kV", Elkraft System Ltd., April 2004; Technical regulations for grid connection at www.elkraft-system.dk.

[9] "Wind turbines connected to grids to voltages over 100 kV", Elkraft System Ltd., September 2004 Preliminary version available at www.elkraft-system.dk.

“Monitoring of power system events at transmission and distribution level”

O. Samuelsson, M. Hemmingsson, A.H. Nielsen, K.O.H. Pedersen, J. Rasmussen

Accepted for the IEEE Transactions on Power Systems,
IEEE PES Letter

Monitoring of power system events at transmission and distribution level

O. Samuelsson[1], M. Hemmingsson[1], A.H. Nielsen[2], K.O.H. Pedersen[2], J. Rasmussen[3]

Abstract—**Monitoring of events in the power system provides a great deal of insight into the behavior of the system. Events with impact on the entire power system typically occur in or near the transmission network and are therefore best monitored at transmission system substations. This puts great demands on the equipment and in general restricts the use of the data since it becomes property of the transmission system operator. An alternative is to measure at lower voltage levels. This paper documents the close agreement between voltage and frequency at low and high voltage levels during a remote and a nearby fault in the transmission network. The very high quality of the data suggests that the transmission system can indeed be monitored from lower voltages.**

Index Terms—**power system monitoring, power system dynamic stability, power system faults**

I. INTRODUCTION

The power system is continuously exposed to different disturbances. These range from small with negligible impact on operation to large with severe consequences possibly including a blackout. To gain knowledge about the disturbances and their impact it is necessary to monitor the system at sufficiently many geographical locations using measurement equipment with sufficient bandwidth. The collected data must also be condensed into useful information and properly analyzed. Historically each system operator monitors his own system. Transmission system operators (TSOs) equip the system to be able to track the state of the system during normal operation, detect abnormalities and analyze disturbances. Neighboring TSOs also exchange data for mutual benefit. Due to the nature of distribution systems, distribution system operators (DSOs) have more limited monitoring capabilities focusing on monitoring the state only at key points, fault detection and clearing and excluding the use of fault recorders. The distribution network connects to the transmission system at one or few points, but since these are usually geographically close, the DSO has limited insight into the transmission system. The dynamic behavior of the overall system is thus visible only to the TSO with appropriate equipment. This paper proposes a monitoring solution that is an alternative to the historical structures: Power system monitors are placed at suitable geographical locations covering a large part of the power system and transfer data across the Internet. The monitors are connected at customer voltage, which has several advantages. Monitoring equipment can be made simpler since design for substation use is not necessary. The use of the recorded data is not heavily restricted, which is expected for TSO-operated monitor networks such as the WECC WAMS [1].The insight into system behavior, which can be gained with such a monitoring system, can have great value to several organizations. Manufacturers of control and monitoring equipment could get to know the process their products are designed for. The fact that tripping of generators and HVDC links are reported at the NordPool website [2] indicate that actors on the electricity market may have strategic use of knowing the state of the system. Universities could base their expertise and teaching on the real system instead of simulation models. Also TSOs can benefit since points for monitoring can be more freely selected, even outside their service area, which would simplify monitoring of inter-area oscillations.The key question is of course if the data quality of the described system is sufficient. To answer the question, this paper presents simultaneous recordings at the 400 kV level and the 400 V level from two transmission system events. It also exemplifies and discusses the impact of distribution system events.

Author affiliations
1) Industrial Electrical Engineering and Automation, Lund University, Sweden
2) Ørsted Institute, Danish Technical University, Denmark
3) Elkraft System, Ballerup, Denmark

II. RECORDINGS

In connection with a project on phasor measurements involv-ing the authors, one phasor measurement unit (PMU) has been connected to the 400 V mains in a laboratory at the Danish Technical University and two PMUs monitor 400 and 132 kV bus bars in a nearby substation. The 400 V PMU measures single phase, while the others are connected to three phases and record positive sequence. Simultaneous recordings from a remote short-circuit and fault in the monitored 400 kV station are shown.

A. Remote Short-Circuit Fault

A short-circuit at a 400 kV substation in southwestern Sweden caused a voltage dip in a large part of the 400 kV network. The dip was clearly visible at the monitored points 200 km away, Fig. 1. The 400 kV voltage went from 414 kV down to 356 kV and the 400 V voltage went from 393 V down to 351 V. Scaling the 400 V curve so that prefault values match reveals that the dip is deeper at 400 kV, but that the postfault waveforms agree well.

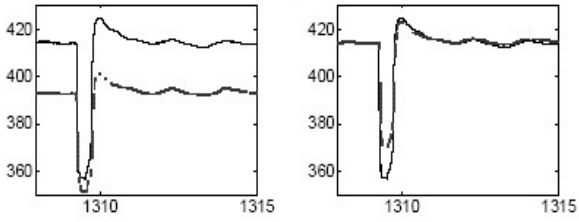

Fig. 1 Voltage dip caused by remote short-circuit at 400 kV in Sweden measured at 400 kV (solid in kV) in Denmark. Simultaneous nearby measurement at 400 V (dashed) shown in V (left) and scaled to same prefault value (right). Time is shown in seconds.

The short-circuit caused tripping of some 800 MW generation in Sweden. This caused a drop in system frequency see Fig. 2, where the curves from 400 kV and 400 V levels coincide.

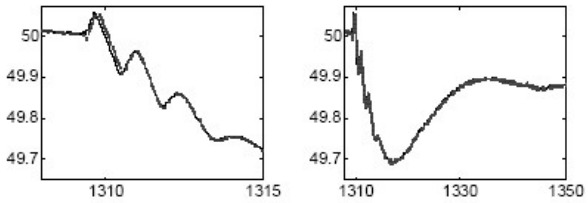

Fig. 2 Frequency transient at tripping of generation in Sweden measured in Denmark at 400 kV (solid) and 400 V (dashed). Time scales are shown in agreement with voltage dip (left) and to show settling to stationary level (right). Time is shown in seconds.

B. Fault in the Monitored 400 kV Station

A fault right in the monitored 400 kV station caused tripping of 400 kV lines. This weakened the system and reduced damping minutes later leading to oscillations with a frequency of 0.45 Hz involving several nearby generating units. The oscillations are clearly visible both in voltage and frequency, see Fig. 3. Since the 400 kV bus bar is de-energized, recordings from the 132 kV level in the same substation are used here. These agree well and obviously the 400 V data again give a good idea about system dynamics. Due to the proximity of the fault, local dynamics are excited. These are not visible in frequencies but in the difference in phase angle at 400 V and 132 kV, see Fig.3.

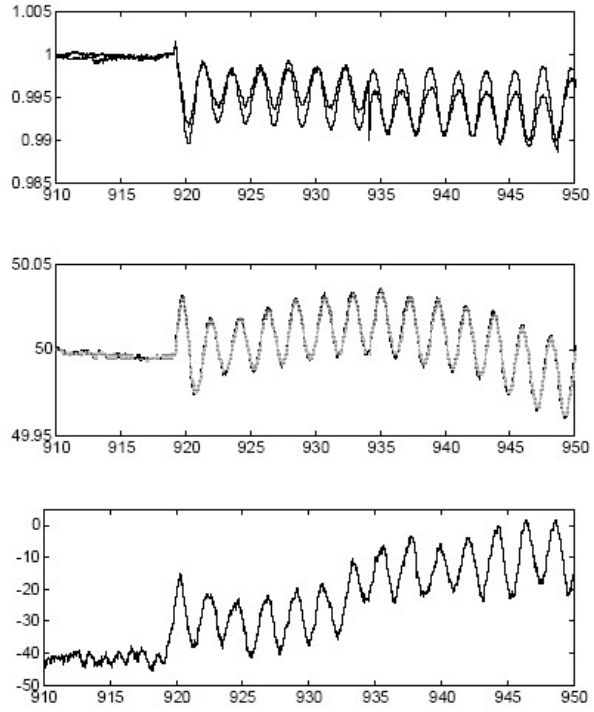

Fig. 3 Per unit voltage (top) scaled to same prefault voltage at 132 kV (thin) and 400 V (bold) during oscillations. Frequency in Hz at 400 V and 132 kV shown with thin lines (middle). Angle difference in degrees between 132 kV and 400 V (below). Time in seconds.

III. IMPACT OF DISTRIBUTION SYSTEM

With the monitors located at low voltage they will capture also events on lower voltage levels. While local oscillations as in Fig. 3 are only occasional the power consumption constantly changes during normal operation. The associated random variations in voltage magnitude and phase angle are a key difference between lower and higher voltages. The larger variations of the 400 V voltage in Fig. 4 make it easy to distinguish this from the high 400 kV voltage. Since these variations are small during normal operation, they are not mistaken for transmission system events. One source for load variations is customer behavior. Others are tap changer action and switching of reactive compensation, which primarily affect the voltage. The effect of these switching operations will be visible in low voltage measurements in one distribution system, but not in others. Access to measurements from several distribution networks makes it straightforward to classify events as occurring on transmission or lower levels.

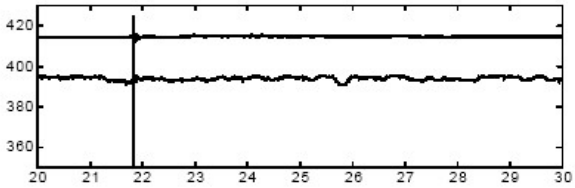

Fig. 4 Voltage measured at 400 kV (upper curve in kV) and 400 V (lower curve in V) . Note that time is shown in minutes. The voltage dip also shown in Fig. 1 is clearly visible.

III. CONCLUSIONS

The presented measurements prove that dynamic behavior of the transmission system can be monitored at a lower voltage level with high quality. This is shown both for a remote and for a nearby fault. A network of phasor measurement units installed at a lower voltage level is thus expected to deliver valuable system-wide data sets, where the phase angle information makes it possible to pinpoint the location of transmission system events. These include short-circuits and electro-mechanical oscillations shown here but also sudden generation-load mismatch, loss of AC or DC lines and voltage collapse. Future work aims at setting up such a network and to collect and analyze data. This is done in Sweden in connection with PMU activities reported in [3].

V. ACKNOWLEDGEMENT

The measurements from 400 kV and 132 kV are used with permission of Elkraft System who has sponsored the project. The support is gratefully acknowledged.

VI. REFERENCE

[1] J. F. Hauer, W. A. Mittelstadt, R. Adapa, W. H. Litzenberger, and M. K. Donnelly, "Direct Analysis of Wide Area Dynamics". Section 11.8: pp 11-82 through 11-120 of *The Electric Power Engineering Handbook*, L. L. Grigsby ed., CRC Press, 2001.

[2] Urgent Market Messages at www.nordpool.com

[3] Karlsson, D., M. Hemmingsson, S. Lindahl, "Wide Area System Monitoring and Control," *IEEE Power & Energy Magazine*, Sep./Oct. 2004, Vol. 2, No.5, pp 68-76.

“Phasor measurement units in the Eastern Danish Power System”

A.H. Nielsen, K.O.H. Pedersen, J. Rasmussen, J. Havsager, S.K. Olsen, P.Jørgensen

Accepted for publication in CIGRE 2006 Conference Proceedings

21, rue d'Artois, F-75008 PARIS

CIGRE 2006

http : //www.cigre.org

C2-204

Phasor measurement units in the Eastern Danish Power System

A.H. Nielsen[1 *], K.O.H. Pedersen[1], J. Rasmussen[2]
J. Havsager[2], S.K. Olsen[2], P. Jørgensen[2]

[1] Centre for Electric Technology (CET), Technical University of Denmark
[2] Energinet.dk

Denmark

SUMMARY

In the eastern Danish transmission system four Phasor Measurement Units (PMU's) are installed at 400 kV and 132 kV voltage level. The PMU's continuously record voltage and current phasors each 20 ms. Data are stored locally on the PMU's and are also transferred to a database at Centre for Electric Technology. After power system events data can be extracted and analyzed offline. The purpose of the project is to do research within various utilizations of PMU data.

On 8 January 2005 a severe storm passed Denmark, and wind speeds were so high, that wind turbines disconnected from the transmission grid because of their self protection. Nysted offshore wind farm was among the wind power units that disconnected from the grid, and PMU data from that event are analyzed. The case illustrates the close relation between voltages, power flows and voltage phase angles over a wide area. The voltage phase angle measurements complements the traditional voltage and power flow measurements.

KEYWORDS

PMU, phase angle, transmission system, wind farm, wind turbine, Nysted, storm

1. INTRODUCTION

Energinet.dk is the independent system operator (ISO) in Denmark. Until 2005 Elkraft System was the ISO in Eastern Denmark, and this project was run as an Elkraft System project in corporation with Centre for Electric Technology at Technical University of Denmark.

The transmission grid in Eastern Denmark encompasses overhead lines and cables at the two highest voltage levels, i.e. 132 kV and 400 kV, and the interconnections with South Sweden and Germany. The link to Germany is a 400-kV DC interconnection with a transmission capacity of 600 MW. The interconnection with Sweden consists of AC interconnections with a total capacity of some 1900 MW. The link with Sweden also serves as an interconnection with the Nordic grid. The maximum load in Eastern Denmark is about 2870 MW and the total installed capacity is 4360 MW. The eastern Danish transmission system is shown in figure 1.

During the last fifteen years the amount of wind production has increased from negligible to cover 15% of the total electric energy consumption. The amount of wind power has taken a significant step upwards when a 150 MW off shore wind farm at Rødsand near Nysted south of Zealand was put into service in autumn 2003 (see figure 1). A 200 MW offshore wind farm is expected to be in operation in 2008. These wind farms together with most part of the on land wind turbines is placed in the sparsely populated areas, where the transmission system is significantly weak. Beside the increased amount of wind power, there have been installed a number of combined heat and power units in the system. This new production displaces production from conventional power plants. Consequently the ISO has to handle a changing pattern of electric energy production. Furthermore, the deregulation of the electric energy market makes the power flow less predictable.

As the increase in utilization of wind energy and combined heat and power is expected to continue, it will become more important to gather precise information about voltages and power flows in the transmission system.

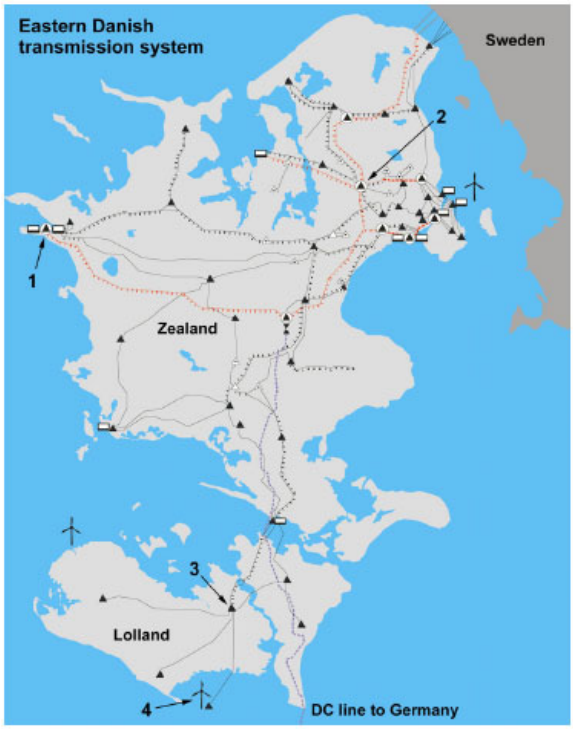

Figure 1. **Eastern Danish transmission system**
Red lines are 400 kV
Black lines are 132 kV
1. PMU at Asnæsværket, 400 kV
2. Two PMU's in Hovegård, 132 kV and 400 kV
3. PMU in Radsted, 132 kV
4. Nysted 150 MW offshore windfarm

2. MEASUREMENT SYSTEM

On that background, a total of four PMU units have been installed in the 400 kV and the 132 kV system in Eastern Denmark. The PMU units are developed and built in collaboration between Elkraft System and Centre for Electric Technology (CET) on Technical University of Denmark. Since the PMU's are built at CET all information about the measurement method are known in every detail. The locations of the four PMU's are shown in figure 1.

The PMU's are based on an industrial PC design with analog and digital I/O card and a GPS especially designed for timing purposes rather than positioning. The excellent timing in the GPS system makes it possible to use a 20 ms shift in the UTC time (Coordinated Universal Time) as reference for the phase of a sinusoidal 50 Hz voltage or current signal. The UTC time has global simultaneity and phases measured with this reference are comparable even if they are measured hundreds or thousands of kilometres apart. The phase angle of a 50 Hz signal can be measured with an accuracy of 0.01 degree, which indicates that the time uncertainty is less than 0.56 μs. The greatest phase uncertainty lies in the phase shift of the conventional voltage and current transformers used in the transmission system. The PMU's continuously measures a three phase voltage phasor and up to four three phase current phasors each 20 ms. After major power system events, relevant data can be extracted from a database at CET and analyzed offline.

3. AIMS OF THE PROJECT

The main purpose with the PMU project is to do research work. In the future PMU data is expected to become a helpful tool in daily control room routines and system protection.

In the first hand, the research work covers the following subjects:

PMU measurement method. Dependent on the used measurement method in the PMU's, they have different responses during transient states in frequency, phase or amplitude. Since the PMU's are built at CET, it is possible to do experiments with different measurement methods.

Model verification. After major events in the transmission system, measured dynamic responses are compared to calculated responses in order to verify the used dynamic models in the dynamic calculation tools. The phase information in the PMU data gives an improved verification of the mathematical models.

Stability assessment. PMU data can improve online stability assessment of angular and voltage stability.

System protection schemes. An industrial PhD project regarding System Protection Schemes utilizing PMU advantages is completed at Elkraft System and CET.

Oscillation modes. Power oscillations in the transmission grid can be investigated by analyzing the frequency or phase information in the PMU data.

4. CASE: STORM IN DENMARK 8 JANUARY 2005

On 8 January a severe storm with wind speeds up to 28 m/s passed Denmark. Because of high mechanical and electrical loads at such high wind speeds, the wind turbines must be disconnected from the grid and shut down. This also happened for the Nysted offshore wind farm located south of Lolland (figure 1), which disconnected from the grid app. at 13:30 .

Figure 2 shows the production of active power from the Nysted offshore wind farm on 8 January 2005 from 13.00 to 14.00. In the first half hour the production was stable and at rated power

because of good wind. During the five minutes from 13.30 to 13.05, all of the wind turbines one by one disconnected from the grid because of too hard wind. After a period with zero power production on the wind farm, some of the wind turbines reconnected to the grid and resumed their production.

The Nysted offshore wind farm is connected to the grid at Radsted (132 kV) on Lolland. Figure 3 shows the voltage in Radsted 132 kV in the same time period as in figure 2. In the first half hour the voltage increases due to disconnection of on land wind turbines. At 13.08 and 13.25 the voltage on Lolland is decreased by disconnecting capacitor banks in the area. At 13.30 the voltage increases due to the gradually disconnection of the Nysted wind turbines. At 13.33 more capacitors are disconnected, and the voltage stabilises at 137 kV.

Figure 4 shows the voltage phase difference Radsted 132 kV minus Hovegård 132 kV. A positive phase difference indicates a north going power flow from Radsted towards Hovegård. At 13.08 and 13.25 the phase difference increases due to voltage drops in Radsted (figure 3). At 13.30 the phase difference decreases concurrently with the decreasing production at Nysted wind farm and hence the decreasing north going power flow. At reconnection of some of the Nysted wind turbines the phase difference increases again.

Figure 5 shows the reactive power flow in a north going line from Radsted towards Sealand. A positive value indicates a south going reactive power flow in that line. The figure clearly shows that a decreasing voltage in Radsted (figure 3) causes an increase in south going reactive power flow and vice versa. The figure also shows that the south going reactive power flow decreases as the Nysted wind turbines disconnects.

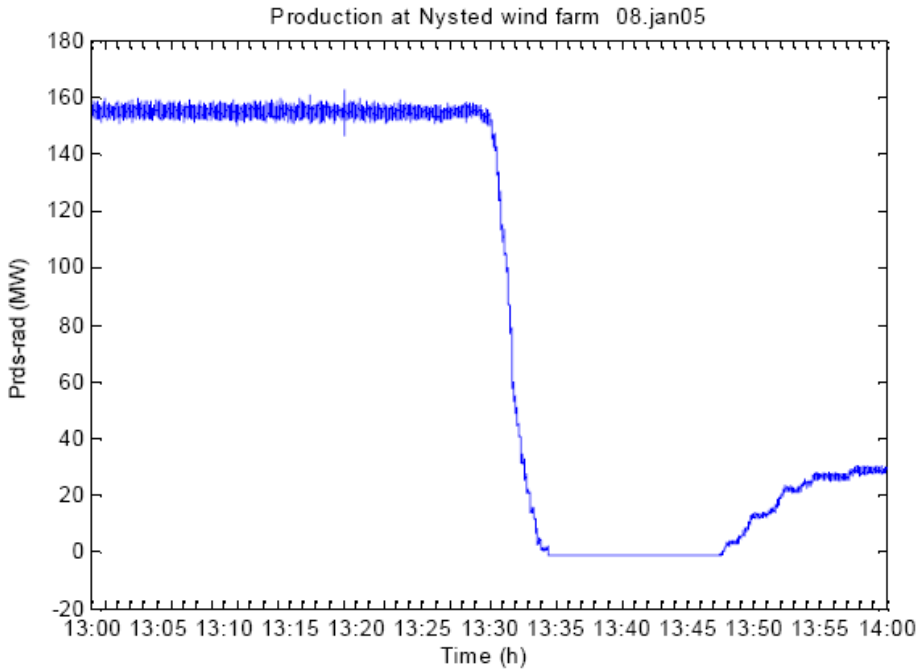

Figure 2. Active power production from Nysted 150 MW offshore wind farm connected at Radsted 132 kV.

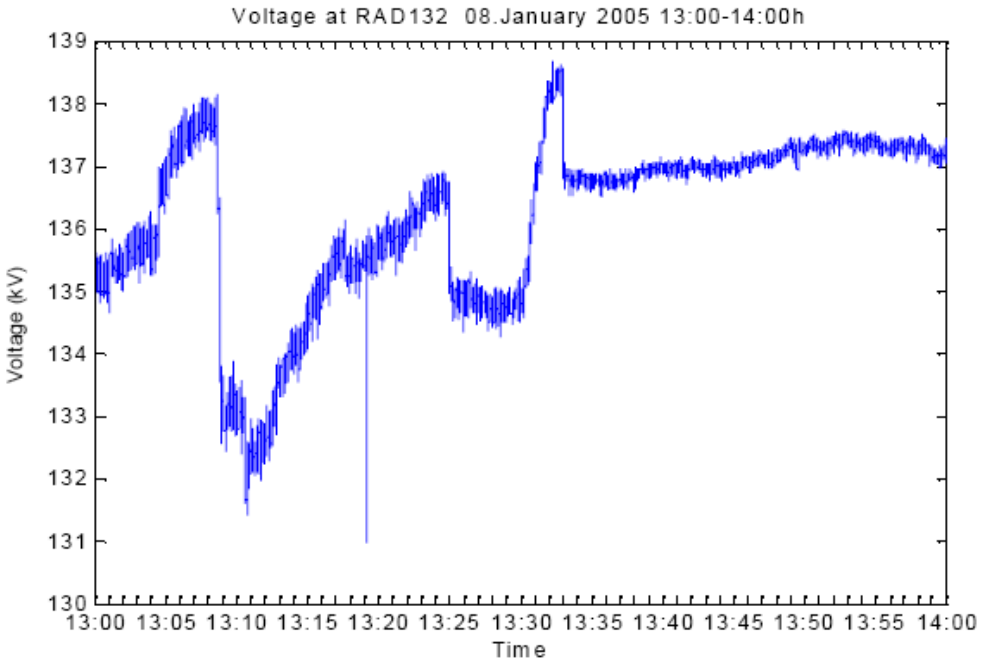

Figure 3. Voltage in Radsted 132 kV.

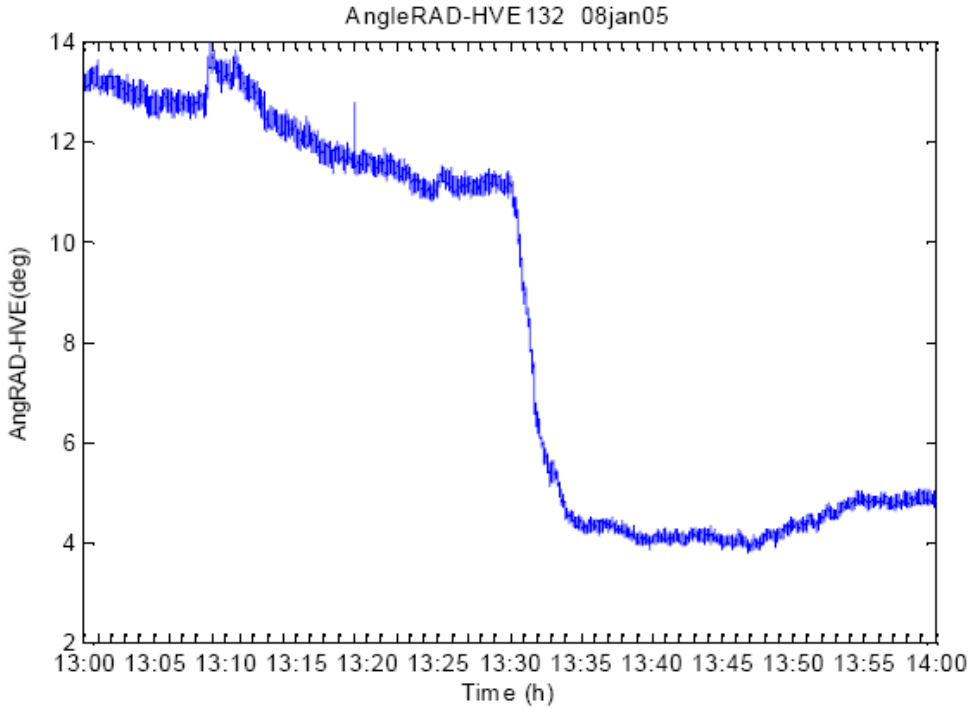

Figure 4. Phase difference between Radsted 132 kV and Hovegård 132 kV. A positive value indikates a north going active power flow.

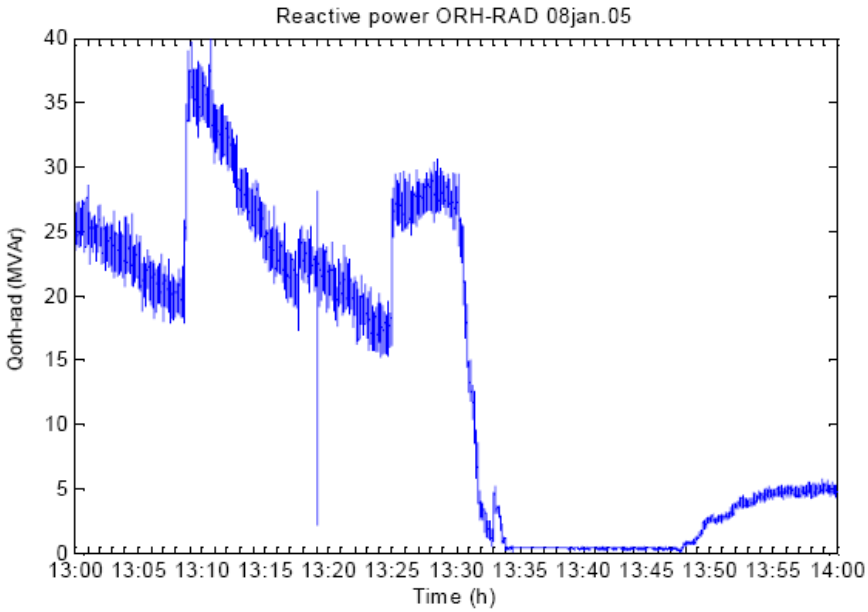

Figure 5. Reactive power flow in a north going line from Radsted towards Sealand. A positive value indicates a south going reactive power flow in that line.

5. CONCLUSION

The case from the storm 8 January 2005 underlines the close relation between voltages, power flows and phase angles over a wide area. The phase angle information supplement the traditional voltage and power flow measurements in a transmission system and in the future the phase angle measurements is expected to become a helpful parameter for daily control room routines and for new system protection devices. At Energinet.dk and Centre for Electric Technology work about utilization of the phase angle measurements in the most beneficial way is going on.

Appendix 2 - Power system data

Load Flow input data:

Central generation	Total load	Wind power 0 MW (0%)		Wind power 133 MW (20%)		Wind power 412 MW (50%)		Wind p. 597 MW (70%)		Wind power 876 MW (100%)	
Generation at power plants (MW)	Total load (MW) (% of peak load)	on-land	off-shore	on-land	off-shore	on-land	off-shore	on-land	off-shore	on-land	off-shore
700 MW	**980 MW** (35%)	0	0	81	52	203	209	284	313	**470**	**406**
1090 MW	**1400 MW** (50%)	0	0	81	52	203	209	284	313	**470**	**406**
1715 MW	**2100 MW** (75%)	0	0	81	52	203	209	284	313	**470**	**406**
1820 MW	**2800 MW** (100%)	0	0	81	52	203	209	284	313	**470**	**406**

Table 1A. Network with NHP1 and NHP2 off-shore wind farms and SVC at RAD

Total load (% of peak)	Generation at power plants (MW) at 100 % wind	Off-shore wind farms at 100 % wind
35 % load	Amager3: 210 MW (-76,6 MVAr) Asnæs2: 80 MW (-18,6 MVAr) Avedøre1: 210 MW (-20,6 MVAr) Small CHP: 200 MW	Nysted 1: 166 MW Nysted 2: 200 MW Mid.grund: 40 MW
50 % load	Amager3: 210 MW (21 MVAr) Asnæs2: 80 MW (13,6 MVAr) Avedøre1: 210 MW (6,5 MVAr) Avedøre2: 350 MW (11,6 MVAr) H.C.Ørsted7:40 MW (7,5 MVAr) Small CHP: 200 MW	Nysted 1: 166 MW Nysted 2: 200 MW Mid.grund: 40 MW
75% load	Amager3: 210 MW, (3,0 MVAr) Asnæs5: 500 MW, (38,7 MVAr) Avedøre1: 210 MW, (9,7 MVAr) Avedøre2: 350 MW, (62,8 MVAr) HCØrsted7: 40 MW (-1,1 MVAr) Svanemøl.7: 55MW (-0,7 MVAr) Small CHP: 350 MW	Nysted 1: 166 MW Nysted 2: 200 MW Mid.grund: 40 MW
100% load	Amager3: 210 MW (87,8 MVAr) Asnæs2: 80 MW (57,4 MVAr) Asnæs5: 500 MW (111,3 MVAr) Avedøre1: 210MW (71,3 MVAr) Avedøre2: 350 MW (74,6 MVAr) H.C.Ørsted7: 40 MW (31,2 MVAr) H.C.Ørsted8: 25 MW (10 MVAr) Svanemøl.7: 55MW (21,2 MVAr) Small CHP: 350 MW	Nysted 1: 166 MW Nysted 2: 200 MW Mid.grund: 40 MW

Table 2A: Generation units for different system conditions

Simulation results:

Load / Wind	35% load		50% load		75% load		100 % load		Network configuration
0% wind	ΔQ_{post} - $\Delta Q_{prefault}$	0,8	ΔQ_{post} - $\Delta Q_{prefault}$	1,8	ΔQ_{post} - $\Delta Q_{prefault}$	3,6	ΔQ_{post} - $\Delta Q_{prefault}$	6,5	Intact $\Delta Q_{prefault}$
	0	0,8	0	1,8	0	3,6	0	6,5	Single line $\Delta Q_{postfault}$
	0	0,8	0	1,8	0	3,6	0,1	6,6	Double line $\Delta Q_{postfault}$
20% wind	ΔQ_{post} - $\Delta Q_{prefault}$	1,0	ΔQ_{post} - $\Delta Q_{prefault}$	1,7	ΔQ_{post} - $\Delta Q_{prefault}$	3,3	ΔQ_{post} - $\Delta Q_{prefault}$	6,0	Intact $\Delta Q_{prefault}$
	0	1,0	0	1,7	0	3,3	0	6,0	Single line $\Delta Q_{postfault}$
	0,3	1,3	0,2	1,9	0,2	3,5	0,1	6,1	Double line $\Delta Q_{postfault}$
50% wind	ΔQ_{post} - $\Delta Q_{prefault}$	6,4	ΔQ_{post} - $\Delta Q_{prefault}$	6,5	ΔQ_{post} - $\Delta Q_{prefault}$	7,3	ΔQ_{post} - $\Delta Q_{prefault}$	9,1	Intact $\Delta Q_{prefault}$
	0,4	6,8	0,4	6,9	0,4	7,7	0,2	9,3	Single line $\Delta Q_{postfault}$
	3,1	9,5	3,1	9,6	2,9	10,2	2,5	11,6	Double line $\Delta Q_{postfault}$
70% wind	ΔQ_{post} - $\Delta Q_{prefault}$	15	ΔQ_{post} - $\Delta Q_{prefault}$	13,9	ΔQ_{post} - $\Delta Q_{prefault}$	14,4	ΔQ_{post} - $\Delta Q_{prefault}$	15,6	Intact $\Delta Q_{prefault}$
	1	16	0,9	14,8	0,8	15,2	0,7	16,3	Single line $\Delta Q_{postfault}$
	6,8	21,8	6,5	20,4	6,2	20,6	5,9	21,5	Double line $\Delta Q_{postfault}$
100% wind	ΔQ_{post} - $\Delta Q_{prefault}$	32,2	ΔQ_{post} - $\Delta Q_{prefault}$	31,8	ΔQ_{post} - $\Delta Q_{prefault}$	30,9	ΔQ_{post} - $\Delta Q_{prefault}$	Non converg. solution	Intact $\Delta Q_{prefault}$
	2,0	34,2	1,9	33,7	2,0	32,9		Non conver. solution	Single line $\Delta Q_{postfault}$
		Non- conver. solution				Non-conver. solution		Non- conver. solution	Double line $\Delta Q_{postfault}$

Table 3A. Summary of reactive power losses for base case studies with SVC (65 MVAr)

Wind turbine generator

In the dynamic analysis identical input data is applied for all induction generators for on-land wind turbines, which is based on equivalent scheme for standard 600 kW wind generator. Another data set is used for the equivalent off-shore wind turbines at Nysted and Middelgrund. Here the data is based on a standard 2,3 MW wind turbine generator. Z_{source} is equivalent generator impedance used in load flow calculations.

Parameter	Standard on-land WT	Standard off-shore WT
X_s [p.u.]	0,0745	0,144
X_m [p.u.]	3,7959	3,145
R_2 [p.u.]	0,01806	0,00704
X_r [p.u.]	0,1214	0,0505
R_s [p.u.]	0,0048	0,00549
Z_{source} [p.u.]	0,1921	0,1937

Table 4A: Typical data for on-land and off-shore wind turbines generators

Relay model data

Parameter	Relay settings (p.u.)		Measuring time constant (sec.)	Tripping time of relay (sec.)
Undervoltage 1	0.800	0.805	0.010	0.500
Overvoltage 1	1.100	1.095	0.010	60.00
Overvoltage 2	1.150	1.140	0.010	0.500
Underfrequency 1	-0.060	-0.059	0.010	0.200
Overfrequency 1	0.020	0.019	0.010	0.200
Overcurrent 1	2.00	1.950	0.010	0.040
Overcurrent 2	100	100	100	100
Overspeed 1	0.900	-1.000	0.200	0.050

Table 5A: Relay settings for on-land wind turbines

Parameter	Relay settings (p.u.)		Measuring time constant (sec.)	Tripping time of relay (sec.)
Undervoltage 1	0.693	0.700	0.010	2.00
Overvoltage 1	1.089	1.080	0.010	11.00
Overvoltage 2	1.188	1.180	0.010	0.100
Underfrequency 1	-0.060	-0.059	0.010	0.300
Overfrequency 1	0.060	0.059	0.010	0.300
Overcurrent 1	5.64	5.63	0.010	0.045
Overcureent 2	100.0	100.0	0.010	100.0
Overspeed 1	0.080	0.075	0.010	0.440

Table 6A: Relay settings for off-shore wind turbines (Nysted1)

Appendix 3 - Considerations on PMU placement

Appendix 3 considers different issues for implementation of Phasor Measurement Units at three locations in the Eastern Danish transmission system.

Re. Hovegård

Frequency, f (Hz)	
$\lvert U_{HVE400} \rvert, \angle U_{HVE400}$	3 channels
$\lvert U_{HVE132} \rvert, \angle U_{HVE132}$	3 channels
$\lvert I_{HVE\text{-}GØR} \rvert, \angle I_{HVE\text{-}GØR}$	3 channels
$\lvert I_{HVE\text{-}SAN} \rvert, \angle I_{HVE\text{-}SAN}$	3 channels
Input total:	12 channels

By monitoring substation data as bus voltage and line current phasors from limited number of key locations in the power system it is possible to cover a considerable portion of the transmission system. The calculation of phasor applied takes precautious against problems with oscillating sign.

$$\begin{aligned} P &= \sqrt{3} \cdot (\mathrm{Re}\{U\}\mathrm{Re}\{I\} + \mathrm{Im}\{U\}\mathrm{Im}\{I\}) \\ Q &= \sqrt{3} \cdot (\mathrm{Im}\{U\}\mathrm{Re}\{I\} - \mathrm{Re}\{U\}\mathrm{Im}\{I\}) \end{aligned} \qquad (1A)$$

Selected input signals from potential and current transformers[40] are suggested as follows:

$$\begin{aligned} P_{HVE-GØR} &= \sqrt{3} \cdot (\mathrm{Re}\{U_{HVE400}\}\mathrm{Re}\{I_{HVE-GØR}\} + \mathrm{Im}\{U_{HVE400}\}\mathrm{Im}\{I_{HVE-GØR}\}) \\ Q_{HVE-GØR} &= \sqrt{3} \cdot (\mathrm{Im}\{U_{HVE400}\}\mathrm{Re}\{I_{HVE-GØR}\} - \mathrm{Re}\{U_{HVE400}\}\mathrm{Im}\{I_{HVE-GØR}\}) \end{aligned} \qquad (2A)$$

$$\begin{aligned} P_{HVE-SAN} &= \sqrt{3} \cdot (\mathrm{Re}\{U_{HVE400}\}\mathrm{Re}\{I_{HVE-SAN}\} + \mathrm{Im}\{U_{HVE400}\}\mathrm{Im}\{I_{HVE-SAN}\}) \\ Q_{HVE-SAN} &= \sqrt{3} \cdot (\mathrm{Im}\{U_{HVE400}\}\mathrm{Re}\{I_{HVE-SAN}\} - \mathrm{Re}\{U_{HVE400}\}\mathrm{Im}\{I_{HVE-SAN}\}) \end{aligned} \qquad (3A)$$

One channel for each phase is accounted for voltage and current magnitudes as well as phase angle measurements at 400 kV and 132 kV level. The primary motivation for direct measurement of $\angle U_{HVE\ 400kV}$ and $\angle U_{HVE\ 132kV}$ is to obtain a voltage phase angle reference for the measuring points $\angle U_{ASV\ 400kV}$ and $\angle U_{RAD\ 132kV}$ respectively. For directly measured U_{HVE400}, $I_{HVE\text{-}GØR}$ and $I_{HVE\text{-}SAN}$

[40] available for protective relays

phasors it is possible to calculate complex 400 kV voltages at SAN (Söderåsen, Sweden) and at GØR (Gørløse) as follows:

$$\begin{aligned} \overline{U}_{SAN} &= \overline{U}_{HVE} - \overline{Z}_{HVE-SAN} \cdot \overline{I}_{HVE-SAN} \\ \overline{U}_{GØR} &= \overline{U}_{HVE} - \overline{Z}_{HVE-GØR} \cdot \overline{I}_{HVE-GØR} \end{aligned} \qquad (4A)$$

Another reason for selecting $I_{HVE\text{-}GØR}$ & $I_{HVE\text{-}SAN}$ phasor measurements is to supply better utilization of the existing digital fault recorder in HVE, which today is used as a power swing monitor.

Re. Asnæs station

It is planned to monitor a voltage phasor at ASV 400 kV bus bar, current phasors in the double outgoing 130 kV line to Bjæverskov and current flow in the 130 kV transformer ASV:

Frequency, f (Hz)	
$\lvert U_{ASV\mathbf{400}}\rvert, \angle U_{ASV\mathbf{400}}$	3 channels
$\lvert I_{ASV\text{-}BJS1}\rvert, \angle I_{ASV\text{-}BJS1}$	3 channels
$\lvert I_{ASV\text{-}BJS2}\rvert, \angle I_{ASV\text{-}BJS2}$	3 channels
$\lvert I_{ASV400/132\ trafo}\rvert, \angle I_{ASV400/132\ trafo}$	3 channels
In total:	12 channels

$$\begin{aligned} P_{ASV-BJS1} &= \sqrt{3} \cdot (\mathrm{Re}\{U_{ASV\,400}\}\mathrm{Re}\{I_{ASV-BJS1}\} + \mathrm{Im}\{U_{ASV\,400}\}\mathrm{Im}\{I_{ASV-BJS1}\}) \\ Q_{ASV-BJS1} &= \sqrt{3} \cdot (\mathrm{Im}\{U_{ASV\,400}\}\mathrm{Re}\{I_{ASV-BJS1}\} - \mathrm{Re}\{U_{ASV\,400}\}\mathrm{Im}\{I_{ASV-BJS1}\}) \end{aligned} \qquad (5A)$$

$$\begin{aligned} P_{ASV-BJS2} &= \sqrt{3} \cdot (\mathrm{Re}\{U_{ASV\,400}\}\mathrm{Re}\{I_{ASV-BJS2}\} + \mathrm{Im}\{U_{ASV\,400}\}\mathrm{Im}\{I_{ASV-BJS2}\}) \\ Q_{ASV-BJS2} &= \sqrt{3} \cdot (\mathrm{Im}\{U_{ASV\,400}\}\mathrm{Re}\{I_{ASV-BJS2}\} - \mathrm{Re}\{U_{ASV\,400}\}\mathrm{Im}\{I_{ASV-BJS2}\}) \end{aligned} \qquad (6A)$$

$$\begin{aligned} P_{ASV\,400/132} &= \sqrt{3} \cdot (\mathrm{Re}\{U_{ASV\,400}\}\mathrm{Re}\{I_{ASV\,400/132}\} + \mathrm{Im}\{U_{ASV\,400}\}\mathrm{Im}\{I_{ASV\,400/132}\}) \\ Q_{ASV\,400/132} &= \sqrt{3} \cdot (\mathrm{Im}\{U_{ASV\,400}\}\mathrm{Re}\{I_{ASV\,400/132}\} - \mathrm{Re}\{U_{ASV\,400}\}\mathrm{Im}\{I_{ASV\,400/132}\}) \end{aligned} \qquad (7A)$$

The complex voltage $U_{ASV400kV}$ & the double line current to BJS can be used to calculate the voltage in BJS station:

$$\overline{U}_{BJS400} = \overline{U}_{ASV\,400} - \overline{Z}_{(ASV-BJS1)} \cdot \overline{I}_{(ASV-BJS1)1} \qquad (8A)$$

This information can be utilized for calculation of line currents $I_{BJS\text{-}HVE}$ and $I_{BJS\text{-}ISH}$:

$$\bar{I}_{HVE-BJS} = \frac{\overline{U}_{HVE} - \overline{U}_{BJS}}{\overline{Z}_{HVE-BJS}} \qquad (9A)$$

Placing PMUs at Asnæs and Hovedgård station the following 400kV key voltage phasors in the backbone network are directly[41] or indirectly[42] available:

$$\overline{U}_{ASV}, \overline{U}_{BJS}, \overline{U}_{HVE}, \overline{U}_{GØR}, \overline{U}_{SAN}$$

The voltage $U_{ASV\mathbf{132}}$ is not between the planned measurements in normal operation, since it does not influence significantly the voltage regulation in the Lolland- Falster region (long electrical distance between ASV_{132} and RAD_{132}. Asnæs substation is MVAr neutral seen from the 132 kV busbar ASV132 kV, because the reactive power produced at the power plant is used to cover transformer reactive power loss under normal operating conditions. The reason for suggesting measurement of $I_{ASV400/132\ trafo}$ phasor is that the flow via the ASV 400/132 kV transformer gives valuable information about change in reactive power (MVAr) flow in emergency situation.

Re. Radsted

At the 132 kV busbar in Radsted it is suggested to measure frequency, three phase voltage magnitude, phase angle as well as 132 kV currents in the outgoing lines from Radsted to Nysted wind farm (NHP), Vestlolland (VLO) substation as well as the double 132 kV connection north up to Orehoved (ORH) and Blangslev (BLA).

f_{RAD} (Hz)	
$\lvert U_{RAD\mathbf{132}}\rvert, \angle U_{RAD\mathbf{132}}$	3 channels
$\lvert I_{RAD\text{-}VLO}\rvert, \angle I_{RAD\text{-}VLO}$	3 channels
$\lvert I_{RAD\text{-}NHP}\rvert, \angle I_{RAD\text{-}NHP}$	3 channels
$\lvert I_{RAD\text{-}ORH}\rvert, \angle I_{RAD\text{-}ORH}$	3 channels
$\lvert I_{RAD\text{-}BLA}\rvert, \angle I_{RAD\text{-}BLA}$	3 channels
In total:	15 channels

$$\begin{aligned} P_{RAD-VLO} &= \sqrt{3} \cdot (\mathrm{Re}\{U_{RAD132}\}\mathrm{Re}\{I_{RAD-VLO}\} + \mathrm{Im}\{U_{RAD132}\}\mathrm{Im}\{I_{RAD-VLO}\}) \\ Q_{RAD-VLO} &= \sqrt{3} \cdot (\mathrm{Im}\{U_{RAD132}\}\mathrm{Re}\{I_{RAD-VLO}\} - \mathrm{Re}\{U_{RAD132}\}\mathrm{Im}\{I_{RAD-VLO}\}) \end{aligned} \qquad (10A)$$

$$\begin{aligned} P_{RAD-NHP} &= \sqrt{3} \cdot (\mathrm{Re}\{U_{RAD132}\}\mathrm{Re}\{I_{RAD-NHP}\} + \mathrm{Im}\{U_{RAD132}\}\mathrm{Im}\{I_{RAD-NHP}\}) \\ Q_{RAD-NHP} &= \sqrt{3} \cdot (\mathrm{Im}\{U_{RAD132}\}\mathrm{Re}\{I_{RAD-NHP}\} - \mathrm{Re}\{U_{RAD132}\}\mathrm{Im}\{I_{RAD-NHP}\}) \end{aligned} \qquad (11A)$$

[41] direct PMU measurement

[42] calculated quantity using Kirchhoff's and Ohm's law

$$P_{RAD-ORH} = \sqrt{3} \cdot (\mathrm{Re}\{U_{RAD132}\}\mathrm{Re}\{I_{RAD-ORH}\} + \mathrm{Im}\{U_{RAD132}\}\mathrm{Im}\{I_{RAD-ORH}\})$$
$$Q_{RAD-ORH} = \sqrt{3} \cdot (\mathrm{Im}\{U_{RAD132}\}\mathrm{Re}\{I_{RAD-ORH}\} - \mathrm{Re}\{U_{RAD132}\}\mathrm{Im}\{I_{RAD-ORH}\}) \quad (12\ A)$$

$$P_{RAD-BLA} = \sqrt{3} \cdot (\mathrm{Re}\{U_{RAD132}\}\mathrm{Re}\{I_{RAD-BLA}\} + \mathrm{Im}\{U_{RAD132}\}\mathrm{Im}\{I_{RAD-BLA}\})$$
$$Q_{RAD-BLA} = \sqrt{3} \cdot (\mathrm{Im}\{U_{RAD132}\}\mathrm{Re}\{I_{RAD-BLA}\} - \mathrm{Re}\{U_{RAD132}\}\mathrm{Im}\{I_{RAD-BLA}\}) \quad (13A)$$

Phasor measurement of the mentioned line currents is also required for calculation of voltage at the following buses that are adjacent to Radsted:

$$\begin{aligned}
\overline{U}_{VLO} &= \overline{U}_{RAD} - \overline{Z}_{RAD-VLO} \cdot \overline{I}_{RAD-VLO} \\
\overline{U}_{NHP} &= \overline{U}_{RAD} - \overline{Z}_{RAD-NHP} \cdot \overline{I}_{RAD-NHP} \\
\overline{U}_{BLA} &= \overline{U}_{RAD} - \overline{Z}_{RAD-BLA} \cdot \overline{I}_{RAD-BLA} \\
\overline{U}_{ORH} &= \overline{U}_{RAD} - \overline{Z}_{RAD-ORH} \cdot \overline{I}_{RAD-ORH}
\end{aligned} \quad (14A)$$

The complex voltages at VLO, NHP, BLA and ORH can be subsequently used to estimate voltage drop (ΔU), as well as active and reactive power flow across the four lines. These quantities are very important in evaluating potential problems with voltage instability.